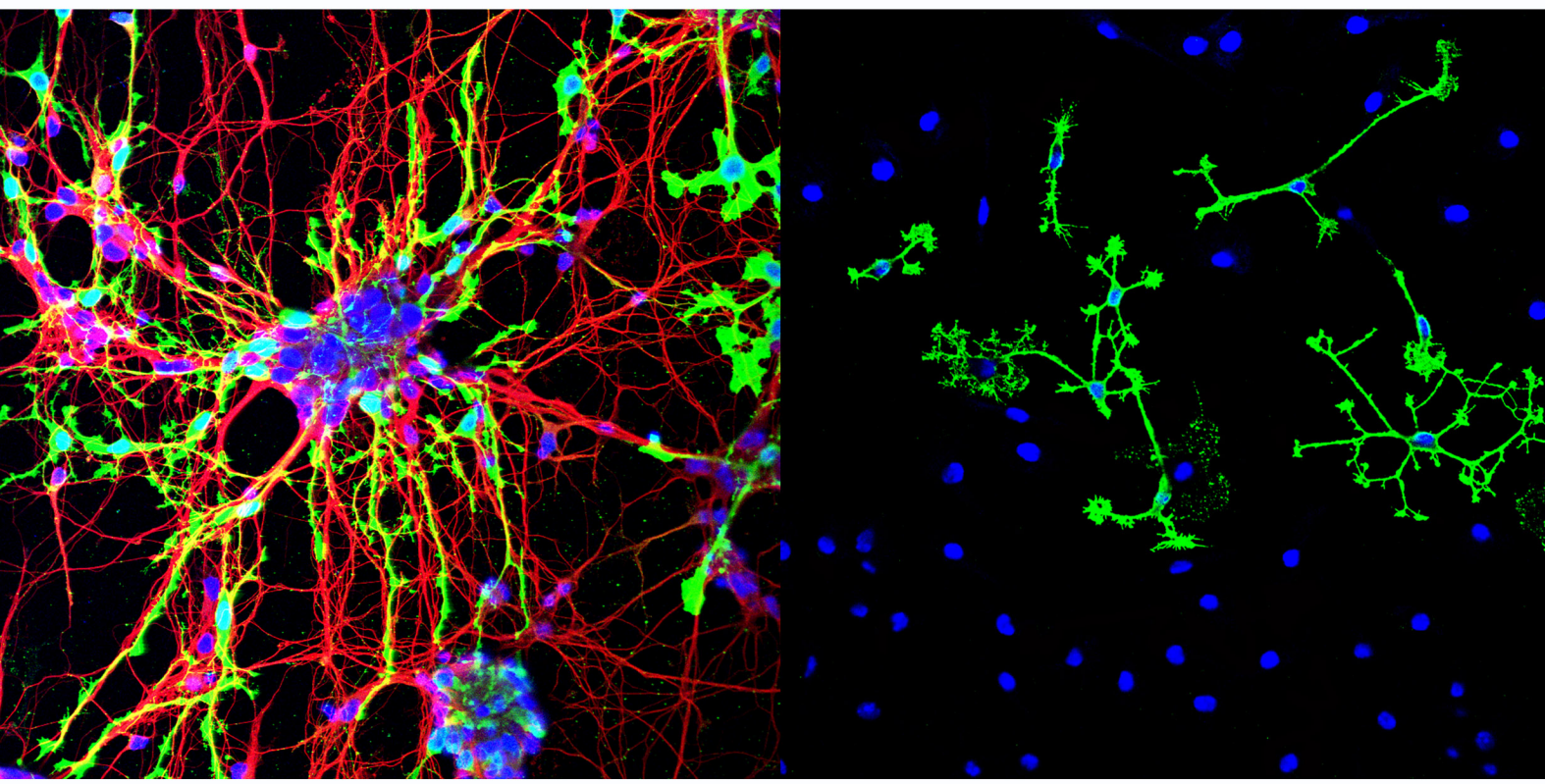
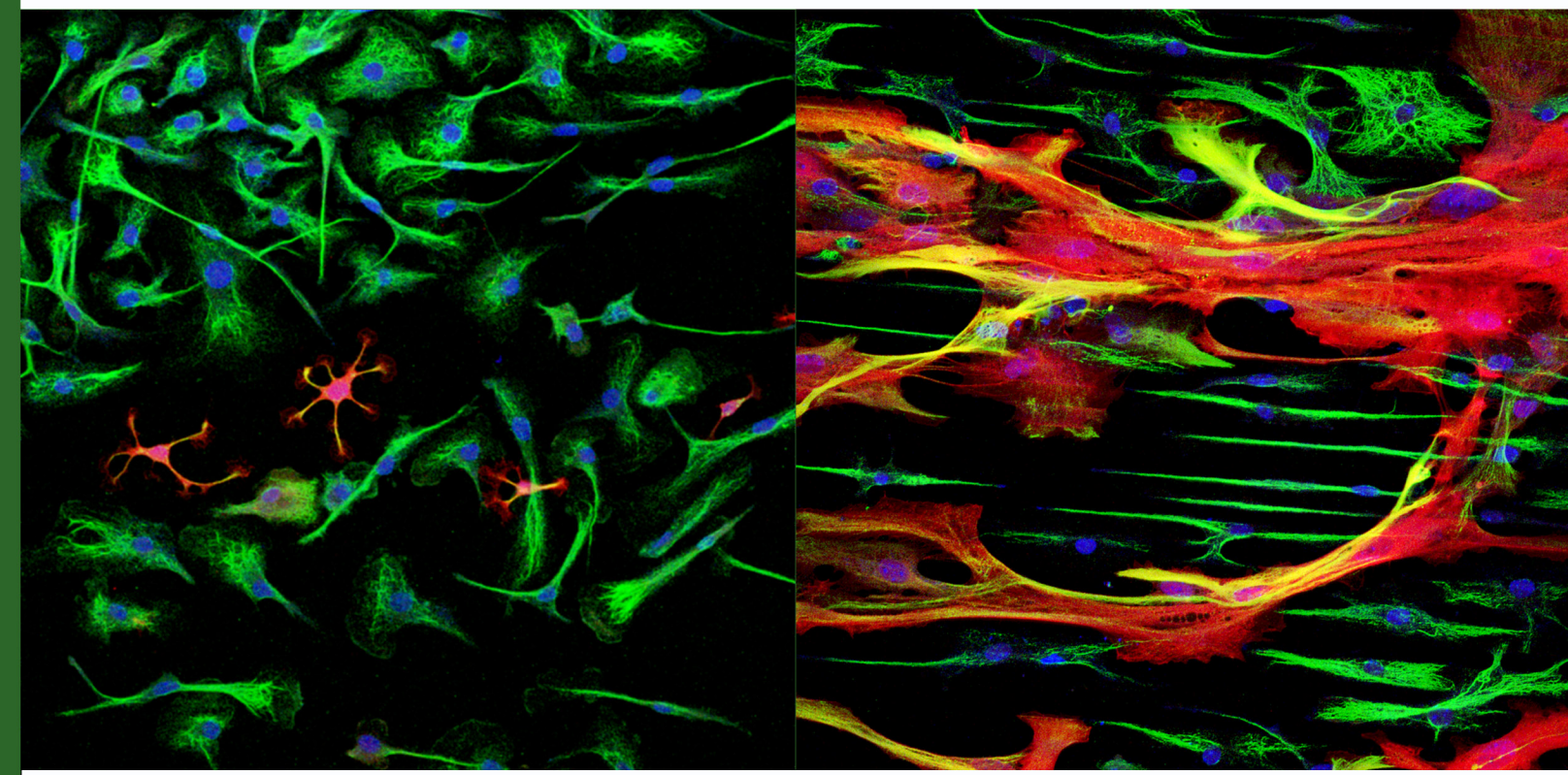


BIOLOGICAL RESPONSE TO STRUCTURED AND FUNCTIONALIZED SUBSTRATES FOR NERVE TISSUE REGENERATION



BIOLOGICAL RESPONSE TO STRUCTURED AND FUNCTIONALIZED SUBSTRATES FOR NERVE TISSUE REGENERATION



PhD program in Biomedical Engineering



UNIVERSITAT POLITÈCNICA
DE CATALUNYA

Department of Material Science and Metallurgical Engineering
Technical Superior School of Industrial Engineering of Barcelona (ETSEIB)
Polytechnic University of Catalonia (UPC)
PhD program in Biomedical Engineering

Biological response to structured and functionalized substrates for nerve tissue regeneration

PhD thesis

Marta Mattotti

July 2012

Director: Dr.^a Elisabeth Engel

Co-director: Dr.^a Soledad Alcántara (University of Barcelona, UB)

A mio papà

*“Fâ e disfâ al è dut un lavorâ”
(To do and to undo are both ways of working)
Proverb from Friuli, Italia*

Agradecimientos

Parecía imposible llegar a este punto del camino. Todo parece imposible hasta cuando se hace. Hay que tener un poco de locura, un poco de paciencia y justo un pellizco de determinación. Llenar esta hoja es lo que me ha dado la motivación durante los momentos de desánimo en este largo proceso formativo y creativo. En los últimos dos años he pensado muchas veces en como escribir los agradecimientos, y ahora que es el momento no voy a pensar, y que salgan solos. Aquí vienen...

Primero que todo, como se suele hacer de protocolo, quiero agradecer a mi jefas Elisabeth Engel y Soledad Alcántara. Dos mujeres increíbles. Gracias por haberme dado la oportunidad de tener una experiencia de vida tanto intensa y variada como solo puede ser un doctorado. Gracias para el apoyo sobre los múltiples frentes, desde lo científico hasta lo burocrático, sin nunca olvidar el humano.

Gracias a Josep A. Planell, por apoyar este proyecto y por dar ejemplo de cómo poco a poco se puede transformar el mundo y hacer que las ideas se hagan realidad.

Gracias a mis compañeros de viaje, Zaida, Alberto, Nuno, Aina y Greti. Llenar todas las páginas de esta tesis no sería suficiente para describir como me habéis llenado el día a día en estos años. Ni me pongo a hacer ejemplos, todos sabemos que hemos pasado juntos unos momentos muy especiales, y otros muy normales, que son los peores de aguantar.

Gracias a mis “compaesanos” Tiziano y Andrea, para los consejos y el buen humor.

Gracias al Benja, el rey de los servicios científicos técnicos, la perfecta combinación entre profesionalidad e ironía.

Gracias a Luis y Conrado para la colaboración con el quitosano.

Gracias a todo el grupo del IBEC Biomaterials for regenerative therapies, y en general a todos los colegas que coincidieron conmigo en algo.

Gracias al grupo de George Altankov.

Gracias a los que financiaron este proyecto (IBEC, UB, beca FPU).

Gracias a Thomas. Gracias a Eva.

Gracias a todos los amigos cercanos y lejanos que de alguna manera me regalaron su energía.

Gracias a mi familia.

Gracias a mi novio Nicolás para ser mi apoyo, mi maestro y mi inspiración.

Y gracias a la música para llenarme la vida.

Index

| | <i>page nº</i> |
|---|----------------|
| Index | I |
| Figures and tables index | V |
| Abbreviations list | XII |
| Abstract | XIV |
| | |
| <u>INTRODUCTION</u> | |
| | |
| 1. THE CENTRAL NERVOUS SYSTEM (CNS) | 3 |
| 1.1 Central Nervous System (CNS) | 3 |
| 1.2 Cerebral cortex | 4 |
| 1.3 Composition of adult cerebral cortex | 6 |
| <i>1.3.1 General characteristics of neurons</i> | 6 |
| <i>1.3.2 Pyramidal neurons and interneurons</i> | 7 |
| 1.4 Composition of adult cerebral cortex: glial cells | 8 |
| <i>1.4.1 General characteristics of glial cells</i> | 8 |
| <i>1.4.2 Glial cells types</i> | 9 |
| 1.5 Composition of adult cerebral cortex: the extracellular matrix (ECM) | 12 |
| 1.6 Cerebral cortex development | 12 |
| <i>1.6.1 Anatomic overview</i> | 12 |
| <i>1.6.2 Cell events overview</i> | 13 |
| <i>1.6.3. Step 1: Early development</i> | 14 |
| <i>1.6.4. Step 2: Neurogenesis</i> | 14 |
| <i>1.6.5. Step 3: Gliogenesis</i> | 18 |
| <i>1.6.6. Step 4: Adult NSC</i> | 21 |
| 1.5 Statements | 24 |
| | |
| 2. CNS RESPONSE TO INJURY | 25 |
| 2.1 Overview | 25 |
| 2.2 Neurons in response to injury | 27 |
| <i>2.2.1 Neuronal damage</i> | 27 |
| <i>2.2.2 Regenerative capacity of neurons</i> | 29 |
| 2.3 Glial cells in response to injury | 32 |
| <i>2.3.1 Gliosis and glial scar</i> | 32 |
| <i>2.3.2 Regenerative capacity of glial cells</i> | 35 |
| 2.4 Current treatments approaches | 36 |
| | |
| 3. BIOMATERIALS IN CNS TISSUE ENGINEERING | 39 |
| 3.1 Tissue engineering | 39 |
| 3.2 Biomaterials for CNS regeneration | 40 |
| 3.3 First, second and third generation of biomaterials | 41 |
| 3.4 Materials used in this thesis work | 43 |
| <i>3.4.1 PMMA</i> | 43 |
| <i>3.4.2 Chitosan</i> | 43 |
| 3.5 Material formulations and structuring | 44 |
| 3.6 Cell-material interaction: the role of biomaterial properties | 47 |

| | |
|---|-----------|
| 3.6.1 Wettability and surface charge | 49 |
| 3.6.2 Stiffness | 49 |
| 3.6.3 Topography | 51 |
| 4. REFERENCES | 54 |
| <u>RATIONAL OF THE THESIS & GOALS</u> | |
| 1. RATIONAL OF THE THESIS | 62 |
| 2. GOALS | 62 |
| <u>RESULTS</u> | |
| 1. INDUCING FUNCTIONAL RADIAL GLIA-LIKE PROGENITORS FROM CORTICAL ASTROCYTE CULTURES USING MICROPATTERNED PMMA | 64 |
| 1.1. Introduction | 65 |
| 1.2. Materials and methods | 67 |
| 1.2.1 PMMA characterization and microstructuring | 67 |
| 1.2.2 Cell culture | 67 |
| 1.2.3 Western blot | 69 |
| 1.2.4 Immunocytochemistry and primary antibodies | 69 |
| 1.2.5 Flow cytometry analysis | 70 |
| 1.2.6 Scanning electron microscopy (SEM) | 70 |
| 1.2.7 Video time lapse analysis | 71 |
| 1.2.8 Imaging and analysis of cell orientation and co-localization | 71 |
| 1.2.9 Statistical analysis | 72 |
| 1.3. Results | 72 |
| 2.3.1 Glial cell orientation and morphology | 72 |
| 1.3.2 Biochemical characterization of glial cells | 75 |
| 1.3.3 Glial cell differentiation on patterned PMMA | 79 |
| 1.3.4 Neuronal adhesion and migration on topography- modified glial cells | 80 |
| 1.5. Discussion | 84 |
| 1.6. Conclusions | 89 |
| 1.6 References | 90 |
| 2. NEURAL CELL BEHAVIOUR IN VITRO AND IN VIVO ON FLAT AND MICRO PATTERNED CHITOSAN FILMS | 93 |
| 2.1. Introduction | 95 |
| 2.2 Materials & Methods | 95 |
| 2.2.1 Preparation of flat and micropatterned films of | 95 |

| | |
|---|------------|
| <i>chitosan</i> | |
| 2.2.2 Material characterization | 96 |
| 2.2.3 Cell culture | 97 |
| 2.2.4 Implant into brain cortex in vivo | 98 |
| 2.2.5 Immunochemistry | 98 |
| 2.2.6 Western Blot | 99 |
| 2.2.7 Imaging and data analysis | 99 |
| 2.2.8 Statistical analysis | 100 |
| 2.3 Results | 100 |
| 2.3.1 Material characterization | 100 |
| 2.3.2 Neuronal response to flat and micropatterned chitosan | 102 |
| 2.3.3 Glial cells response to flat and micro patterned chitosan | 105 |
| 2.3.4 Effect of flat and micro patterned chitosan on neuron to glia cell-cell adhesion | 110 |
| 2.3.5 In vivo response | 111 |
| 2.4. Discussion | 113 |
| 2.5 Conclusions | 117 |
| 2.6 References | 119 |
| | |
| 3. EFFECT OF MODEL SURFACES ON GLIAL ADHESION AND DIFFERENTIATION | 122 |
| | |
| 3.1 Introduction | 123 |
| 3.2. Materials and methods | 125 |
| 3.2.1 Preparation of model surfaces | 125 |
| 3.2.2 Surface characterization | 126 |
| 3.2.3 Primary mouse glial cell culture | 126 |
| 3.2.4 Cell count and overall cell morphology | 127 |
| 3.2.5 Immunocytochemistry | 128 |
| 3.2.6 Statistical analysis | 128 |
| 3.3 Results | 129 |
| 3.3.1. Glial cells adhesion and survival | 129 |
| 3.3.2 Glial cells morphometric characterization after 5h | 130 |
| 3.3.3 Glial cells differentiation after 5 DIV | 131 |
| 3.4. Discussion | 133 |
| 3.5 Conclusions | 135 |
| 3.6 References | 136 |
| | |
| <u>GENERAL DISCUSSION & CONCLUSIONS</u> | |
| | |
| 1. GENERAL DISCUSSION | 140 |
| 1.1 Wettability | 141 |
| 1.2. Surface chemistry and charge | 143 |
| 1.3. Stiffness | 145 |
| 1.4. Topography | 145 |
| 1.5 Final statements | 146 |

| | |
|---|-----|
| 2. CONCLUSIONS | 148 |
| 3. EPILOGUE | 149 |
| 4. REFERENCES | 151 |
| <u>APPENDIX</u> | |
| 1. SCIENTIFIC COMMUNICATIONS DERIVED FROM THE THESIS | 153 |

Figures and tables index

Figures *page n^o*

INTRODUCTION

1. THE CENTRAL NERVOUS SYSTEM (CNS)

| | |
|---|----|
| Figure 1. Central nervous system: brain, spinal cord and meninges. | 3 |
| Figure 2. White matter and grey matter in brain and spinal cord. | 4 |
| Figure 3. Human and mouse cerebral cortex. | 5 |
| Figure 4. A. Representation of cortical layers by Ramon and Cajal and B. cortical columnar functional units. Left: 3D reconstructions of the dendrites from these nerve cells; right: 3D reconstruction of axons that yield input to the neural networks within a cortical column. | 6 |
| Figure 5. Basic cell type in cerebral cortex of monkey. A. glutamatergic neuron (pyramindal cells and stellate cells) and B. GABAergic neuron. | 7 |
| Figure 6. Glial cell types. | 9 |
| Figure 7. Example of protoplasmic astrocytes (a) and fibrous astrocytes (b). Gray matter protoplasmic astrocytes have highly branched fine processes, while white matter fibrous astrocytes, have thicker and less branched processes. | 11 |
| Figure 8. Developement of central nervous system. | 13 |
| Figure 9. Main cellular events in cerebral cortex development in a temporal overview. Solid arrows are supported by experimental evidence; dashed | 13 |

arrows are hypothetical. Colors depict symmetric, asymmetric, or direct transformation. IPC, intermediate progenitor cell; MA, mantle; MZ, marginal zone; NE, neuroepithelium; nIPC, neurogenic progenitor cell; oIPC, oligodendrocytic progenitor cell; RG, radial glia; SVZ, subventricular zone; VZ, ventricular zone.

Figure 10. Neuroepithelial cells in the neural tube. 14

Figure 11. Neurogenic radial glia 15

Figure 12. Radial migration and formation of cerebral cortex layer. 16

Figure 13. Tangential migration and GABAergic neurons 17

Figure 14. Schematical representation of neural progenitor cells and glial cell lineage according to *in vivo* and *in vitro* experiments. 20

Figure 15. Schematic representation of evolution of neuroepithelial cells and radial glia and the main used antigenic features. 22

2. CNS RESPONSE TO INJURY

Figure 16. Brain injury. 26

Figure 17. Schematic representation of neuronal response to injury. 28

Figure 18. Drawings by Ramon y Cajal of axonal bulbs in abortive regeneration. 29

Figure 19. Compensatory plasticity. 30

Figure 20. Increased cell proliferation in neurogenic regions after experimental TBI. An increase in the number of bromodeoxyuridine (BrdU)-labeled cells (brown), was observed after 2days in the ipsilateral dentate gyrus in injury group (B) compared to control animal group (A, sham). These cells are mainly clustered in the subgranular zone (B, arrows). Similarly, BrdU labeling in the ipsilateral subventricular zone of sham animals (C) significantly increases after injury (D, arrows). 31

Figure 21. Glial scar. 32

Figure 22. Quiescent and reactive markers and their main markers. 33

Figure 23. NG2-positive cells after injury in cerebellum of adult rats. At 4 and 10 days post-injury, the NG2-expressing cells have formed small plaques at the injury site. These plaques correspond to the glial scar. 34

3. BIOMATERIALS IN CNS TISSUE ENGINEERING

| | |
|--|----|
| Figure 24 Tissue engineering approach to brain injury. | 39 |
| Figure 25. Properties of the ideal nerve guidance channel. The desired physical properties of a nerve conduit include (from the top and clockwise): bioactive factor delivery; supporting cell incorporation; oriented matrix to favour cell migration; intraluminal channels to mimic the structure of nerve fascicles; electrical activity; biodegradability and porosity. | 45 |
| Figure 26. Self assembling amphiphilic peptides a. structure; b. overall gelly appearance; c. in vitro neural stem cell cultures differentiated in neurons (stained for neuronal marker β -tubulin III) | 46 |
| Figure 27. Cell-ECM interactions. | 47 |
| Figure 28. Development of glial encapsulation on an intracortical microelectrode. (A) Acute neural injury caused by inserting a microelectrode into the brain cortex. Astrocytes and microglial cells become activated and migrate to the site of injury. (B) Chronic response showing a dense sheath around implanted probes, which contains fibroblasts, macrophages and astrocytes. (C,D) The reactive astrocytes, immunohistochemically labeled here for GFAP, encapsulate the neural probes forming a dense cellular sheath. Calibration bar = 50 μ m (Marin and Fernandez 2010). | 48 |
| Figure 29. Effect of substrate elasticity on mesenchomal stem cell differentiation. | 50 |
| Figure 30. Cultures of dissociated embrionic cerebral cortices at 1 week in vitro on soft (A) and hard (B) polyacrylamide (PA) gels and soft (250Pa)(D) and hard (2,1 kPa)€ fibrin gels. The prevalence of astrocytes is apparent on hard PA gels and to a lesser extent on hard fibrin gels, which are still much softer than the hardest PA gels. The pertange of total cells on soft PA gels (C) and fibrin gels (F) that were neurons was significantly higher that on hard gels. Red= β III tubulin, neurons; green= GFAP, astrocytes; blue=DAPI, nuclei. | 51 |
| Figure 31. SEM pictures of chick embryo neural cells on poly-lysine coated steps. A-C 4 μ m steps; D,E, 2 μ m deep, 7 μ m wide grooves. Arrow in C indicates the point of encounter of a growing process, the path of the growth cone having been deflected to the left. Bars: A,B, 40 μ m; C 10 μ m; D, E, 20 μ m. | 52 |
| Figure 32. Nano imprinting lithography and soft lithography patterning techniques. | 53 |

RESULTS**1. INDUCING FUNCTIONAL RADIAL GLIA-LIKE PROGENITORS FROM CORTICAL ASTROCYTE CULTURES USING MICROPATTERNED PMMA**

Figure 1: White light interferometer 3D images and profiles of 10 μm and 2 μm patterned PMMA. 73

Figure 2: Effect of PMMA and micropattern on glial cells morphology and orientation. A-F, Confocal images of actin staining (phalloidin, red) and nuclei (TO-PRO-3, blue). G, Graphic representing cell alignment by FTT-Oval profile measurement. Flat line indicates random distribution; peak at 90° indicates alignment parallel to the topography. H, SEM pictures of glial cells on NP and 2 μm lines PMMA. Scale bar A-F= 100 μm ; Scale bar H = 30 μm . ** indicates statistical significance respect to control $p \geq 0.001$. 74

Figure 3: Cellular composition of glial cultures. Confocal images of glial cells immunostained for different glial and progenitor markers: GFAP and BLBP for astroglia, Nestin for progenitors, and NG2 and A2B5 for different glia restricted progenitors. Nuclei are stained with TO-PRO-3 (blue). Scale bar = 50 μm . 76

Figure 4: Biochemical characterization of glial differentiation. A, Western Blots showing the expression of different progenitors and glial differentiation markers. B-D, Quantitative representation of the western blot densitometry (intensity values normalized to actin) grouped by categories: B, mature and reactive glial markers (GFAP, Vimentin and EAAT-2); C, progenitor glial markers (BLBP, Nestin and PH3); and D, neurogenic progenitor markers (Pax6 and Tbr2). E, Graph representing the percentage of immunoreactive cells for glial restricted progenitors markers (NG2 and A2B5) respect the total number of cells by unit area. Prog = progenitor; React = reactive glia; C = control (tissue culture plate); NP = no patterned PMMA; Ln10 = 10 μm line patterned PMMA; Ln2 = 2 μm line patterned PMMA. ** indicates statistical significance respect to control $p < 0.01$. 77

Figure 5: Graft from flow cytometry analysis showing the evolution of the total cell number and dead cell number on control and PMMA Ln2 during 4 days. * indicates statistical significance between control and PMMA Ln2, $p < 0.05$; # indicates statistical significance with respect to 1div in each substrate, # $p < 0.05$, ## $p < 0.01$ 80

Figure 6: Effect Role of pattern-induced RGLC in neural growth and axonal guidance. A, B, Images showing explants from E16 cerebral cortex cultured on glial cells grown on NP PMMA (A) or Ln2 PMMA (B). Cell nuclei are marked with TO-PRO-3 (blue) and neurons with Tuj-1 antibody (red). Frequency plots representing axonal outgrowth orientation on PMMA NP (C) and PMMA Ln2 (D) substrates. E-F, explants from E16 GFP mice cerebral 81

cortex seeded on top of on glia grown on PMMA ln2. E = bright field and F = GFP fluorescence. Neurons exiting from the explants are identified by GFP expression. Scale bars = 200µm (A, B); 100 µm (E, F).

Figure 7: Role of pattern- induced RGLC in neural migration. Representative time lapse images of E16 GFP neurons (green) seeded on glial cells grown on control (A) and ln2 PMMA (B) of glial cells (bright field). White arrows indicate the position of a representative neuronal body showing its stativity on control condition (A) and its migration on ln2 induced RGLC process (B). C-D, Frequency plot showing the distribution of the speed (µm/h) of migrating neurons (n=24) in control and ln2 PMMA conditions. E, Particle tracks showing neuronal trajectories in control and ln2 PMMA during a 3h record. F-G, GFP neurons (green) grown on WT glial cells stained with BLBP (red) after 5div in control (F) and ln2 PMMA (G) and their Z projections. H-I, neurons labeled with Tuj1 (green) grown on glial cells labeled with BLBP (red) in control (H) and ln2 PMMA (I) substrates. (J). Graph representing the Pearson's coefficient for neuron/glia co-localization in those cultures. $0 \leq R_r \leq 1$, where 1= max colocalization and 0= maximal exclusion. ** indicates statistical significance, $p < 0.01$. Scale bar = 100µm. Scale bars (A) =50µm; (B, F, G) =25µm; (E) =20µm; (H, I) 100 µm.

2. NEURAL CELL BEHAVIOUR *IN VITRO* AND *IN VIVO* ON FLAT AND MICRO PATTERNED CHITOSAN FILMS

Figure 1: A. Degradation of chitosan films and B.. White light interferometer 3D images of 10 µm and 2µm patterned chitosan. 101

Figure 2: Effect of chitosan on neuronal cultures composition and protein expression. **A.** Confocal images of neuronal cell cultures. Scale bar = 100µm; **B.** Western Blots showing the expression of different neuronal and glial markers. **C-D.** Quantitative representation of the western blot densitometry (intensity values normalized to actin) of neuronal markers (C) and glial markers (D). Tuj1 is a marker for post mitotic neurons, Pax6 for neural progenitors, GFAP and BLBP for astroglial cells. * $p < 0.05$ and ** $p < 0.01$. 102

Figure 3: Neurons alignment on micropatterned chitosan films. **A.** Confocal images of Tuj1 and MAP2 (dendrites) stainings. The bottom right picture is a visual example of how axonal staining was obtained for alignment quantification (Tuj1-MAP2). Scale bar = 50 µm and 15 µm; **B.-C.** Graphic representation of **B.** axons and **C.** dendrite alignment by FTT-Oval profile measurement. Flat line indicates random distribution; peak at 90o indicates alignment parallel to the topography. ** indicates statistical significance respect to control $p \geq 0.01$. 104

Figure 4: Effect of serum concentration on chitosan adhesion. **A.** Cell attachment after 2h at different serum concentration. **B.** Confocal pictures of glial cells on chitosan and control after 5div in presence of 3% or 10% NHS. Cell are stained for actin (phalloidin, red) **C.** Cell count after 5div in 106

presence of 3% or 10% NHS. Scale bar = 200 μ m.

Figure 5: Effect of flat and patterned chitosan on glial cells culture composition and protein expression. **A.** Confocal images of glial cells immunostained for different glial and progenitor markers. Nuclei are stained with TO-PRO-3 (blue). Scale bar = 50 μ m; **B.** Western Blots showing the expression of glial differentiation markers; **C.** Quantitative representation of the western blot densitometry (intensity values normalized to actin). GFAP and BLBP are markers for astroglia, Nestin for progenitors. * $p < 0.05$ and ** $p < 0.01$. 108

Figure 6: Glial cell alignment on micropatterned chitosan films. **A.** Confocal images of glial cells on control, no patterned chitosan (Ch NP) and In2 patterned chitosan (Ch In2). Cell are stained for actin (phalloidin, red). Scale bar = 200 μ m and 15 μ m; **B.** Graphic representing cell alignment by FTT-Oval profile measurement. Flat line indicates random distribution; peak at 90o indicates alignment parallel to the topography. μ m; ** indicates statistical significance respect to control $p \geq 0.01$. 109

Figure 7: Confocal images of neurons cultured on top of pre-seeded glial cells on control, no patterned (NP), In10 and In2 patterned chitosan. Neurons are stained with Tuj1 (red) and glial cells with BLBP (green). 110

Figure 8: Response to chitosan implants in brain cortex after 21 days in vivo. Confocal images of imunohistochemistry performed on brain cortex section of mice that received a chitosan film or only an injury (control). **A.** Astroglial markers (GFAP: activated astrocytes; BLBP: astroglial cells; NG2: oligodendrocytes); **B.** Neuronal markers for parvalbumina (PV), macrophage and microglial markers F4/80 and extracellular matrix marker laminin (LN). Chitosan is delimited by discontinuos line, while injury site in control condition is indicated by *. All the pictures are oriented with meninges on the bottom. Scale bar = 50 μ m. 112

3. EFFECT OF MODEL SURFACES ON GLIAL ADHESION AND DIFFERENTIATION

Figure 1. Glial cell attachment on model surfaces with increasing hydrophobicity after 5h and 5 DIV and the respective percentage of cell survival. Significant difference ** $p \leq 0.01$ respect to Glass. 129

Figure 2. Glial cell morphology and morpholmetric parameters after 5 h on model surfaces with increasing hydrophobicity. **A.** Confocal pictures for actin staining. Scale bar = 40 μ m. **B.** Glial cells area (pixels) and cell circularity. Circularity index values range from 0 to 1, where 0 = linear shape and 1= circular shape. * $p \leq 0.05$ and ** $p \leq 0.01$ respect to Glass. 131

Figure 3. Cellular composition of glial cultures. Confocal images of glial cells immunostained for GFAP (astroglia) and Nestin (progenitors). Nuclei are 132

stained with TO-PRO-3 (blue). Scale bar = 100µm.

Tables

page nº

INTRODUCTION

3. BIOMATERIALS IN CNS TISSUE ENGINEERING

Table 1. Biomaterials used in CNS tissue engineering. 42

RESULTS

2. NEURAL CELL BEHAVIOUR *IN VITRO* AND *IN VIVO* ON FLAT AND MICRO PATTERNED CHITOSAN FILMS

Table 1. Surface and mechanical properties of chitosan films and control glass (uncoated and Lysin coated). 101

3. EFFECT OF MODEL SURFACES ON GLIAL ADHESION AND DIFFERENTIATION

Table 1. Values of water contact angle of model surfaces. Values of OH and CH₃ are from (Coelho et al. 2010), while values of COOH and NH₂ are from (Coelho et al. 2011) 126

Abbreviation list

aIPC: astrocytes progenitor cell
APCs: astrocyte precursor cells
BLBP: brain lipidic binding protein
Bmi1: polycomb transcription factor
CNS: central nervous system
CA: contact angle
CP: cortical plate
CSPGs: chondroitin sulphate proteoglycans
Cx: cerebral cortex
dBAMPc: dibutyryl cyclic adenosine monophosphate
DIV: days *in vitro*
DMEM: dulbecco's modified eagle medium
DMSO: dimethylsulfoxide
DRG: dorsal root ganglions
EA: ethyl acrylate
EAAT2: glutamate transporter expressed on astrocyte (GLT-1)
ECL: electrogenerated chemiluminescence
ECM: extracellular matrix
EGF: endothelial growth factor
EM: experimental medium
ePTFE: expanded poly(tetrafluoroethylene), Gore-Tex
FCS: fetal calf serum
FDA: food and drug administration
FGF-2: fibroblast growth factor 2
G5: supplement
GE: ganglionar eminence
GFAP: glial fibrillary acidic protein
GFP: green fluorescent protein
GLAST: glutamate transporter (EEAT1)
GM: growing medium
GRP: glial restricted precursors
HEA: hydroxyethyl acrylate
ICC: imunocytochemistry
IPC: intermediate progenitor cell
IZ: intermediate zone
Ki67: cellular marker for proliferation
Ln: line
LN: laminin
Lys: poly-D-lysine
MAG: myelin-associated glycoprotein
MAI: myelin associates inhibitors
MBP: myelin basic protein
MOG: myelin oligodendrocyte glycoprotein

MZ: marginal zone
NB: neurobasal medium
NE: neuroepithelium
Nestin: type VI intermediate filament (IF) protein
NG2: “neuron-glia” type 2 astrocytes, polydendrocytes
NHS: normal horse serum
NIL: nano imprinting lithography
nIPC: neurogenic progenitor cell
Nogo-A: inhibitor of neurite outgrowth specific to the central nervous system
NP: no patterned
NPC: neural progenitor cells
NRG: neuregulina
O2A: oligodendrocyte and type-2 astrocyte precursors (**OPC**)
OEC: olfactory bulb ensheathing cells
oIPC: oligodendrocytic progenitor cell
PAGE: polyacrylamide gel electrophoresis
PBS: phosphate buffered saline
PCL: poly caprolactone
PFA: paraformaldehyde
PI: propidium iodide
PLA: polylactic acid
PMMA: polymethylmethacrilate
PNS: peripheral nervous system
PP: preplate
PV: parvalbumina
RG: radial glia
RGC: radial glia cells
RGLC: radial glia like-cells
SAMs: self assembling monolayers
SCI: spinal cord injury
SDS: sodium dodecyl sulfate
SEM: scanning electron microscopy
SP: subplate
SVZ: subventricular zone
TBI: traumatic brain injury
Tg: glass transition temperature
Tuj-1: β III Tubulin
Vimentin: intermediate filament protein
VSI: vertical scanning interferometry
VZ: ventricular zone
WT: wild type

Abstract

After a lesion in the CNS, glial cells play a fundamental role, being the mediators of both the inhibitory and the beneficial response for neural regeneration. The tissue engineering approach consists in the use of biomaterials to help the regeneration and guide the regenerative capable cells to create a permissive environment. The main working hypothesis of this thesis is that we can promote a favourable environment for CNS regeneration identifying material properties which can modulate neuronal cells behaviour.

In a first place we analyzed glial and neuronal response to two very different biopolymers, PMMA and chitosan. Wettability, surface and mechanical properties were characterized for both materials. Then line pattern of different dimensions in the micrometrical range were introduced. The response of glial cell and neurons were analyzed in terms of cell adhesion, morphology and differentiation state.

Finally, we studied the behaviour of glial cells on glass model surfaces functionalized by self assembling monolayers with different wettability (OH, COOH, NH₂, CH₃), in order to identify the specific role that wettability plays in determining cell response.

The dates suggest that the adhesion, the morphology and the differentiation state of neuron and glial cells can be controlled by choosing the proper combination of material properties and physical patterns. Overall, line patterns resulted to be a suitable tool to use in biomaterial design for nerve regeneration. However, the performance of each material must be analyzed with attention, since the combination of material properties, which most of the time is not predictable, play important roles in the biological activity.

INTRODUCTION

This chapter aims to give the background to this thesis work.

- The first section, describe the central nervous system (CNS) and cerebral cortex organization, as well as their cellular composition and the developmental origin;
- The second section approaches the consequences of injury. Overall consequences and cellular event are described and endogenous potentials of regeneration are reported;
- The third part talks about the tissue engineering approach to treat injury in the CNS and the recent advances in the field of material science.

The cost of complexity.

“Evolutionarily speaking, it is tempting to wonder why more advanced vertebrate species would lose the ability to regenerate after CNS injury. In feral animals, selection pressure has little or no role in favouring CNS regenerative capability. The types of injury that would damage the CNS would almost certainly lead to rapid demise in the wild before regeneration could take place. Therefore, the more likely evolutionary explanation for the 'loss' of CNS regenerative capacity is that this is an unselected by-product of gaining the increasingly complex nervous systems that selection pressures have favoured over time.”

Noam Harel
(Harel and Strittmatter 2006)

“The chief function of the body is to carry the brain around.”
Thomas A. Edison

1. THE CENTRAL NERVOUS SYSTEM

1.1 Central nervous system (CNS)

The CNS consists in the brain and the spinal cord. The spinal cord transmits information from the brain to the peripheral nervous system and back. The brain receives sensory information from the spinal cord and from cranial nerves (optical, auditory and olfactory nerves), processes all the inputs and coordinates the appropriate responses.

Brain and spinal cord are covered by three layers of connective tissue: the dura mater, the arachnoid mater, and the pia mater, collectively referred to as the meninges. The subarachnoid space, between the arachnoid and pia mater, is filled with cerebrospinal fluid (**Fig. 1**).

Central nervous system (CNS)

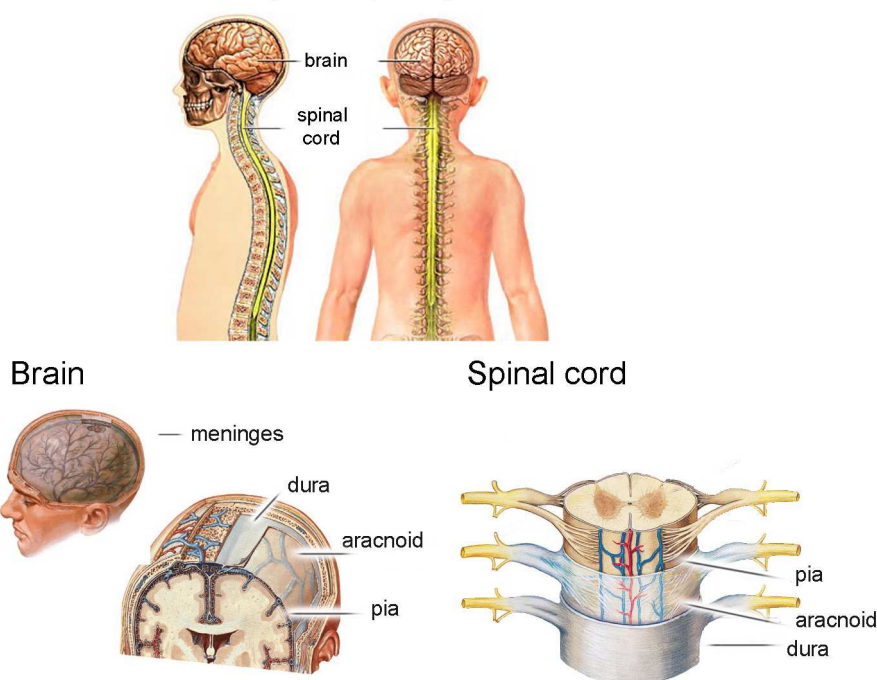


Figure 1. Central nervous system: brain, spinal cord and meninges. Adapted from www.nlm.nih.gov/medlineplus.

CNS tissue consists in white matter and grey matter. Grey matter is formed mainly by neuron cell bodies and unmyelinated fibers, while white matter is formed predominantly by myelinated axonal tracts. In mammalian brains, grey matter is at the outer surface and white matter at the inner part, while in spinal cord the pattern is reversed (**Fig. 2**) (Schmidt and Leach 2003; Gumera, Rauck et al. 2011).

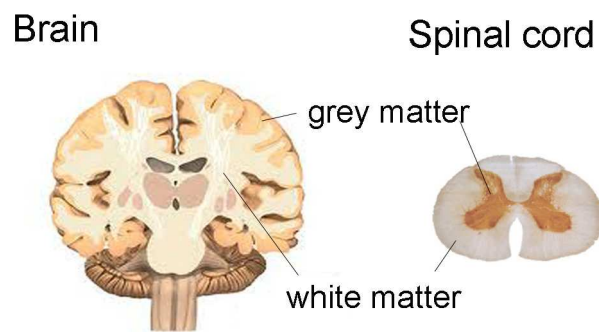


Figure 2. White matter and grey matter in brain and spinal cord. Adapted from www.nlm.nih.gov/medlineplus.

1.2 Cerebral cortex

The cerebral cortex is the outer part of the cerebrum of mammals. In human, it is extremely developed and it is the responsible of the highest motor functions, such as talking, writing, dancing, memory and perceptual awareness. It has a stratified cytoarchitecture that vary among different areas. Based on a phylogenetic classification, the cerebral cortex can be divided into three areas, named archicortex, paleocortex and neocortex (**Fig. 3**). In the **Figure 3** human and mouse cerebral cortex are shown, since mouse model is used in this thesis work.

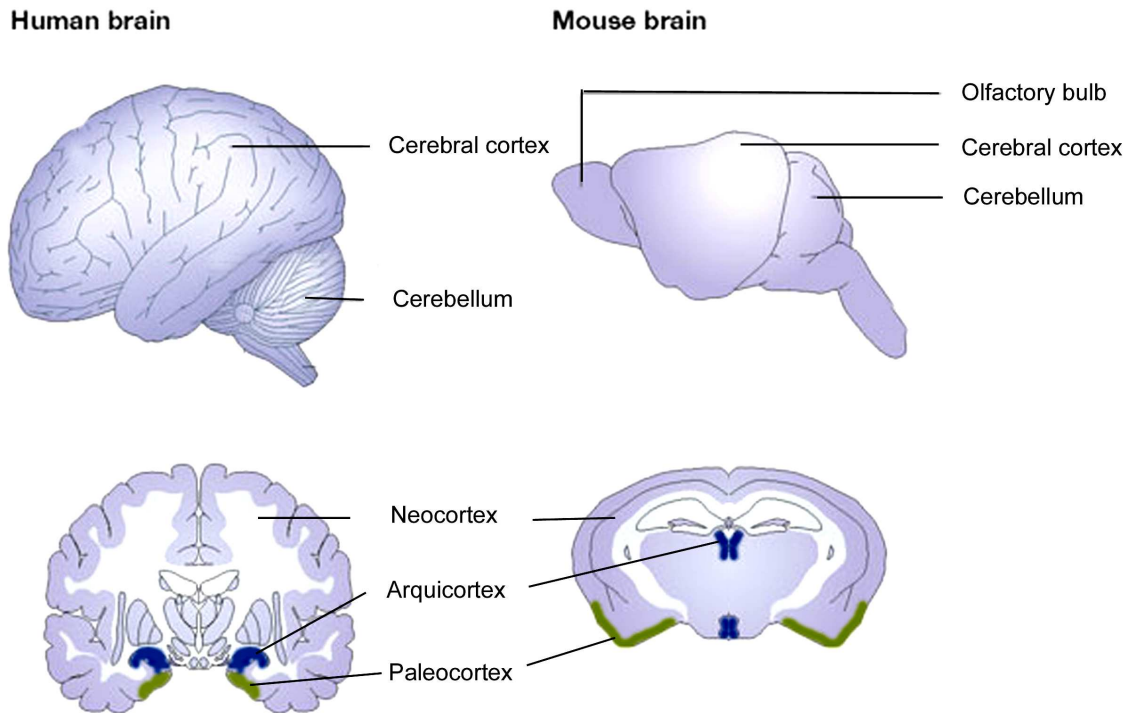


Figure 3. Human and mouse cerebral cortex. Top: lateral view; bottom: coronal sections. Adapted from (Cryan and Holmes 2005) and <http://www.med.ufro.cl>

The neocortex, phylogenetically the most recent part, consists of six horizontal neuronal layers which have different thickness and neuronal composition depending on the cortical region. Neurons from different layers connect vertically forming functional units, called columns (**Fig. 4**) (Oberlaender, de Kock et al. 2011). Neurons send and receive connections with subcortical areas, however most of the connections are between neurons into the cerebral cortex (Valverde 2002) (Kandel 2000).

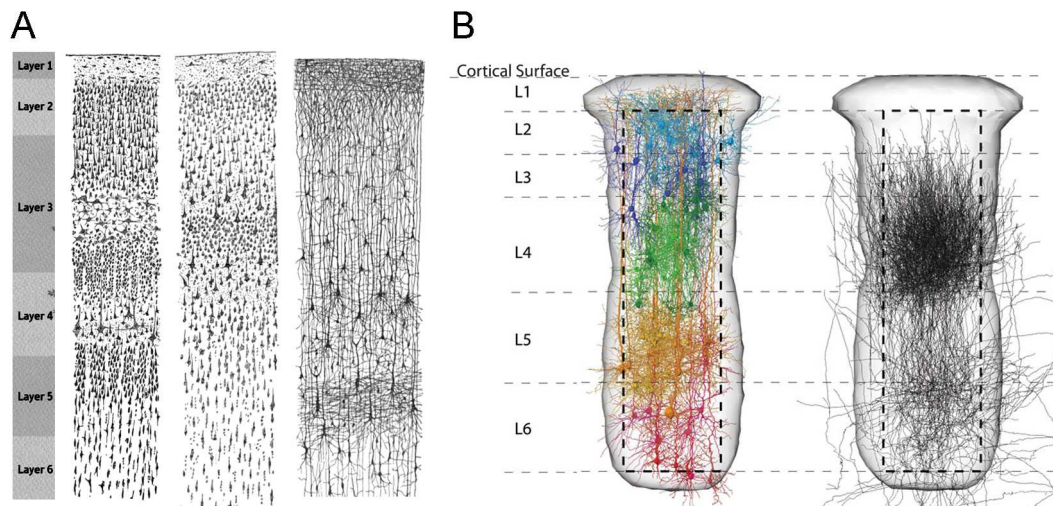


Figure 4. **A.** Representation of cortical layers by Ramon and Cajal and **B.** cortical columnar functional units. Left: 3D reconstructions of the dendrites from these nerve cells; right: 3D reconstruction of axons that yield input to the neural networks within a cortical column. (Oberlaender, de Kock et al. 2011).

1.3 Composition of adult cerebral cortex: neurons

1.3.1 General characteristics of neurons

Neurons are the basic functional cells of the nervous system. They are highly polarized cells that transmit impulses through out the nervous system. They consist of a cell body, also called soma, axon and dendrites. Axons are the longest projection and are responsible for conducting electrical impulses from the soma, while dendrites are branched projections which receive electrical impulses towards the soma. Neurons create neural networks through the formation of contacts between axons and dendrites, called synapses.

Neuronal membranes exhibit a voltage difference known as membrane potential, which gives them the ability to depolarize and propagate action potential. At synaptic junctions, the action potential causes the release of neurotransmitters, a family of biomolecules with various chemical natures. Neurotransmitters activate one or more types of receptor in the post synaptic button. This cause several functions, like the firing or the inhibition of action potentials (Stocum 2008).

1.3.2 Pyramidal neurons and interneurons

In the cerebral cortex two types of neurons can be differentiated: pyramidal neurons and interneurons (**Fig. 5**). Pyramidal neurons represent almost 80% of neurons, and they are named also glutamatergic neurons, due to the fact that their axons release glutamate as a neurotransmitter in the synapses, exerting excitatory action. They send axons to other areas of the cortex and to distant parts of the brain. They display triangular shape cell bodies with apical, oblique and basal dendrites and a single axonal arborisation (**Fig. 5A**) (Valverde 2002).

Interneurons are known also as GABAergic neurons, since they use gamma aminobutyric acid (GABA) as neurotransmitter. GABAergic inhibitory Interneurons make only local connections and they have inhibitory action. By contrast with pyramidal neurons, GABAergic interneurons are extensively heterogeneous. They differ by their axonal and dendritic morphologies, biochemical markers, as well as connectivity and physiology (**Fig. 5B**) (Vitalis and Rossier 2011). They express different patterns of calcium-binding proteins, like parvalbumin (PV), calbindin (CB), and calretinin (CR). The content of those proteins is strictly related to the type of fired action-potential (Schwark and Li 2000). With the exception of neural stem cells and a few other types of neurons, neurons do not undergo cell division (Nowakowski 2006).

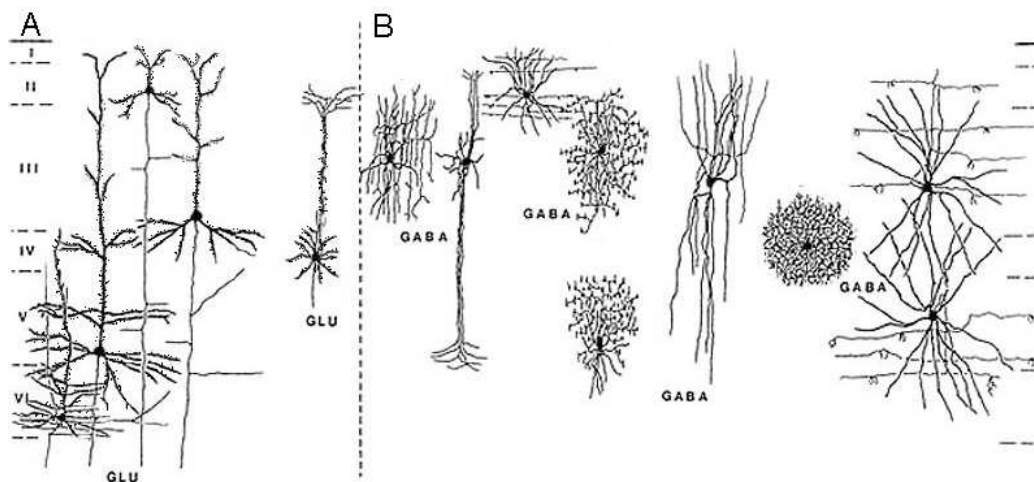


Figure 5. Basic cell type in cerebral cortex of monkey. **A.** glutamatergic neuron (pyramidal cells and stellate cells) and **B.** GABAergic neuron. Adapted from <http://webvision.med.utah.edu>.

1.4.1 General characteristics of glial cells

The term “glia,” derives from the Greek word for “glue”, which highlights the property of brain support and, more particularly, the support of neurons (Rock, Gekker et al. 2004). Glial cells are the most abundant type in mammalian brain, they are highly heterogeneous and they cover several and diverse important functions. Glial cells surround and ensheat neuronal cell bodies, axons and synapses throughout the nervous system. They serve as physical and trophic support for neurons, since they are the main secretors of ECM molecules and the responsible of providing nutrients from blood vessels. Glial cells help the neural transmission, one side forming myelin sheets around axons and on the other side regulating the ion and neurotransmitter concentration at the synaptic junctions. Glial cells are able to remove and secrete several substances, included neurotransmitters and neurotropic factors. They are key players in the repair and scarring process of the brain and spinal cord following traumatic injuries. Glial cells also constitute the immunity of nervous system, that is different form the rest of the body (Vaccarino, Fagel et al. 2007; Barres 2008).

1.4.2 Glial cells types

Glial cells comprehend **microglia** and **macroglia**, which is composed basically by *astrocytes*, *oligodendrocytes* and *polydenrocytes* (Fig. 6).

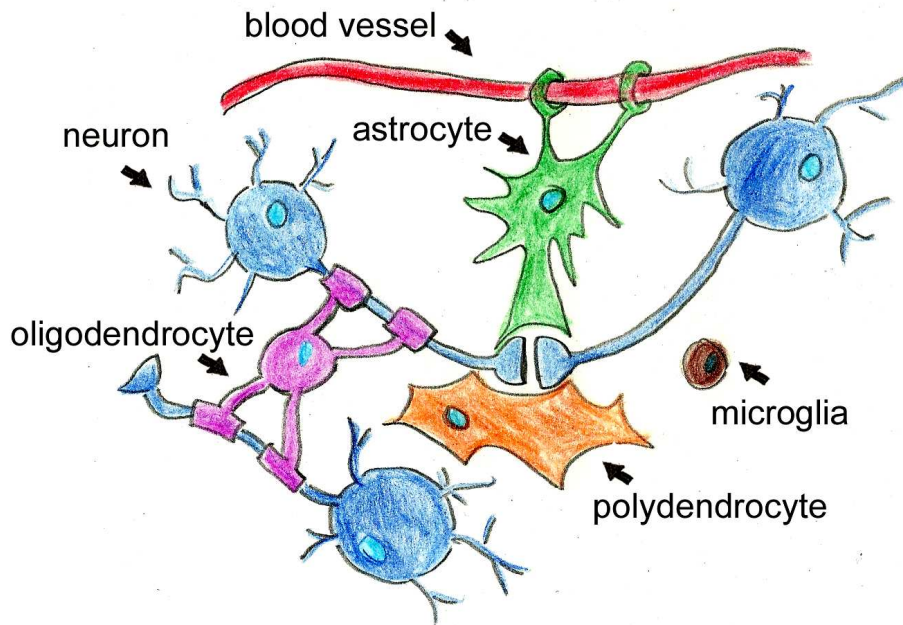


Figure 6. Glial cell types. Adapted from (Allen and Barres 2009).

Microglia

Microglia are the resident macrophages of the brain and spinal cord. They protect the brain from damage and infection, engulfing dead cells and debris. After an injury they activate and help the re-growth of neural tissue by synaptic remodeling, secretion of anti-inflammatory cytokines and recruitment of neurons and astrocytes to the damaged area. They are immunoreactive for F4/80, a specific macrophage glycosylated glycoprotein and for Iba1, a calcium binding protein that is upregulated in activated macrophages and microglia (Saura 2007; Allen and Barres 2009).

Oligodendrocytes

Oligodendrocytes produce a lipid-rich membrane called myelin, which enwraps axons, thereby speeding up the conduction of electrical impulses. They are essential for rapid electrical communication between neurons and their targets. Myelin is constituted of extensions of oligodendrocyte plasma membranes containing approximately 70% lipids

and 30% proteins. Proteins found in myelin include myelin basic protein (MBP), myelin oligodendrocyte glycoprotein (MOG) and myelin-associated glycoprotein (MAG) (Saura 2007; Allen and Barres 2009).

Astrocytes

Astrocytes are the major macroglial cell types in the adult brain. Astrocytes were already described by Santiago Ramon y Cajal at the beginning of the 20th century as a star shaped glia that acts maintaining the homeostasis in the brain. They are uniformly distributed along the adult CNS parenchyma surface, where they exert distinct functions such as the formation of a basal lamina around blood vessels and meninges, the regulation of extracellular ions concentration, modification of synaptic efficacy, inactivation of neurotransmitters like glutamate, induction and maintenance of the blood-brain barrier, and providing nutrients and trophic support for neurons and oligodendrocytes. (Stocum 2006).

The principal general characteristics that define mature astrocytes are a stellate or spread morphology and a high expression of intermediate filaments composed of glial fibrillary acidic protein (GFAP) (Vacarino, Fagel et al. 2007). However, astrocytes comprise a heterogeneous population of cells with diverse morphological features, functions and protein expression, varying widely with their developmental state, distribution in the CNS and pathological conditions (reviewed in (Bachoo, Kim et al. 2004; White and Jakeman 2008). For this reason, attempts to classify astrocytes have been made since their discovery.

For instance in 1984 Martin Raff and colleagues distinguish between Type 1 and Type 2 astrocytes, based on lineage and antigenic features of *in vitro* cultures (Miller and Raff 1984). Type 1 Astrocytes are described as cells with a flat polygonal morphology that appear early during development, while Type 2 Astrocytes have a stellate morphology (Nishiyama, Komitova et al. 2009).

Another common classification based on morphology and location *in vivo*, distinguishes between protoplasmic and fibrous astrocytes (**Fig.7**). Protoplasmic astrocytes are found in the grey matter, intimately associated with neuronal cell

bodies and synapses; they have many branching processes whose end-feet envelop synapses, while fibrous astrocytes have fewer, thinner and longer processes than protoplasmic astrocytes and are found in the white matter, associated with neuronal axons (Allen and Barres 2009).

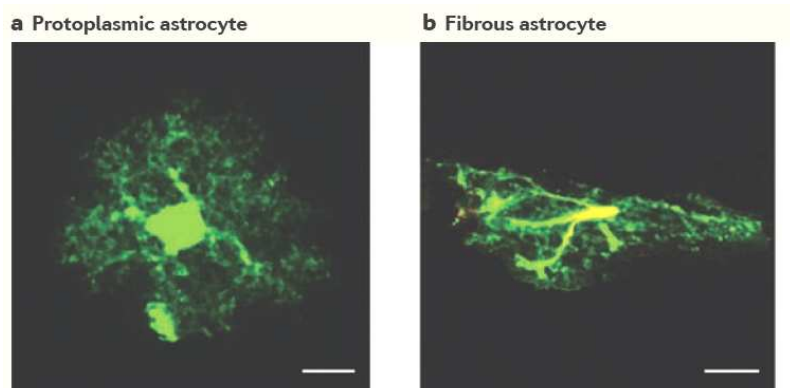


Figure 7. Example of protoplasmic astrocytes (a) and fibrous astrocytes (b). Gray matter protoplasmic astrocytes have highly branched fine processes, while white matter fibrous astrocytes, have thicker and less branched processes (Robel, Berninger et al. 2011).

In addition to the described type of astrocytes, modifications of glial cells with specific functions exist in specific parts of the brain. For instance, lining the ventricular system we can find ependymal cells, while in cerebellum and in the olfactory bulb we can find respectively Bergmann glia and olfactory ensheathing glial cells. The knowledge about astrocytes and therefore their classification continues to expand with the discovery of molecular markers that can be used to follow cell lineages *in vitro* and *in vivo*.

Polydendrocytes

Polydendrocytes are a particular kind of glial cells that have been described in the last decade. They are known for their highly ramified morphology and their immunoreactivity for the NG2 proteoglycan. They are found through all the grey matter and white matter and they have intermediate characteristics between neurons (N) and glia (G), from which it comes the name “NG”. They are able to receive synaptic signals since they possess Na^+ and K^+ voltage sensitive channels, thus it is thought that they form an active part of neural networks. In adults they are a source of oligodendrocytes, and play key roles in re-myelinating axons after injuries (Nishiyama, Komitova et al. 2009; Richardson, Young et al. 2011).

1.5 Composition of adult cerebral cortex: the extracellular matrix (ECM)

About 20% of the total brain volume is occupied by extracellular matrix (ECM). ECM helps the functional organization of the CNS structure. ECM plays important roles in synapses formation and stabilization, in the neurogenic niche, and in astrocytic endfeet. In more details, it rules the compartmentalization of diffusible molecules, ion channels and transporters. ECM consists in chondroitin sulfate proteoglycans (CSPGs), tenascins, link proteins, and hyaluronan. The majority of the CSPGs belongs to the lectican family that includes brevican, neurocan, aggrecan, and versican (Dours-Zimmermann, Maurer et al. 2009). CSPGs are the main components of perineuronal networks associated with mature neurons, a basal lamina-like ECM that is localized at the blood– brain barrier and in neurogenic niches. ECM plays important roles during development and after injury, determining pathways for neuronal and glial location and differentiation. Additionally, the ECM modulates the mechanical properties of the CNS, which in general is very soft (Dityatev, Seidenbecher et al. 2010; Gumerá, Rauck et al. 2011).

1.6 Cerebral cortex development

Most of the regenerative processes somehow try to recapitulate embryonic development. For this reason, in this thesis we report an overview of the most important CNS developmental steps and the main classes of progenitor cells.

1.6.1 Anatomic overview

The CNS develops from the most anterior part of the neural plate, a specialized part of the embryonic ectoderm. The neural plate folds and closes to form the neural tube. From the cavity inside the neural tube develops the ventricular system, and, from the epithelial cells of its walls, the neurons and glia of the nervous system. The telencephalon, which is the most frontal part of the neural tube, gives rise to the cerebral hemispheres and cortex (**Fig. 8**). (Noctor, Flint et al. 2001)

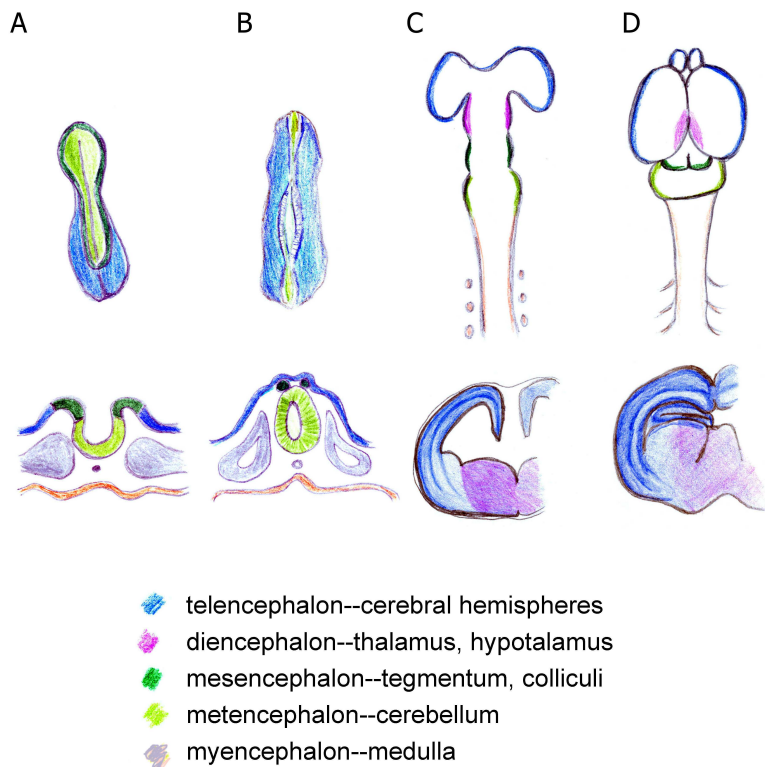


Figure 8. Development of central nervous system.

1.6.2 Cell events overview

Based on the review of Kriegstein and Alvarez-Buylla (Kriegstein and Alvarez-Buylla 2009), cerebral cortex development can be simplified in four steps (Fig. 9).

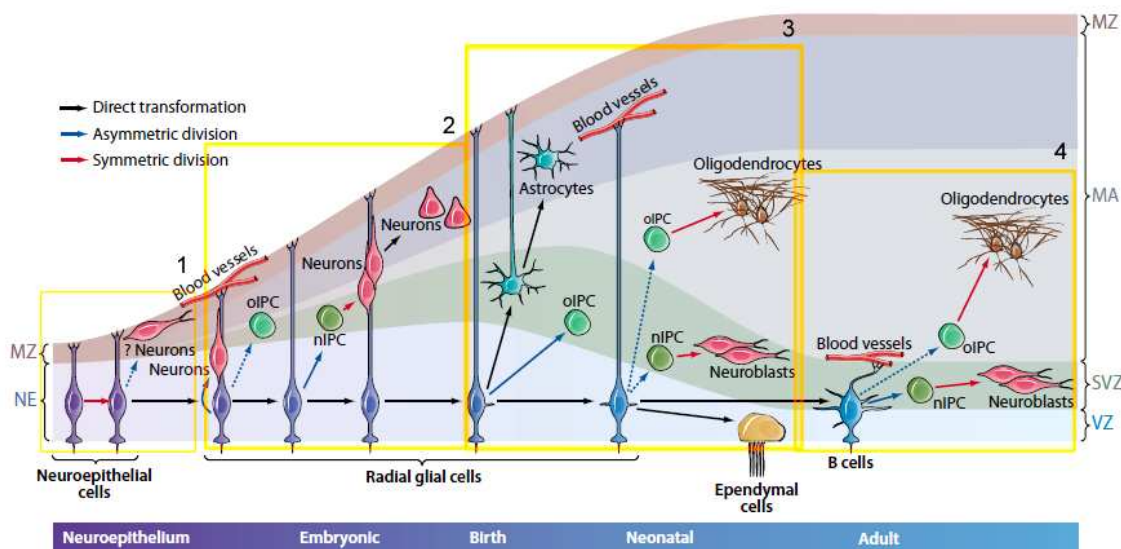
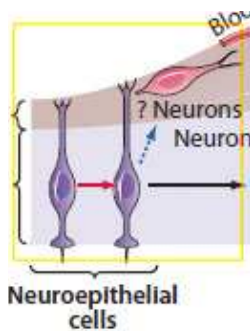


Figure 9. Main cellular events in cerebral cortex development in a temporal overview. Solid arrows are supported by experimental evidence; dashed arrows are hypothetical. Colors depict symmetric, asymmetric, or direct transformation. IPC, intermediate progenitor cell; MA, mantle; MZ, marginal zone; NE, neuroepithelium; nIPC, neurogenic progenitor cell; oIPC, oligodendrocytic progenitor cell; RG, radial glia; SVZ, subventricular zone; VZ, ventricular zone. (Kriegstein and Alvarez-Buylla 2009).

1.6.3. Step 1: Early development



At the early stage of development, proliferating progenitors in the ventral neuroepithelium of the neural tube are known as **neuroepithelial** cells. Neuroepithelial cells are highly polarized along their apical–basal axis (**Fig. 10**). Neuroepithelial cells divide symmetrically to generate more neuroepithelial cells and some likely generate early neurons. (Rao 1999; Kriegstein and Alvarez-Buylla 2009).

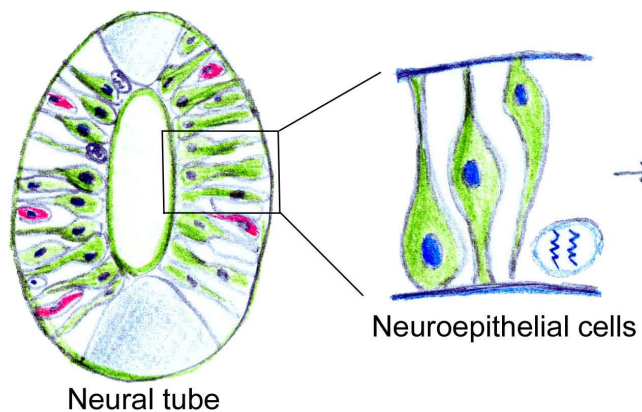
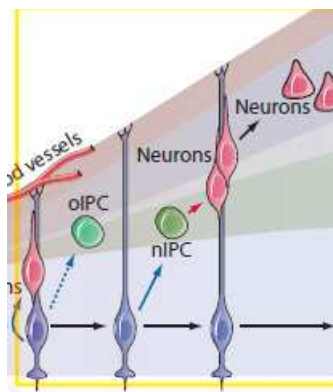


Figure 10. Neuroepithelial cells in the neural tube.

1.6.4. Step 2: Neurogenesis



Around E10 in the mouse neurogenesis begins and the brain cortex starts to expand and become thicker. Neuroepithelial cells transform into radial glia cells (RGC). RGC maintain the radial orientation spanning the thickness of the cerebral cortex, from the ventricular zone (VZ) to the outer pial surface. RGC maintain their proliferating cell bodies in the ventricular zone (VZ).

RGC divide symmetrically to maintain the pool of proliferative progenitors, and asymmetrically to generate neurons and some early NG2⁺ oligodendrocytes precursor cells (oIPC) (Richardson, Young et al. 2011). RGC generate neurons directly or indirectly through intermediate progenitor cells (nIPCs). IPCs can be distinguished from RGC by their position, morphology and by the expression of characteristic transcription

factors. Englund and collaborators clearly described the sequential expression pattern in the cerebral cortex of Pax6→Tbr2→Tbr1 transcription factors during the differentiation of Pax6+ RGC to Tbr2+ IPC and the resulting newborn Tbr1+ neuron (Fig. 11)(Englund, Fink et al. 2005).

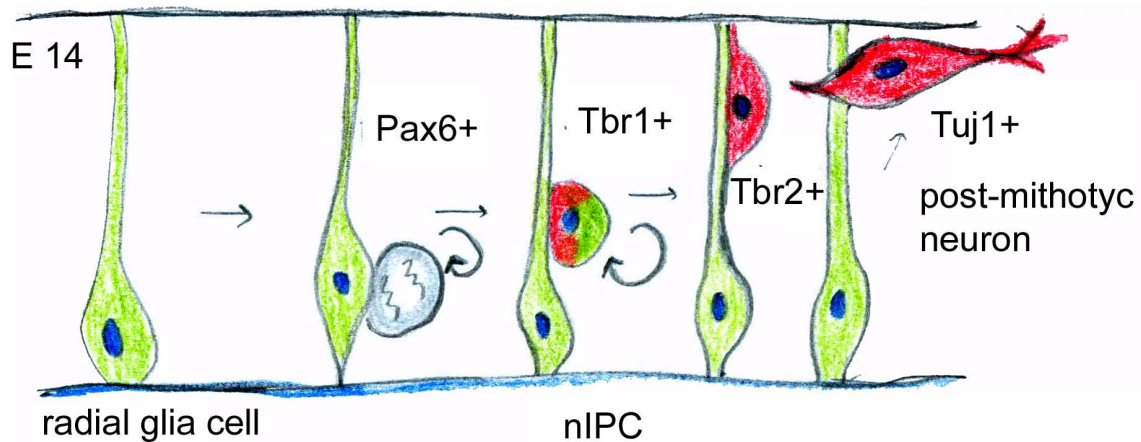


Figure 11. Neurogenic radial glia (Englund, Fink et al. 2005).

As the progeny from RGC and IPCs move into the mantle for differentiation, the neuroepithelium becomes a multi-cell-layered tissue, where the newly formed neurons find their final position. RGC function as a scaffold providing a framework for the migration of newborn neurons from the ventricular and subventricular zones to their final position in the developing brain. This process is known as radial migration.

Radial migration and layer formation

Radial migration is crucial during neurogenesis, which in mouse occurs from embryonic day (E) 11.5 to E17.5. Neurons organize in 6 layers in an inside-out model, where the earliest born neurons generated in the VZ migrate radially, constituting the deeper layers, while later neuronal cohorts pass the previously formed neurons and settle within upper most layers (Molyneaux, Arlotta et al. 2007).

The first wave of cortical neurons accumulates on the top of the VZ giving rise to the preplate (PP). Subsequent generated neurons invade the PP forming the cortical plate (CP) and dividing the PP in two different regions separated by the CP: the marginal zone (MZ), or layer I, just beneath pial surface, and a deeper zone composed by the

subplate (SP) neurons and incoming axons of the intermediate zone (IZ). As neurogenesis proceeds, an additional proliferative region known as the subventricular zone (SVZ), is formed above the VZ. Next newly born neurons from VZ and SVZ will generate the layers VI, V and IV according to a very organized program, shaping the final 6-layers cortex (**Fig. 12**) (Meyer, Schaaps et al. 2000) (Molyneaux, Arlotta et al. 2007).

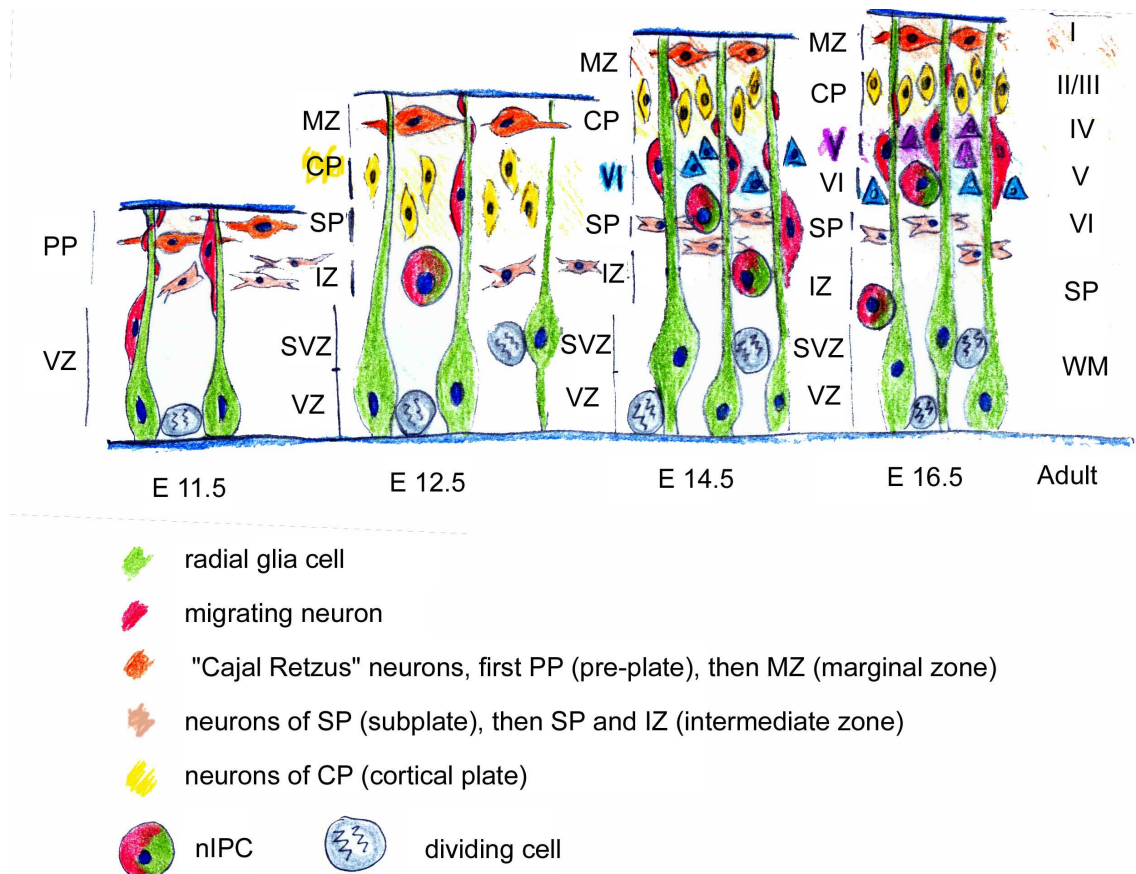


Figure 12. Radial migration and formation of cerebral cortex layer.

Cajal Retzius neurons and RGC direct the stages of radial migration communicating where and when a neuron may stop, detach or differentiate. To do that, they provide surface and extracellular matrix signals. RGC express surface adhesive molecules that can be recognized by neuronal integrins. The most common and studied one is laminin.

RGC influence neuronal migration, but this is not a one-way relationship. Indeed, neurons also communicate with glial cells regulating their differentiation state. For

instace, neurons produce neuregulin (NRG), that through erbB receptor signaling induce astrocytes to extend a process along which neurons can migrate (Schmid, McGrath et al. 2003). Moreover, neuronal contact also induces expression of the radial glia brain lipid binding protein (BLBP). Thus, cell-cell contacts are key event in the formation and maintenance of radial glia.

Tangential migration

Tangential migration is referred to the non radial mode of neuronal translocation that does not require the direct contact with RGC. Tangential migration is characteristic of GABAergic interneurons, which are generated in the ganglionic eminence (GE) (Fig.13). During development, interneurons reach the cerebral cortex migrating dorsally and following different chemical cues. Once they enter in the cerebral cortex, they reach their final position moving ventrally or dorsally following RGC (Anderson, Marin et al. 2001; Marin and Rubenstein 2001; Metin, Baudoin et al. 2006).

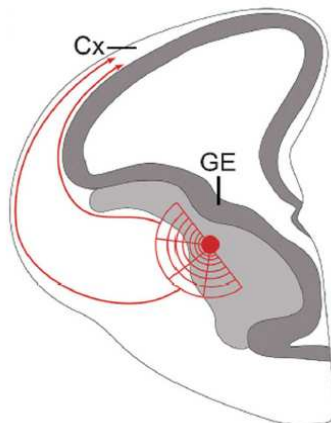
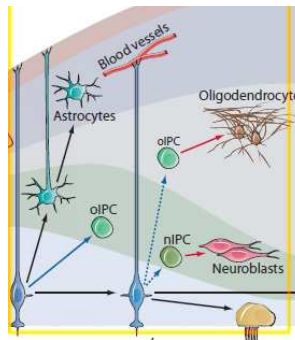


Figure 13. Tangential migration. GABAergic interneurons originate in the ganglionic eminence (GE) and migrate tangentially into the cerebral cortex (Cx). Adapted from (Metin, Baudoin et al. 2006).

1.6.5. Step 3: Gliogenesis



At the end of neurogenesis, around E18-19 in mouse, RGC lose their ventricular attachment and migrate toward the cortical plate by a process of somal translocation. RGC morphology changes from bipolar to unipolar, that subsequently become multipolar and progressively takes on astrocyte or oligodendrocyte morphology. Most RGC transform into astrocytes, and this event is coincident with the disappearance of RGC. A subpopulation of RGC retains apical contact and continues functioning as NSCs in the neonate. These neonatal RG continue to generate neurons and oligodendrocytes, while some convert into ependymal cells (Kriegstein and Alvarez-Buylla 2009).

Glial intermediate progenitors

In the last years it has become clear that multipotent RGC do not generate fully differentiated cells directly, rather they generate intermediate precursors that undergo progressive maturation to give rise to postmitotic mature cells. However, some individual RGC that produces neurons can transform into an astroglial cell, thus switching from a neurogenic to a gliogenic profile *in situ* (Noctor, Martinez-Cerdeno et al. 2008).

The identification and definition of intermediate progenitors is a hard and confusing task. In the literature they have several names, due to the fact that experiments have been performed either *in vitro* or *in vivo*, using different animal models and observing different parts of the CNS (brain cortex, spinal cord, optic nerve etc). However, here we report some classification attempts made by experts in the field.

Kriegstein and A. Alvarez-Buylla name intermediate progenitor cells “IPC”. IPC can be neuron, astrocyte or oligodendrocyte committed (nIPC, aIPC and oIPC respectively), according to time and location during development. Into the aIPC and oIPC cell lineage group, we can differentiate, according to the classifications by Rowitch et al and Liu and Rao et al. (**Fig. 14**) (Rowitch, Lu et al. 2002; Liu and Rao 2004):

- glial restricted precursors (**GRPs**),
- oligodendrocyte and type-2 astrocyte precursors (**O2A** cells), also known as oligodendrocytes precursors cells (**OPC**) or **polydendrocytes** or **synantocytes**
- astrocyte precursor cells (**APCs**)

Other progenitors also have been identified, like motoneuron-oligodendrocyte precursors (MNOPs) and white matter progenitors (WMPCs)(Liu and Rao 2004).

GRP

Glial restricted precursors (GRPs) were observed early in the development (E12-E14) and can be distinguished from neuroepithelial cells by the acquisition of A2B5 immunoreactivity. They are nestin+, and they differ from O2-A for being NG2- (Rao and Mayer-Proschel 1997; Liu and Rao 2004). Those prgenitors are the earliest glial precursors not neurogenic and are able to give rise to type 1 astrocytes, oligodendrocytes and, under appropriate conditions, type 2 astrocytes. Thus, neuroepithelial cells generate GRPs that subsequently differentiate into even more restricted glial precursors, the O2A cells and APC cells.

O2A or OPC:

The main characteristic of this kind of progenitors is NG2 imunoreactivity. Apart from this, OPC cells are also A2B5+ , and they are committed progenitor cell that mainly generates oligodendrocytes (Nishiyama, Komitova et al. 2009).

The relationship between NG2+ OPC and adult NG2+ polydendrocytes is current matter of study. In a recent work, it is shown that NG2+ cells isolated from postnatal hippocampus are multipotent and can differentiate into neurons (Belachew, Chittajallu et al. 2003). This indicates that NG2 as a marker characterize distinct group of cells depending on the developmental stage assessed.

APCs: Astrocytes precursos cells express GFAP and A2B5+ and acquire stellate-shape typical of astrocytes (Culican, Baumrind et al. 1990). APCs can give rise to type 1 astrocytes.

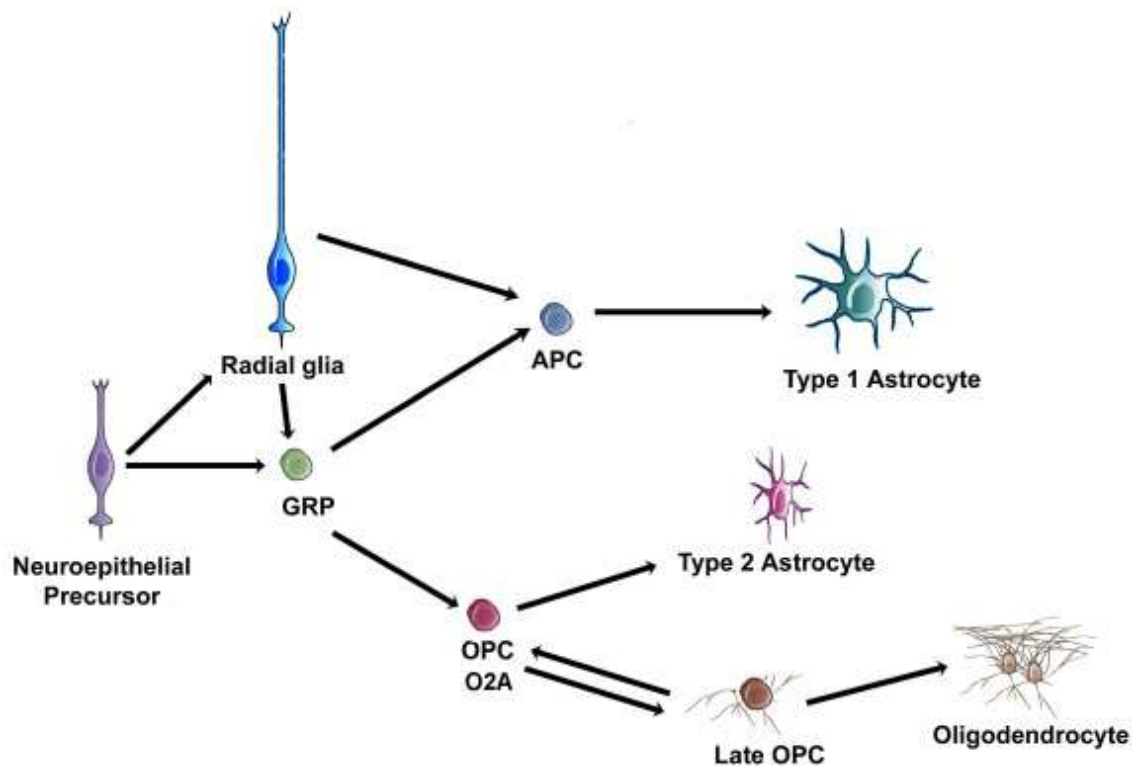
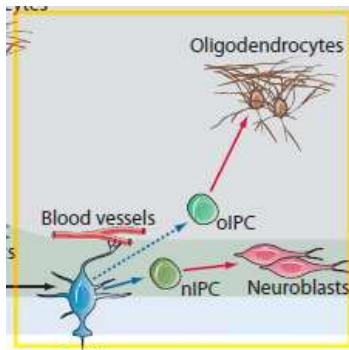


Figure 14. Schematic representation of neural progenitor cells and glial cell lineage according to *in vivo* and *in vitro* experiments. Adapted from (Cano 2011).

1.6.6. Step 4: Adult NSC



In adulthood most of RGC differentiate into mature astrocytes and oligodendrocytes. However, some astrocyte population acts as primary progenitors generating new neurons and glial cells in restricted germinal regions in the adult mammalian brain (Alvarez-Buylla and Lim 2004). Nowadays is generally accepted that adult NSCs are present specifically in the subventricular zone (SVZ) of the lateral ventricle wall and the subgranular zone (SGZ) of the hippocampal dentate gyrus. Interestingly, NSCs have also been derived *in vitro* from a variety of adult CNS regions, including hippocampus and spinal cord, yet it remains controversial whether those regions harbor similar NSCs and enable neurogenesis under physiological conditions *in vivo* (Ming and Song 2005; Ma, Bonaguidi et al. 2009). Adult NSCs retain epithelial properties, including the extension of a thin apical process that ends on the ventricle and a basal process ending on blood vessels. They stay relatively quiescent and in response to stimuli they give rise to proliferating cells that can then give rise to neurons and some glial cells.

A concrete example is represented by B cells, a specific adult kind of NSC that give rise to immature neuroblasts which migrate in chains to the olfactory bulb, where they differentiate into interneurons. B cells display ultrastructural characteristics and markers of astroglial cells, including the expression of GFAP, GLAST, and other astroglial markers. (Merkle and Alvarez-Buylla 2006). B cells also generate oligodendrocytes through a NG2+ oIPC (Doetsch, Caille et al. 1999; Merkle and Alvarez-Buylla 2006).

Richardson et al. (2011) reviewed the role of NG2+ cells as adult NSC, summarizing the recent knowledge about this kind of cells. They compare *in vitro* and *in vivo* studies. For instance, they highlight NG2+ cell plasticity reporting a study of Kondo and Raff, in which *in vitro* post natal derived-NG2+ cells are re-programmed into NSC-

neurospheres, able to give rise to neurons, type-1 astrocytes and oligodendrocytes (Kondo and Raff, 2000). They conclude hypothesizing a close relationship between SVZ B cells, type-2 astrocytes and NG2-glia.

Antigenic characteristics of radial glia during development and in adult

Trying to simplify the complicated world of differentiation state markers, in this paragraph the most used immunocytochemical markers to identify the different kind of NPC are reported.

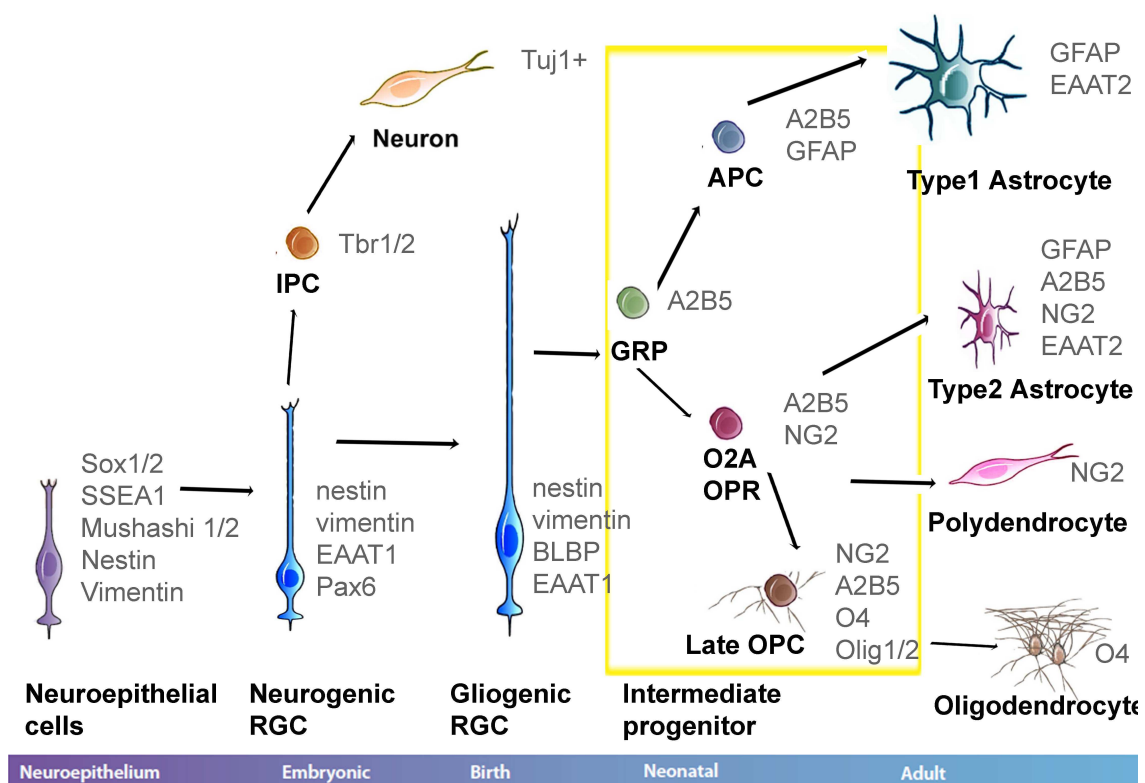


Figure 15. Schematic representation of evolution of neuroepithelial cells and radial glia and the main used antigenic features. Image adapted from (Kriegstein and Alvarez-Buylla 2009; Cano 2011). Marker definition adapted from (Baumann and Pham-Dinh 2001 ; Liu and Rao 2004; Vaccarino, Fagel et al. 2007; White and Jakeman 2008; Kriegstein and Alvarez-Buylla 2009; Freeman 2010 ; Cano 2011).

1. Neuroepithelial cells.

They express stem cells markers, like the transcription factors Sox1/2, CD133, SSEA1, and Mushashi1/2, and neural progenitors markers, like the intermediate filament Nestin (White and Jakeman 2008).

2. Neurogenic RGC

During neurogenesis, all neural progenitors express the intermediate filament proteins Nestin (Tohyama, Lee et al. 1992; McDermott, Barry et al. 2005) and, in some species, Vimentin (Dahl, Rueger et al. 1981; McDermott, Barry et al. 2005). In the cerebral cortex Pax6 is also considered a marker of radial glia still not committed to a neurogenic or gliogenic profile (Englund, Fink et al. 2005). The elongated glial precursors that go on to form neurons do not express BLBP. (Vacarino, Fagel et al. 2007).

3. Gliogenic RGC

After neurogenesis is completed, radial glial cells that will go on to differentiate into Astrocytes begin to express BLBP. Expression of BLBP is commonly used as a specific marker for the identification of astrocytic radial glial progenitors (McDermott, Barry et al. 2005). RGC also begin to express astroglial markers such as the astrocyte-specific glutamate transporter (EAAT-1, known also as GLAST)(White and Jakeman 2008). They also express a variety of intermediate filament proteins including nestin, vimentin, and in some species the astroglial intermediate filament, glial fibrillary acidic protein (GFAP) (Kriegstein and Alvarez-Buylla 2009).

4. Intermediate progenitors

Intermediate progenitors GRP, APC and OPC, were introduced and explained in the previous paragraph. To sum up, they are characterized by the expression of A2B5, and they express GFAP when they are committed to astrocyte type 1, while they express NG2 when they are committed to astrocyte type-2, polydendrocytes and oligodendrocytes.

5. Adulthood

In postnatal stages of development, the immature astrocytes down-regulate the expression of BLBP and Nestin, and retain the expression of the glutamate transporter GLAST (EAAT-1) (Eng, Vanderhaeghen et al. 1971; Sims and Robinson 1999; McDermott, Barry et al. 2005; Vaccarino, Fagel et al. 2007). Then, each cell type increase specific mature markers. Type 1 astrocytes express GFAP and the glutamate transporter EAAT-2, Type 2 Astrocytes express GFAP, EAAT-2 and in addition A2B5 and NG2 (Nishiyama, Komitova et al. 2009), polydendrocytes express NG2 and oligodendrocytes O4.

1.5 Statements

Many efforts are put in the study of the adult population of progenitors because of their potential as regenerative therapy. Those glial progenitor cells likely play important roles in response to injury. This subject is treated in more details in the section **2.3 “Glial cells in response to injury”**. It must to be taken into account that the model used in this work is *in vitro*, where changes in cell behaviour and phenotype are susceptible to culture conditions. However, is good to keep in mind the existing knowledge derived from *in vivo* developmental studies.

2. CNS RESPONSE TO INJURY

2.1 Overview

Injuries in the CNS have several causes, like tumors, vascular diseases or infectious diseases. However, the most common reason for injuries is trauma, and they are known as traumatic brain injury (TBI) and traumatic spinal cord injury (SCI).

Consequences of TBI are manifested by diverse symptoms, ranging from headaches and dementia through to severe functional impediments such as paraplegia or tetraplegia. It is estimated that every year there are between 175 and 200 cases per 100,000 inhabitants of TBI and 500 cases of SCI per million people. Data from the Guttman Institute for rehabilitations report that the number of people attended per year has been on the rise since 2002. (<http://www.guttmann.com>). (Schmidt and Leach 2003; Lane 2008).

During the impact, the injury can be inflicted by contusion or by the simple ricocheting of the brain inside the skull, resulting in hematomas. At the site of injury, a fluid filled cavity is formed, which becomes surrounded by a dense glial scar. Reactive astrocytes, immune cells, glycosaminoglycans and other inhibitory molecules prevent neurons and other cells from infiltrating the injury site, resulting in a loss of axonal connections and a loss of motor function. Neuron degeneration, scar tissue formation and the release of inhibitory axon growth factors can lead to the formation of voids in tissue (**Fig. 16**). The process referred to the physical insult to tissue that leads to tissue disruption, vascular rupture, cellular death and tissue necrosis is known as primary injury (Schmidt and Leach 2003; Pettikiriachchi 2010).

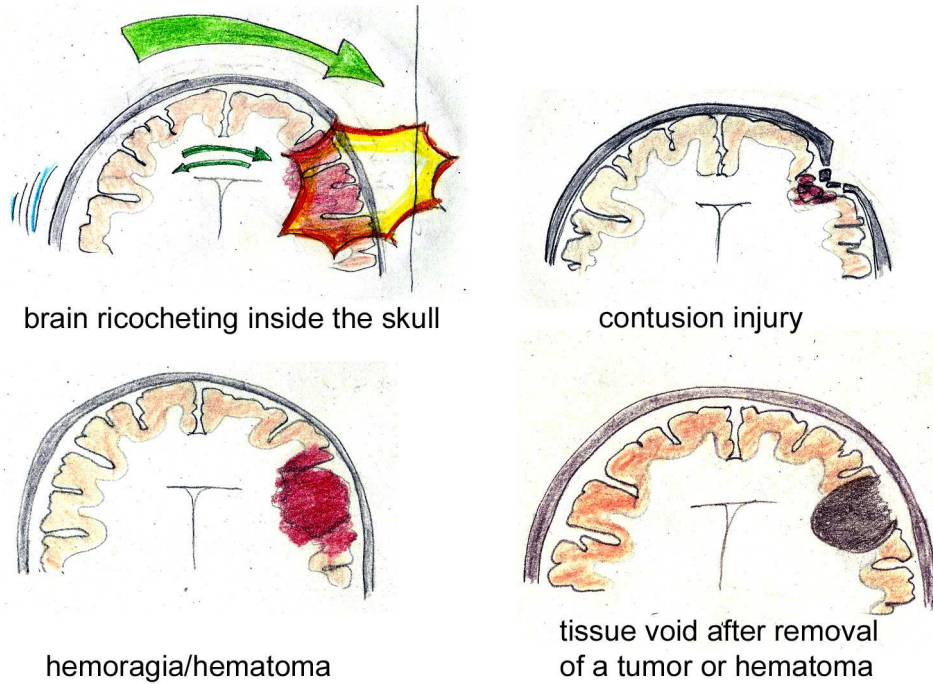


Figure 16. Brain injury.

The primary injury is followed by a secondary injury, whereby cells that do not sustain direct injury become vulnerable to a later cell death. The secondary tissue injury is characterized by oxidative stress and excitotoxicity. The equilibrium is broken by the delivery in the extracellular space of reactive oxygen species (ROS), resulting in lipid membrane peroxidation and rupture, and excitatory neurotransmitters, like glutamate and aspartate, that cause the malfunction of Ca^{2+} , $\text{Na}^{+}/\text{K}^{+}$ ionic pumps. Secondary cell death is frequently associated with concomitant vascular damage and edema. The influx of plasma proteins is detrimental to neuronal viability, while edema can cause compression of surrounding tissue, cell swelling and death (Schmidt and Leach 2003; Lane 2008; Gumerá et al. 2011).

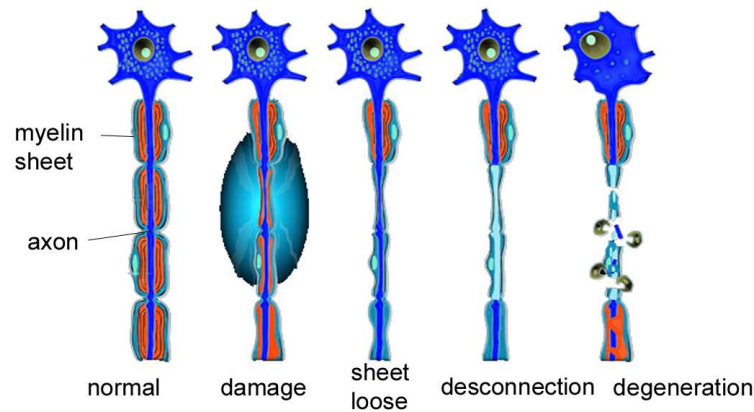
2.2 Neurons in response to injury

2.2.1 Neuronal damage

The axons of neurons that do not die immediately, suffer axotomy. Axotomy is an interruption of axonal continuity due to transection or severe compression. The main consequence of axotomy is a progressive death of the distal axonal segment, since the metabolic maintenance and integrity of the axon is primarily dependent on synthetic activity in the cell body and anterograde axonal transport. This phenomenon is referred to as Wallerian or anterograde degeneration. During Wallerian degeneration, axons and their myelin layers disintegrate over a period of several days. This process causes a release of myelin proteins that are inhibitory for axonal regeneration (Stocum 2006; Lane 2008).

Neuronal cell bodies after axotomy suffer chromatolysis. This process is characterized by a prominent migration of the nucleus toward the periphery of the cell and an increased size of nucleolus. During chromatolysis, the neuronal rough endoplasmic reticulum, also known as Nissl Bodies and responsible for protein synthesis, progressively dissolves, while neural soma swells and synaptic terminals are lost or retracted (**Fig. 17**). (Liu et al. 2011).

Wallerian degeneration



Chromatolysis

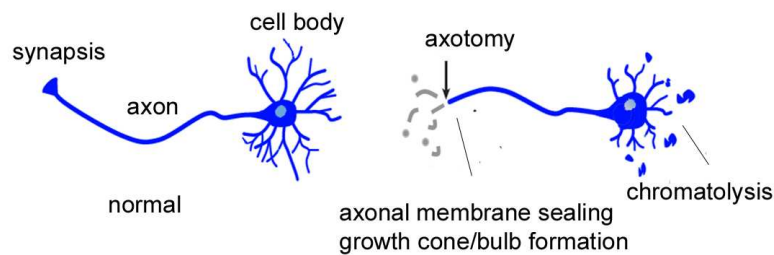


Figure 17. Schematic representation of neuronal response to injury. Adapted from (Schmidt and Leach 2003; Liu et al. 2011).

While the distal axonal extremity undergoes Wallerian degeneration, the proximal lesion site reseals the damaged axonal membrane in order to preserve the integrity of the cell. The cut axonal end attempt to transform into a growth cone–like structure, that can integrate extracellular signals and orchestrate the use of cellular materials for axon re-growth. This is a critical step for axon regeneration and it often fails in CNS, leading to the formation of a retraction bulb (Hill et al. 2001). Axons that could develop a growth cone face an inhibitory chemical environment. Growth cone behaviors such as advancing, retracting, turning, and branching are regulated by the dynamic reorganization of actin filaments and microtubules, which in turn are linked to the receptors for molecules such as netrins, slits, semaphorins, and ephrins (Kalil and Dent 2005). Growth cones integrate complex cues, which vary in both time and space, and may also be synergistic or competitive. New growth cones extend very short distances before stabilizing and then receding. This transient re-growth of axons within the CNS is known with the name of abortive regeneration, and it was observed for the first

time in the late 1800 by the German scientist H. Stroebe and later verified by the renowned Spanish neuroscientist Santiago Ramon y Cajal (**Fig. 18**) (Liu et al. 2011).

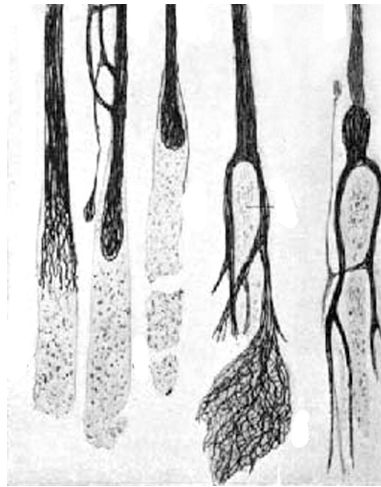


Figure 18. Drawings by Ramon y Cajal of axonal bulbs in abortive regeneration.

2.2.2 Regenerative capacity of neurons

CNS has an inner plasticity and capacity to adapt to changes. For instance during perinatal periods, neural circuits and synaptic formation of neurons can be either powered or inhibited in an experience-dependent manner. After an injury, the most likely compensative mechanism that leads to functional improvement is the compensatory axonal sprouting from uninjured neurons. This kind of plasticity leads to the formation of alternative neural circuits to restore the lost connections (**Fig. 19**).

However, this kind of plasticity is limited by environmental cues represented mostly by glial cell and ECM, which in adulthood stabilize and seal the neural networks and synaptic circuits. It is well known that neural plasticity decreases with age. Some studies attribute this change to the maturation of astrocytes and oligodendrocytes, which secrete CSPG perineural network and myelinate axons. It has been proved that the chemical removal of CSPG and myelin associated proteins (MAP) in new born animals prolongs the plasticity period. Thus, a strategy to encourage this type of regenerative response, could be repressing inhibiting cues presented by glial cell in order to re-establish a permissive environment to synaptic remodeling (Harel and Strittmatter 2006).

Compensatory plasticity

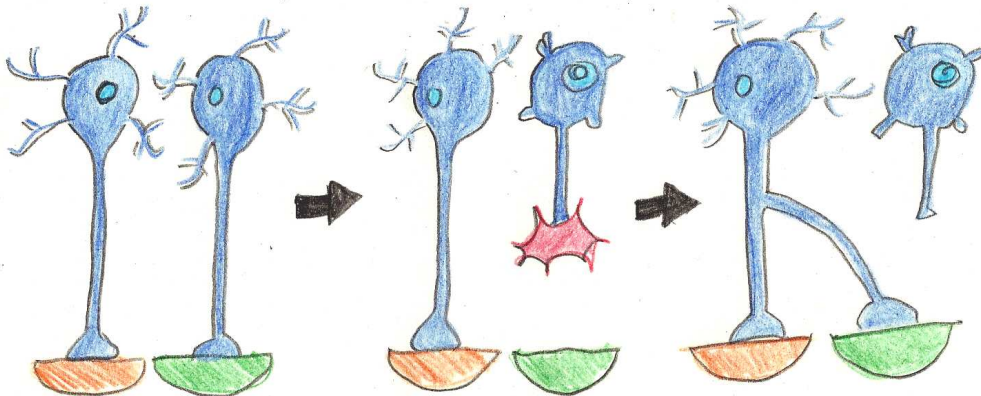


Figure 19. Compensatory plasticity.

There are evidences that neural stem cells become activated in certain parts of the brain after trauma. Activated progenitors and new neurons have been found, for instance, in the dentate gyrus (Richardson et al. 2007), in the hippocampus and in the cerebral cortex, while normally this would occur only during early development and in the postnatal stage (Harel and Strittmatter 2006).

In cerebral cortex, it has been shown that after a perinatal hypoxic insult, neurogenesis is greatly enhanced. Within one week after cessation of hypoxia, the amount of proliferating BLBP+/vimentin+ astroglial in the SVZ more than doubles compared to normoxic controls; these cells give rise to neuronal and glial progenitors that migrate into the cortex. (Fagel et al. 2006) (Vacarino et al. 2007) (Ong et al. 2005). Another example is reported by Richardson et al, which showed increased proliferation in dentate gyrus after induced experimental TBI (**Fig. 20**)

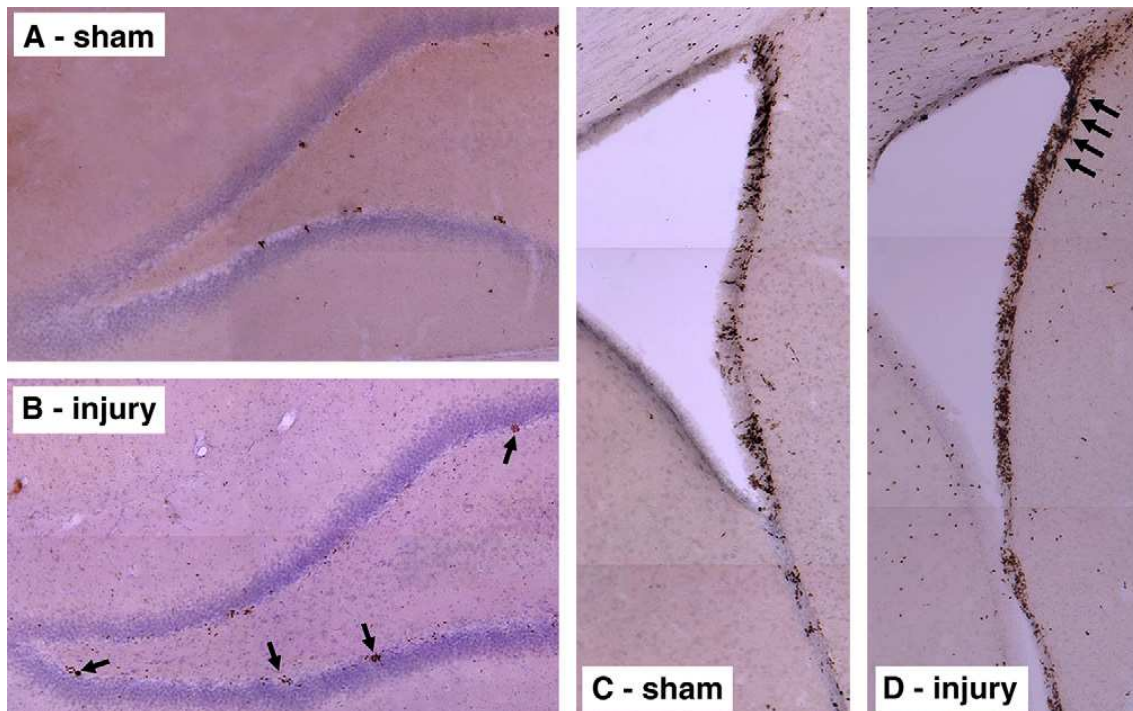


Figure 20. Increased cell proliferation in neurogenic regions after experimental TBI. An increase in the number of bromodeoxyuridine (BrdU)-labeled cells (brown), was observed after 2days in the ipsilateral dentate gyrus in injury group (B) compared to control animal group (A, sham). These cells are mainly clustered in the subgranular zone (B, arrows). Similarly, BrdU labeling in the ipsilateral subventricular zone of sham animals (C) significantly increases after injury (D, arrows). (Richardson et al. 2007)

However, this is a controversial subject, since it has to be considered that from the experimental point of view, it becomes difficult to differentiate between stem/progenitor cells within the dentate gyrus and activated or reactive astrocytes. Markers like nestin, Sox 2, vimentin, and glial fibrillary associated protein (GFAP) are not specific for neural stem and progenitor cells but may also be expressed in astrocytes following injury (Ridet et al. 1997). Furthermore, it is still unclear whether the activation of progenitors results in stable and productive neurogenesis and, if enhancing this process is beneficial after injury (Richardson et al. 2007).

Kernie et al., in his interesting review about insult induced-neurogenesis, points out the potential drawbacks of post-traumatic aberrant neurogenesis, which could result in epilepsy or tumor development. Therefore, although enhancing neurogenesis following TBI remains a compelling strategy, many issues regarding specificity,

mechanism, and potential toxicity need to be investigated before clinical interventions can occur (Kernie and Parent 2010).

2.3 Glial cells in response to injury

2.3.1 Gliosis and glial scar

After TBI, breaches in the brain-blood barrier enable the migration of macrophages and other cell types to the injury site. The loss of tissue associated with neuroinflammation, Wallerian degeneration and cell damage, triggers an astroglial response. The overall astrocytic response is referred to as gliosis or astrogliosis, which in conjunction with other cell types form glial scars (**Fig. 21**).

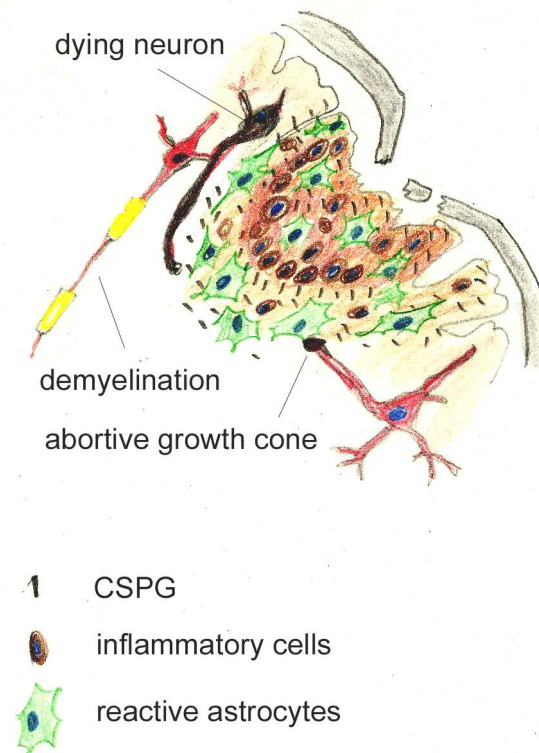


Figure 21. Glial scar. Inspired by (Pettikiriarachchi 2010; Gumera et al. 2011)

Following detection of signs of infection or tissue injury, microglial cells adopt an activated state and produce numerous pro-inflammatory cytokines. Molecules secreted by microglial cells activate astrocytes, which become reactive and secrete themselves pro-inflammatory molecules. Chemokins secreted by reactive astrocytes attract macrophages from the periphery to the site of the injury (Otto et al. 2002), generating positive feedback cross-talk (Saijo and Glass 2011 167).

Reactive astrocytes mainly undergo hypertrophy, proliferate, migrate, differentiate and form a dense network bordering the lesion site (White and Jakeman 2008). Changes in the morphology of reactive glial cells are associated to alteration in protein expression. GFAP level increases, as well as the glutamate transporter EAAT-1; many of the markers expressed during development are re-expressed, like for instance nestin and vimentin (**Fig. 22**) (White and Jakeman 2008). Inhibitory extracellular matrix molecules are also overexpressed, such as CSPGs, ephrins, myelin associated glycoproteins and Nogo (Bandtlow and Zimmermann 2000), which can inhibit growth into the lesion, as well as growth past the lesion site into the denervated CNS (Asher et al. 2002).

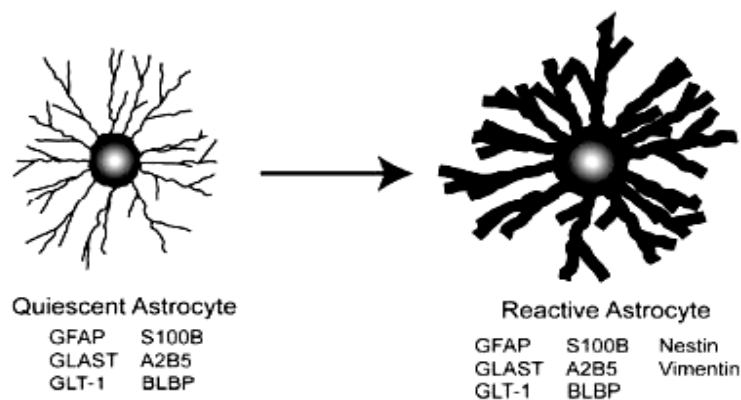


Figure 22. Quiescent and reactive astrocytes and their main markers. Adapted from (White and Jakeman 2008).

Reactive astrocytes can arise either from progenitor cells or from quiescent astrocytes that proliferate in response to an injury. A recent fate mapping study has shown that quiescent, mature astrocytes can proliferate and give rise to astrocytes that contribute to the glial scar (Buffo et al. 2008). These cell populations are considered to be adult stem cells that proliferate and differentiate into glial cells, including astrocytes, after injury (Mothe and Tator 2005).

The up regulation of NG2 expressing cells was also demonstrated in response to injury in the CNS at early time points (**Fig. 23**). However, the role of this kind of cells is not

Introduction: 2. CNS response to injury

very clear because on one hand, NG2+ cells are considered to be a kind of progenitor cells, thus beneficial for regeneration, while on the other hand NG2 molecule have been shown to be inhibitory for neurite growth (Tan et al. 2005).

Overall, the glial scar, as a result of reactive astrocytes, microglia and invading meningeal fibroblasts, presents an inhibitory cellular and molecular microenvironment for axon regeneration and tissue repair.

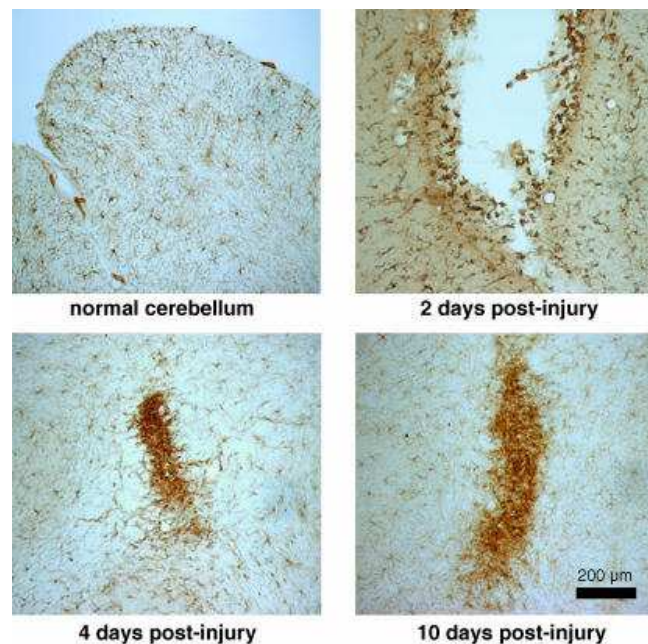


Figure 23. NG2-positive cells after injury in cerebellum of adult rats. At 4 and 10 days post-injury, the NG2-expressing cells have formed small plaques at the injury site. These plaques correspond to the glial scar (Tan et al. 2005).

From a different point of view, astroglial scarring is a form of wound healing and it effectively serve as a fence to protect the damaged tissue. For instance, in the case of laceration injuries with bone fragments entering the CNS, astrocytes respond by forming a limiting membrane along the exposed CNS neural parenchyma. This forms a glial capsule that can be one or more layers thick and isolate the interior of CNS tissue from non-CNS elements in the lesion (Stocum 2006; White and Jakeman 2008).

Astrocyte response to injury includes several actions that contribute to endogenous neuroprotection and repair. Astrocytes produce neurotrophic factors, such as brain

derived neurotrophic factor (BDNF) (Ikeda et al. 2001), ciliary neurotrophic factor (CNTF), nerve growth factor (NGF), and fibroblast growth factor (FGF-2) (White and Jakeman 2008). They play a key role in reducing excitotoxic death after injury by upregulating their expression of glutamate transporters, like EAAT-1 and EAAT-2, and they also produce extracellular matrix molecules that are supportive to axon growth, such as laminin (Costa et al. 2002) and fibronectin (Tom et al. 2004). In addition, experiments using GFAP-deficient mice have shown that without astrocytes, the degree of secondary tissue damage is much greater (Lepekhn et al. 2001; Otani et al. 2003).

2.3.2 Regenerative capacity of glial cells

In recent years has become clear that the predominant proliferative response after injury in the CNS arise from glial progenitors that are resident in the parenchyma. Glial progenitor cells present in the parenchyma proliferate and participate in reforming the brain-blood barrier, and remyelinating demyelinated tracts. This response is robust and has been observed in multiple models of disease, suggesting that cues exist to direct glial progenitors to proliferate, migrate to an injured site, and participate in the repair process (Han et al. 2004).

More recent work has begun to identify the characteristics of the glial cells that respond to an injury. It has been observed that the cells that respond to an injury are mostly Olig2 and NG2 positive. This precursor cell is capable of surviving in the damaged environment and migrate into the lesion site to participate in remyelination of the damaged tissue (Vaccarino et al. 2007; Nishiyama et al. 2009).

In spinal cord, it has been observed that radial glial progenitors are reactivated and up-regulated in areas of neurodegeneration following injury, supplying progenitors for repair (Shibuya et al. 2003). This response was also observed after implantation of a chitosan channel in a rat spinal cord injury model. The increased presence of nestin positive radial glia like cells led to an improvement in neural regeneration (Nomura et al. 2010).

Vaccarino et al report studies where following perinatal insult, the reactivation of GFAP+ proliferative glial cells also led to the formation of new neurons (Bi et al.

2011). It appears that proliferating astroglial cells in the SVZ may give rise to neuroblasts, which migrate into brain cortex (Ganat et al. 2006; Vaccarino et al. 2007)

However, neurogenesis arising from glial cells rarely occurs. Even though a glial progenitor can generate neurons under specific conditions, inhibitory cues prevent stem cells or glial progenitors from differentiating into neurons. Liu and Rao showed that this inhibition is likely at the transition from ependymal cell to neuron restricted precursor and that if one bypasses that stage then neurons can survive and integrate even in white matter compartments (Liu and Rao 2004).

Taken together, these observations lead to the hypothesis that modulating the glial response by the mobilization of endogenous reparative precursors may be a logical intervention for obtaining a therapeutic improvement. These findings are encouraging for this study, as supporting that glial cells could be directed toward a more permissive state by presenting the proper information.

2.4 Current treatments approaches

Current clinical treatments focus on prevention of the secondary injury after the initial trauma, and on partial function recovery with drug therapy and rehabilitation. However, the results are far from ideal and new therapeutic methods must be established for better treatment.

Basic therapy of TBI consist in maintain the brain in a low-metabolic state by sedation and hypothermia. Systemic delivery of neuroprotective molecules, like methylprednisolone and gacyclidine, is the only clinically used therapy. Antagonist glutamate receptor and calcium antagonists, free radicals scavengers and cyclosporine are currently being investigating as possible therapeutic agents (Clausen and Bullock 2001; Marklund and Hillered 2011).

A field of research focuses on improving the delivery of drugs that promote neuronal regeneration, anti-inflammatory drugs, neurotrophins like NGF, BDNF, NT-3, or other growth factors. The main problem for local drug delivery in the nervous system is crossing the brain-blood barrier, which is highly selective for the entrance of

molecules. The most common techniques for targeted drug delivery, like scaffold based systems, microspheres, immobilized drugs or electrically controlled devices are described by Willert et al. (Willerth and Sakiyama-Elbert 2007).

Other strategies to treat injuries in the central nervous system are the use of artificial electrical prosthesis to recover functionality, solution already used for some clinical cases. However, they are extremely expensive and not free from drawbacks (Giszter 2008).

An interesting approach is to inhibit the unfavorable glial scar. This consists in targeting key molecules responsible for neuronal inhibition. Nogo-A, myelin associated glycoprotein (MAG), oligodendrocytes-myelin glycoprotein (Omgp) and CSPG are some of the identified molecules responsible of axon growth inhibition, and since their discovering some neutralizing methods have been developed. The molecular approaches to CNS regeneration are reviewed by (David and Lacroix 2003; Baptiste and Fehlings 2008; Tohda and Kuboyama 2011).

For instace, ongoing work involving myelin associates inhibitors (MAI) antagonism or CSPG inhibition in mice shows great promise in allowing plastic sprouting responses to compensate for different types of CNS injury (Harel and Strittmatter 2006; Tohda and Kuboyama 2011).

Thanks to the stem cell research, many approaches involving cell therapy have been taken over in the last decade. Stem cells have been implanted in animal models and in humans in clinical trials. The aim of this kind of therapy is to replace the lost cells, give trophic support and help axonal re-growth. In human, autologous bone marrow stem cells, olfactory ensheathing cells, macrophages and T- cells have been administrated to patients with injury in central nervous system in spinal cord. V. Sahanni recently reviewed the main achievements and rationales for their use in the clinic. He mainly explains that clinical trials reported no adverse effects, such as cystis or tumor formation, but we are still far from claiming improvements (Sahni and Kessler 2010).

Controversial opinions about stem cell therapy arise from the experience of the Geron company (Wilson 2009). Geron received FDA approval to start Phase 1 clinical trial using GRNOPC1, an embryonic stem cell based drug designed to treat spinal cord injury promoting remyelination. The trial was based on *in vivo* studies on rats which demonstrated functional improvement after injury (Keirstead et al. 2005). However, the trial shut down after treating 4 patients and seen no effects (Pollak 2011). Moreover, at the same time, a patient treated in Moscow developed multiple tumors after stem cell implant in brain. The same authors of the study suggest that these results “do not imply that the research in stem cell therapeutics should be abandoned. They do, however, suggest that extensive research into the biology of stem cells and in-depth preclinical studies, especially of safety, should be pursued in order to maximize the potential benefits of regenerative medicine while minimizing the risks” (Amariglio et al. 2009).

Together with stem cells research, tissue engineering also did tremendous advances in the last years. With the development of biomaterial science and nanotechnologies, a whole field of research expanded, providing new options for CNS injury treatment. The idea of tissue engineering is implanting a biomaterial at the injury site that carries enough information to stimulate resident competent cells. This comprises the delivery of drugs or neurotrophic factors, as the stimulation by physical and chemical properties. The tissue engineering approach, among all the reviewed ones, is the one that gives the background to this thesis. A multitude of materials and formulations have been used experimentally. The types of materials and the advances made in CNS, as future therapies that incorporate multiple cues into unique devices are treated in detail in the next chapter.

3. BIOMATERIALS IN CNS TISSUE ENGINEERING

3.1 Tissue engineering

The approach that gives the background to this thesis is the tissue engineering one, which is based on the use of biomaterials to temporally replace and induce the restoring of a damaged organ. The basic idea of tissue regeneration therapy is to take advantage of the natural healing potentials of patients themselves (Stocum 2006).

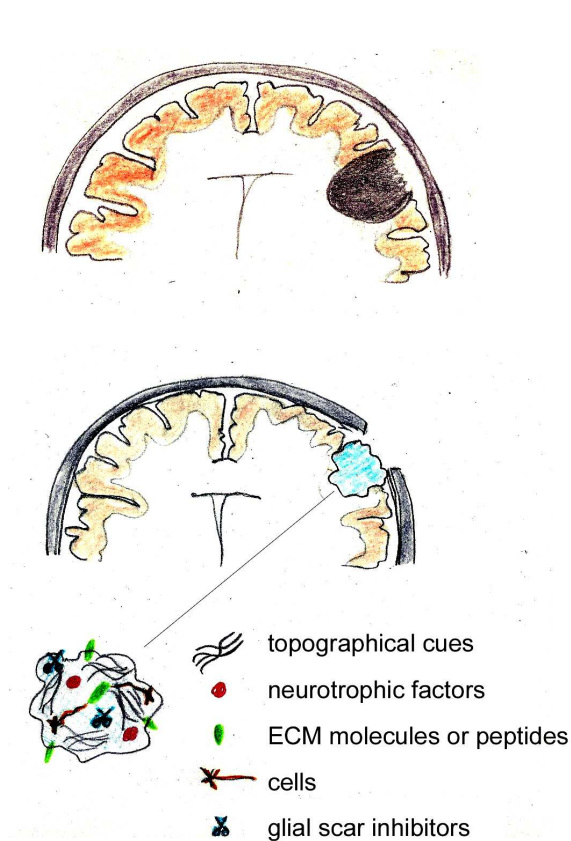


Figure 24. Tissue engineering approach to brain injury. Inspired by (Pettikiriachchi 2010; Gumera, Rauck et al. 2011)

Damage to the brain leads often to the formation of a glial scar and a lesion cavity. When surgery is required after TBI, placing implantable biomaterial construct into the damaged area or cavity may provide support for the surrounding brain tissue, function as a substrate for cell infiltration and growth, axon regeneration and neurite formation (Orive, Anitua et al. 2009; Pettikiriachchi 2010). Apply a scaffold in TBI treatment could be useful to prevent tissue collapse, as well as to provide cells with an artificial ECM network (**Fig. 24**).

In the field of neuronal tissue engineering many researchers are presently focusing efforts on creating physical or chemical pathways to facilitate the regenerating axons. These devices can include physical or chemical topographical cues, biomolecular signals like neurotrophic factors, ECM molecules, or glial scar inhibitors, and neural stem or progenitor cells that differentiate into the appropriate neural lineages (**Fig. 24**) (Schmidt and Leach 2003; Li and Hoffman-Kim 2008; Orive, Anitua et al. 2009; Pettikiriachchi 2010; Gumera, Rauck et al. 2011).

3.2 Biomaterials for CNS regeneration

In a recent review concerning biomaterials for brain regeneration, C. Gumera et al. classify the materials that have been studied according to their physico-chemical properties into natural, biodegradable synthetic, and bio-stable synthetic (Gumera, Rauck et al. 2011). Herein I report their classification and a table (**Table 1**) listing some examples, to give an idea about the variety of possibilities that are currently explored in the research field.

- Natural materials comprehend chitosan, collagen, fibronectin, fibrin, hyaluronic acid, silk fibroin, and xyloglucan. Proteins derived from ECM molecules, like fibronectin derived RGD sequence and laminin derived IKVAV sequence, can also be considered part of this group. Naturally derived materials possess good biocompatibility when processed properly and may exhibit inherent bioactivity that can facilitate cell recognition and tissue integration. This class of materials can be degraded by enzymes in the body. Among all of these materials, chitosan was selected for the second experimental part of this thesis work.
- The biodegradable synthetic materials studied include PGA (poly-glycolic acid), PLA (polylactic acid), PLGA (polylactic-co-glycolic acid), PCL (polycaprolactone), PHB (polyhydroxyl butyrate), PGS (polyglycerol sebacate) and synthetic peptide amphiphiles. Compared to natural derived materials they are advantageous because proper synthesis and manufacturing protocols avoid complications due to the batch-to-batch variability and the potential for disease transmission. Biodegradable synthetic materials can be degraded, absorbed or remodeled by the body, which results in material replacement by new tissue as the nerve grows, thus minimizing potential physical interference with the regenerating nerve.
- Bio-stable synthetic materials generally are not ideal for *in vivo* applications since they are not biodegradable. This means that the material would remain inside the body or that a second surgery would be necessary to remove the material

after regeneration occurred, with all the clinical implications that it implies. However, there are examples of bio-stable materials applied in clinical settings in peripheral nervous system, like silicon tubes, expanded poly(tetrafluoroethylene) or ePTFE (Gore-Tex) and acrylates like poly-methylmetacrylate (PMMA). Even if in the future the use of those materials for regenerative purposes is up to being abandoned, they still remain valuable tools for studying cellular behavior *in vitro*. For the first experimental part of this thesis work, we used PMMA as *in vitro* model.

3.3 First, second and third generation of biomaterials

Hench defined biomaterials in relation with their interaction with the body. He classified biomaterials in 1st, 2nd and 3rd generation.

Biomaterials of the 1st generation were mostly inert and biostable. Materials were selected on the basis that they would be non-toxic, non-immunogenic, non-thrombogenic, non-carcinogenic, non-irritant and so on. The definition of biocompatibility consisted mainly in such a list of negatives characteristics. Examples are metallic systems, like stainless steels, cobalt–chromium alloys, titanium alloys, or synthetic polymeric materials like PTFE, PMMA, polyethylene and silicones (David F. 2008).

Biomaterials of the 2nd generation were designed to be either bioactive or resorbable. Examples of bioactive materials are bioactive glasses, ceramics, glass-ceramics, and composites. In their formulation we see the inclusion of bioactive components that could elicit a controlled action and reaction in the physiological environment. Concerning resorbable biomaterials, examples are PLA, PLGA and other biodegradable synthetic materials.

Biomaterials of the 3rd generation combine these two properties. Bioactive materials are being made resorbable and resorbable polymers are being made bioactive. The aim is developing materials that, once implanted, will help the body to heal itself. This

Introduction: 3. Biomaterials in CNS tissue engineering

implies molecular modifications of resorbable systems, in order to elicit specific interactions with cells and thereby direct cell proliferation, differentiation, and extracellular matrix production and organization (Hench and Polak 2002).

Table 1. Biomaterials used in CNS tissue engineering. Adapted from (Wyatt Potter 2008) and (Gumera, Rauck et al. 2011)

| <i>Material</i> | <i>Application and reference</i> |
|------------------------------------|--|
| Natural | |
| Matrigel | culture substrate |
| hyaluronic acid | hydrogel with conjugated poly D-lysine for brain tissue repair |
| collagen I | 3D culture matrix, support neuronal differentiation |
| collagen IV | combined with PHEMA, Schann cell transplant |
| Alginate | direct axonal regrowth in spinal cord |
| chitosan | support nerve cell growth (Freier, Koh et al. 2005; Freier, Montenegro et al. 2005) attach YIGSR, IKVAV in tube for spinal nerve repair |
| fibrin | 3D scaffold directing ESC to neural lineage |
| gelatin | amenable to peptide modification, can crosslink |
| silk fibroin | support nerve cell attachment and NGF release (Uebersax, Mattotti et al. 2007) |
| laminin | cell adhesion, coating |
| fibronectin | cell adhesion, coating |
| polylysine | cell adhesion, coating |
| Peptide sequences | |
| RGD | many ECM proteins: cellular adhesion, migration |
| PHSRNG6RGD | fibronectin: promote cellular adhesion, migration beyond RGD |
| IKVAV | laminin: cell adhesion |
| IKVAV nanofiber | cell scaffold, selective neuronal differentiation |
| YIGSR | laminin: cell adhesion |
| PDSGR | laminin: cell adhesion |
| PRGDSGYRGDS | collagen IV: cell adhesion |
| SKPPGGTSS | bone marrow homing protein-1: tight adhesion, neurite spreading |
| PFSSTKT | bone marrow homing protein-2: tight adhesion, neurite spreading |
| Biodegradable Synthetic | |
| PLA | attachment to PEG to increase cellular affinity |
| PLLA | culture substrate |
| PDLLA | nerve guidance channel |
| PGA | cell scaffold for transplantation, attach to PEG |
| PLGA | cell scaffold, blended with PCL forming sponges for TBI (Wong, Hollister et al. 2007) |
| self-assembling peptide nanofibers | culture substrate, can attach peptide |
| PCL | electrospun cell scaffold, blended with collagen (Schnell, Klinkhammer et al. 2007) |
| Biostable Synthetic | |
| PHEMA | used as hydrogel |
| PMMA | axonal guidance on nanopatterns or microcontact printed stripes of laminin (Schmalenberg, Buettner et al. 2004; Johansson, Carlberg et al. 2006) |
| silicon | peripheral nerve tubulization (Valero-Cabre, Tsironis et al. 2004) |
| PEG | cell scaffold, attachment of peptides/polymers |
| PHPMA | attachment of RGD, spinal cord repair |

3.4 Materials used in this thesis work

3.4.1 PMMA

PMMA is a bio-stable synthetic polyacrylate commonly applied for implants in orthopedics. PMMA tissue biocompatibility was discovered when Plexiglas fragments were accidentally introduced in the eyes and other body tissue of World War II fighter pilots during aircraft crashes. After being used as an essential ingredient in making dentures, PMMA is used in orthopedic surgery as a common bone grafting material mainly in the fixation of orthopedic prosthetic materials for hips, knees, and shoulder since mid-1950s. Thanks to its good optical properties, PMMA is used for implantable ocular lenses and hard contact lenses. For the same reason, PMMA is an excellent material to use for *in vitro* studies. It has to be pointed out that several biopolymers, such as PCL or PLA, may be not totally transparent, and for this reason they cause complications when used for microscopy. Thanks to its thermoplastic properties, PMMA is easy to pattern up to the nm scale by NIL. More over, previous works in our lab were conducted with mesenchymal stem cells. For all these reasons, PMMA was chosen as an *in vitro* model to study glial cell response to line patterns (Atala A 2008).

3.4.2 Chitosan

Chitosans are a family of biodegradable cationic polysaccharides consisting of glucosamine and randomly distributed N-acetylglucosamine linked in a $\beta(1-4)$ manner. Chitosans are derived from the alkaline N-deacetylation of chitin, a component of the protective layer of shellfish. The molecular weight of chitosan ranges from 300 to over 1000KDa, depending on the preparation procedure and the degree of deacetylation, which is the ratio of glucosamine and N-acetylglucosamine (Dornish, Kaplan et al. 2001). The degree of acetylation has been show to play an important role in the rate of degradation and it is directly related to the ability of the material to support cell attachment, with a higher degree of deacetylation being more favorable for cell attachment (Mao, Cui et al. 2004). *In vivo*, chitosan is degraded primarily by lysozime into oligosaccharides giving as degradation products D-glucosamine and N-acetyl-D-glucosamine. Those compounds are non-toxic and non-immunogenic. Thanks to his cationic nature, chitosan interacts with glycosaminoglycans

and other negatively charged particles, including various water soluble anionic polymers. Furthermore, the N-acetylglucosamine moiety on chitosan is analogous to that on glycosaminoglycans and suggests that additional biological activity may be attributed to this naturally occurring scaffold (Atala A 2008).

Chitosan films can be easily microstructured by soft lithography techniques, as reported by Fernandez et al (Fernandez, Mills et al. 2008; Fernandez, Mills et al. 2009). Moreover, chitosan offer the possibility to be structured into films, tubes, fibers, gels, particles etc (Di Martino, Sittinger et al. 2005; Silva, Mano et al. 2010). For all these properties, chitosan was chosen as a possible candidate material to be use for *in vivo* CNS regeneration.

3.5 Material formulations and structuring

Most of the materials mentioned above can be structured in many ways depending on the application. Tubes or guidance channels have been widely investigated for applications in peripheral nervous system or spinal cord. For this kind of “formulations” there are parameters that play important roles, like elasticity, biodegradability and porosity. Nerve guidance channels are supposed to bridge the gap between the injured nerves, and can also serve as drug carriers, can have cell components or directional cues, like grooves or fibers, or can be electrically conductive (**Fig. 25**) (Schmidt and Leach 2003).

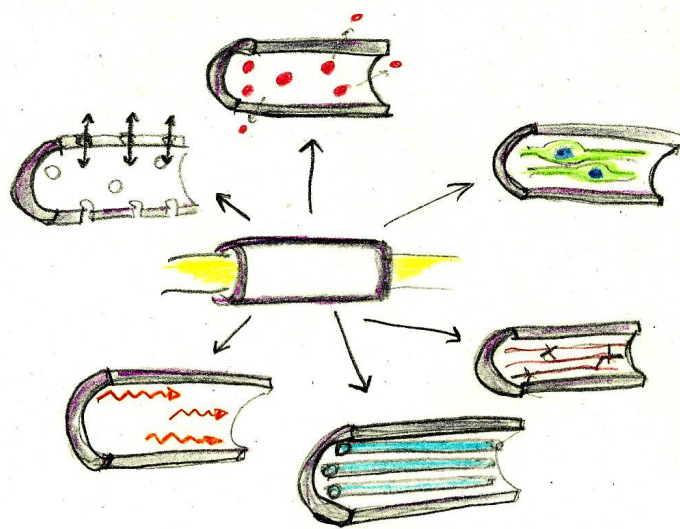


Figure 25. Properties of the ideal nerve guidance channel. The desired physical properties of a nerve conduit include (from the top and clockwise): bioactive factor delivery; supporting cell incorporation; oriented matrix to favour cell migration; intraluminal channels to mimic the structure of nerve fascicles; electrical activity; biodegradability and porosity. Adapted from (Schmidt and Leach 2003)

However, in the brain the concept of guidance channel is not applicable; therefore other formulations have been investigated. Hydrogels, nanofibers or self-assembling peptides are the most suitable for brain tissue, since they have similar mechanical compliance. Examples of hydrogels are agarose, alginate, chitosan, collagen or matrigel. For instance, chitosan have been investigated as an hydrogel blended together with methylcellulose or agarose, showing good neuronal attachment and neurite extension (Zuidema, Pap et al.; Cao, Gilbert et al. 2009). Crompton et al. also developed a polylysine functionalized thermoresponsive hydrogel biocompatible with neuronal growth (Crompton, Goud et al. 2007; Jain and Bellamkonda 2007).

Concerning the research on nanofibers, there are some advances that have to be mentioned. Nisbet et al, for instance, developed PCL nanofibers and tested them in rat cerebral cortex. Electrospun fibers showed neurite infiltration and low immune response, indicating that the material is compatible for CNS applications (Nisbet, Forsythe et al. 2009).

Self assembling amphiphilic peptides are also promising tools toward CNS regeneration. Ellis-Behnke and Schneider recently reviewed their use in CNS (Ellis-Behnke and Schneider 2011). They have been developed in Stupp laboratories, and they consisted in molecules with a hydrophilic peptide head group and a hydrophobic carbon tail joined by a peptide spacer region that under physiological conditions, self-assembly into elongated micelles (**Fig. 26**). Doing so, a dense nanofiber matrix is produced, which forms a gel due to the embedding of the surrounding aqueous environment. During the self assembling process, cells can be encapsulated. (Hartgerink, Beniash et al. 2002 ; Silva 2006).

For instance, Silva et al reported a study in which neural stem cells were encapsulated *in vitro* into IKVAV presenting self-assembling nanofibers. They observed a rapid differentiation of cells into neurons, while the appearance of glial phenotype was discouraged (Silva, Czeisler et al. 2004).

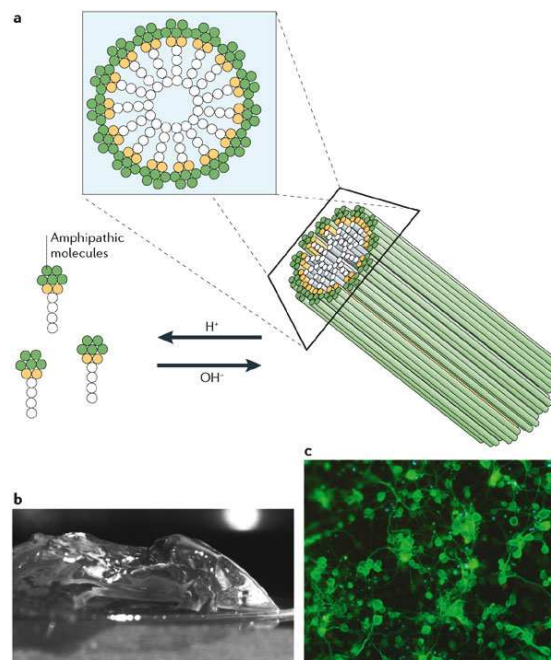


Figure 26. Self assembling amphiphilic peptides a. structure; b. overall gelly appearance; c. *in vitro* neural stem cell cultures differentiated into neurons (stained for neuronal marker β -tubulin III) (Silva, Czeisler et al. 2004; Silva 2006)

3.6 Cell-material interaction: the role of biomaterial properties

The cell-material interaction is a complex bi-directional and dynamic process that mimics to a certain extent the natural interactions of cells with the extracellular matrix. Cells in the tissues are constantly receiving information from their environment, including the extracellular matrix (ECM) (**Fig. 27**). At the same time, cells produce signals their selves and secrete their own ECM (Shekaran and Garcia 2011).

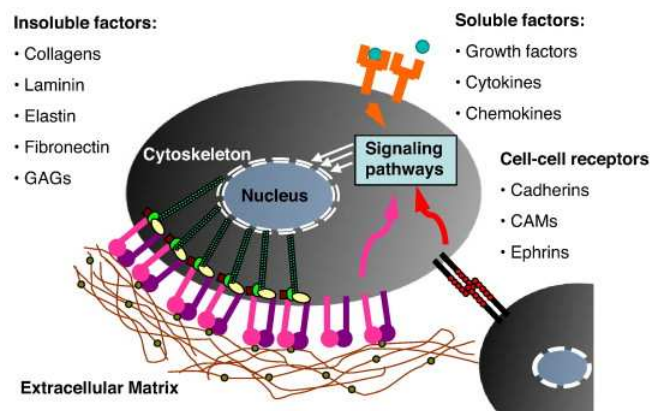


Figure 27. Cell-ECM interactions. (Shekaran and Garcia)

Therefore, when a foreign material is implanted in the body, or when cells are grown on a biomaterial *in vitro*, the properties of the material are crucial to determine the cell response (Llopis-Hernández, Rico et al. 2011). A typical adverse response to a material is encapsulation, which results in the formation of a scar around the implanted material. An example is reported in **Fig. 28**. The figure represents schematically a typical reaction to an electrode that was implanted in brain. The use of this kind of electrode for neuroprosthetic devices has grown rapidly in the latest years. They have been used as deep brain stimulators for pain management, and for control of motor disorders such as Parkinson's disease, or as cochlear implants for restoring auditory function (Marin and Fernandez 2010).

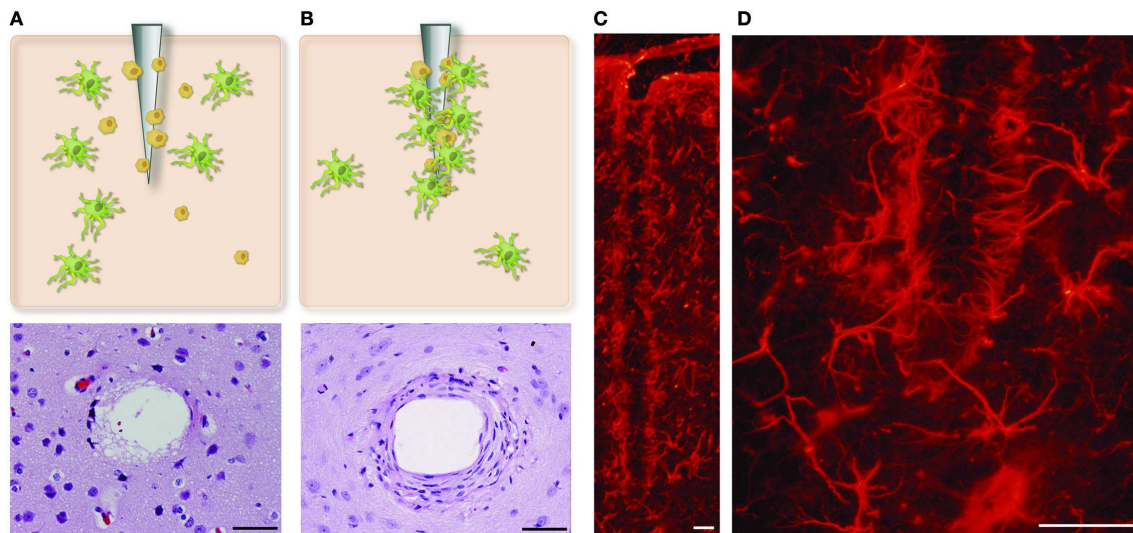


Figure 28. Development of glial encapsulation on an intracortical microelectrode. **(A)** Acute neural injury caused by inserting a microelectrode into the brain cortex. Astrocytes and microglial cells become activated and migrate to the site of injury. **(B)** Chronic response showing a dense sheath around implanted probes, which contains fibroblasts, macrophages and astrocytes. **(C,D)** The reactive astrocytes, immunohistochemically labeled here for GFAP, encapsulate the neural probes forming a dense cellular sheath. Calibration bar = 50 μm (Marin and Fernandez 2010).

After *in vivo* implant, serum proteins are the ones that most likely contact the surface of the material. Cells do not recognize the material itself, which often is not bioactive, but they interact with ECM proteins that adsorb on it. This phenomena also occur in *in vitro* systems. The interaction between surface and ECM proteins is a matter of study in the field of tissue engineering. In the literature there are several studies that investigate the effect of adhesive protein adsorption on model surfaces that vary only in one property, like wettability, charge, stiffness or rugosity (Arima and Iwata 2007; Barrias, Martins et al. 2009; Palacio, Schricker et al. 2010; Coelho, Gonzalez-García et al. 2011).

A strategy to minimize adverse tissue reaction and improve cell response is the chemical modification of the material surface by biomolecules. For instance, coating with adhesion proteins, peptides, sugars or growth factors are widely used (Marin and Fernandez 2010).

Anyway, coated or not, it is clear that material properties influence protein absorption and therefore cell behavior. Thus, understanding the role of material properties allows

controlling the desired cell response. Herein material properties involved in driving cell response such as wettability, surface charge, stiffness and surface topography are described.

3.6.1 Wettability and surface charge

Wettability strongly affects the conformation of ECM molecules that adsorb to the materials, changing the integrin-mediated signals for cell adhesion. There are some interesting studies that use mostly model surfaces with variable chemistry. For instance, Coelho et al observed how Collagen type IV and laminin change their conformation on polymeric well-defined surfaces with different density of hydroxyl groups. AFM studies revealed that on hydrophobic surfaces both proteins arrange in networks, while on hydrophilic substrates they are present in a single molecule arrangement. This is reflected on cellular behaviour in a strange way, having two optima, on the hydrophilic ($XOH = 1$) and on the hydrophobic ($XOH = 0.3$) surfaces, in terms of cell adhesion and morphology and development of focal adhesion complexes (Coelho, Gonzalez-García et al. 2011).

Another example is the study by Soria et al, in which they grow brain explants on polymeric surfaces with different contact angles prepared from polyacrylamide, ethyl acrylate (EA), and hydroxyethyl acrylate (HEA) in various blend ratios, methyl acrylate and chitosan. They observed that neural cells attached and differentiate better on chitosan, poly-(methyl acrylate), and the 50% wt copolymer of EA and HEA, which have respectively a very low, very high or intermediate contact angle. They conclude that the biological performance of the biomaterials is modulated more by other material's parameters, rather than correlating directly with the surface wettability (Soria JM 2006).

3.6.2 Stiffness

It has been demonstrated several times that cells can sense the stiffness and acquire different phenotypes depending on the Young modulus. In their natural environment, cells are surrounded by a tissue and each tissue has its specific mechanical properties.

This properties will lead progenitor cells to differentiate in each specific tissue. On this base, Engler et al proved that human mesenchymal stem cells can turn into osteoblast-like or neuron-like cells only varying the stiffness of the presented substrate (**Fig. 29**) (Engler, Sen et al. 2006).

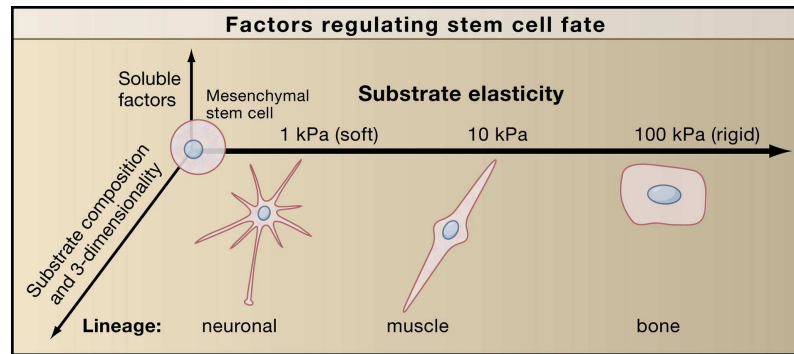


Figure 29. Effect of substrate elasticity on mesenchymal stem cell differentiation. (Engler, Sen et al. 2006)

The preference for soft substrates by neurons was also observed in a study involving adult neural stem cells. Leipzig et al showed that neural stem cells better differentiate into neurons on substrates with stiffness under 1 kPa. Soft substrates also promoted the oligodendrocytes maturation and myelin production. (Leipzig and Shoichet 2009)

Willits and Skornia studied the effects of mechanical stiffness on chick DRG neurons. By varying the concentration of collagen used to gel the matrix, several stiffnesses (2.2–17 Pa) were generated. After 4 days in culture, softer matrices led to longer neurite lengths (Willits and Skornia 2004).

Substrate stiffness can also influence cell type adhesion, as observed in a study by Georges et al (**Fig. 30**). The authors see that on soft gels of polyacrylamide with a shear modulus of 200 Pa, suppression of astrocyte growth appears. Astrocytes on soft substrates exhibit a low attachment and spreading and had a disorganized cytoskeleton. Neuron-glia coculture experiments showed a significantly higher proportion of cortical neurons than astrocytes on the soft gel compared to the hard gel (9 kPa shear modulus) (Georges, Miller et al. 2006).

Moshayedi et al, studied the mechanosensitivity of astrocytes on optimized poly-lysine coated polyacrylamide gels. Quantitative morphometry showed that astrocytes cultured on stiff substrates (shear storage moduli (G') = 10 KPa) were significantly bigger and ramified compared to those cultured on compliant substrates ($G' = 100$ Pa), remarking the importance of substrate stiffness on cell behaviour (Moshayedi, Costa Lda et al. 2012).

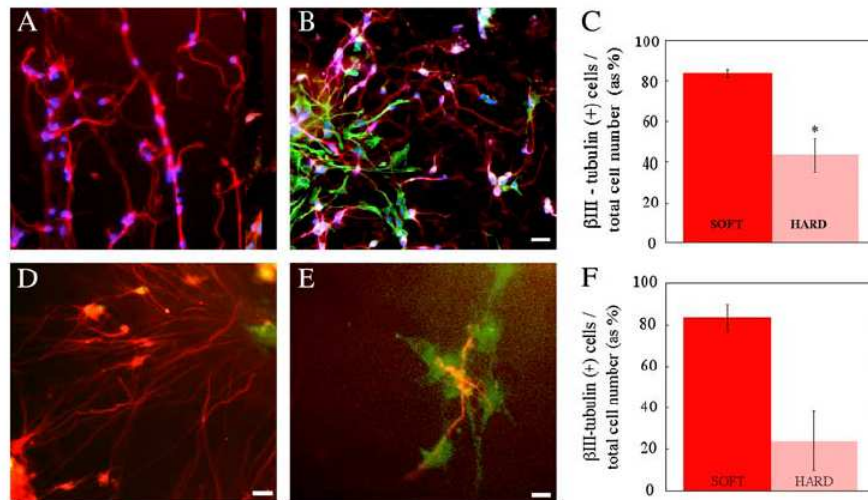


Figure 30. Cultures of dissociated embryonic cerebral cortices at 1 week in vitro on soft (A) and hard (B) polyacrylamide (PA) gels and soft (250Pa)(D) and hard (2,1 kPa) fibrin gels. The prevalence of astrocytes is apparent on hard PA gels and to a lesser extent on hard fibrin gels, which are still much softer than the hardest PA gels. The percentage of total cells on soft PA gels (C) and fibrin gels (F) that were neurons was significantly higher than on hard gels. Red= β III tubulin, neurons; green= GFAP, astrocytes; blue=DAPI, nuclei (Georges, Miller et al. 2006).

3.6.3 Topography

The idea that cells respond to the topography is intuitive and was observed for the first time in 1945, when Paul Weiss described how contact guidance is one of the basic methods by which cells can migrate from their source to their destination (Weiss 1947). Some years later, Curtis et al. used topography to control cell behavior (Curtis 1964). In 1987, Clark and colleagues observed that cell response to line micropatterns was cell type and size dependent. They also observed that chicken neural cells cultured on poly-lysine coated substrates carrying micrometric line patterns extend aligned neurite (Fig. 31).

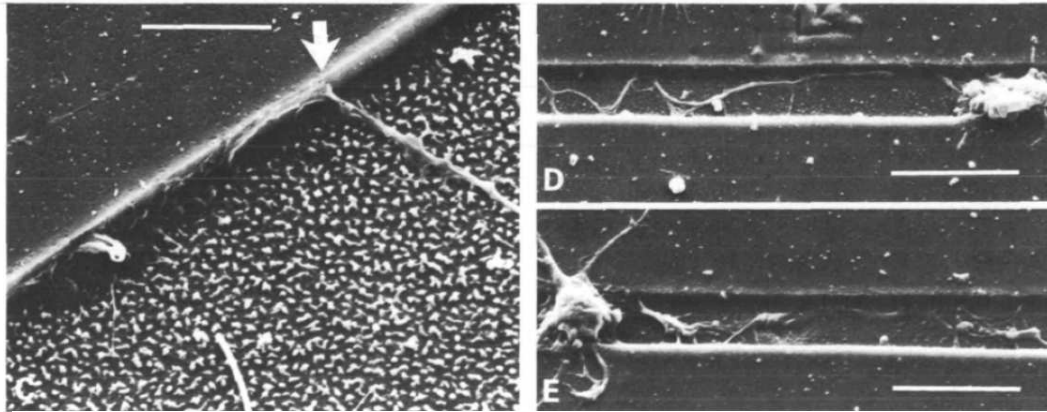
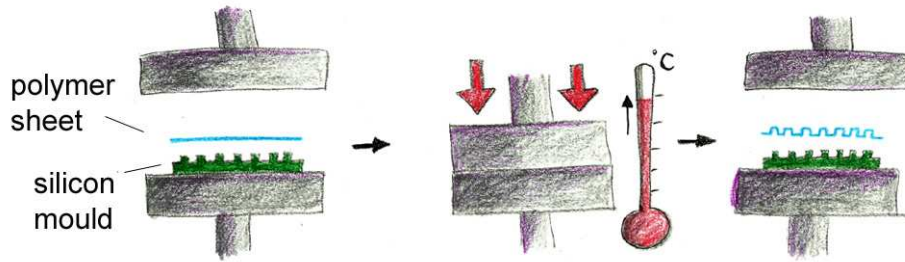


Figure 31. SEM pictures of chick embryo neural cells on poly-lysine coated steps. A-C 4 μ m steps; D,E, 2 μ m deep, 7 μ m wide grooves. Arrow in C indicates the point of encounter of a growing process, the path of the growth cone having been deflected to the left. Bars: A,B, 40 μ m; C 10 μ m; D, E, 20 μ m.

From that time and with the development of nanotechnologies, many advances have been made. Nanotechnologies developed patterning techniques with nanometric resolution. They comprehend lithographic techniques, such as soft lithography and nanoimprinting lithography, used in this thesis work (**Fig. 32**).

The most important *in vitro* studies concerning neuronal cells response to topography have been reviewed by Hoffman-Kim et al. The review gives an exhaustive overview of the methods used to assess neural response to topography, studies *in vitro* employing patterned surfaces, nanofibers and examples *in vivo* using nerve guidance channels (Hoffman-Kim, Mitchel et al. 2010).

Nano imprinting lithography (NIL)



Soft lithography by solvent casting

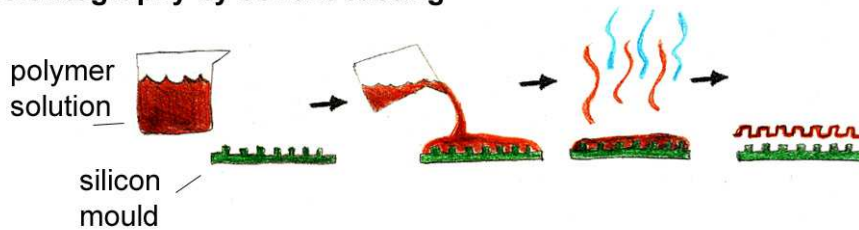


Figure 32. Nano imprinting lithography and soft lithography patterning techniques.

Line patterns can be presented to cells in several ways: these include patterned surfaces, cell inspired surfaces or electrospun fibers. For instance, it has been shown that NPC, Schwann cells and astrocytes orient themselves preferentially along the axis of surface textures. Schwann cells align when cultured on microgrooved chitosan substrates (Hsu, Lu et al. 2007) or on laminin coated patterned PLA films (Miller, Shanks et al. 2001), while Schnell et al. (Schnell, Klinkhammer et al. 2007) reported that cells form dorsal root ganglions (DRG) and olfactory bulb ensheathing cells (OEC) align when cultured on electrospun fibers of meshed poly-3-caprolactone (PCL)-collagen.

4. REFERENCES

- Allen, N. J. and B. A. Barres (2009). "Neuroscience: Glia: more than just brain glue." **457**(7230): 675-677.
- Alvarez-Buylla, A. and D. A. Lim (2004). "For the long run: maintaining germinal niches in the adult brain." Neuron **41**(5): 683-6.
- Amariglio, N., A. Hirshberg, et al. (2009). "Donor-Derived Brain Tumor Following Neural Stem Cell Transplantation in an Ataxia Telangiectasia Patient." PLoS Med **6**(2): e1000029 EP.
- Anderson, S. A., O. Marin, et al. (2001). "Distinct cortical migrations from the medial and lateral ganglionic eminences." Development **128**(3): 353-63.
- Arima, Y. and H. Iwata (2007). "Effect of wettability and surface functional groups on protein adsorption and cell adhesion using well-defined mixed self-assembled monolayers." Biomaterials **28**(20): 3074-3082.
- Asher, R. A., D. A. Morgenstern, et al. (2002). "Versican is upregulated in CNS injury and is a product of oligodendrocyte lineage cells." J Neurosci **22**(6): 2225-36.
- Atala A, L. R., Thomson J, Nerem R (2008). Principles of regenerative medicine, Elsevier.
- Bachoo, R. M., R. S. Kim, et al. (2004). "Molecular diversity of astrocytes with implications for neurological disorders." Proc Natl Acad Sci U S A **101**(22): 8384-9.
- Bandtlow, C. E. and D. R. Zimmermann (2000). "Proteoglycans in the developing brain: new conceptual insights for old proteins." Physiol Rev **80**(4): 1267-90.
- Baptiste, D. C. and M. G. Fehlings (2008). "Emerging drugs for spinal cord injury" Exp Op on Emerg Drugs **13**(1): 63-80
- Barres, B. A. (2008). "The mystery and magic of glia: a perspective on their roles in health and disease." Neuron **60**(3): 430-40.
- Barrias, C. C., M. C. L. Martins, et al. (2009). "The correlation between the adsorption of adhesive proteins and cell behaviour on hydroxyl-methyl mixed self-assembled monolayers." Biomaterials **30**(3): 307-316.
- Baumann, N. and D. Pham-Dinh (2001). "Biology of Oligodendrocyte and Myelin in the Mammalian Central Nervous System " Physiological Reviews **81** (2): 871-927.
- Belachew, S., R. Chittajallu, et al. (2003). "Postnatal NG2 proteoglycan-expressing progenitor cells are intrinsically multipotent and generate functional neurons." J Cell Biol **161**(1): 169-86.
- Bi, B., N. Salmaso, et al. (2011). "Cortical Glial Fibrillary Acidic Protein-Positive Cells Generate Neurons after Perinatal Hypoxic Injury" J Neurosci **31**(25): 9205-9221.
- Buffo, A., I. Rite, et al. (2008). "Origin and progeny of reactive gliosis: A source of multipotent cells in the injured brain." Proc Natl Acad Sci U S A **105**(9): 3581-6.
- Cano, J. A. O. (2011). "Function and regulation of bone morphogenetic protein 7 (BMP7) in cerebral cortex development" Doctoral Thesis, Dep. Experimental Patology and Therapeutics. University of Barcelona.
- Cao, Z., R. J. Gilbert, et al. (2009). "Simple agarose-chitosan gel composite system for enhanced neuronal growth in three dimensions." Biomacromolecules **10**(10): 2954-9.
- Clausen, T. and R. Bullock (2001). "Medical treatment and neuroprotection in traumatic brain injury." Curr Pharm Des **7**(15): 1517-32.
- Coelho, N. M., C. González-García, et al. (2011). "Arrangement of type IV collagen on NH2 and COOH functionalized surfaces." Biotechnology and Bioengineering **108**(12): 3009-3018.
- Costa, S., T. Planchenault, et al. (2002). "Astroglial permissivity for neuritic outgrowth in neuron-astrocyte cocultures depends on regulation of laminin bioavailability." Glia **37**(2): 105-13.
- Crompton, K. E., J. D. Goud, et al. (2007). "Polylysine-functionalised thermoresponsive chitosan hydrogel for neural tissue engineering." Biomaterials **28**(3): 441-9.

Introduction: References

- Cryan, J. F. and A. Holmes (2005). "The ascent of mouse: advances in modelling human depression and anxiety." *J Neurosci* **4**(9): 775-790.
- Culican, S. M., N. L. Baumrind, et al. (1990). "Cortical radial glia: identification in tissue culture and evidence for their transformation to astrocytes." *J Neurosci* **10**(2): 684-92.
- Curtis, V. (1964). "Control of cell behavior: topological factors." *J. Natl. Cancer Inst.* **33**: 15-26.
- Dahl, D., D. C. Rueger, et al. (1981). "Vimentin, the 57 000 molecular weight protein of fibroblast filaments, is the major cytoskeletal component in immature glia." *Eur J Cell Biol* **24**(2): 191-6.
- David F., W. (2008). "On the mechanisms of biocompatibility." *Biomaterials* **29**(20): 2941-2953.
- David, S. and S. Lacroix (2003). "Molecular approaches to spinal cord repair." *Annu Rev Neurosci* **26**: 411-40.
- Di Martino, A., M. Sittinger, et al. (2005). "Chitosan: A versatile biopolymer for orthopaedic tissue-engineering." *Biomaterials* **26**(30): 5983-5990.
- Dityatev, A., C. I. Seidenbecher, et al. (2010). "Compartmentalization from the outside: the extracellular matrix and functional microdomains in the brain." *Trends in Neurosciences* **33**(11): 503-512.
- Doetsch, F., I. Caille, et al. (1999). "Subventricular zone astrocytes are neural stem cells in the adult mammalian brain." *Cell* **97**(6): 703-16.
- Dornish, M., D. Kaplan, et al. (2001). "Standards and guidelines for biopolymers in tissue-engineered medical products: ASTM alginate and chitosan standard guides." *Ann N Y Acad Sci* **944**: 388-97.
- Dours-Zimmermann, M. a. T., K. Maurer, et al. (2009). "Versican V2 Assembles the Extracellular Matrix Surrounding the Nodes of Ranvier in the CNS" *J Neurosci* **29**(24):7731-7742.
- Ellis-Behnke, R. G. and G. E. Schneider (2011). "Peptide amphiphiles and porous biodegradable scaffolds for tissue regeneration in the brain and spinal cord." *Methods Mol Biol* **726**: 259-81.
- Eng, L. F., J. J. Vanderhaeghen, et al. (1971). "An acidic protein isolated from fibrous astrocytes." *Brain Res* **28**(2): 351-4.
- Engler, A. J., S. Sen, et al. (2006). "Matrix Elasticity Directs Stem Cell Lineage Specification." *Cell* **126**(4): 677-689.
- Englund, C., A. Fink, et al. (2005). "Pax6, Tbr2, and Tbr1 are expressed sequentially by radial glia, intermediate progenitor cells, and postmitotic neurons in developing neocortex." *J Neurosci* **25**(1): 247-51.
- Fagel, D. M., Y. Ganat, et al. (2006). "Cortical neurogenesis enhanced by chronic perinatal hypoxia." *Exp Neurol* **199**(1): 77-91.
- Fernandez, J. G., C. A. Mills, et al. (2008). "Micro- and nanostructuring of freestanding, biodegradable, thin sheets of chitosan via soft lithography." *J Biomed Mater Res A* **85**(1): 242-7.
- Fernandez, J. G., C. A. Mills, et al. (2009). "Complex microstructured 3D surfaces using chitosan biopolymer." *Small* **5**(5): 614-20.
- Freeman, M. R. (2010). "Specification and Morphogenesis of Astrocytes" *Science* **330**(6005):774-778.
- Freier, T., H. S. Koh, et al. (2005). "Controlling cell adhesion and degradation of chitosan films by N-acetylation." *Biomaterials* **26**(29): 5872-8.
- Freier, T., R. Montenegro, et al. (2005). "Chitin-based tubes for tissue engineering in the nervous system." *Biomaterials* **26**(22): 4624-32.
- Ganat, Y. M., J. Silbereis, et al. (2006). "Early postnatal astroglial cells produce multilineage precursors and neural stem cells in vivo." *J Neurosci* **26**(33): 8609-21.
- Georges, P. C., W. J. Miller, et al. (2006). "Matrices with compliance comparable to that of brain tissue select neuronal over glial growth in mixed cortical cultures." *Biophys J* **90**(8): 3012-8.
- Giszter, S. F. (2008). "Spinal Cord Injury: Present and Future Therapeutic Devices and Prostheses." *Neurotherapeutics* **5**(1):147-162.

Introduction: References

- Gumera, C., B. Rauck, et al. (2011). "Materials for central nervous system regeneration: bioactive cues." J Mat Chemis **21**(20): 7033-7051.
- Han, S. S., Y. Liu, et al. (2004). "Transplantation of glial-restricted precursor cells into the adult spinal cord: survival, glial-specific differentiation, and preferential migration in white matter." Glia **45**(1): 1-16.
- Harel, N. Y. and S. M. Strittmatter (2006). "Can regenerating axons recapitulate developmental guidance during recovery from spinal cord injury?" Nat Rev Neurosci **7**(8): 603-16.
- Hartgerink, J. D., E. Beniash, et al. (2002). "Peptide-amphiphile nanofibers: A versatile scaffold for the preparation of self-assembling materials" Proceedings Nat Acc Sci **99**(8): 5133-5138.
- Hench, L. L. and J. M. Polak (2002). "Third-Generation Biomedical Materials" Science **295**(5557):1014-1017.
- Hill, C. E., M. S. Beattie, et al. (2001). "Degeneration and sprouting of identified descending supraspinal axons after contusive spinal cord injury in the rat." Exp Neurol **171**(1): 153-69.
- Hoffman-Kim, D., J. A. Mitchel, et al. (2010). "Topography, cell response, and nerve regeneration." Annu Rev Biomed Eng **12**: 203-31.
- Hsu, S.-h., P. Lu, et al. (2007). "Fabrication and evaluation of microgrooved polymers as peripheral nerve conduits." Biomedical Microdevices **9**(5): 665-674.
- Ikeda, O., M. Murakami, et al. (2001). "Acute up-regulation of brain-derived neurotrophic factor expression resulting from experimentally induced injury in the rat spinal cord." Acta Neuropathol **102**(3): 239-45.
- Jain, A., Ravi V. Bellamkonda et al. (2007) "Nano- and Micro-Technology to Spatially and Temporally Control Proteins for Neural Regeneration" BioMEMS and Biomedical Nanotechnology I: 3-22.
- Johansson, F., P. Carlberg, et al. (2006). "Axonal outgrowth on nano-imprinted patterns." Biomaterials **27**(8): 1251-8.
- Kalil, K. and E. W. Dent (2005). "Touch and go: guidance cues signal to the growth cone cytoskeleton." Current Opinion in Neurobiology **15**(5): 521-526.
- Kandel, E. R. S., James H.; Jessell, Thomas M. (2000). Principles of Neural Science Fourth Edition, United State of America: McGraw-Hill.
- Keirstead, H. S., G. Nistor, et al. (2005). "Human Embryonic Stem Cell-Derived Oligodendrocyte Progenitor Cell Transplants Remyelinate and Restore Locomotion after Spinal Cord Injury" J Neurosci **25**(19): 4694-4705.
- Kernie, S. G. and J. M. Parent (2010). "Forebrain neurogenesis after focal Ischemic and traumatic brain injury." Neurobiol Dis **37**(2): 267-74.
- Kriegstein, A. and A. Alvarez-Buylla (2009). "The glial nature of embryonic and adult neural stem cells." Annu Rev Neurosci **32**: 149-84.
- Lane, P. J. R. a. M. A. Rier (2008). "Degeneration, Regeneration, and Plasticity in the Nervous System" Neuroscience in Medicine United States of America:Humana Press.
- Leipzig, N. D. and M. S. Shoichet (2009). "The effect of substrate stiffness on adult neural stem cell behavior." Biomaterials **30**(36): 6867-78.
- Lepekhn, E. A., C. Eliasson, et al. (2001). "Intermediate filaments regulate astrocyte motility." J Neurochem **79**(3): 617-25.
- Li, G. N. and D. Hoffman-Kim (2008). "Tissue-engineered platforms of axon guidance." Tissue Eng Part B Rev **14**(1): 33-51.
- Liu, K., A. Tedeschi, et al. (2011). "Neuronal Intrinsic Mechanisms of Axon Regeneration" Ann Rev Neurosci **34**(1):131-152.
- Liu, Y. and M. S. Rao (2004). "Glial progenitors in the CNS and possible lineage relationships among them." Biol Cell **96**(4): 279-90.
- Llopis-Hernandez, V., P. Rico, et al. (2011). "Role of Surface Chemistry in Protein Remodeling at the Cell-Material Interface." PLoS ONE **6**(5): e19610 EP.

Introduction: References

- Ma, D. K., M. A. Bonaguidi, et al. (2009). "Adult neural stem cells in the mammalian central nervous system." Cell Res **19**(6): 672-682.
- Mao, J. S., Y. L. Cui, et al. (2004). "A preliminary study on chitosan and gelatin polyelectrolyte complex cytocompatibility by cell cycle and apoptosis analysis." Biomaterials **25**(18): 3973-81.
- Marin, C. and E. Fernandez (2010). "Biocompatibility of intracortical microelectrodes: current status and future prospects." Front Neuroeng **28**:3-8.
- Marin, O. and J. L. Rubenstein (2001). "A long, remarkable journey: tangential migration in the telencephalon." Nat Rev Neurosci **2**(11): 780-90.
- Marklund, N. and L. Hillered (2011). "Animal modelling of traumatic brain injury in preclinical drug development: where do we go from here?" Br J Pharmacol **164**(4): 1207-29.
- McDermott, K. W., D. S. Barry, et al. (2005). "Role of radial glia in cytotogenesis, patterning and boundary formation in the developing spinal cord." J Anat **207**(3): 241-50.
- Merkle, F. T. and A. Alvarez-Buylla (2006). "Neural stem cells in mammalian development." Curr Opin Cell Biol **18**(6): 704-9.
- Metin, C., J. P. Baudoin, et al. (2006). "Cell and molecular mechanisms involved in the migration of cortical interneurons." Eur J Neurosci **23**(4): 894-900.
- Meyer, G., J. P. Schaaps, et al. (2000). "Embryonic and early fetal development of the human neocortex." J Neurosci **20**(5): 1858-68.
- Miller, C., H. Shanks, et al. (2001). "Oriented Schwann cell growth on micropatterned biodegradable polymer substrates." Biomaterials **22**(11): 1263-1269.
- Miller, R. H. and M. C. Raff (1984). "Fibrous and protoplasmic astrocytes are biochemically and developmentally distinct." J Neurosci **4**(2): 585-92.
- Ming, G.-I. and H. Song (2005). "Adult neurogenesis in the mammalian central nervous system" Annual Rev Neurosci **28**(1): 223-250.
- Molyneaux, B. J., P. Arlotta, et al. (2007). "Neuronal subtype specification in the cerebral cortex." Nat Rev Neurosci **8**(6): 427-37.
- Moshayedi, P., F. Costa Lda, et al. (2012). "Mechanosensitivity of astrocytes on optimized polyacrylamide gels analyzed by quantitative morphometry." J Phys Condens Matter **22**(19): 194114.
- Mothe, A. J. and C. H. Tator (2005). "Proliferation, migration, and differentiation of endogenous ependymal region stem/progenitor cells following minimal spinal cord injury in the adult rat." Neuroscience **131**(1): 177-87.
- Nisbet, D. R., J. S. Forsythe, et al. (2009). "Review Paper: A Review of the Cellular Response on Electrospun Nanofibers for Tissue Engineering " J Biomat App **24**(1): 7-29.
- Nishiyama, A., M. Komitova, et al. (2009). "Polydendrocytes (NG2 cells): multifunctional cells with lineage plasticity." Nat Rev Neurosci **10**(1): 9-22.
- Noctor, S. C., A. C. Flint, et al. (2001). "Neurons derived from radial glial cells establish radial units in neocortex." Nature **409**(6821): 714-20.
- Noctor, S. C., V. Martinez-Cerdeno, et al. (2004). "Cortical neurons arise in symmetric and asymmetric division zones and migrate through specific phases." Nat Neurosci **7**(2): 136-44.
- Noctor, S. C., V. Martinez-Cerdeno, et al. (2008). "Distinct behaviors of neural stem and progenitor cells underlie cortical neurogenesis." J Comp Neurol **508**(1): 28-44.
- Nomura, H., H. Kim, et al. (2010). "Endogenous radial glial cells support regenerating axons after spinal cord transection." NeuroReport **21**(13): 871-876.
- Nowakowski, R. S. (2006). "Stable neuron numbers from cradle to grave." Proc Natl Acad Sci U S A **103**(33): 12219-20.

Introduction: References

- Oberlaender, M., C. P. J. de Kock, et al. (2011). "Cell type specific three-dimensional structure of thalamocortical circuits in a column of rat vibrissal cortex "Cerebral Cortex doi: 10.1093/cercor/bhr317.
- Ong, J., J. M. Plane, et al. (2005). "Hypoxic-ischemic injury stimulates subventricular zone proliferation and neurogenesis in the neonatal rat." Pediatr Res **58**(3): 600-6.
- Orive, G., E. Anitua, et al. (2009). "Biomaterials for promoting brain protection, repair and regeneration." **10**(9): 682-692.
- Otani, N., H. Nawashiro, et al. (2003). "A role of glial fibrillary acidic protein in hippocampal degeneration after cerebral trauma or kainate-induced seizure." Acta Neurochir Suppl **86**: 267-9.
- Otto, V. I., S. M. Gloor, et al. (2002). "The production of macrophage inflammatory protein-2 induced by soluble intercellular adhesion molecule-1 in mouse astrocytes is mediated by src tyrosine kinases and p42/44 mitogen-activated protein kinase." J Neurochem **80**(5): 824-34.
- Palacio, M., S. Schricker, et al. (2010). "Morphology and protein adsorption characteristics of block copolymer surfaces." Journal of Microscopy **240**(3): 239-248.
- Parnavelas, J. G. (2000). "The origin and migration of cortical neurones: new vistas." Trends Neurosci **23**(3): 126-31.
- Pettikiriachchi, J. T. S., Parish, C. L., Shoichet, M. S., Forsythe, J. S., Nisbet, D. R. (2010). "Biomaterials for Brain Tissue Engineering." J Australian Journal of Chemistry **63**(8): 1143-1154.
- Pollak, A. (2011). "Geron Is Shutting Down Its Stem Cell Clinical Trial" The New York Times. New York: B2.
- Rao, M. S. (1999). "Multipotent and restricted precursors in the central nervous system." Anat Rec **257**(4): 137-48.
- Rao, M. S. and M. Mayer-Proschel (1997). "Glial-restricted precursors are derived from multipotent neuroepithelial stem cells." Dev Biol **188**(1): 48-63.
- Richardson, R. M., D. Sun, et al. (2007). "Neurogenesis after traumatic brain injury." Neurosurg Clin N Am **18**(1): 169-81.
- Richardson, W. D., K. M. Young, et al. (2011). "NG2-glia as multipotent neural stem cells: fact or fantasy?" Neuron **70**(4): 661-73.
- Ridet, J. L., S. K. Malhotra, et al. (1997). "Reactive astrocytes: cellular and molecular cues to biological function." Trends Neurosci **20**(12): 570-7.
- Robel, S., B. Berninger, et al. (2011). "The stem cell potential of glia: lessons from reactive gliosis." Nat Rev Neurosci **12**(2): 88-104.
- Rock, R. B., G. Gekker, et al. (2004). "Role of Microglia in Central Nervous System Infections" Clin Microb Rev **17**(4): 942-964.
- Rowitch, D. H., Q. R. Lu, et al. (2002). "An 'oligarchy' rules neural development." Trends Neurosci **25**(8): 417-22.
- Sahni, V. and J. A. Kessler (2010). "Stem cell therapies for spinal cord injury." Nat Rev Neurol **6**(7): 363-372.
- Saijo, K. and C. K. Glass (2011). "Microglial cell origin and phenotypes in health and disease." Nat Rev Immunol **11**(11): 775-787.
- Saura, J. (2007). "Microglial cells in astroglial cultures: a cautionary note." J Neuroinflammation **4**: 26.
- Schmalenberg, K. E., H. M. Buettner, et al. (2004). "Microcontact printing of proteins on oxygen plasma-activated poly(methyl methacrylate)." Biomaterials **25**(10): 1851-7.
- Schmid, R. S., B. McGrath, et al. (2003). "Neuregulin 1-erbB2 signaling is required for the establishment of radial glia and their transformation into astrocytes in cerebral cortex." Proc Natl Acad Sci U S A **100**(7): 4251-6.
- Schmidt, C. E. and J. B. Leach (2003). "Neural tissue engineering: strategies for repair and regeneration." Annu Rev Biomed Eng **5**: 293-347.
- Schnell, E., K. Klinkhammer, et al. (2007). "Guidance of glial cell migration and axonal growth on electrospun nanofibers of poly-epsilon-caprolactone and a collagen/poly-epsilon-caprolactone blend." Biomaterials **28**(19): 3012-25.

Introduction: References

- Schwark, H. D. and J. Li (2000). "Distribution of neurons immunoreactive for calcium-binding proteins varies across areas of cat primary somatosensory cortex." Brain Research Bulletin **51**(5): 379-385.
- Shekaran, A. and A. J. Garcia (2011). "Nanoscale engineering of extracellular matrix-mimetic bioadhesive surfaces and implants for tissue engineering." Biochim Biophys Acta **1810**(3): 350-60.
- Shibuya, S., O. Miyamoto, et al. (2003). "Temporal progressive antigen expression in radial glia after contusive spinal cord injury in adult rats." Glia **42**(2): 172-83.
- Silva, G. A. (2006). "Neuroscience nanotechnology: progress, opportunities and challenges." Nat Rev Neurosci **7**(1): 65-74.
- Silva, G. A., C. Czeisler, et al. (2004). "Selective differentiation of neural progenitor cells by high-epitope density nanofibers." Science **303**(5662): 1352-5.
- Silva, S. S., J. o. F. Mano, et al. (2010). "Potential applications of natural origin polymer-based systems in soft tissue regeneration" Crit Rev Biotech **30**(3): 200-221.
- Sims, K. D. and M. B. Robinson (1999). "Expression patterns and regulation of glutamate transporters in the developing and adult nervous system." Crit Rev Neurobiol **13**(2): 169-97.
- Soria J.M., M. R. C., Manuel Salmerón Sánchez, et al. (2006). "Survival and differentiation of embryonic neural explants on different biomaterials." J Biomed Mat Res Part A **79A**(3): 495-502.
- Soria J.M., M. R. C., O. Bahamonde et al. (2007). "Influence of the substrate's hydrophilicity on the *in vitro* Schwann cells viability." J Biomed Mat Res Part A **83A**(2): 463-470.
- Stocum, D. L. (2006). Regenerative biology and medicine, Elsevier.
- Stocum, D. L. (2008). "Developmental mechanisms of regeneration." Principles of regenerative medicine. Academic press.
- Tan, A. M., W. Zhang, et al. (2005). "NG2: a component of the glial scar that inhibits axon growth." J Anat **207**(6): 717-725.
- Tohda, C. and T. Kuboyama (2011). "Current and future therapeutic strategies for functional repair of spinal cord injury." Pharmacology & Therapeutics **132**(1): 57-71.
- Tohyama, T., V. M. Lee, et al. (1992). "Nestin expression in embryonic human neuroepithelium and in human neuroepithelial tumor cells." Lab Invest **66**(3): 303-13.
- Tom, V. J., C. M. Doller, et al. (2004). "Astrocyte-associated fibronectin is critical for axonal regeneration in adult white matter." J Neurosci **24**(42): 9282-90.
- Ubersax, L., M. Mattotti, et al. (2007). "Silk fibroin matrices for the controlled release of nerve growth factor (NGF)." Biomaterials **28**(30): 4449-60.
- Vaccarino, F. M., D. M. Fagel, et al. (2007). "Astroglial cells in development, regeneration, and repair." Neuroscientist **13**(2): 173-85.
- Valero-Cabre, A., K. Tsironis, et al. (2004). "Peripheral and spinal motor reorganization after nerve injury and repair." J Neurotrauma **21**(1): 95-108.
- Valverde, F. (2002). "Structure of the cerebral cortex. Intrinsic organization and comparative analysis of the neocortex." Rev Neurol **34**(8):758-80.
- Vitalis, T. and J. Rossier (2011). "New insights into cortical interneurons development and classification: Contribution of developmental studies." Develop Neurobiol **71**(1): 34-44.
- Weiss, P. (1947). "The problem of specificity in growth and development." Yale J. Biol. Med. **19**(3): 235-78.
- White, R. E. and L. B. Jakeman (2008). "Don't fence me in: harnessing the beneficial roles of astrocytes for spinal cord repair." Restor Neurol Neurosci **26**(2-3): 197-214.
- Willerth, S. M. and S. E. Sakiyama-Elbert (2007). "Approaches to neural tissue engineering using scaffolds for drug delivery." Ad Drug Delivery Rev **59**(4-5): 325-338.

Introduction: References

Willits, R. K. and S. L. Skornia (2004). "Effect of collagen gel stiffness on neurite extension." J Biomater Sci Polym Ed **15**(12): 1521-31.

Wilson, J. M. (2009). "A History Lesson for Stem Cells" Science **324**(5928):727-728.

Wong, D. Y., S. J. Hollister, et al. (2007). "Poly(epsilon-caprolactone) and poly (L-lactic-co-glycolic acid) degradable polymer sponges attenuate astrocyte response and lesion growth in acute traumatic brain injury." Tissue Eng. **13**(10):2515-23.

Wyatt Potter, R. E. K., Weiyuan J. Kao (2008). "Biomimetic material systems for neural progenitor cell-based therapy." Frontiers in Bioscience **13**: 806-821.

Zuidema, J. M., M. M. Pap, et al. "Fabrication and characterization of tunable polysaccharide hydrogel blends for neural repair." Acta Biomater **7**(4): 1634-43.

RATIONAL OF THE THESIS & GOALS

1. RATIONAL OF THE THESIS

After a lesion in the CNS, glial cells mediate both the inhibitory and the beneficial response for neural regeneration. Thus, the main working hypothesis of this thesis is that we can induce a favorable environment for CNS regeneration modulating material properties, like wettability and surface topography.

For this purpose, two biopolymers with very different properties were selected. The first one was poly-methylmetacrylate (PMMA), a slightly hydrophobic not biodegradable synthetic polymer, while the second one was chitosan, a hydrophilic biodegradable natural derived material. Line patterns with different dimensions in the micrometric scale were then introduced to the selected materials.

As a biological model, primary neuron and glial cells from mouse cerebral cortex were used. This choice was made because primary cell culture mimics better the reality and mice is widely studied as a model in developmental neurobiology.

2. GOALS

The work is divided in three parts:

1. Assess the effect of PMMA presenting micropatterns on glial cells and neurons;
2. Assess the effect of chitosan presenting micropatterned on glial cells and neurons;
3. Identify key parameters which regulate glial cell response using model surfaces.

RESULTS

In this section are reported the main experimental findings of this thesis work, according to the planned goals.

- In the first session, the effects of PMMA presenting micropatterns on glial cells and neurons are studied;
- The second session treats about the effects of chitosan presenting micropatterns on glial cells and neurons;
- In the third part, key parameters which regulate glial cell response are studied by the aid of model surfaces.

1. INDUCING FUNCTIONAL RADIAL GLIA-LIKE PROGENITORS FROM CORTICAL ASTROCYTE CULTURES USING MICROPATTERNED PMMA

Abstract

Radial glia cells (RGC) are multipotent progenitors that generate neurons and glia during CNS development, and which also served as substrate for neuronal migration. After a lesion, reactive glia are the main contributor to CNS regenerative blockage, although some reactive astrocytes are also able to de-differentiate *in situ* into radial glia-like cells (RGLC), providing beneficial effects in terms of CNS recovery. Thus, the identification of substrate properties that potentiate the ability of astrocytes to transform into RGLC in response to a lesion might help in the development of implantable devices that improve endogenous CNS regeneration. Here we demonstrate that functional RGLC can be induced from *in vitro* matured astrocytes by using a precisely-sized micropatterned PMMA grooved scaffold, without added soluble or substrate adsorbed biochemical factors. RGLC were extremely organized and aligned on 2 μ m line patterned PMMA and, like their embryonic counterparts, express nestin, the neuron-glial progenitor marker Pax6, and also proliferate, generate different intermediate progenitors and support and direct axonal growth and neuronal migration. Our results suggest that the introduction of line patterns in the size range of the RGC processes in implantable scaffolds might mimic the topography of the embryonic neural stem cell niche, driving endogenous astrocytes into a RGLC phenotype, and thus favoring the regenerative response *in situ*.

1.1. Introduction

Despite the presence of multipotent neural stem cells (NSC) in the adult central nervous system (CNS), their ability to regenerate after an injury is very limited and there is currently no effective treatment to improve CNS healing. The formation of a glial scar is one of the most important causes of the lack of spontaneous CNS regeneration. Reactive astrocytes, fibroblasts and other glial cells within the scar produce inhibitory molecules for axon growth (Yiu and He 2006; Fitch and Silver 2008). However, current evidence indicate that astrocytes also play beneficial effects for CNS recovery, as they restart the hemato-encephalic barrier, secrete neurotrophic factors and provide support and guidance for axonal growth (Leavitt 1999; White and Jakeman 2008; Rolls, Shechter et al. 2009) . Moreover, a pool of early reactive astrocytes changes their phenotype adopting many of the molecular traits of embryonic radial glia and NSC (Lang 2004; Buffo 2010). Therefore, a promising strategy can be enhancing the beneficial astrocytic response to obtain a permissive glial environment for neural growth and the re-establishment of functional connections after an injury.

Cell-based approaches to CNS regeneration have had little success, partly because of the limited survival and integration of the implanted cells, which is probably due to the absence of biochemical and topographical cues normally present at the NSC niche. To overcome this problem, the tissue engineering approach aims to provide instructive information to regenerative capable cells through the implantation of intelligent materials that mimic the natural NSC microenvironment. There is increasing evidence that surface topography can modulate the cell response by changing cell morphology and differentiation state. The most recent findings and theories have been elegantly reviewed by Bettinger et al (Bettinger 2009) and Hoffman-Kim (Hoffman-Kim, Mitchel et al. 2010), the latter focusing specifically on nerve regeneration. Among the results they mention, micropatterned or aligned fibers of poly-caprolactone enhanced the differentiation of retinal progenitor cells into neurons and glia (Steedman 2010) or Schwann cells maturation (Chew, Mi et al. 2008), respectively, while the diameter of electrospun fibers influenced NSC differentiation (Christopherson, Song et al. 2009). Furthermore, mature astrocytes have been shown to de-differentiate *in vitro* under

Results: 1. Inducing functional radial glia-like progenitors from cortical astrocytes cultures using micropatterned PMMA

certain specific conditions. For instance, induction of the polycomb transcription factor Bmi1 and exposure to FGF-2 or sulphated hyaluronan can induce stem cell-like features in quiescent astrocytes (Moon, Yoon et al. 2008; Yamada, Sawada et al. 2008). Astrocytes may also de-differentiate by physical methods, such as freeze-thawing (Yu, Cao et al. 2006) or by mechanical and scratch insults (Lang 2004). These findings suggest that differentiated glial cells retain a certain plasticity that might be manipulated to evoke a reparative response to damage by presenting the appropriate signals.

Several recent studies have used micropatterned polymer substrates to direct the growth and differentiation of NSC (Recknor, Sakaguchi et al. 2006). However, glial cells and, in particular, astrocytes are the most likely cell types to contact the material after *in vivo* implant. To identify instructive cues that could induce astrocytes to adopt a radial glia-like phenotype permissive for neural growth, we analyzed *in vitro* the differentiation of glial cells in response to linear patterns imprinted on a substrate of poly(methyl methacrylate) (PMMA).

PMMA is a transparent synthetic material that, thank to its thermoplastic nature, can be structured by hot embossing with high resolution (Mills, Fernandez et al. 2007; Martinez, Engel et al. 2008; Engel, Martinez et al. 2009). It has been used for nerve tissue engineering *in vitro* (Johansson, Carlberg et al. 2006; Martínez-Ramos, Lainez et al. 2008) and has recently been successfully employed for rat sciatic nerve regeneration *in vivo* (Merolli, Rocchi et al. 2009). Here therefore, we used uncoated PMMA films carrying line topographies of different dimensions in order to determine whether the introduction of topographical cues might bias glial differentiation toward a supportive phenotype for neuronal growth.

1.2. Materials and methods

1.2.1 PMMA characterization and microstructuring

Characterization of PMMA wettability was achieved via contact-angle measurements using an OCA 20 system (Dataphysics, GmbH, Germany). Advancing contact angle measurements were taken using 3 μ L Milli-Q water. Four substrates and at least four different measurements were performed on each. Z-potential measurements were carried out using a SurPASS apparatus and VisioLab software (Anton Paar Ltd. - UK). All the measurements were performed four times at the pH of the electrolyte (KCL 1mM, pH 5.5) after 2h of equilibration using the Adjustable Gap Cell for small samples (20 mm x 10 mm).

Micropatterns were introduced on 125 μ m thick PMMA sheets (Goodfellow Ltd., UK) by nano-imprinting lithography (NIL) (Obducat AB, Sweden) and following the protocol described by Mills et al (Mills, Fernandez et al. 2007). Micropatterns consisted of 2 μ m and 10 μ m wide lines (In2 and In10), all 1 μ m deep/tall and 1.5" length. The silicon moulds were provided by AMO GmbH (Aachen, DE) and consisted of 1.5" x 1.5" silicon squares. For cell culture, PMMA films were sterilized with 70% ethanol for 15min and cut to fit in 60mm ϕ tissue culture dishes. The characterization of patterned PMMA films was achieved by white light interferometry (WYKO NT1100 apparatus and the software Vision 32 V2.303 (Veeco Instruments, Inc, USA)).

1.2.2 Cell culture

All animal housing and procedures were approved by the Institutional Animal Care and Use Committee in accordance with Spanish and EU regulations. Glial cells were derived from brain cortex of postnatal mice as described elsewhere (Ortega Cano 2011). Briefly, P0 brain cortices were dissected out free of meninges in dissection buffer (PBS 0.6% glucose (Sigma), 0.3% BSA (Sigma)) and digested with trypsin (Biological Industries) and DNase I (Sigma) for 10 min at 37 $^{\circ}$ C. The tissue was dissociated in Dulbecco's Modified Eagle Medium (DMEM, Biological Industries) 10% normal horse serum (NHS, GIBCO), 1% penicillin-streptomycin (Pen-Strep, Biological Industries), and 2mM L-glutamine (Biological Industries), referred to in this text as growing medium

Results: 1. Inducing functional radial glia-like progenitors from cortical astrocytes cultures using micropatterned PMMA

(GM). After centrifugation and resuspension, cells were plated and grown to confluence at 37° C, 5% CO₂ (approximately 25-30 days *in vitro*, DIV). All the experiments were performed using glial cells from the first passage (Ps1).

To assess the influence of different line topographies on glial cell morphology and differentiation state, Ps1 cells were cultured at a density of 2×10^5 cells/cm² for 5 DIV in Neurobasal™ (NB), 3% NHS, 1% Pen-Strep, and 2 mM L-glutamine (experimental medium = EM) on PMMA In2, In10 or flat (non patterned = NP). To avoid any confusion caused by the heterogeneity of glia culture types described in the literature, we defined three reference conditions within the *in vitro* system used here to compare biochemical changes of glial cells on PMMA. Control glia were Ps1 glial cells cultured on non-coated culture plastic (for Western blotting) or glass (for ICC) under the same conditions as for PMMA. Reactive/mature glia were obtained by culturing Ps1 glial cells for 8 DIV in EM and with EM supplemented with dibutyryl cyclic AMP (dcAMP, 500mM, SIGMA) during 7 more days (Fedoroff 1984; Wu 1998). Progenitor glia were obtained by culturing Ps1 glial cells for 24h in EM and then in NB supplemented with G5 (GIBCO) for 7 DIV. G5 supplement contains mitogens, such as FGF-2 and EGF, and it is used to maintain neural stem cells in culture; it significantly promotes the proliferation of neuronal precursor cells, radial glial cells and astrocytes *in vitro* (Gregg and Weiss 2003; Yu, Cao et al. 2006). The choice of culture conditions for progenitor and reactive glia, and of the EM, was made after numerous preliminary studies using different culture mediums, supplements, serum types and concentrations.

Neurons were obtained from embryonic brains. Brain cortices from E16 mice were isolated in dissection buffer, digested with trypsin-DNAse I, dissociated and preplated for 30 min in preplating medium (CO₂-equilibrated Neurobasal™ supplemented with 5% NHS, 1% Pen-Strep, 0.5 mM L-glutamine, 5.8 µl/ml NaHCO₃ (Sigma-Aldrich, Saint Louis, MO)). The supernatant was then collected, centrifuged and resuspended in serum-free neuronal culture medium (NB, 1% Pen-Strep, 0.5 mM L-glutamine, 1x B27, 5.8 µl/ml NaHCO₃). Neurons were plated at a density of 2.5×10^5 cells/cm², directly on

Results: 1. Inducing functional radial glia-like progenitors from cortical astrocytes cultures using micropatterned PMMA

top of 5DIV glial cell cultures, and then cultured for 5 more days in neuronal culture medium.

Explants were obtained from the cerebral cortex of E16 actin-GFAP transgenic mice. Brains were isolated and then cut into 350µm thick slices with a McIlwain Tissue Chopper (Camden Instruments, UK). Explants of approximately 300 µm diameter were obtained by microdissection, incubated in preplating medium for 1h and seeded on top of glial layers in neuronal culture medium for 2 DIV.

1.2.3 Western blot

Total extract proteins were separated by SDS-polyacrylamide gel and electro-transferred to a nitrocellulose membrane. Membranes were first blocked in 5% non-fat milk and then incubated with primary antibodies overnight at 4° C, followed by their corresponding secondary HRP-conjugated antibodies (1:3000, Santa Cruz Biotechnology, San Diego). Protein signal was detected using the ECL chemiluminescent system (Amersham, Buckinghamshire, UK). Densitometric analysis, standardized to actin as a control for protein loading, was performed using ImageJ software (National Institutes of Health, USA). For quantification, triplicate samples were analyzed.

1.2.4 Immunocytochemistry and primary antibodies

For immunofluorescence, fixed samples (4% PFA for 1h at RT) were incubated with primary antibodies and appropriate Alexa488 or Alexa555 secondary antibodies (1:500, Molecular Probes, Eugene, Oregon). Phalloidin was used to stain F-actin (1:2000, Sigma-Aldrich, Saint Louis, MO) and To-Pro-3 iodide (1:500, Molecular Probes, Eugene, Oregon) to stain nuclei. Finally, the preparations were coverslipped with Mowiol (Calbiochem, San Diego) for imaging.

The following primary antibodies were used: rabbit anti-GFAP (mature and reactive glia marker, 1:500-1:8000, Dako), mouse anti-Vimentin (reactive glia marker 1:1000, Santa Cruz Biotechnology, INC), rabbit anti-EAAT-2 (mature glia marker 1:500, Cell

Results: 1. Inducing functional radial glia-like progenitors from cortical astrocytes cultures using micropatterned PMMA

Signaling) rabbit anti-BLBP (radial glia marker, 1:1000-1:8000, Chemicon), mouse anti-Nestin (progenitor and radial glia marker, 1:250, Abnova Corporation), goat anti-Actin (cytoskeleton Marker, 1:2000, Santa Cruz Biotechnology,INC), mouse anti-Tuj-1 (neuronal marker 1:10000, Covance) and rabbit anti-PH3 (proliferation marker, 1:250, Millipore), goat anti-Pax6 (neurogenic radial glia marker, 1:250, Santa Cruz Biotechnology,INC) and rabbit anti-TBR2 (neurogenic intermediate progenitor cells marker, 1:500, Abcam), rabbit anti-NG2 (oligodendrocytes precursor cells marker, 1:200, Millipore), rabbit anti-Ki67 (proliferation marker, 1:500, Abcam), mouse anti A2B5 (glial precursor cell marker, 1:100, Miltenyi Biotec) and goat anti-Tuj-1 (neuronal marker 1:1000, Covance).

1.2.5 Flow cytometry analysis

The absolute number of living and dead cells was determined at 1-4 DIV by flow cytometry using a FACScalibur apparatus (Becton Dickinson). For absolute live/dead cell number counts we used propidium iodide (PI, Sigma, 5 µg/mL) to label dead cells and CountBright™ absolute counting beads (Molecular Probes, Invitrogen), according to the protocol suggested by the provider. Ps1 cells were cultured at a density of 2×10^5 cells/cm², then trypsinized at 1-4 DIV, and resuspended in 1ml of PBS. Ten thousand CountBright™ counting beads (Molecular Probes, Invitrogen) were recorded and cell populations were determined based on cell size (FSC) and granularity of the cytoplasm (SSC). The cell suspensions were analyzed after PI incubation. Percentage of positive cells and sample relative fluorescence were calculated for each window, as determined by the monoparametric analysis. All the samples were measured in triplicates.

1.2.6 Scanning electron microscopy (SEM)

For SEM imaging, samples were fixed in 2.5% glutaraldehyde in 0.1M PB for 2h at 4°C, washed three times, frozen in liquid nitrogen and dehydrated by freeze-drying over 24h. Then they were gold sputter-coated and observed using a Jeol JSM-6400 scanning electron microscope.

1.2.7 Video time lapse analysis

For video time lapse analysis, neurons were obtained from the cerebral cortex of E16 actin-GFP transgenic mice and cultured on top of pre-seeded glial cells as described above. After 8h, the co-cultured cells were placed in the incubation chamber of an Observer.Z1m inverted fluorescent microscope (Carl Zeiss, USA) at 37 °C with 5% CO₂. Cells were imaged in phase contrast and under 488-nm wavelength light. Pictures were taken every 3 min during 3h. Cell displacement, speed and trajectory were calculated by the aid of the “Manual Tracking” plug in of the ImageJ software (National Institutes of Health, USA).

1.2.8 Imaging and analysis of cell orientation and co-localization

Cells were observed using an Axiovert 40 CFL light inverted microscopy (Carl Zeiss, USA). Digital images were taken throughout experimentation using a digital camera controlled by software. Fluorescent preparations were visualized and micrographs were captured with either a Leica TCS-SL Spectral confocal microscope (Leica Microsystems, Mannheim, Germany) or a Nikon Eclipse 800 light microscope (Nikon, Tokyo, Japan). Images were assembled in Adobe Photoshop (v. 7.0), with adjustments for contrast, brightness and color balance to obtain optimum visual reproduction of data. Morphometric and quantitative image analysis was performed using ImageJ software (National Institutes of Health, USA).

Cell alignment was quantified using the FTT-Oval Profile method described previously by Alexander et al. (Alexander, Fuss et al. 2006). This method generates plots that represent alignment by a peak at 90° and randomness by a flat line. To this end, astrocytes stained for actin, BLBP and GFAP were considered. Neuron-glia co-localization was quantified using the Intensity Correlation Analysis plug-in on pictures of glial cells stained with BLBP and neurons stained with Tuj1. Co-localization was represented by Pearson’s correlation coefficient (Rr), whose values range between 1 and -1, where 1 represent maximal co-localization and -1 maximal exclusion (Comeau, Costantino et al. 2006). Axon alignment from brain explants was analyzed fitting a line along the emitted axons, measuring their angles and plotting their relative frequencies.

The percentage of immunoreactive cells for the distinct differentiation markers was calculated with respect to the total number of cell nuclei stained with TO-PRO-3. Cells were counted manually on a minimum of 10 pictures for each condition.

1.2.9 Statistical analysis

Statistical analysis was performed using the Statgraphic-plus software. One-way ANOVA and Fisher's least significant difference (LSD) procedure were used to discriminate between the means.

1.3. Results

2.3.1 Glial cell orientation and morphology

Besides their distinct composition, glass PMMA and culture plastic (polypropylene) are harder than brain and considered stiff substrates (<http://matbase.com>; <http://goodfellow.com>). PMMA and glass were slightly hydrophobic and negatively charged (contact angle: $76^{\circ}\pm 4$ and 73° ; Z potential: $-45\pm 5\text{mV}$ and $-80\pm 14\text{mV}$ respectively), while tissue culture treated polystyrene was slightly hydrophilic and negatively charged (van Kooten, Spijker et al. 2004).

The choice of the pattern type and dimension was taken after an initial screening of different geometries (lines and posts) and width (2, 5, 10 and $20\mu\text{m}$) based on previous studies involving the alignment of osteoblast-like cells (Mills, Fernandez et al. 2007), and mesenchymal stem cells (Martinez, Engel et al. 2008). Glial cells spread in posts (not shown) and aligned in lines of all sizes. Glial cells on $2\mu\text{m}$ lines exhibit better alignment and higher nestin expression than in $10\mu\text{m}$ and $20\mu\text{m}$ lines were they behave similarly. Thus, lines of $2\mu\text{m}$ and $10\mu\text{m}$ were selected for the present study. The replication of micropatterns on PMMA was confirmed by white light interferometry imaging (**Fig. 1**). Height and width of both $2\mu\text{m}$ and $10\mu\text{m}$ line patterns were replicated faithfully (ln2: height $0.76\pm 0.3\mu\text{m}$, width $1.92\pm 0.2\mu\text{m}$; ln10: height $0.97\pm 0.02\mu\text{m}$, width $9.9\pm 0.31\mu\text{m}$; n=5).

Results: 1. Inducing functional radial glia-like progenitors from cortical astrocytes cultures using micropatterned PMMA

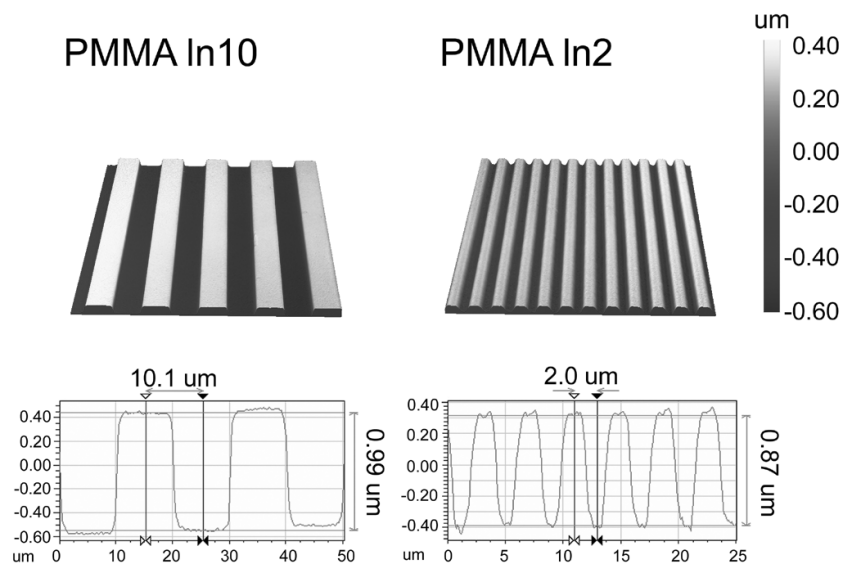


Figure 1: White light interferometer 3D images and profiles of 10 μm and 2 μm patterned PMMA.

Using E16 primary neuronal cultures we determined that neurons do not attach to uncoated PMMA films, glass or culture plastic (not shown). By contrast, primary glial cultures from P0 cortices attached and grew on uncoated PMMA, glass and culture plastic. Cells were then stained with phalloidin or actin antibodies for morphometric analysis. Glial cells grown in the control condition (glass and culture plastic) adopted a flattened and well-spread morphology, with the occasional presence of elongated, bipolar or small ramified cells (**Fig. 2A**). In the presence of dcAMP, the reactive/mature condition, glial cells acquired a stellar morphology with a highly ramified cytoskeleton characteristic of reactive glia (**Fig. 2B**), while cells grown in the progenitor condition were elongated and bipolar with reduced cytoplasm, a morphology that resembles radial glia and progenitor cells (**Fig. 2C**). On flat PMMA, as in controls, well-spread astrocytes, small ramified cells and bipolar radial glia-like cells (RGLC) were present (**Fig. 2D**). However, the branched cytoskeleton arrangements typical of reactive glia were not observed. In the presence of grooved topographies, glial cells adopted elongated shapes resembling RGLC and aligned following the pattern (**Fig. 2E-F**).

Results: 1. Inducing functional radial glia-like progenitors from cortical astrocytes cultures using micropatterned PMMA

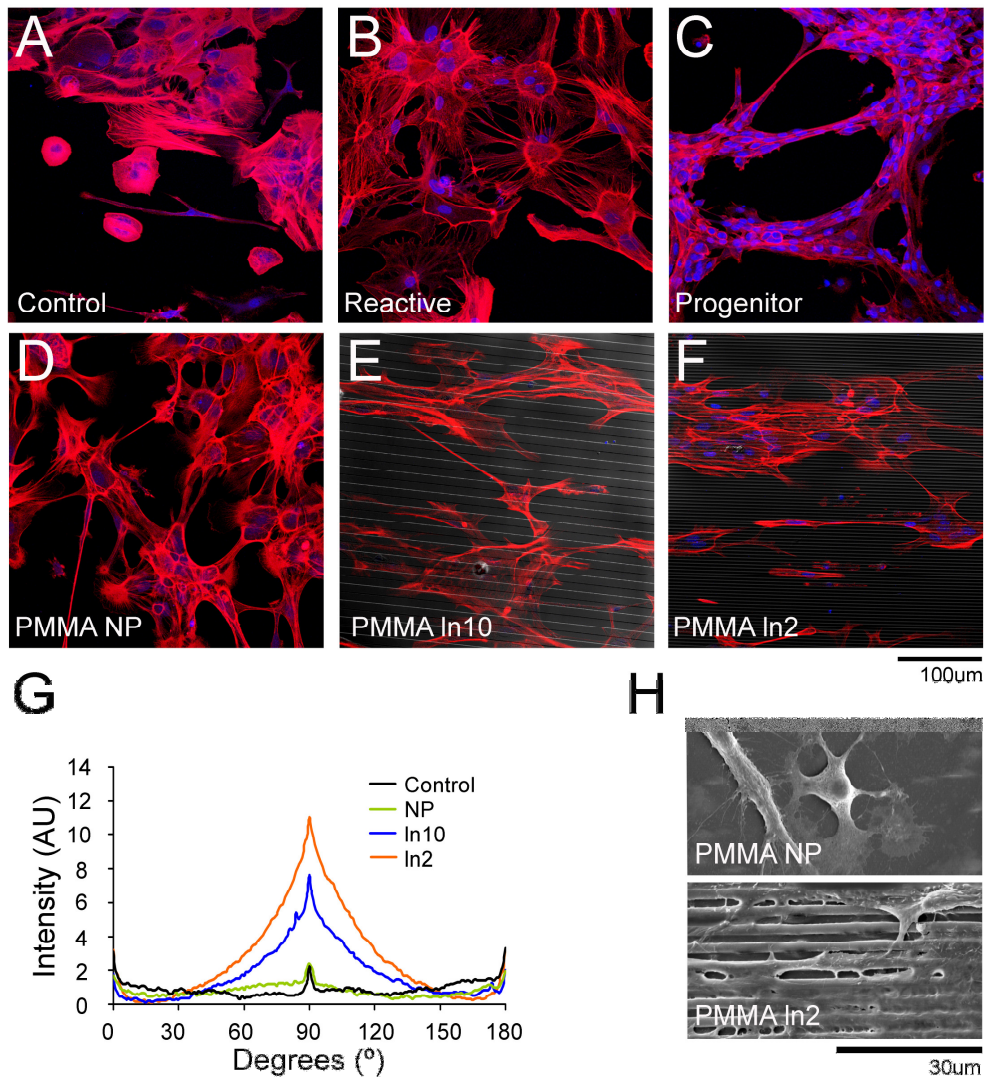


Figure 2: Effect of PMMA and micropattern on glial cells morphology and orientation. A-F, Confocal images of actin staining (phalloidin, red) and nuclei (TO-PRO-3, blue). G, Graphic representing cell alignment by FTT-Oval profile measurement. Flat line indicates random distribution; peak at 90° indicates alignment parallel to the topography. H, SEM pictures of glial cells on NP and 2 μm lines PMMA. Scale bar A-F= 100 μm; Scale bar H = 30 μm. ** indicates statistical significance respect to control $p \geq 0.001$.

FTT- Oval Profile analysis demonstrated that the alignment was better on In2 than on In10 (**Fig. 2G**), which is represented by a higher peak at 90°. SEM images revealed that elongated glial cells extended their processes, with a preference towards the mesa of the topography. They grew on top of the pattern and covered the grooves only in the case of higher cell density (**Fig. 2H**).

1.3.2 Biochemical characterization of glial cells

In order to determine whether micropatterns can induce RGLC we characterized glial cultures by immunocytochemistry and Western blot. Glial cultures were immunostained with antibodies against GFAP and BLBP to identify astrocytes, and against nestin to identify progenitors and radial glia-like cells (Fig. 3). Astrocytes expressing GFAP predominated in the reactive, control, NP and In10 PMMA conditions (78±10%, 75±13%, 89±9%, 81±11% respectively), while they were reduced in progenitor and In2 PMMA conditions (25±3% and 45±7% respectively). BLBP+ astrocytes predominated in the progenitor condition (93±11%), being less abundant in the reactive, control, NP, In10 and In2 PMMA (61±17%, 69±13%, 63±21%, 65±6% and 68±4% respectively). Many astrocytes expressed both GFAP and BLBP and when we analyzed their morphology, the number of bipolar cells was significantly increased in the In2 and In10 PMMA conditions (43±17% and 27±7% respectively) with respect to NP PMMA and control conditions (17±3% and 16±11% respectively). Nestin+ progenitors were scarce in the control and reactive conditions (26±8% and 23±1% respectively), they were abundant in the progenitor condition (81±6%) and intermediate levels were found in NP, In10 and In2 PMMA (35±11%, 33±16% and 55±18% respectively).

Results: 1. Inducing functional radial glia-like progenitors from cortical astrocytes cultures using micropatterned PMMA

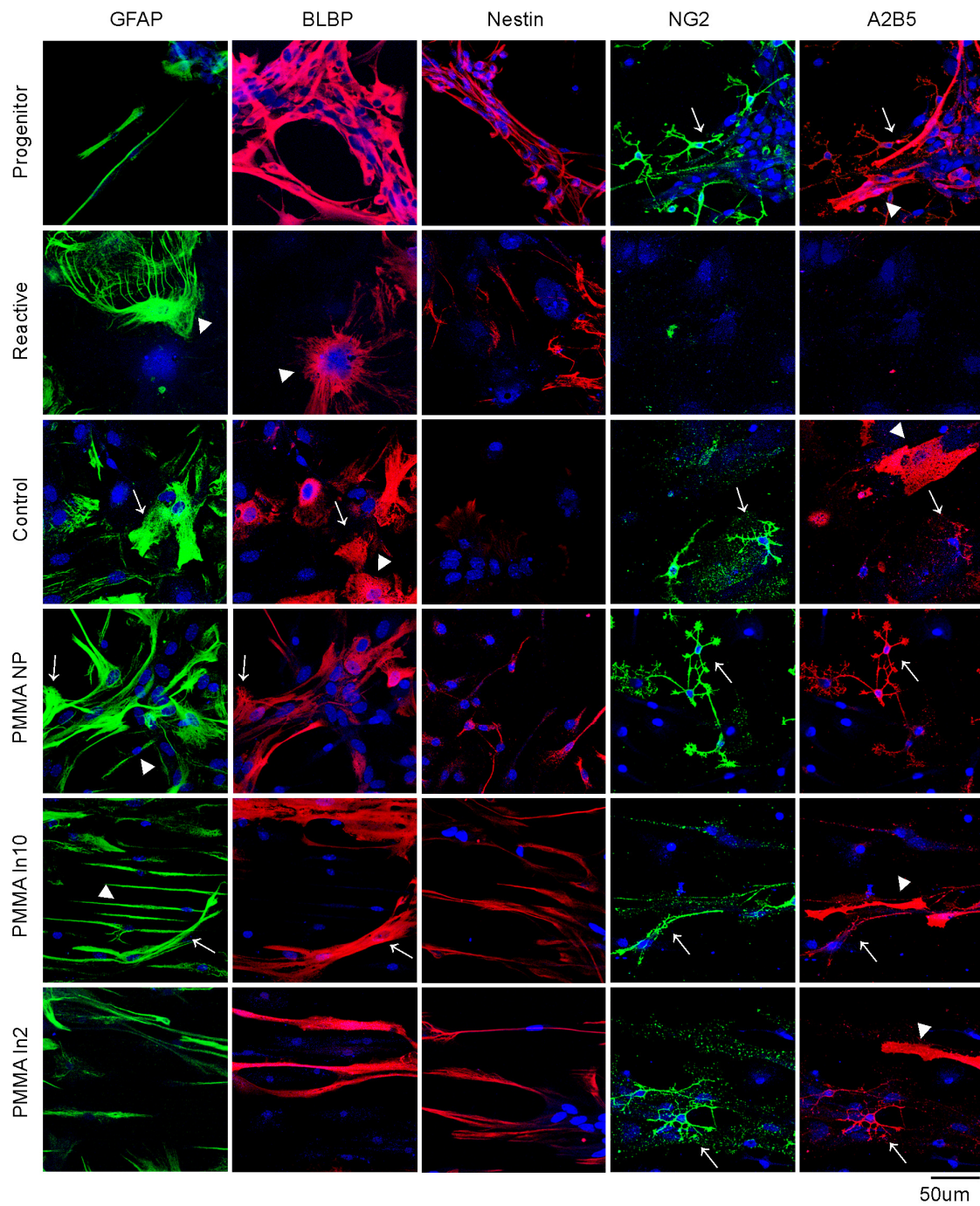


Figure 3: Cellular composition of glial cultures. Confocal images of glial cells immunostained for different glial and progenitor markers: GFAP and BLBP for astroglia, Nestin for progenitors, and NG2 and A2B5 for different glia restricted progenitors. Nuclei are stained with TO-PRO-3 (blue). Scale bar = 50µm.

Results: 1. Inducing functional radial glia-like progenitors from cortical astrocytes cultures using micropatterned PMMA

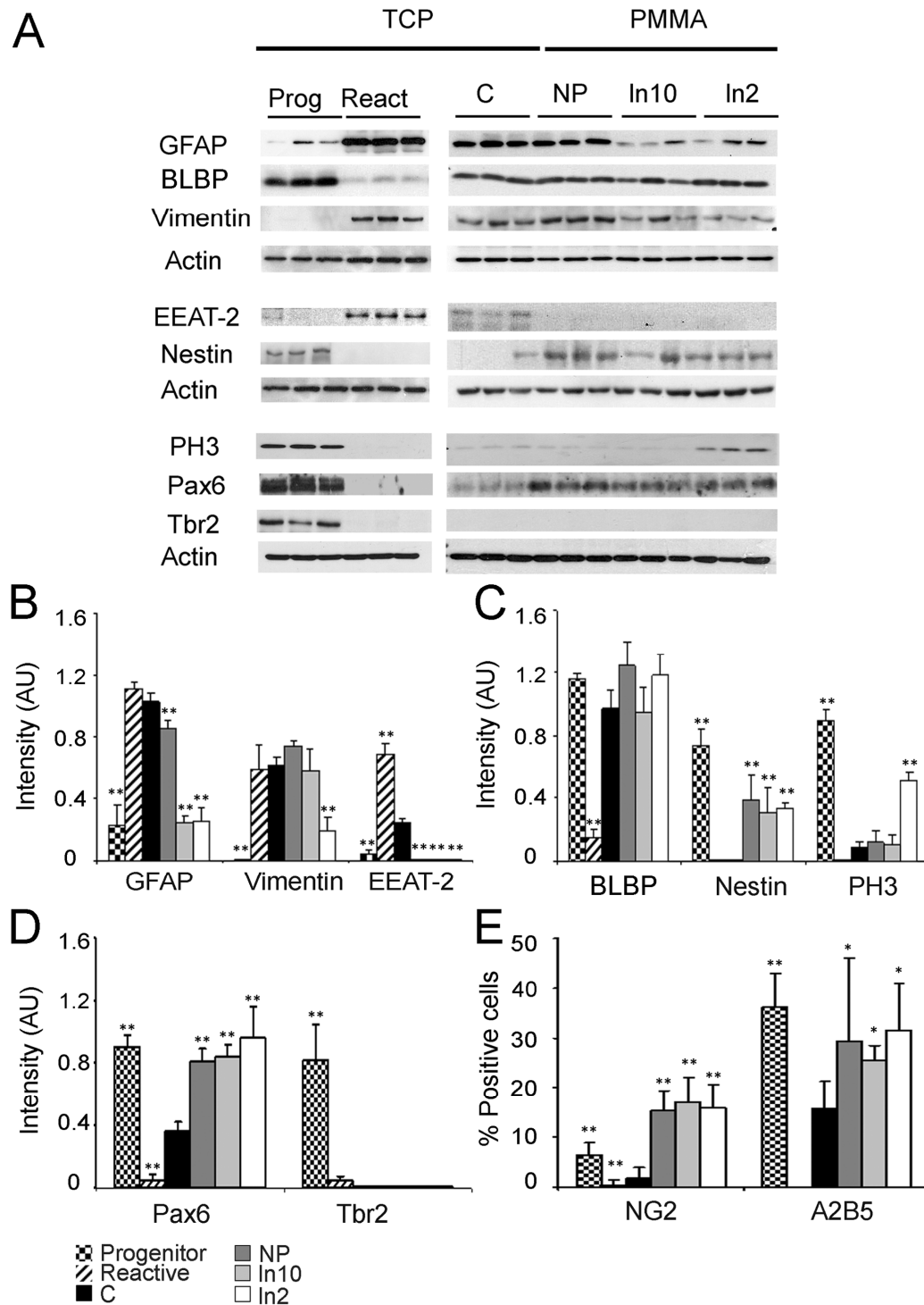


Figure 4: Biochemical characterization of glial differentiation. A, Western Blots showing the expression of different progenitors and glial differentiation markers. B-D, Quantitative representation of the western blot densitometry (intensity values normalized to actin) grouped by categories: B, mature and reactive glial markers (GFAP, Vimentin and EAAT-2); C, progenitor glial markers (BLBP, Nestin and PH3); and D, neurogenic progenitor markers (Pax6 and Tbr2). E, Graph representing the percentage of immunoreactive cells for glial restricted progenitors markers (NG2 and A2B5) respect the total number of cells by unit area. Prog = progenitor; React = reactive glia; C = control (tissue culture plate); NP = no patterned PMMA; In10 = 10 μ m line patterned PMMA; In2 = 2 μ m line patterned PMMA. ** indicates statistical significance respect to control $p < 0.01$.

Results: 1. Inducing functional radial glia-like progenitors from cortical astrocytes cultures using micropatterned PMMA

Western blotting was then used to quantify the relative proportion of the different cell types and their maturation state (**Fig. 4A**). Densitometry analysis revealed that when glial cells were grown in the progenitor condition the expression of immaturity markers, such as nestin, and the mitotic marker PH3 dramatically increased with respect to the control, while maturity and reactive markers such as GFAP, vimentin, and the glutamate transporter EAAT-2 were markedly reduced. By contrast, the opposite was observed in the reactive condition where EAAT-2 increased while immature and progenitor markers dramatically decreased with respect to control (**Fig. 4B, C**). Glial cells grown on PMMA increased the expression of immaturity markers while maturation markers decreased. The induction of a progenitor-like phenotype was more dramatic on In2 PMMA, where proliferation (identified by PH3 expression) was also increased (**Fig. 4B, C**).

To investigate whether gliogenic or neurogenic progenitors were favored by the micropattern, we analyzed by Western blot the expression of several lineage-specific markers. Pax6 homeodomain transcription factor was used to identify radial glia-like cells that can produce neurons and glia, along with Tbr2, a T-domain transcription factor expressed by intermediate progenitors that produce only neurons, and Tuj-1, a neuronal tubulin expressed by postmitotic neurons (Englund, Fink et al. 2005). Tuj-1 expression was never found in our glial cultures, indicating the absence of differentiated neurons (not shown). Pax6 expression was induced by culture in the progenitor condition and by PMMA whereas Tbr2 expression was only induced by culture in the progenitor condition (**Fig. 4A, D**).

We then analyzed whether the use of PMMA substrates favored the development of specific subpopulations of glial progenitors. A2B5 ganglioside is a marker of glial-restricted progenitors, Olig2 is a helix-loop-helix transcription factor that is early expressed by oligodendrocyte progenitors, while NG2 proteoglycan is expressed by the recently described NG2 glia, a progenitor cell type that can generate oligodendrocytes and protoplasmic astrocytes (Zhu 2008). Olig2 was not detected by Western blot or ICC in our culture conditions (not shown), while A2B5 and NG2 could only be detected by

Results: 1. Inducing functional radial glia-like progenitors from cortical astrocytes cultures using micropatterned PMMA

ICC. A2B5+ glia-restricted progenitors were mostly small bipolar or multipolar cells, although large and elongated flat cells were also occasionally seen. They were abundant in glial cultures grown in the progenitor condition and on Ln2 PMMA ($36\pm 6,8$ and $30,5\pm 5$ respectively), less frequently seen in control or on flat and Ln10 PMMA ($21,4\pm 8,7$; $21,3\pm 5,6$ and $25,1\pm 6,9$ respectively) and absent in the reactive condition (0 ± 0). NG2+ progenitors were small bipolar or mostly multipolar cells, and double labeling studies revealed that most of them were also A2B5 positive. NG2 cells were rare in the control and reactive conditions ($1,7\pm 2,2$ and $0,5\pm 0,9$ respectively), whereas their number increased significantly in the progenitor condition ($6,4\pm 2,4$) and even greatly on PMMA (flat $15,3\pm 4,1$; Ln10 $17,2\pm 5,1$; Ln2 $15,9\pm 4,6$) (**Figs. 3, 4E**). Taken together these data suggest that PMMA and more dramatically Ln2 PMMA induce RGLC and progenitor phenotypes on glial cultures.

1.3.3 Glial cell differentiation on patterned PMMA

Ln2 PMMA substrate might induce RGLC through different mechanisms. RGLC might be: 1) the progeny of RGC that contaminated the initial culture; 2) the result of cell selection through induced death of particular cell sub-populations; or 3) the product of the de-differentiation of mature astrocytes. Therefore, we analyzed the level of cell death and total number of cells in glial cultures grown in control and Ln2 PMMA conditions from 1 to 4 div. The total number of cells during the 4 days period analyzed remains almost constant in controls while was slightly reduced at day 4 in Ln2 PMMA (**Fig. 5A**). Only minor differences were found between control and Ln2 PMMA substrates at 1 and 4 div. Cell number doubling was not achieved in this 4 days period in neither condition, a result that is concordant with the cell cycle asynchronicity and extremely low proliferation rates observed in our primary culture conditions. The number of dead cells labeled with PI was low and decreased with time, between 9% (control) and 12% (Ln2 PMMA, $p < 0.05$) at day 1, and between 2% (control) and 3% (Ln2 PMMA) at day 4 (**Fig. 5B**). These small changes in cell death and proliferation suggest that the most probable source of RGLC in Ln2 PMMA is the de-differentiation of mature astrocytes.

Results: 1. Inducing functional radial glia-like progenitors from cortical astrocytes cultures using micropatterned PMMA

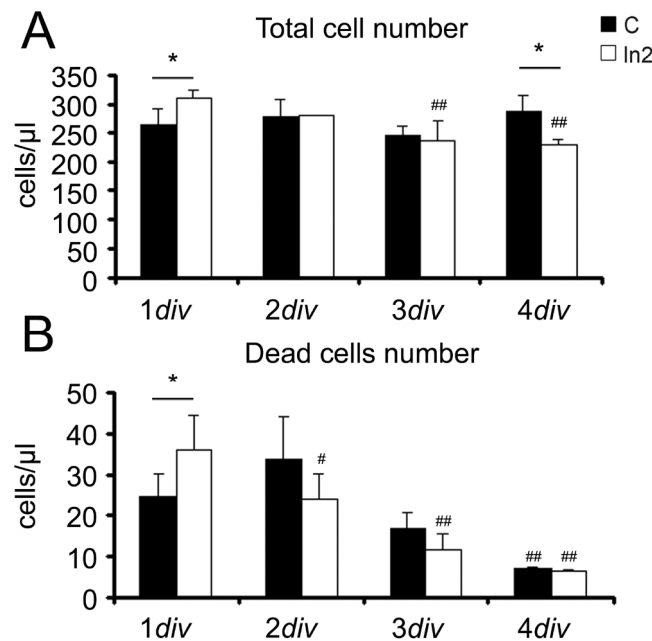


Figure 5: Graft from flow cytometry analysis showing the evolution of the total cell number and dead cell number on control and PMMA Ln2 during 4 days. * indicates statistical significance between control and PMMA Ln2, $p < 0.05$; # indicates statistical significance with respect to 1div in each substrate, # $p < 0.05$, ## $p < 0.01$.

1.3.4 Neuronal adhesion and migration on topography-modified glial cells

In the developing CNS newborn neurons attach to radial glia which is the main substrate for neuronal migration. Thus, we then analyzed the neuronal supportive behavior of RGLC induced by PMMA substrates. To determine whether oriented RGLC can direct neuronal migration and neurite growth, explants from E16 cerebral cortex were grown on top of aligned (Ln 2 PMMA) or random (NP PMMA) glial cells.

After 36–48 h axons and some neurons were able to migrate outside the explants. Neuronal outgrowth was radial when grown in random oriented glia with only the 14% of axons aligned (**Fig. 6A, C**), while on Ln2 PMMA they follow the pattern of the aligned glia underneath, with the 80% of axons having an angle less than 20° (**Fig. 6B, D**). In addition to fibers, neurons also abandoned the explants in some cases, migrating on the aligned glia (**Fig. 6E, F**).

Results: 1. Inducing functional radial glia-like progenitors from cortical astrocytes cultures using micropatterned PMMA

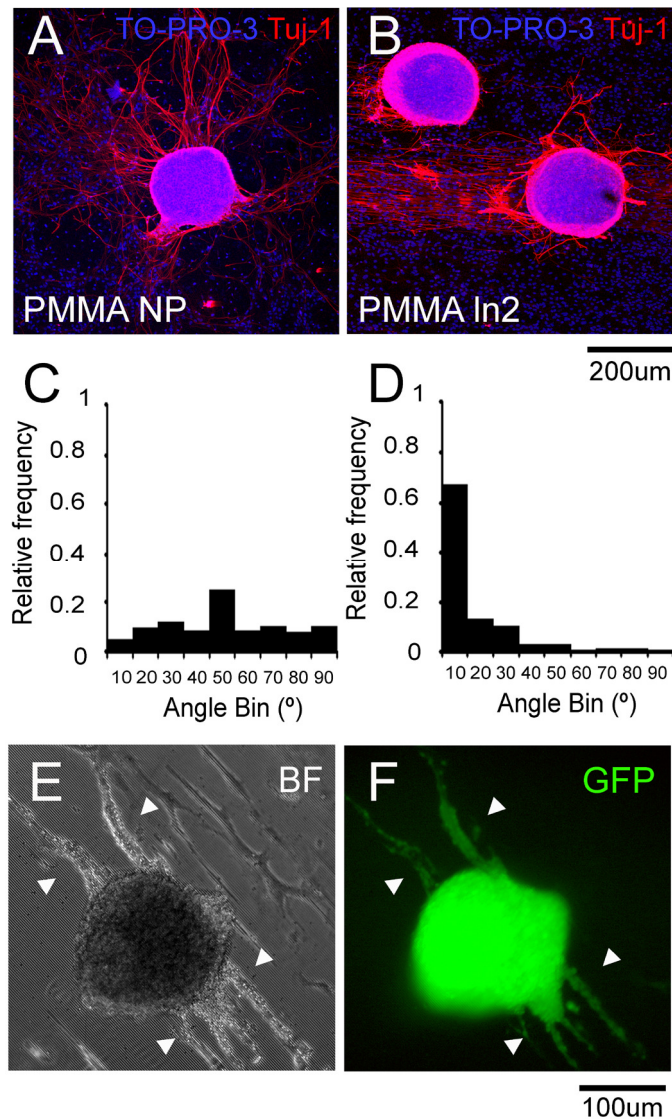


Figure 6: Effect Role of pattern-induced RGLC in neural growth and axonal guidance. A, B, Images showing explants from E16 cerebral cortex cultured on glial cells grown on NP PMMA (A) or Ln2 PMMA (B). Cell nuclei are marked with TO-PRO-3 (blue) and neurons with Tuj-1 antibody (red). Frequency plots representing axonal outgrowth orientation on PMMA NP (C) and PMMA Ln2 (D) substrates. E-F, explants from E16 GFP mice cerebral cortex seeded on top of on glia grown on PMMA Ln2. E = bright field and F = GFP fluorescence. Neurons exiting from the explants are identified by GFP expression. Scale bars = 200µm (A, B); 100 µm (E, F).

To corroborate whether topography induced RGLC support and directed neuronal migration we used video time lapse microscopy. Glial cultures from wild type mice were first grown on control (uncoated glass) and Ln2 PMMA for 5 DIV, and dissociated E16 neurons from actin-GFP transgenic mice were then seeded on top of them in serum free neuronal medium. After 8 h, neurons were attached to the subjacent glia and the co-cultures were then placed in the microscope incubation chamber and

Results: 1. Inducing functional radial glia-like progenitors from cortical astrocytes cultures using micropatterned PMMA

recorded every 3 min for 3h. In the control conditions GFP+ neurons remained static or exhibited a minimal random movement with an average speed of $14 \pm 12 \mu\text{m/h}$ ($n=24$), and final displacement of $7 \pm 6 \mu\text{m}$ (**Fig. 7A, C, G**). On In2 PMMA neurons migrate for relative long distances on RGLC ($37 \pm 23 \mu\text{m}$) with an average speed of $39 \pm 11 \mu\text{m/h}$ ($n=24$) (**Fig. 7B, D, E**). Neurons moved along the RGLC, and in some cases, they reverted their direction of movement when they reach the end of the RGLC.

To discard the possibility that the neuronal cultures provided RGC that act as substrates for migration, WT glial co-cultures with GFP neurons were left for a further 5 *div*, fixed and stained for BLBP to identify the origin of glial cells (**Fig. 7F, G**). In both control and In2 PMMA conditions, neurons were GFP+ and almost all BLBP+ glial cells were negative for GFP. This data indicate that embryonic neuronal dissociates does not provide a significant number of glial cells. After 5div, in the control condition BLBP+ glial cells were flattened and well spread and GFP+ neurons were well developed and exhibited ramified dendritic branches (**Fig. 7F**). However, in In2 PMMA glial cells were elongated and GFP+ neurons were mostly bipolar, oriented along the BLBP+ RGLC processes and with few or none dendritic branches (**Fig. 7G**). In both conditions, Z reconstruction showed that neurons grew on the top of glial cells. To quantify the differences in neuron-glia attachment we stained WT co-cultures with Tuj-1 and BLBP. Then we measured the degree of Tuj-1/BLBP co-localization, using the intensity correlation analysis 5 days after the neuronal seeding. The degree of co-localization can be calculated according to the value of Pearson's coefficient (R_r), where R_r equal to 1 indicates maximal co-localization and R_r of -1 indicates maximal exclusion. Glia-neuron co-localization was significantly higher in In2 PMMA culture ($R_r: 0.59 \pm 0.11$) than in control ($R_r: 0.15 \pm 0.08$) (**Fig. 7H-J**). Taking together, those results indicate that In2 PMMA-induced RGLC recapitulates the functions of embryonic RG, providing a good substrate for neural attachment and promoting directional neuronal migration.

Results: 1. Inducing functional radial glia-like progenitors from cortical astrocytes cultures using micropatterned PMMA

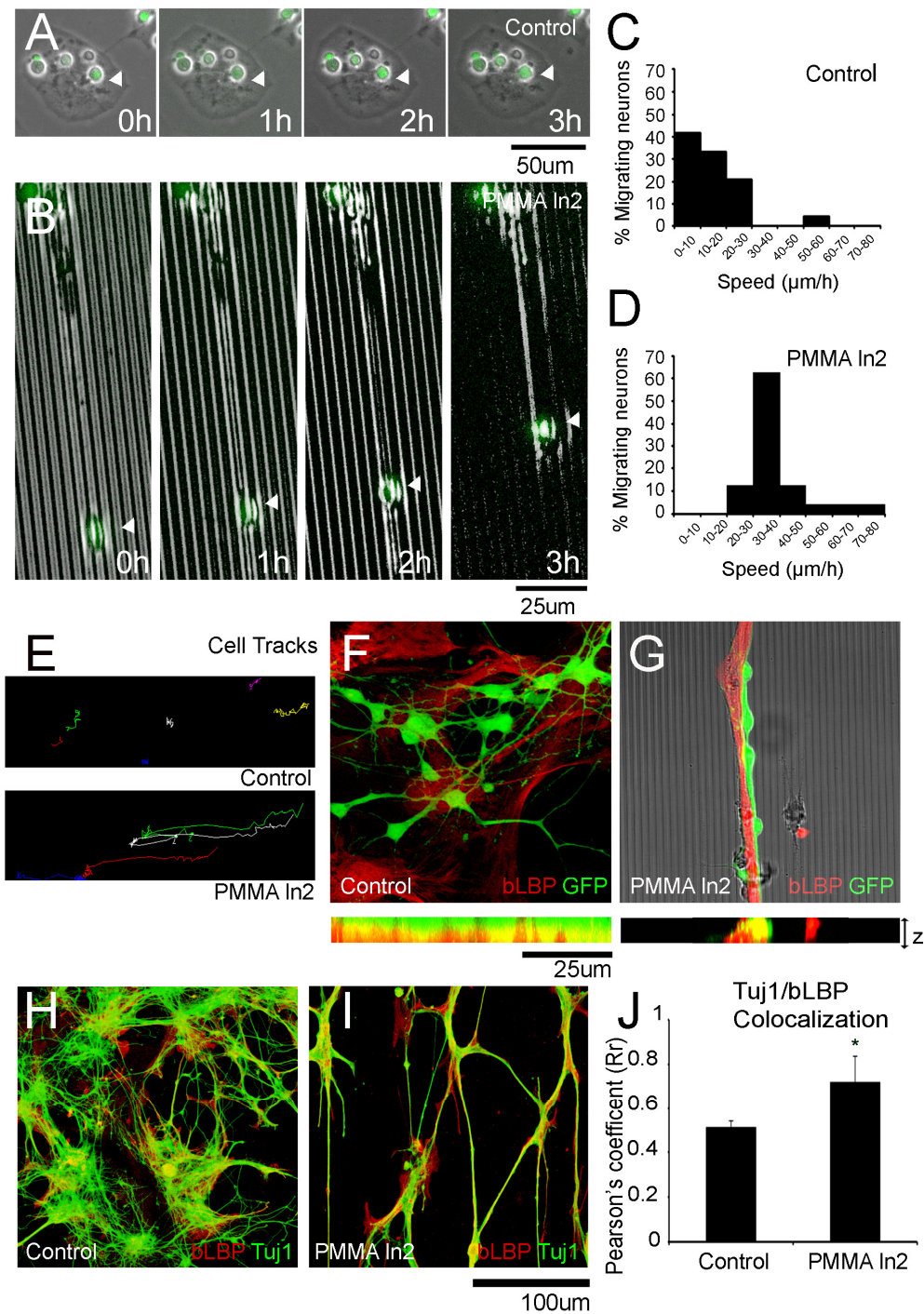


Figure 7: Role of pattern- induced RGLC in neural migration. Representative time lapse images of E16 GFP neurons (green) seeded on glial cells grown on control (A) and In2 PMMA (B) of glial cells (bright field). White arrows indicate the position of a representative neuronal body showing its stativity on control condition (A) and its migration on In2 induced RGLC process (B). C-D, Frequency plot showing the distribution of the speed ($\mu\text{m/h}$) of migrating neurons ($n=24$) in control and In2 PMMA conditions. E, Particle tracks showing neuronal trajectories in control and Ln2 PMMA during a 3h record. F-G, GFP neurons (green) grown on WT glial cells stained with BLBP (red) after *5div* in control (F) and In2 PMMA (G) and their Z projections. H-I, neurons labeled with Tuj1 (green) grown on glial cells labeled with BLBP (red) in control (H) and In2 PMMA (I) substrates. (J). Graph representing the Pearson's coefficient for neuron/glia co-localization in those cultures. $0 \leq Rr \leq 1$, where 1= max colocalization and 0= maximal exclusion. ** indicates statistical significance, $p < 0.01$. Scale bar = $100\mu\text{m}$. Scale bars (A) = $50\mu\text{m}$; (B, F, G) = $25\mu\text{m}$; (E) = $20\mu\text{m}$; (H, I) $100\mu\text{m}$.

1.4. Discussion

Although glial cells have long been regarded as responsible for the lack of CNS regeneration, due to the formation of the non-permissive glial scar, it is now clear that they are also beneficial and may play an active role in the induction of neurogenesis from adult neural stem cells (Song, Stevens et al. 2002; Vaccarino, Fagel et al. 2007; Buffo 2010). During embryonic development, radial glia generate directly or indirectly most CNS neurons (Kriegstein and Alvarez-Buylla 2009), while at the end of neurogenesis most radial glia transform into parenchymal astrocytes (Voigt 1989), and also originate the adult neural stem cells (Alvarez-Buylla, Garcia-Verdugo et al. 2001; Chojnacki 2009). The direction of differentiation can be partially reverted after a lesion *in vivo*, and some astrocytes can de-differentiate into a radial glia-like phenotype that supports the migration of embryonic transplanted neurons (Leavitt 1999). On this basis, a recent experimental strategy for CNS regeneration is to develop mechanisms that restore the embryonic radial glia neurogenic competence into parenchymal astrocytes (Berninger 2010; Costa 2010). Extracellular stimuli, including soluble and adhesive factors *in vivo* and in culture media are important modulators of glial cell phenotype and function (Discher 2005; White and Jakeman 2008). However these factors are usually derived from animal sources, they are expensive, and it is difficult to control their optimum concentration and side effects. Recent evidence claims that topographical cues cause changes in cell phenotype (Thompson and Buettner 2001; Recknor, Recknor et al. 2004; Yang, Co et al. 2005; Martinez-Ramos, Lainez et al. 2008). For instance, Evelyn K.F. Yim et al., promoted hMSC transdifferentiation into neuronal lineages using a collagen coated PDMS carrying line patterns of 350nm (Yim 2007) , while MR Lee et al. obtained the same from hESC (Lee 2010). Thus it can be assumed that by providing appropriate physical stimuli it is possible to bias the response of glial cells to injury, i.e. from the reactive to the radial glia phenotype, the later being more supportive for successful endogenous repair.

The major finding of this study is that *in vitro* matured astrocytes can be reverted to a RGLC phenotype by a precisely-sized micropatterned PMMA scaffold without added biochemical factors. As do their embryonic counterparts, induced RGLC express the

Results: 1. Inducing functional radial glia-like progenitors from cortical astrocytes cultures using micropatterned PMMA

neuron-glial progenitor marker Pax6, and also proliferate, generate intermediate A2B5 and NG2 progenitors, and support and direct neuronal migration and axonal outgrowth.

The composition and physiological status of a primary glial culture is highly heterogeneous and depends on several factors, including the tissue origin and mode of preparation, the selected growth substrate and substrate coating, and the culture medium composition. To overcome this heterogeneity we defined three reference conditions: progenitor, reactive/mature and control (see material and methods for detailed definitions), thus enabling us to compare the physiological changes of cortical glial cells on the different substrates. In these reference conditions, progenitor glia were small bipolar cells characterized by a high proliferation rate and the expression of the progenitor markers (nestin, Pax6, A2B5), whereas reactive/mature glia were large cells with flat or ramified shapes, mostly quiescent, and expressing high levels of maturity markers (GFAP, EAAT-2). Control glia were mostly flat and well-spread, proliferated slowly, and expressed high levels of mature markers, characteristics that define them as cells closer to the reactive/mature condition. When PMMA was used as the substrate, the glial morphology and biochemical marker expression indicate a bias towards a more immature RGLC progenitor phenotype that was dramatically potentiated when PMMA was micropatterned, with grooves no bigger than $2\mu\text{m}$ wide/ $1\mu\text{m}$ deep. These results suggest that intrinsic material properties might act synergistically with the micro-topography in the modulation of the astrocytic phenotype. Biophysical and material cues regulate stem cell behavior (reviewed in (Keung 2010). For example, substrate stiffness differentially directs neural stem cells differentiation to neural and glial phenotypes (Saha 2008; Hynes 2009; Leipzig 2009.) and substrate hydrophobicity regulates glial cells adhesion and proliferation (Biran 1999; Soria 2007). PMMA is the most hydrophobic substrate we used here and the study of Biran et al., demonstrated that astrocytes exhibit lower adhesion and increased proliferation with increasing material hydrophobicity. Material chemistry and surface energy affect the adsorption of ECM proteins and thus might regulate cell adhesion and proliferation by modulating integrin signaling (Soria 2007). ECM protein

Results: 1. Inducing functional radial glia-like progenitors from cortical astrocytes cultures using micropatterned PMMA

adsorption on PMMA is 5-10 times smaller than the amount adsorbed in tissue culture treated polystyrene (Alaerts 2001). Thus, one possibility is that the hydrophobicity and low protein adsorption of PMMA might act synergistically with the micro-topography in the induction of the RGLC phenotype.

After initial seeding, primary glial cultures were grown *in vitro* for 1 month until reach confluence, reflecting the extremely slow proliferation rate in our experimental conditions. One possibility is that the threefold increase in RGLC in Ln2 PMMA was the progeny of RGC that contaminated the initial culture, selected through induced death of particular cell sub-populations. However, our data strongly argue against this possibility because cell number doubling was not achieved in any substrate in the first 4 days of the study, and the number of dead cells was similar in Ln2 PMMA and control substrates. Therefore, although complementary experiments will be required to fully resolve this question, our results support that the most probably source of RGLC is the dedifferentiation of mature astrocytes.

Recent studies have focused on the effect of nano- and microtopography on cell function (reviewed by Bettinger et al.(Bettinger 2009)), and grooved substrates have been tested for neural tissue engineering purposes showing a size-dependent response (Hoffman-Kim, Mitchel et al. 2010). For instance, line topographies larger than the cell body (30-200 μ m) promote perpendicular alignment, called "cell bridging", in several cell types such as dorsal root ganglion and Schwann cells (Goldner 2006). Moreover, mesenchymal stem cell differentiation and cell fate might be directed by changing the groove dimension (Yim 2007; Saha 2008; Hynes 2009; Tay 2010). Cell shape elongation on grooved surfaces is mostly due to oriented mechanical tension created by integrin and focal adhesion rearrangements. The elongation of cytoskeleton and nucleus has been correlated with changes in cell function and differentiation, in part through intracellular calcium regulation (Biran 1999; Dalby 2003; Itano 2003; Leipzig 2009.). Nevertheless the strong proliferative induction of 2 μ m grooves that we observed here was rather surprising, as it is reported in the literature that, in general, cells grown on grooved topographies exhibit lower

Results: 1. Inducing functional radial glia-like progenitors from cortical astrocytes cultures using micropatterned PMMA

proliferation rates (Saha 2008; Bettinger 2009). However, in most studies the material surface was modified by adding reactive groups or through coatings with extracellular matrix proteins to improve cell adhesion. It is known that strong cell adhesion to stiff substrates favors the formation of focal contacts and actin-myosin stress fibers (Engler 2006; Discher 2009), thus probably limiting cell division. We have observed that RGLC on PMMA or in the progenitor condition gradually lose their adhesion to the substrate, and some of their radial processes detach from them. NSC proliferate when grown as neurospheres, and differentiate when they are forced to adhere to stiff substrates through the addition of adhesive molecules (Alaerts 2001; Martinez, Engel et al. 2008; Discher 2009). Thus, a loose adherent phenotype might be a requisite to maintain NSC competence and proliferative capacity, and optimizing cell adhesion to the substrate might therefore introduce a bias towards cell differentiation.

Recent evidences strongly support the idea that in order to maintain or promote proliferation it is also necessary to recreate certain physical characteristics of the specialized progenitor niche (Keung 2010). In the embryonic CNS, progenitors and neuroblasts are densely packed in the ventricular areas, with the long processes of radial glia spanning from the ventricular surface to the surrounding pia mater. As the size of radial glia processes is around 2 μm (Anton 1997) one possibility is that 2 μm grooves mimic the physical structure of the NSC niche during brain development.

Lineage tracing experiments suggest that CNS neural progenitors are heterogeneous and mostly arise from sequential differentiation of an early multipotent neuroepithelial progenitor that progressively transforms into radial glia. Radial glia cells, which express Pax6 in the cerebral cortex, can originate neurons and glia, and as development proceeds they also generate different intermediate neuronal restricted (TBR2 positive) or glial restricted (A2B5 positive) amplifying progenitors (Englund, Fink et al. 2005; Baracska 2007; Yim 2007). In our experimental conditions, RGLC and glia-restricted progenitors could be induced by material chemistry and topographical cues, but this was not the case of neuronal-restricted progenitors or mature neurons,

Results: 1. Inducing functional radial glia-like progenitors from cortical astrocytes cultures using micropatterned PMMA

suggesting that the cues which guide progenitor specification to neuronal and glial lineages might be different.

During embryonic development, RGC not only act as NSC but also serve as scaffold for directed neuronal migration (Vacarino, Fagel et al. 2007). The ability of glial cells to support and orient neural growth has already been studied by other authors. For instance, dorsal root ganglions grew longer neurites on aligned astrocytes and meningeal-coated substrates (Biran 2003), while neurons grew and oriented on electric field-induced aligned astrocytes (Alexander, Fuss et al. 2006). One interesting study reported that neurons could align on top of an astrocyte monolayer even after 3 weeks, and they were able to read the pattern “buried” beneath astrocytes (Sørensen 2007). In our experimental conditions, embryonic cortical neurons adhered to glial cells but not to the substrates themselves; thus, changes in neuronal adhesion directly reflect different glial physiology. RGLC induced by 2 μ n grooved PMMA provided better neuronal substrates than did glial cells grown on naive PMMA, glass or culture plastic, and neuronal bodies and neurites align perfectly with the oriented glia. Moreover, neurons migrate relatively long distances using the RGLC as rails, at a speed that is comparable with the embryonic neuronal radial migration (Youn, Pramparo et al. 2009). Significant participation of contaminant RGC from neural cultures was also ruled out, as GFP+/BLBP glial cells were rarely observed in our co-cultures. Thus, induced RGLC are functional and reproduce the normal roles of RGC during development, providing a guiding substrate for migrating neurons.

Embryonic neurons are known in turn to direct astrocyte transformation into radial glia through neuregulin secretion and BLBP induction in astrocytes (Tay 2010). Here we found that 2 μ m patterned PMMA synergizes with embryonic neurons, potentiating astrocyte de-differentiation into RGLC. This effect was manifested by a reduction of the surface covered by glial cells, since they adopted bipolar shapes, and an increase in neuron-glia co-localization compared to control (from 15% to 60%).

The present work report morphological and physiological RGLC progenitor induction from *in vitro* matured astrocytes in response to material composition and topography without the concurrence of biochemical cues. Although PMMA is not the material of choice for *in vivo* implantation after a lesion, our results suggest that substrate-mediated induction of RGLC phenotype in mature astrocytes might improve their ability to sense and respond to other potential regenerative cues, whether provided externally or already present locally.

Our results also suggest that the design of an implantable device to promote CNS regeneration must take in account the glial cell response. Although much more work remains to be done, the findings raise the possibility of designing implantable devices that restore *in situ* the embryonic radial glia competence into parenchymal astrocytes. Successful regeneration might then require that implantable materials not only promote neuronal cell growth, but also drive glial physiological responses into a neuron permissive or even a neurogenic phenotype. In this regard, the introduction of line patterns within the size range of RGC processes in implantable scaffolds might mimic the topography of the embryonic neural stem cell niche, and could be a useful tool for driving endogenous astrocytes into a neurogenic RGLC phenotype and a regenerative response *in situ*.

1.5. Conclusions

This study has demonstrated that in the absence of other biochemical cues, the intrinsic composition and line topography of PMMA is sufficient to drive glial cell de-differentiation into RGLC progenitors. Glial cells, and in particular astrocytes, align and orient in a wide range of line topographies, although, only those in the size range of normal RGC processes (~2 μm) strongly induced astrocyte transformation into RGLC progenitors. These cells reproduce *in vitro* some of the normal functions of radial glia itself, including the generation of different types of intermediate progenitors and the support and orientation of neuronal growth.

Results: 1. Inducing functional radial glia-like progenitors from cortical astrocytes cultures using micropatterned PMMA

1.6 References

- Alaerts, J. A., De Cupere, V.M., Moser, S., et al. (2001). "Surface characterization of poly(methyl methacrylate) microgrooved for contact guidance of mammalian cells." Biomaterials **22**: 1635-1642.
- Alexander, J. K., B. Fuss, et al. (2006). "Electric field-induced astrocyte alignment directs neurite outgrowth." Neuron Glia Biol **2**(2): 93-103.
- Alvarez-Buylla, A., J. M. Garcia-Verdugo, et al. (2001). "A unified hypothesis on the lineage of neural stem cells." Nat Rev Neurosci **2**(4): 287-93.
- Anton, E. S., Marchionni, M.A., Lee, K.F., Rakic, P. (1997). "Role of GGF/neuregulin signaling in interactions between migrating neurons and radial glia in the developing cerebral cortex." Development **124**: 3501-3510.
- Baracska, K. L., Kidd, G.J., et al. (2007). "NG2-positive cells generate A2B5-positive oligodendrocyte precursor cells." Glia **55**(10): 1001-1010.
- Berninger, B. (2010). "Making neurons from mature glia: a far-fetched dream?" Neuropharmacology **58**(6): 894-902.
- Bettinger, C., Langer R, Borenstein JT. (2009). "Engineering substrate topography at the micro- and nanoscale to control cell function." Angew Chem Int Ed Engl . **48**(30): 5406-5415.
- Biran, R., Noble, M.D., Tresco, P.A. . (1999). "Characterization of cortical astrocytes on materials of different surface chemistry." J Biomed Mater Res. **46**(2): 150-159.
- Biran, R., Noble, M.D., Tresco, P.A. . (2003). "Directed nerve outgrowth is enhanced by engineered glial substrates." Exp Neurol **184**(1): 141-152.
- Buffo, A., Rolando, C., Ceruti, S. (2010). "Astrocytes in the damaged brain: Molecular and cellular insights into their reactive response and healing potential." Biochem Pharmacol **79**(2): 77-89.
- Chew, S. Y., R. Mi, et al. (2008). "The effect of the alignment of electrospun fibrous scaffolds on Schwann cell maturation." Biomaterials **29**(6): 653-61.
- Chojnacki, A. K., Mak, G.K., Weiss, S. (2009). "Identity crisis for adult periventricular neural stem cells: subventricular zone astrocytes, ependymal cells or both?" Nat Rev Neurosci **10**(2): 153-163.
- Christopherson, G. T., H. Song, et al. (2009). "The influence of fiber diameter of electrospun substrates on neural stem cell differentiation and proliferation." Biomaterials **30**(4): 556-64.
- Comeau, J. W., S. Costantino, et al. (2006). "A guide to accurate fluorescence microscopy colocalization measurements." Biophys J **91**(12): 4611-22.
- Costa, M. R., Gotz, M., Berninger, B. (2010). "What determines neurogenic competence in glia?" Brain Res Rev. **63**(1-2): 47-59.
- Dalby, M. J., Riehle, M.O., Yarwood, S.J., Wilkinson, C.D., Curtis, A.S. (2003). "Nucleus alignment and cell signaling in fibroblasts: response to a micro-grooved topography." Exp Cell Res. **284**(2): 274-282.
- Discher, D. E., Janmey, P., Wang, Y.L. (2005). "Tissue cells feel and respond to the stiffness of their substrate. ." Science **310**(5751): 1139-1143.
- Discher, D. E., Mooney, D.J., Zandstra, P.W. . (2009). "Growth factors, matrices, and forces combine and control stem cells." Science **324**(5935): 1673-1677.
- Engel, E., E. Martinez, et al. (2009). "Mesenchymal stem cell differentiation on microstructured poly (methyl methacrylate) substrates." Ann Anat **191**(1): 136-44.
- Engler, A. J., Sen, S., Sweeney, H.L., Discher, D.E. (2006). "Matrix elasticity directs stem cell lineage specification." Cell **126**(4): 677-689.
- Englund, C., A. Fink, et al. (2005). "Pax6, Tbr2, and Tbr1 are expressed sequentially by radial glia, intermediate progenitor cells, and postmitotic neurons in developing neocortex." J Neurosci **25**(1): 247-51.

Results: 1. Inducing functional radial glia-like progenitors from cortical astrocytes cultures using micropatterned PMMA

- Fedoroff, S., McAuley, W.A., et al. (1984). "Astrocyte cell lineage. V. Similarity of astrocytes that form in the presence of dBcAMP in cultures to reactive astrocytes in vivo." J Neurosci Res **12**(1): 14-27.
- Fitch, M. T. and J. Silver (2008). "CNS injury, glial scars, and inflammation: Inhibitory extracellular matrices and regeneration failure." Exp Neurol **209**(2): 294-301.
- Goldner, J. S., Bruder, J.M., Li, G., et al. (2006). "Neurite bridging across micropatterned grooves." Biomaterials **27**(3): 460-472.
- Gregg, C. and S. Weiss (2003). "Generation of functional radial glial cells by embryonic and adult forebrain neural stem cells." J Neurosci **23**(37): 11587-601.
- Hoffman-Kim, D., J. A. Mitchel, et al. (2010). "Topography, cell response, and nerve regeneration." Annu Rev Biomed Eng **12**: 203-31.
- Hynes, S. R., Millicent, F.R., Bertram, J.P., Lavik, E.B. (2009). "A library of tunable poly(ethylene glycol)/poly(L-lysine) hydrogels to investigate the material cues that influence neural stem cell differentiation." J Biomed Mater Res A **2**: 499-509.
- Itano, N., Okamoto, S., et al. (2003). "Cell spreading controls endoplasmic and nuclear calcium: a physical gene regulation pathway from the cell surface to the nucleus." Proc Natl Acad Sci U S A **100**(9): 5181-5186.
- Johansson, F., P. Carlberg, et al. (2006). "Axonal outgrowth on nano-imprinted patterns." Biomaterials **27**(8): 1251-8.
- Keung, J. A., Kumar, S., Schaffer, D.V. (2010). "Presentation counts: microenvironmental regulation of stem cells by biophysical and material cues." Annu. Rev Cell Dev Biol **26**: 533-56.
- Kriegstein, A. and A. Alvarez-Buylla (2009). "The glial nature of embryonic and adult neural stem cells." Annu Rev Neurosci **32**: 149-84.
- Lang, B., Liu, H.L., et al. (2004). "Astrocytes in injured adult rat spinal cord may acquire the potential of neural stem cells." Neurosci **128**(4): 775-783.
- Leavitt, B. R., Hernit-Grant, C.S., Macklis, J.D. (1999). "Mature astrocytes transform into transitional radial glia within adult mouse neocortex that supports directed migration of transplanted immature neurons." Exp Neurol **157**(1): 43-57.
- Lee, M. R., Kwon, K.W., Jung, H., Kim, H.N., Suh, K.Y., Kim, K., et al. (2010). "Direct differentiation of human embryonic stem cells into selective neurons on nanoscale ridge/groove pattern arrays." Biomaterials **31**(15): 4360-4366.
- Leipzig, N. D., Shoichet, M.S. (2009). "The effect of substrate stiffness on adult neural stem cell behaviour." Biomaterials **30**: 6867-6878.
- Martinez-Ramos, C., S. Lainez, et al. (2008). "Differentiation of Postnatal Neural Stem Cells into Glia and Functional Neurons on Laminin-Coated Polymeric Substrates." Tissue Engineering Part A **14**(8): 1365-1375.
- Martinez, E., E. Engel, et al. (2008). "Focused ion beam/scanning electron microscopy characterization of cell behavior on polymer micro-/nanopatterned substrates: a study of cell-substrate interactions." Micron **39**(2): 111-6.
- Merolli, A., L. Rocchi, et al. (2009). "In vivo regeneration of rat sciatic nerve in a double-halved stitch-less guide: a pilot-study." Microsurgery **29**(4): 310-8.
- Mills, C. A., J. G. Fernandez, et al. (2007). "Directional alignment of MG63 cells on polymer surfaces containing point microstructures." Small **3**(5): 871-9.
- Moon, J. H., B. S. Yoon, et al. (2008). "Induction of neural stem cell-like cells (NSCLCs) from mouse astrocytes by Bmi1." Biochem Biophys Res Commun **371**(2): 267-72.
- Ortega Cano, J. A. (2011). Function and regulation of bone morphogenetic protein 7 (BMP7) in cerebral cortex development. Experimental Pathology and Therapeutics. Barcelona, University of Barcelona.
- Recknor, J. B., J. C. Recknor, et al. (2004). "Oriented astroglial cell growth on micropatterned polystyrene substrates." Biomaterials **25**(14): 2753-67.

Results: 1. Inducing functional radial glia-like progenitors from cortical astrocytes cultures using micropatterned PMMA

- Recknor, J. B., D. S. Sakaguchi, et al. (2006). "Directed growth and selective differentiation of neural progenitor cells on micropatterned polymer substrates." Biomaterials **27**(22): 4098-108.
- Rolls, A., R. Shechter, et al. (2009). "The bright side of the glial scar in CNS repair." Nat Rev Neurosci **10**(3): 235-41.
- Saha, K., Keung, A.J., et al. (2008). "Substrate modulus directs neural stem cell behaviour." Biophys J **95**: 4426-4438.
- Song, H., C. F. Stevens, et al. (2002). "Astroglia induce neurogenesis from adult neural stem cells." Nature **417**(6884): 39-44.
- Sørensen, A., Alekseeva, T., et al. (2007). "Long-term neurite orientation on astrocyte monolayers aligned by microtopography." Biomaterials **28**(36): 5498.
- Soria, J. M., Martínez Ramos, et al. (2007). "Influence of the substrate's hydrophilicity on the in vitro Schwann cells viability." J Biomed Mater Res A. **83**(2): 463-70.
- Steedman, M., Tao, S, et al. (2010). "Enhanced differentiation of retinal progenitor cells using microfabricated topographical cues." Biomed Microdevices **12**: 363-369.
- Tay, C. Y., Yu, H., et al. (2010). "Micropatterned matrix directs differentiation of human mesenchymal stem cells towards myocardial lineage." Exp Cell Res **316**(7): 1159-1168.
- Thompson, D. M. and H. M. Buettner (2001). "Schwann cell response to micropatterned laminin surfaces." Tissue Eng **7**(3): 247-65.
- Vaccarino, F. M., D. M. Fagel, et al. (2007). "Astroglial cells in development, regeneration, and repair." Neuroscientist **13**(2): 173-85.
- van Kooten, T. G., H. T. Spijker, et al. (2004). "Plasma-treated polystyrene surfaces: model surfaces for studying cell-biomaterial interactions." Biomaterials **25**(10): 1735-47.
- Voigt, T. (1989). "Development of glial cells in the cerebral wall of ferrets: direct tracing of their transformation from radial glia into astrocytes." J Comp Neurol **289**(1): 74-88.
- White, R. E. and L. B. Jakeman (2008). "Don't fence me in: harnessing the beneficial roles of astrocytes for spinal cord repair." Restor Neurol Neurosci **26**(2-3): 197-214.
- Wu, V. W., Schwartz, J.P. (1998). "Cell culture models for reactive gliosis: new perspectives." J Neurosci Res. **51**(6): 675-681.
- Yamada, T., R. Sawada, et al. (2008). "The effect of sulfated hyaluronan on the morphological transformation and activity of cultured human astrocytes." Biomaterials **29**(26): 3503-13.
- Yang, I. H., C. C. Co, et al. (2005). "Spatially controlled co-culture of neurons and glial cells." J Biomed Mater Res A **75**(4): 976-84.
- Yim, E. K., Pang, S.W., Leong, K.W. (2007). "Synthetic nanostructures inducing differentiation of human mesenchymal stem cells into neuronal lineage." Exp Cell Res **313**(9): 1820-1829.
- Yim, E. K. F., Pang, S.W., Leong, K.W. (2007). "Synthetic nanostructures inducing differentiation of human mesenchymal stem cells into neuronal lineage." Exp Cell Res **313**(9): 1820-1829.
- Yiu, G. and Z. He (2006). "Glial inhibition of CNS axon regeneration." Nat Rev Neurosci **7**(8): 617-27.
- Youn, Y. H., T. Pramparo, et al. (2009). "Distinct dose-dependent cortical neuronal migration and neurite extension defects in Lis1 and Ndel1 mutant mice." J Neurosci **29**(49): 15520-30.
- Yu, T., G. Cao, et al. (2006). "Low temperature induced de-differentiation of astrocytes." J Cell Biochem **99**(4): 1096-107.
- Zhu, X., Bergles, D.E., Nishiyama, A. (2008). "NG2 cells generate both oligodendrocytes and gray matter astrocytes." Development. **135**(1): 145-15.

2. Neural cell behaviour *in vitro* and *in vivo* on flat and micro patterned chitosan films

Abstract

Chitosan is a biodegradable natural polysaccharide that has been widely studied for regenerative purposes in the central nervous system. To predict whether chitosan can be successful for tissue regeneration, understanding the behaviour of neurons and glial in terms of differentiation state cells is fundamental. However, little is known about this matter. In this study we assessed the *in vitro* and *in vivo* glial and neuronal response to chitosan either flat or patterned with lines in the micrometric range.

Chitosan demonstrated to be a good substrate for the attachment and growth of both neurons and glial cells. However, it exerted a general maturation/activation effect on glial cells in both cell cultures, as indicated by the increase of the mature astrocytes marker GFAP+. When micropatterns were introduced, neuronal culture responded with an alignment which was selective for axons but not for dendrites. According to line dimensions, axons organized either separately on smaller channels (2µm width), either in bundles on bigger channels (10µm width), mimicking their anatomical structure. In the case of glial cells, alignment involved the cytoskeleton and not the whole cell shape. However, even if glial cells were activated, were capable to support and orient neuronal growth in glial-neuronal co-cultures. When implanted *in vivo*, a mild foreign body reaction was present in both chitosan and injured condition. However, toxicity, cell death and encapsulation were not observed, indicating a good biocompatibility.

In conclusion, line patterned chitosan could be a useful material to be applied in CNS tissue engineering, especially if we want to orient axonal outgrowth. However, it has to be taken into account the activated glial response, which can be interpreted both as beneficial and harmful for the regenerative response.

2.1. Introduction

In order to help regeneration in central nervous system, the final aim of implanting biomaterials is to encourage a permissive environment for neurons that attempt to restore connections. Among the biomaterials used in investigation for this purpose, chitosan outstands thanks to its good affinity for nerve cells (Cheng et al. 2003).

Chitosan is a natural polycationic linear copolymer of beta (1-4)-D-glucosamine and is the second most abundant polysaccharide in nature. Thanks to its biodegradability, water solubility, ability to sustain the release of molecules and support the attachment and proliferation of different cell types, has recently found a range of application in tissue engineering (Bumgardner et al. 2003; Lee et al. 2004). Moreover, it does not show immune rejection, has good and tunable mechanical properties and has hemostatic and antibacterial properties. Chitosan can be easily microstructured by soft lithography techniques up to the nanometric scale (Fernandez et al. 2008). Previous studies involving neural cells growing on line patterned chitosan showed that cells follow the pattern and align, like in the case of Hsu, in which they culture Schwann cells on 20 μm microgrooves (Hsu et al. 2007).

Although many studies have been published regarding chitosan for nerve tissue engineering, there is little information about the behavior of neural cells derived from the cerebral cortex, especially concerning biochemical characterization of cell - biomaterial interaction. Most of the published studies are limited to adhesion, morphology and viability assessment. For instance, Martín-López et al studied the viability of neurons on chitosan based materials (Martín-López et al. 2012). However, in order to interpret the interaction between cells and biomaterials a deeper understanding of cells response is required. Neurons are not the only cell type involved in the reaction to an injury. On the contrary, the most abundant cell type that modulate regeneration is astroglia. Glial cells play crucial roles in the CNS during normal homeostasis, during development and after injury. They serve as physical and trophic support for neurons and they can be permissive for their growth and guidance, like during cerebral cortex development, or can be extremely inhibitory, like after

injury in a glial scar. For this reason, when designing biomaterials for CNS tissue engineering application, is extremely important to study not only neuronal response, but also glial cell response and the interaction between the two cell types.

Thus, the purpose of our study was in a first place, to evaluate the *in vitro* glial and neuronal response to flat and micro patterned chitosan in terms of cell morphology and differentiation state, and in a second place, to assess the *in vivo* biocompatibility of chitosan.

2.2 Materials & Methods

2.2.1 Preparation of flat and micropatterned films of chitosan

Chitosan films were prepared as previously described (Fernandez et al. 2008). Briefly, Medium molecular weight chitosan (75–85% deacetylated, 200–800 cps viscosity), derived from crab shell, was purchased from Aldrich (Sigma-Aldrich Chemical, USA). A 2% (w/v) polymer solution was produced by dissolving the chitosan in diluted glacial acetic acid (1% v/v). The chitosan polymer solution was centrifugated at 15000rpm to get rid of un-dissolved particles.

The solution was casted on flat or patterned moulds. Micro-patterns consisted of 2 μm and 10 μm wide lines (In2 and In10), all 1 μm deep/tall. The silicon moulds were provided by AMO GmbH (Aachen, DE) and consisted of 1.5" \times 1.5" silicon squares. The solution was dried 8h at 37°C and neutralized with 3w/v% NaOH. The films were rinsed in MilliQ water (Millipore, USA). For cell studies, chitosan films were neutralized under sterile conditions, using sterile water and operating under the hood. Standard borosilicate glass (Knittel Glaeses, Germany) or tissue culture plastic (TCP) have been used as control materials, respectively for ICC or Western blotting. Controls were used nude or coated with poly-D-lysine (Sigma-Aldrich, Saint Louis, MO) to allow the adhesion of neurons. Glass was autoclaved as standard procedures at 120°C for 20min.

2.2.2 Material characterization

Characterization of the wettability of the materials was achieved via contact-angle measurements using an OCA 20 system (Dataphysics, GmbH, Germany). The captive bubble method was performed using a custom made PMMA chamber filled with ultrapure water. A 2 μ L bubble of room air was dispensed and allowed to make contact with an upside down sample located at the top of the chamber. The reported value for the contact angle is the complementary angle of the one measured between the air-bubble and the surface of the tested material. A minimum of four different measurements were performed on at least four different samples.

ζ -Potential measurements of chitosan, Glass and LysGlass were carried out using a SurPASS apparatus and a VisioLab software (Anton Paar Ltd. - UK). All the measurements were performed 4 times at the pH of the electrolyte (KCL 1mM, pH 5.5) after 2h of equilibration using the Adjustable Gap Cell for small samples (20 mm x 10 mm).

The percentage of water absorption was calculated weighting the samples in the dried and wet state. Mechanical properties of chitosan films were determined using an uniaxial testing machine (Adamel Lhomargy DY34) equipped with a 100-N load cell under a cross-head speed of 20 mm/s (ASTM D882 method). Measurements were taken at room temperature, maintaining the films in the wet state. All samples were cut into rectangular shape with dimensions of 210 \pm 20*24 \pm 2mm. At least five samples were tested.

The *in vitro* degradation of chitosan films was followed at 37 $^{\circ}$ C over a period of 5 weeks. Four samples (~20mg) were immersed in PBS (250ml PBS: 1g sample), retrieved weekly, dried during 6h at 37 $^{\circ}$ C and weighted with an analytical balance. The percentage of mass loss after certain time (t) of immersion in PBS, % Deg(t), was calculated using the formula %Deg(t)=100(M₀-M_(t))/M₀, where M₀ is the dried weight of the sample at time t=0 and M_(t) is the dried weight at a time=t of immersion in PBS.

Results: 2. Neural cell behaviour *in vitro* and *in vivo* on flat and micro patterned chitosan films

The characterization of patterned chitosan films was performed on a surface of 194x94 μm using a WYKO NT1100 white light interferometer apparatus and the software Vision 32 V2.303 (Veeco Instruments, Inc, USA).

2.2.3 Cell culture

All animal housing and procedures were approved by the Institutional Animal Care and Use Committee in accordance with Spanish and EU regulations. Neurons were obtained from embryonic brains like described previously (Ortega Cano 2011; Mattotti et al. 2012). Brain cortices from E16 mice were isolated in dissection buffer, digested with trypsin-DNAse I, dissociated and preplated for 30 min in preplating medium (CO_2 -equilibrated Neurobasal™ supplemented with 5% NHS, 1% Pen-Strep, 0.5 mml-glutamine, 5.8 $\mu\text{l/ml}$ NaHCO_3 (Sigma–Aldrich, Saint Louis, MO)). The supernatant was then collected, centrifuged and resuspended in neuronal culture medium (NB, 1% Pen-Strep, 0.5 mml-glutamine, 1x B27, 5.8 $\mu\text{l/ml}$ NaHCO_3). Neurons were plated at a density of $2.5 \cdot 10^5$ cells/ cm^2 on chitosan films and on poly-lysine coated control surfaces and cultured for 5 DIV. The medium was supplemented with 1% NHS during the first 24h and then changed for fresh neuronal serum free medium. For mixed glial-neurons co-cultures, neurons were seeded directly on top of 5DIV glial cell cultures and cultured during 5 more days in serum free neuronal culture medium.

Glial cells were derived from brain cortex of newborn mice like described elsewhere (Mattotti et al. 2012). Briefly, brain cortices were dissected out free of meninges in dissection buffer (PBS 0.6% glucose (Sigma), 0.3% BSA (Sigma)) and digested with trypsin (Biological Industries) and DNAse I (Sigma) for 10 min at 37°C. The tissue was dissociated in Dulbecco's Modified Eagle Medium (DMEM, Biological Industries), 10% Normal Horse Serum (NHS, GIBCO), 1% Penicillin-Streptomycin (Pen-Strep, Biological Industries) and 2mM L-Glutamine (Biological Industries), referred to in this text as growing medium (GM). After centrifugation and re-suspension, cells were plated and grown to confluence at 37°C, 5% CO_2 (approximately 25-30 days *in vitro*, DIV). All the experiments were performed using glial cells from the first passage (Ps1). Glial cells were cultured at a density of 2×10^5 cells/ cm^2 either on chitosan films or on control

Results: 2. Neural cell behaviour *in vitro* and *in vivo* on flat and micro patterned chitosan films

surfaces for 5DIV in Neurobasal™ media (NB), 3%NHS, 1% Pen-Sterp, 2mMLGlutamine (Culture Medium, CM). The samples were either fixed in 4% PFA for 15h at RT for immunocytochemistry procedures or used for protein extraction and western blot analysis.

2.2.4 *Implant into brain cortex in vivo*

Postnatal newborn mice at day 4 (P4) were anaesthetized with ice and placed in a stereotaxic frame. An incision was made in one side of the skull in correspondence of the somatosensorial cortex and a bone flap was removed to expose cortical surface. Chitosan films were inserted through these holes by the aid of tweezers below the skull to a depth of no more than 1mm. In the control group, an injury of approximately the same size of the chitosan group was provoked by the insertion of a needle, so that each brain has an internal un-injured hemisphere that serves as a control. After that, bone flaps were placed back.

After 21 days (P25) mice were transcardially perfused with 4% paraformaldehyde (PFA) in 0.1 M phosphate buffer pH 7.3 (PB). Brains were dissected and postfixed for 8–12 h, cryoprotected in 30% sucrose solution in PB, snap frozen with liquid nitrogen, stored at -80 °C and sectioned with a cryostat (Leica). Coronal sections of 40-µm thickness were collected and then processed for histochemical procedures.

2.2.5 *Immunocytochemistry*

Immunostaining of fixed cell cultures or cryostat sections were performed with standard protocols using antibodies against the following antigens: rabbit anti-GFAP (Mature and Reactive Glia marker, 1:500, Dako), rabbit anti-BLBP (Radial Glia marker, 1:1000, Chemicon), mouse anti-Nestin (Radial Glia marker, 1:200, Abnova Corporation), rabbit anti-laminin (extra cellular matrix marker, 1:200, Sigma), rat anti-F4/80 (macrophage and microglia marker, 1:200 Abcam) rabbit anti-NG2 (Oligodendrocytes Precursor Cells marker, 1:200, Millipore), goat anti-Actin (Cytoskeleton Marker, 1:2000, Santa Cruz Biotechnology, INC), rabbit anti-parvalbumina (marker of pyramidal neurons, 1:8000 Swant), goat anti-Tuj-1 (Neuronal Marker 1:1000, Covance) and rabbit anti-MAP2 (Neuronal Dendrites Marker, 1:1000,

Results: 2. Neural cell behaviour *in vitro* and *in vivo* on flat and micro patterned chitosan films

Covance). Appropriate Alexa488 or Alexa555 secondary antibodies (1:500, Molecular Probes, Eugene, Oregon) were used, and the nuclei were counter stained with TO-PRO-3 iodide (1:500, Molecular Probes, Eugene, Oregon). Finally, the preparations were coverslipped with Mowiol (Calbiochem, San Diego) for imaging.

2.2.6 Western Blot

Total extract proteins were separated by SDS-polyacrilamide gel and electro-transferred to a nitrocellulose membrane. Membranes were first blocked in 5% non fat milk and then incubated with primary antibodies overnight at 4°C, followed by their corresponding secondary HRP-conjugated antibodies (1:3000, Santa Cruz Biotechnology, San Diego). Protein signal was detected using the ECL chemiluminescent system (Amersham, Buckinghamshire,UK). Densitometry analysis, standardized to actin as a control for protein loading, was performed using ImageJ software (National Institutes of Health, USA).

The following primary antibodies were used: rabbit anti-GFAP (Mature and Reactive Glia marker, 1:8000, Dako), rabbit anti-BLBP (Radial Glia marker, 1:8000, Chemicon), mouse anti-Nestin (progenitor and Radial Glia marker, 1:250, Abnova Corporation), goat anti-Actin (Cytoskeleton Marker, 1:2000, Santa Cruz Biothechnology,INC), mouse anti-Tuj-1 (Neuronal Marker 1:10000, Covance) and goat anti-Pax6 (Neurogenic Radial Glia Marker, 1:250, Santa Cruz Biothechnology,INC). For quantification triplicate samples were analyzed.

2.2.7 Imaging and data analysis

Imunolabeled cells were imaged using a confocal microscope (Leica). Alignment was measured with the aim of image analysis software (Image J, National Institutes of Health, USA) using the FTT-Oval Profile method described previously by C. Ayres and Alexander JK (Alexander et al. 2006; Ayres et al. 2006). Briefly, grayscale images were processed with the FTT function and the 'Oval Profile' plug in. The summed pixel intensities were plotted between 0° and 180°. Aligned and random tendency are represented respectively by a peak at 90° and a horizontal line. All the images were

aligned with x axis prior analysis. Neurons and glia alignment was measured respectively on Tuj1 and GFAP pictures. Axon images were obtained subtracting MAP2 images to Tuj1 (example in **Fig.4 i.**), while dendrites images were the result of the subtraction of TOPRO-3 to MAP2 staining. Neuron-glia co-localization was quantified using the Intensity Correlation Analysis plug-in on pictures of glial cells stained with BLBP and neurons stained with Tuj1. Co-localization was represented by Pearson's correlation coefficient (R_r), whose values range between 1 and -1, where 1 represent maximal co-localization and -1 maximal exclusion (Comeau et al. 2006).

2.2.8 Statistical analysis

Statistical analysis was performed on all data using the Statgraphic-plus software. For comparison of the different results a One-way ANOVA test was performed using the LSD method and p -values < 0.05 were considered to be statistically significant.

2.3 Results

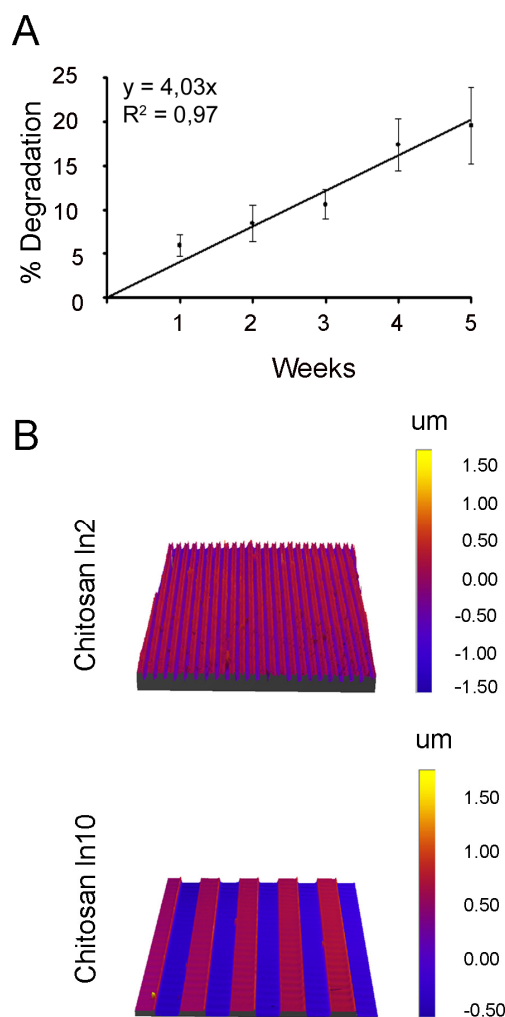
2.3.1 Material characterization

Surface and mechanical properties of chitosan and the materials used as controls, glass and lys-glass are reported in **Table 1**. Concerning wettability and surface charge, chitosan and lys-glass were hydrophilic (contact angle: $34^\circ \pm 3$ and $42^\circ \pm 3$ respectively) and positively charged, (Z potential: 15 ± 3 mV and 3 ± 1 mV respectively). On the contrary, glass was close to hydrophobic (contact angle: $73^\circ \pm 3$) and negatively charged (Z potential: -80 ± 14 mV). Moreover, chitosan showed high water absorption, increasing his mass up to $128 \pm 10\%$, while glass and lys-glass did not. This property has to be taken into account, since different behaviors can be observed in wet or dry state. Concerning mechanical properties, chitosan films can be considered a relatively soft and elastic material (Young's modulus: 5.7 ± 1.4 MPa; tensile strength: 4.31 ± 0.8 MPa; elongation at brake: $56 \pm 14\%$) when compared to glass, which was a hard materials (Young's modulus: 68 ± 4 103 MPa; tensile strength: between 30-100 MPa; elongation at breake: absent) (data obtained for standard borosilicate glass from www.camglassblowing.co.uk/gproperties.htm and www.jmcglass.com, www.knittel-laeser.de).

Results: 2. Neural cell behaviour *in vitro* and *in vivo* on flat and micro patterned chitosan films

| | Chitosan | Glass | LysGlass |
|-------------------------|------------|-----------------------|----------|
| Contact angle (°) | 34 ±3 | 73 ±3 | 42 ±3 |
| Z Potencial (mV) | 15 ±3 | -80 ±14 | 3 ±1 |
| Water absorption (%) | 128 ±10 | - | - |
| Young's modulus (MPa) | 5,7 ±1,4 | 68 ±4 10 ³ | - |
| Tensile strenght (MPa) | 4,31 ±0,81 | 30-100 | - |
| Elongation at break (%) | 56 ±14 | - | - |

Table 1: Surface and mechanical properties of chitosan films and control glass (uncoated and Lysin coated).



Since chitosan is a biodegradable material, a mass loss study was performed. Chitosan exhibit a linear pattern of degradation ($y = 4,03x$, $R^2 = 0,97$), and degrade at an average speed of 0.55% of its mass per day. After 5 weeks the material had lost 17-19% of its initial mass (**Fig.1 A**), thereafter, the samples lost cohesion and were no more usable for the test.

Topography was added to chitosan by patterning lines of 2 and 10 μm width and 1 μm high. White light interferometry showed that microstructures height and widths were replicated faithfully on chitosan (height $0.98 \pm 0.09 \mu\text{m}$ and widths 2.04 ± 0.16 and $9.9 \pm 0.83 \mu\text{m}$ respectively) (**Fig 1 B**).

Figure 1: A. Degradation of chitosan films and B.. White light interferometer 3D images of 10 μm and 2 μm patterned chitosan.

Results: 2. Neural cell behaviour *in vitro* and *in vivo* on flat and micro patterned chitosan films

2.3.2 Neuronal response to flat and micropatterned chitosan

To assess neuronal behavior, dissociated cultures of E16 cerebral cortex were cultured for 5DIV directly on uncoated flat or patterned chitosan films, using lysine coated glass or TCP as controls (for ICC and western blot analysis respectively). To characterize the cellular composition of these cultures, neurons were immunostained with Tuj1 and glial cells with GFAP and BLBP (**Fig. 2A**).

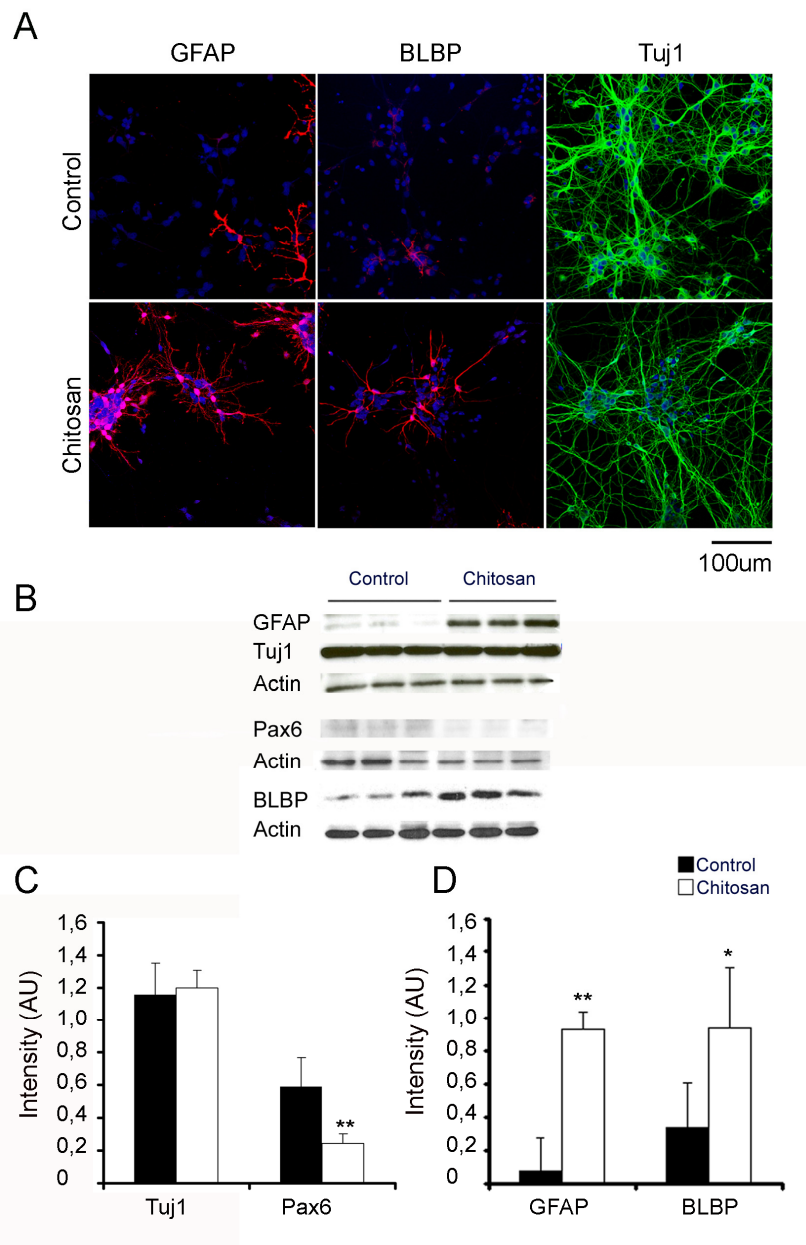


Figure 2: Effect of chitosan on neuronal cultures composition and protein expression. **A.** Confocal images of neuronal cell cultures. Scale bar = 100µm; **B.** Western Blots showing the expression of different neuronal and glial markers. **C-D.** Quantitative representation of the western blot densitometry (intensity values normalized to actin) of neuronal markers (C) and glial markers (D). Tuj1 is a marker for post mitotic neurons, Pax6 for neural progenitors, GFAP and BLBP for astroglial cells. * $p < 0.05$ and ** $p < 0.01$.

Results: 2. Neural cell behaviour *in vitro* and *in vivo* on flat and micro patterned chitosan films

E16 cortical cultures grown in lys-glass conditions were composed essentially by neurons, with low proportion of glial cells (**Fig. 2A**). In chitosan, neurons identified by Tuj-1 immunoreactivity adhered and grown similarly than in control condition, however, glial cells number increased dramatically. Moreover, GFAP+ and BLBP+ astrocytes showed a more ramified and differentiated morphology when grown on chitosan compared to control.

To quantify the differences in the phenotype of cortical neuronal cultures Western blot analysis were performed (**Fig. 2B-D**). E16 neuronal cultures on lysine coated TCP expressed high protein levels of Tuj1 and low levels of BLBP and GFAP, indicative of the essentially neuronal composition of these cultures. In addition, the low levels of Pax6 protein found indicated the presence of a leftover population of radial glia and neuronal progenitors. Cultures grown on chitosan films expressed similar levels of Tuj1 protein than controls, indicating similar neuronal composition. However, GFAP and BLBP were dramatically increased while Pax6 progenitor marker was very low (**Fig 2B-D**), indicating that chitosan induced enrichment in mature astrocytes. As the total cell number was similar in control and chitosan substrates (991 ± 243 and 729 ± 337 cells/mm² respectively), the increase in GFAP and BLBP positive cells was probably due to increased astrocytic differentiation induced by chitosan. The radial glia marker Nestin and the mature neurons marker Synaptophysin were negative in both the conditions, indicating that radial glia cells or mature neurons were not present in any conditions (datas not shown).

When 2 μ m (ln2) and 10 μ m (ln10) line micropatterns on chitosan films were analyzed, Tuj1 positive neurites were aligned and oriented following the patterning direction (**Fig.3A**). To differentiate the behavior of dendrites and axons in response to the linear topography cultures were double stained with Tuj1 and MAP2 antibodies. While Tuj1 recognizes β 3tubulin, a microtubule protein expressed in the neuronal soma, axon and dendrites, MAP2 is a microtubule associated protein expressed only in the neuronal soma and dendrites, and absent in the axon. MAP 2 images were used to analyze dendrites alignment and for axonal alignment axons were discriminated from

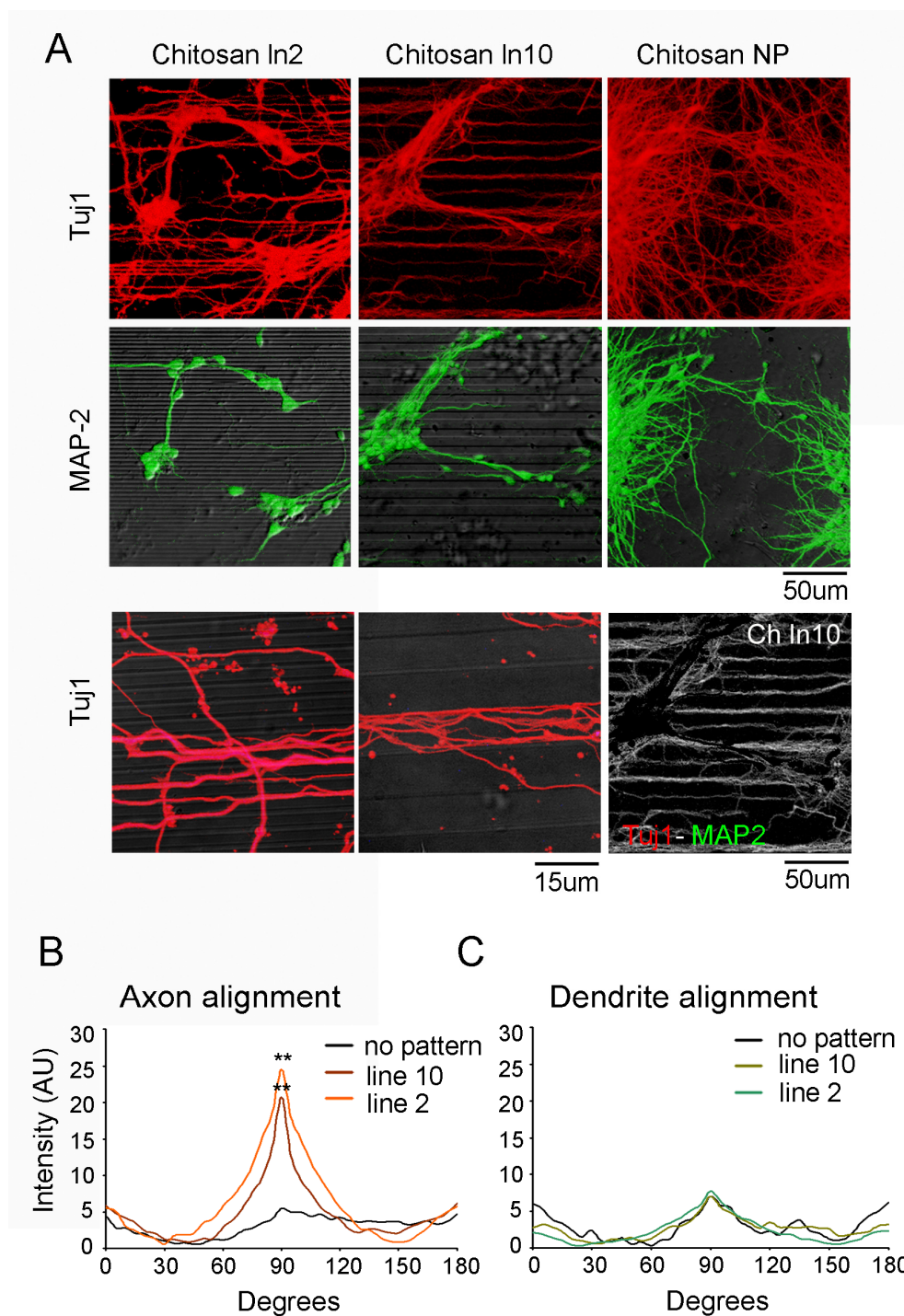


Figure 3: Neurons alignment on micropatterned chitosan films. **A.** Confocal images of TuJ1 and MAP2 (dendrites) stainings. The bottom right picture is a visual example of how axonal staining was obtained for alignment quantification (TuJ1-MAP2). Scale bar = 50 μ m and 15 μ m; **B.-C.** Graphic representation of **B.** axons and **C.** dendrite alignment by FFT-Oval profile measurement. Flat line indicates random distribution; peak at 90° indicates alignment parallel to the topography. ** indicates statistical significance respect to control $p \geq 0.01$.

Results: 2. Neural cell behaviour *in vitro* and *in vivo* on flat and micro patterned chitosan films

dendrites by subtracting MAP2 images from Tuj1 ones. FTT-Oval Profile analysis demonstrated that axons strongly aligned along the pattern with high affinity on In2 and In10, which is represented by a higher peak at 90° (**Fig. 3B**), while dendrites organized randomly (**Fig. 3C**). Moreover, axonal organization was affected by line dimensions. Axons tended to organize singularly on In2 and grew preferentially in the ridges of the grooves. On In10 axons tend to form fascicles in the grooves (**Fig 3A**).

2.3.3 Glial cells response to flat and micro patterned chitosan

To assess glial behavior on chitosan Ps1 glial cell cultures obtained from P0 mice were seeded directly on flat or patterned uncoated chitosan films, and cultured for 5 DIV. Initial experiments using the standard 10% NHS in the medium revealed a negligible glial attachment on chitosan with respect to glass (61 ± 51 and 599 ± 422 respectively after 5DIV). This result was somehow surprising as glial cells attached and differentiated on chitosan when neuronal cultures from E16 cerebral cortex were prepared. Above the cell origin, the principal difference between neuronal and glial cultures was the amount of serum used, 10% in the glial cultures and 1% the first DIV and serum free thereafter in the neuronal cultures. Thus we analyzed the effect of serum concentration on glial attachment. Ps1 glial cultures were allowed to seed for 2 hours on uncoated flat chitosan films or glass, in medium containing different concentrations of NHS from 0% to 10%. Serum concentration influenced negatively glial cell adhesion both on glass and chitosan films (**Fig. 4A**). Good glial cells adhesion rates were observed at NHS concentrations up to 3% while a dramatic decrease of cell adhesion was found at higher concentrations, in particular in the case of chitosan, Therefore, the rest of the experiments with glial cells were performed with 3% NHS. This medium composition was also used in our previous study (Mattotti et al. 2012). In such conditions glial cells attached and grew well both on chitosan and glass (1480 ± 586 and 1079 ± 476 respectively after 5DIV) (**Fig. 4B-C**).

Results: 2. Neural cell behaviour *in vitro* and *in vivo* on flat and micro patterned chitosan films

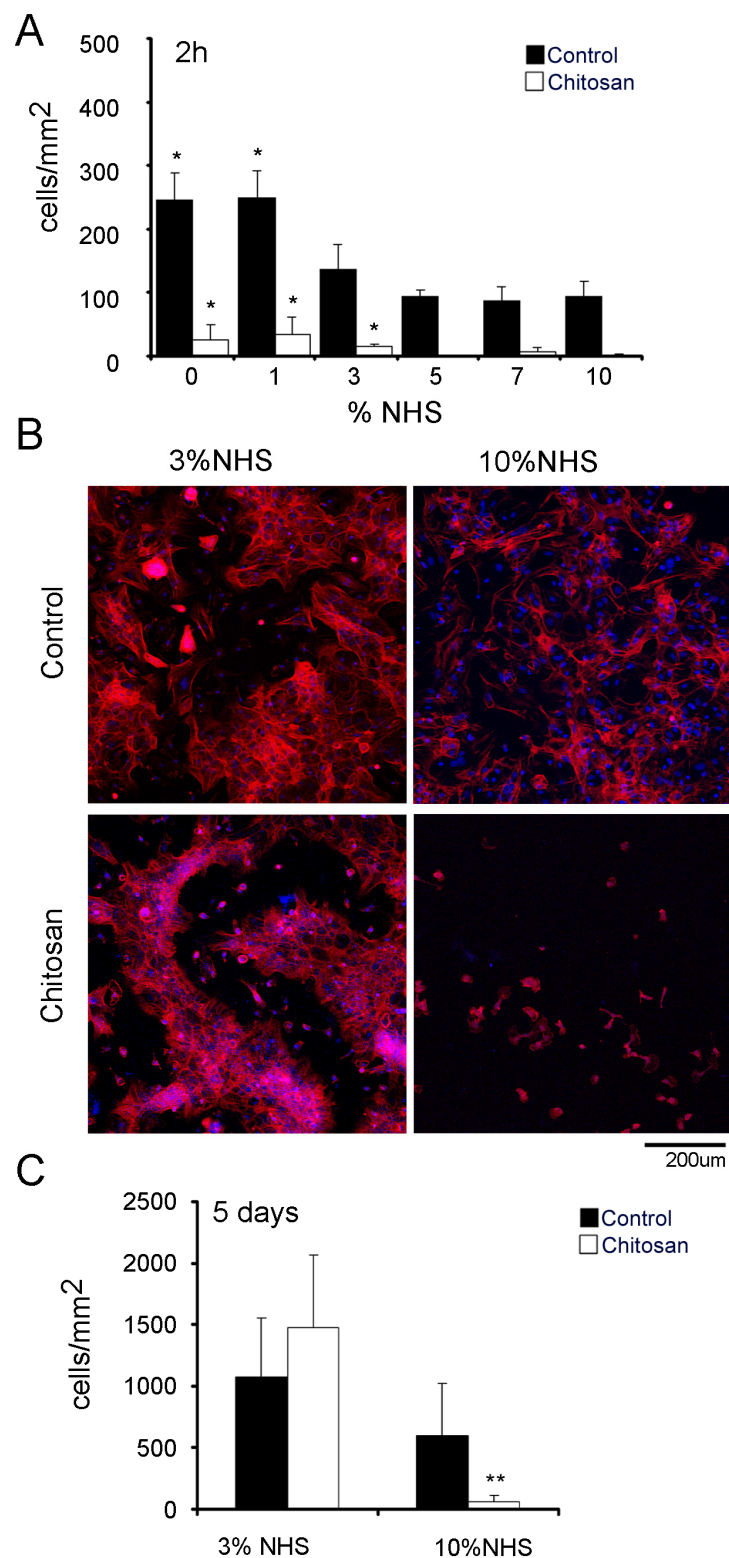


Figure 4: Effect of serum concentration on chitosan adhesion. **A.** Cell attachment after 2h at different serum concentration. **B.** Confocal pictures of glial cells on chitosan and control after 5

in presence of 3% or 10% NHS. Cell are stained for actin (phalloidin, red) **C.** Cell count after 5

in presence of 3% or 10% NHS. Scale bar = 200 μ m.

Results: 2. Neural cell behaviour *in vitro* and *in vivo* on flat and micro patterned chitosan films

To assess glial behaviour on chitosan films, cells were seeded directly on flat or patterned films without the aim of any coating and cultured for 5 DIV. In a previous work using 2µm and 10µm line-patterned PMMA, we observed that glial cells exhibited better alignment on In2 and a dramatic increase in bipolar cell morphologies (Mattotti et al., 2012). Therefore, in this study glial cell differentiation and alignment was only analyzed on In2 chitosan films. Glial cultures were immunostained with antibodies against GFAP and BLBP to identify astrocytes and against nestin to identify radial glia-like progenitors. Glial cells on flat chitosan had a similar morphology compared to control glass. Astrocytes expressing GFAP predominated in all conditions, while BLBP+ and Nestin+ cells were less present in flat and patterned chitosan substrates. Opposite to the expected results, glial cells on patterned chitosan did not exhibit the stretched and elongated morphology, as observed in a previous study using In2 patterned PMMA (Mattotti et al., 2012).

In order to quantify the relative proportion of the different cell types and their maturation state in the different substrates and conditions (**Fig.5**) western blot analysis were performed. Chitosan promoted an overall maturation of glial cells. Densitometry analysis revealed that when glial cells were grown on chitosan films, the expression of radial glia marker nestin and the immature astroglial marker BLBP decreased respect to the control, while the maturity marker GFAP did not change. Markers of proliferating cell (PH3) and early progenitor (Pax6) were not observed in any case, indicating the absence of proliferative progenitors in the culture (data not shown).

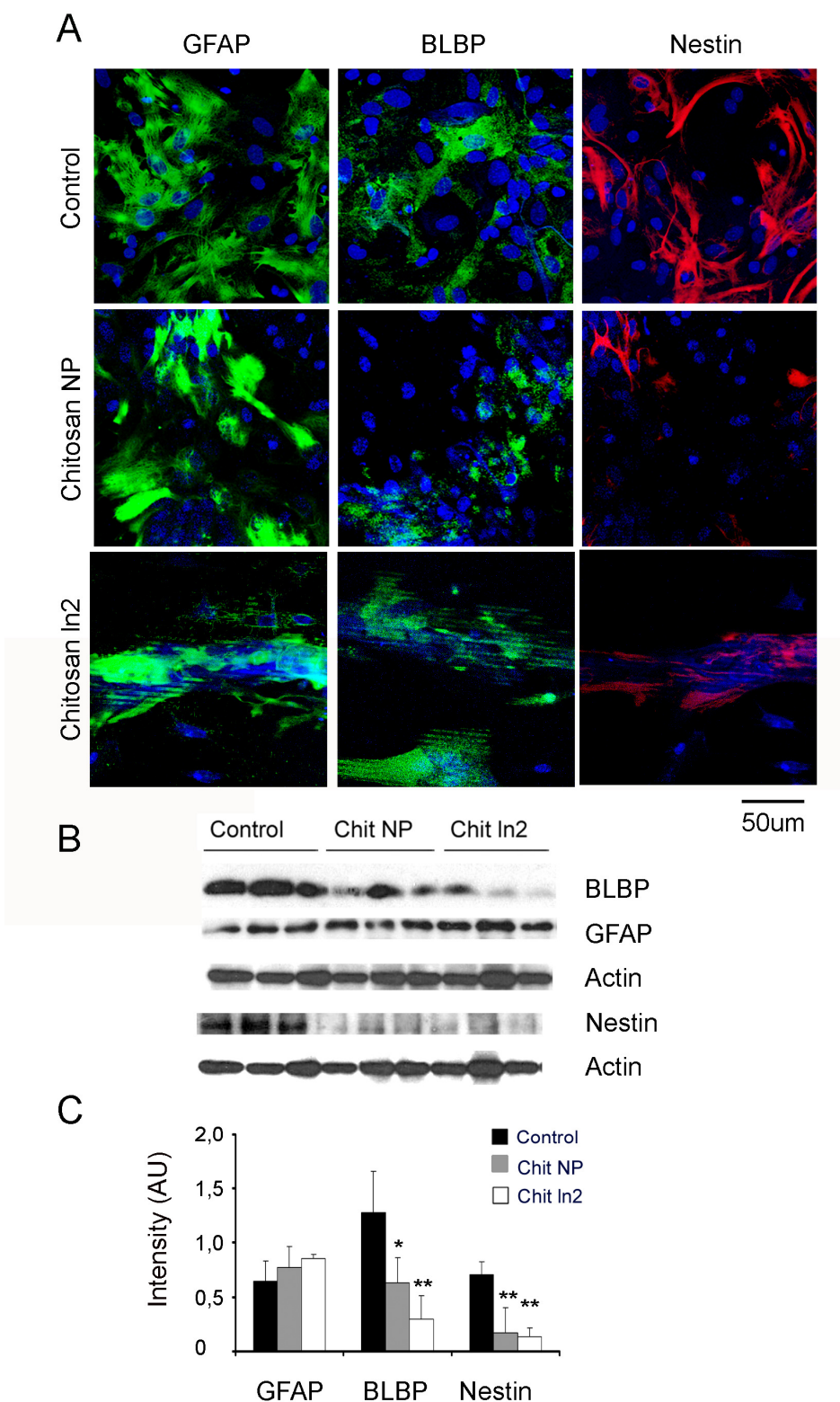


Figure 5: Effect of flat and patterned chitosan on glial cells culture composition and protein expression. **A.** Confocal images of glial cells immunostained for different glial and progenitor markers. Nuclei are stained with TO-PRO-3 (blue). Scale bar = 50µm; **B.** Western Blots showing the expression of glial differentiation markers; **C.** Quantitative representation of the western blot densitometry (intensity values normalized to actin). GFAP and BLBP are markers for astroglia, Nestin for progenitors. * $p < 0.05$ and ** $p < 0.01$.

Results: 2. Neural cell behaviour *in vitro* and *in vivo* on flat and micro patterned chitosan films

FTT-Oval profile analysis showed that glial cells on In2 patterned chitosan align following the pattern (**Fig.6B**). However, bipolar morphologies were only rarely seen and glial cells remained flat and clustered. The alignment concerned mostly the actin cytoskeleton that organized following the lines, rather than the whole cell shape (**Fig. 6A**).

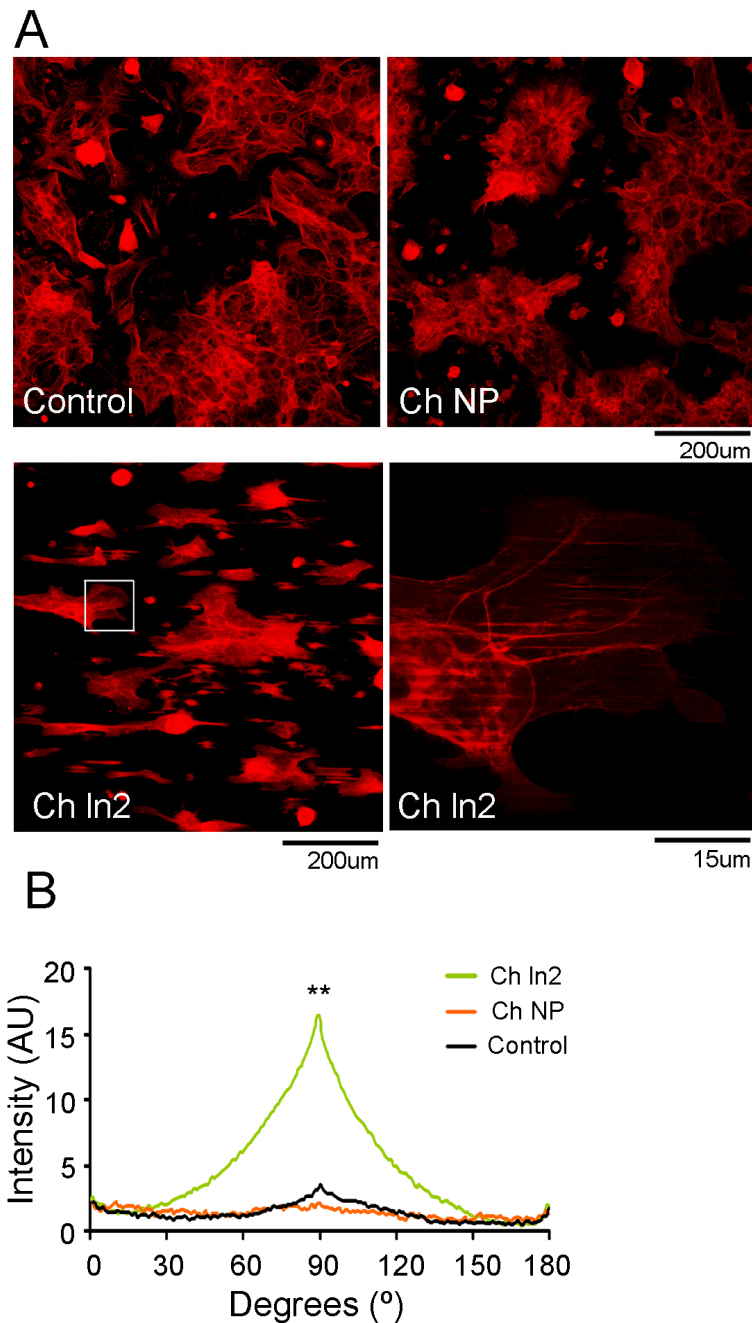


Figure 6: Glial cell alignment on micropatterned chitosan films. **A.** Confocal images of glial cells on control, no patterned chitosan (Ch NP) and In2 patterned chitosan (Ch In2). Cell are stained for actin (phalloidin, red). Scale bar = 200 μm and 15 μm ; **B.** Graphic representing cell alignment by FTT-Oval profile measurement. Flat line indicates random distribution; peak at 90° indicates alignment parallel to the topography. μm ; ** indicates statistical significance respect to control $p \geq 0.01$.

2.3.4 Effect of flat and micro patterned chitosan on neuron to glia cell-cell adhesion

In order to assess whether chitosan influenced glial cells to be permissive or inhibitory for neural growth, E16 neurons were cultured on top of pre-seeded Psg1 P0 glial cells on flat, In2 patterned chitosan and on uncoated glass (control) (**Fig. 7**). Like expected, on glass surfaces neurons could grow only where glial cells were present. Neuronal axons sprouted onto neighbour glial cells but only on spots of high glial cell density. When the distance between glial cells was too long, axons could not cross glass surfaces, leaving empty spaces (**Fig 7**). On the other hand, on all chitosan conditions, neurons could attach and grow in the entire surface, like already demonstrated by pure neuronal cultures. The presence of glial cells did not improve neuronal attachment, neither alignment in patterned surfaces. However, they were not neither inhibitory for neuronal growth, since axons could grow on top of them.

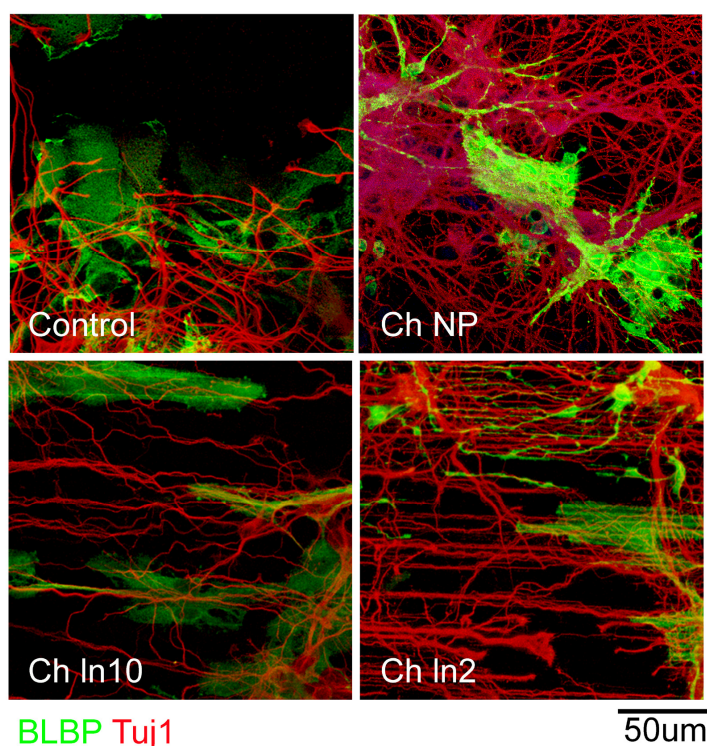


Figure 7: Confocal images of neurons cultured on top of pre-seeded glial cells on control, no patterned (NP), In10 and In2 patterned chitosan. Neurons are stained with Tuj1 (red) and glial cells with BLBP (green).

2.3.5 *In vivo* response

In order to test chitosan *in vivo* biocompatibility, we implanted films in mice P4 cerebral cortex and analyzed them at 21days (P25). Injured brains were used as controls. Generally, chitosan films were easily lost during the processing of the samples, leaving a hole where they were collocated. As a first macro observation, this is indicative of a poor integration within the surrounding brain tissue. Around the injured site, both in chitosan and in injured condition, we observed a diffuse activation of GFAP+, BLBP+ and NG2+ glial cells (**Fig. 8A**). However, activated astrocytes did not encapsulate the film, as observed in the study using GORETEX , Vicryl and ePTFE after 1 months (Kim et al. 2011).

In order to evaluate the inflammatory response, brain sections were stained with F4/80, a marker of microglia and macrophages. An increase of microglia expressing F4/80 was observed in the area surrounding the injury site, both in chitosan and injured condition, indicating that microglial cells were activated. Then we stained the tissue for Laminin, the main component of brain extracellular matrix. The staining was stronger closed to chitosan implant than in injury control, indicating an increase of extracellular matrix production. We identified a neuronal subpopulation with parvalbumina (PV) to analyze neuronal survival in the vicinity of implantation. No reduction in neuronal staining was observed in the presence of implanted chitosan. Some of PV+ cells were next to the zone of the implanted material, indicating that chitosan implants did not cause the death of neighbour neurons. (**Fig.8B**).

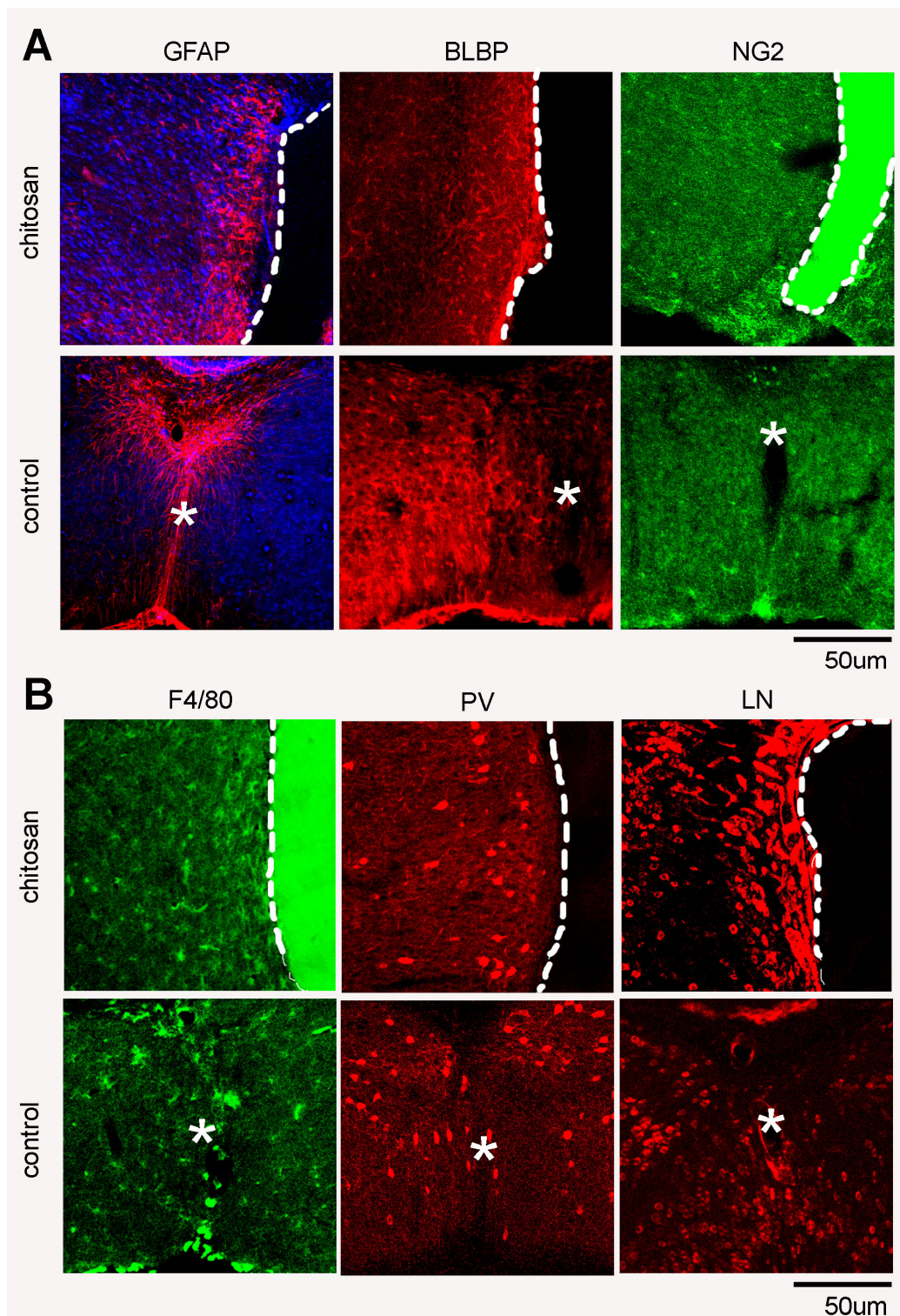


Figure 8: Response to chitosan implants in brain cortex after 21 days *in vivo*. Confocal images of immunohistochemistry performed on brain cortex section of mice that received a chitosan film or only an injury (control). **A.** Astroglial markers (GFAP: activated astrocytes; BLBP: astroglial cells; NG2: oligodendrocytes); **B.** Neuronal markers for parvalbumina (PV), macrophage and microglial markers F4/80 and extracellular matrix marker laminin (LN). Chitosan is delimited by discontinuous line, while injury site in control condition is indicated by *. All the pictures are oriented with meninges on the bottom. Scale bar = 50µm.

2.4. Discussion

Chitosan has been widely used in research toward nervous system tissue engineering. However little is known about cerebral neuronal and glial response to this biomaterial in term of differentiation state. To predict whether a material can be successful for tissue regeneration, understanding the behaviour of both neurons and glial cells is fundamental. Thus, in a first place, in this study we characterized *in vitro* glial and neuronal response to chitosan, either flat or patterned with lines in the micrometric range, in absence of any protein coating.

Chitosan allowed the attachment and growth of both neurons and glial cells. However, glial cells adhered to chitosan in a serum-dependent manner. In our results there was a negative correlation between cell adhesion and serum content. Concentrations of serum at 10% inhibited glial adhesion to chitosan and glass, while when these concentrations were decreased; a better cell attachment was obtained on both materials. This behaviour might be correlated with material surface properties. For instance, it has been demonstrated that surface charge have an important role in protein adsorption. Salloum et al. showed that surfaces of opposite charge to that of the protein were more effective at promoting protein adsorption, even more than the effect of surface wettability (Salloum and Schlenoff 2004). In our study, chitosan films were positively charged (Z potential value: $15\pm 3\text{mV}$) being a great attractor of negatively charged serum proteins at neutral pH. Serum albumin and globulins are the most abundant plasma proteins in mammals. Since albumin (more than 50% of the total protein in plasma) is negatively charged at pH 0 7.4, it would have a higher affinity for the chitosan surface. Moreover, Tangpasuthadol et al. showed in a study with modified chitosan that albumin adsorption increase on chitosan with increasing hydrophilicity (Tangpasuthadol et al. 2003). Chitosan used in this study was also hydrophilic (CA: $34^\circ\pm 3$), thus wettability could play a synergistic role with surface charge in promoting protein adsorption.

Similarly, neurons demonstrated a good affinity for chitosan, probably due to the interaction of the cationic primary amine groups of chitosan and the negative cell

Results: 2. Neural cell behaviour *in vitro* and *in vivo* on flat and micro patterned chitosan films

surface charge (Chung and Wang 2004; Cho et al. 2010). As neuronal cultures were performed in presence of only 1% of serum during the first 24h, the low serum concentration would probably not interfere on the opposite charge attraction between neurons and Ch surface. This result correlates well with previous studies showing that neurons preferentially adhere to and form neural networks on positively charged surfaces such as poly-lysine coated glass (Lakard et al. 2004). In addition, to favour neuronal adhesion, amino groups can promote in some cases neural differentiation (Soria JM 2006; Soria JM 2007; Ren et al. 2009). In this sense, the results showed that chitosan induced the maturation of glial cells indicated by high expression of the mature astroglia marker GFAP and low expression of the radial glia markers BLBP and nestin, both in pure glial cultures and in neuronal enriched embryonic cultures.

Chitosan films loose 0,55% of their mass per day, and it is know that chitosan degrade into chito-oligosaccharides, including D-glucosamine and N-acetyl-D-glucosamine (Chellat et al. 2000), two molecules involved in cellular stress. Therefore, chitosan degradation products might also influence neural cells behaviour. Arvanitis LD showed that hipoxic stress increased the expression of N-acetylglucosamine in ependymal cells, an event that was correlated with an increase of reactive astrocytes (Arvanitis et al. 2011). The same group also showed that N-acetylglucosamine was upregulated by reactive astrocytes following brain lesions (Arvanitis et al. 2001). Increased levels of D-glucosamine in astroglial cells have been also correlated with an increase of markers of endoplasmic reticulum stress (Matthews et al. 2007). In addition, glucosamine is produced also by oligodendrocytes, and was increased after an injury due to the cellular breakdown (Supler 1994). Thus glial cells might interpret biochemical cues from chitosan degradation as stress signals, resulting in an activated phenotype. Nevertheless, the reactive astrocyte phenotype induced by chitosan was not inhibitory for neuron and axonal growth. Moreover, it is known that reactive astrocytes might also play beneficial effects for CNS recovery, as they restart the hemato-encephalic barrier and secrete trophic factors (White et al 2008; Rolls et al., 2009). For example, chitosan induce osteopontin expression in different inflammatory cell types (Ueno et al. 2001), and it has been reported that osteopontin production and secretion by

reactive astrocytes is involved in tissue repair and reorganization after forebrain ischemia (Choi et al. 2007). Moreover, some studies claim that chitosan derived-oligosaccharides have neuro-protective roles, lowering the production of inflammatory cytokines and reducing ROS species (Joodi et al. 2011; Pangestuti and Kim, 2010; Cho et al., 2010). Nevertheless, contradictory results reporting brain inflammatory response to chitosan (Crompton et al. 2007) indicate that further studies would be needed to understand the effect of chitosan and chitosan degradation products on neural cells metabolism.

The introduction of linear patterns has been described to promote cell orientation and alignment (Hsu et al. 2007). Moreover, recent evidences showed that topography can also induce phenotypic changes in cells that underline changes in morphology and protein expression (Bettinger et al., 2009; Hoffman-Kim et al, 2010). In a previous study we demonstrated that glial cells grown on a micropatterned polymer, PMMA, adopt a radial glia-like phenotype, characterized by an elongated morphology, an increase of radial glia markers and the ability of supporting neural migration (Mattotti et al. 2012). The introduction of line patterns on chitosan was then intended to induce a dedifferentiation state of glial cells into a radial glia-like phenotype, in order to facilitate neuronal migration in case of an injury.

The present results showed that although glial cells did align on line patterned chitosan, bipolar morphologies suggestive of radial glia-like cells were barely seen. The biochemical analysis of glial cultures revealed high expression of the mature astroglia marker GFAP in all three substrates, and low or even absent expression of radial glia markers BLBP and nestin.in plane chitosan and more acusated in ln2 chitosan. In contrast with the previous results obtained by our group chitosan induced astroglia maturation and linear patterning synergistically enhances this effect. The observation that similar line patterns induce opposite effects on glial phenotype suggest that the pattern alone is insufficient in determining the cell response and that the material itself plays an important role. In other words, surface pattern cooperate with material chemistry and surface properties in driving cell responses.

Results: 2. Neural cell behaviour *in vitro* and *in vivo* on flat and micro patterned chitosan films

In the case of neurons, we found that the introduction of line patterns promotes neuritic alignment. Interestingly axons and dendrites exhibited different behaviour where axons align with the underlying grooves, while dendrites distribute randomly. This behaviour could be explained taking a look at the development of neurons. It has been shown previously that at the first stages of polarization, neurons extend undifferentiated neurites in random direction and the first to exceed a critical length becomes the axon (Fukata et al. 2002). It was also shown that in absence of biochemical signals, like attractive and repellent molecules, the presence of one more adhesive pathway is sufficient as a trigger to orient neuronal polarity (Vogt et al. 2004). Gomez et al. also demonstrated that axons topographical cues are stronger than biochemical cues in promoting neuronal polarization (Gomez et al. 2007). Thus, physical guidance facilitates the elongation of neurites grown anisotropically, marking their fate as axon.

The dimension of the channels plays a key role on the overall organization of sprouting processes. Anatomically, nerves organize in fascicles composed from groups of nerves, like the cerebellar peduncles, the nerve fibers of corpus callosum or the corticospinal tract (Wakana et al. 2004). On 10 μ m line patterns axons form bundles resembling the anatomical axonal organization, while small patterns isolate the single axons. Promoting fasciculation during regeneration could be helpful for the re-establishment of the original 3D structure. The organization of axons on the grooves between the line patterns suggest that during path finding growth cones sense environmental cues and seem like they are looking for and following the three-dimensional structure. The micro-environment in the valleys may also play a role in axonal guidance. Serum protein adsorption may be different in the grooves and in the ridges, due to local changes in surface free-energy. Curvatures associated to topographic features can trigger changes in protein adsorption and then to cellular behaviour (Von Recum et al. 1996). This could be relevant for axonal migrating growth cones, which filopodia tips are the main site where integrins and laminin receptors are located.

The introduction of chitosan *in vivo* induced an overall foreign body reaction. Astrocytes and microglia/macrophages were slightly activated, indicating a normal inflammation. This kind of response is commonly observed after the implant of a biomaterial. For instance, Tian et al. observed macrophage presence in the first weeks after implantation of lysine coated hyaluronan gel (Tian 2005), and Kim et al. observed elevated microglia/macrophages response after 1 month (Kim et al. 2011).

In this study, implanted chitosan did evoke a mild glial reactivity, but did not cause glial encapsulation and/or fibrosis, at least at the analyzed times. In contrast, in the study by Kim et al., chitosan was implanted *in vivo* in spinal cord, together with vicryl and Goretex as negative control reference materials (Kim et al. 2011). In that study, an evident glial scar and tissue fibrosis could be observed after 30 days. A kind of response that was not observed in the present study.

Overall, the *in vivo* response to chitosan is indicative of a good biocompatibility. However, more studies using other formulations, like microfibers (Nisbet et al. 2009) gel (Tian 2005), sponges (Chirila et al. 1993) or microparticles (Menei et al. 1993), would be desirable to study whether there could be cell invasion and integration.

2.5 Conclusions

In conclusion, uncoated chitosan is a good substrate for glial cells and neurons attachment and growth, eliciting differential responses in both cell types. Chitosan promotes glial cell maturation, which could be interpreted as astroglial activation even when linear patterns were introduced. Nevertheless, those mature/reactive glial cells were permissive for axonal growth. On their side, axons align and organize following the patterns while neuronal dendrites remained indifferent to the topographic cues. The size of linear topographies is also a parameter to take into account as patterns around 10µm help the fasciculation of axons, which can be a desirable response in some applications. Chitosan evoked a mild foreign body reaction *in vivo*. However, toxicity, cell death and encapsulation were not observed, indicating a good

Results: 2. Neural cell behaviour *in vitro* and *in vivo* on flat and micro patterned chitosan films

biocompatibility. Line patterned chitosan could be a candidate to be applied in CNS tissue engineering, in particular if we want to precisely orient the axonal outgrowth. However, it has to be taken into account that the activated glial response to chitosan may have both beneficial and harmful effects on the regenerative response.

Results: 2. Neural cell behaviour *in vitro* and *in vivo* on flat and micro patterned chitosan films

2.6 References

- Alexander, J. K., B. Fuss, et al. (2006). "Electric field-induced astrocyte alignment directs neurite outgrowth." Neuron Glia Biol **2**(2): 93-103.
- Arvanitis, D. L., A. I. Stavridou, et al. (2001). "Reactive astrocytes upregulate one or more gene products that are recognized by monoclonal antibody H." Cell and Tissue Research **304**: 11-19.
- Arvanitis, L. D., K. Vassiou, et al. (2011). "Hypoxia upregulates the expression of the O-linked N-acetylglucosamine containing epitope H in human ependymal cells." Pathol Res Pract **207**(2): 91-6.
- Ayres, C., G. L. Bowlin, et al. (2006). "Modulation of anisotropy in electrospun tissue-engineering scaffolds: Analysis of fiber alignment by the fast Fourier transform." Biomaterials **27**(32): 5524-34.
- Bettinger C. J., R. Langer and J. T. Borenstein. "Engineering substrate topography at the micro- and nanoscale to control cell function." Angew Chem Int Ed Engl 2009;**48**:5406-5415.
- Bumgardner, J. D., R. Wisler, et al. (2003). "Contact angle, protein adsorption and osteoblast precursor cell attachment to chitosan coatings bonded to titanium." J Biomater Sci Polym Ed **14**(12): 1401-9.
- Chellat, F., M. Tabrizian, et al. (2000). "Study of biodegradation behavior of chitosan-xanthan microspheres in simulated physiological media." Journal of Biomedical Materials Research **53**(5): 592-599.
- Cheng, M., W. Cao, et al. (2003). "Studies on nerve cell affinity of biodegradable modified chitosan films." J Biomater Sci Polym Ed **14**(10): 1155-67.
- Chirila, T. V., I. J. Constable, et al. (1993). "Poly(2-hydroxyethyl methacrylate) sponges as implant materials: in vivo and in vitro evaluation of cellular invasion." Biomaterials **14**(1): 26-38.
- Cho, Y., R. Shi, et al. (2010). "Chitosan produces potent neuroprotection and physiological recovery following traumatic spinal cord injury" Journal of Experimental Biology **213** (9): 1513-1520
- Choi, J. S., H. Y. Kim, et al. (2007). "Transient microglial and prolonged astroglial upregulation of osteopontin following transient forebrain ischemia in rats." Brain Research **1151**(0): 195-202.
- Chung, Y., Y. Su, et al. (2004). "Relationship between antibacterial activity of chitosan and surface characteristics of cell wall." Acta Pharmacol Sin **25**(7): 932-936.
- Comeau, J. W., S. Costantino, et al. (2006). "A guide to accurate fluorescence microscopy colocalization measurements." Biophys J **91**(12): 4611-22.
- Crompton, K. E., J. D. Goud, et al. (2007). "Polylysine-functionalised thermoresponsive chitosan hydrogel for neural tissue engineering." Biomaterials **28**(3): 441-449.
- Fernandez, J. G., C. A. Mills, et al. (2008). "Micro- and nanostructuring of freestanding, biodegradable, thin sheets of chitosan via soft lithography." J Biomed Mater Res A **85**(1): 242-7.
- Fukata, Y., T. Kimura, et al. (2002). "Axon specification in hippocampal neurons." Neuroscience Research **43**(4): 305-315.
- Gomez, N., S. Chen, et al. (2007). "Polarization of hippocampal neurons with competitive surface stimuli: contact guidance cues are preferred over chemical ligands" Journal of The Royal Society Interface **4** (13): 223-233
- Haipeng, G., Z. Yinghui, et al. (2000). "Studies on nerve cell affinity of chitosan-derived materials." J Biomed Mater Res **52**(2): 285-95.
- Hoffman-Kim D., J. A. Mitchel, R. V. Bellamkonda. "Topography, cell response, and nerve regeneration." Annu Rev Biomed Eng 2010;**12**:203-231.
- Hsu, S. H., P. Lu, et al. (2007). "Fabrication and evaluation of microgrooved polymers as peripheral nerve conduits." Biomedical Microdevices **9**(5): 665-674.
- Joodi, G., N. Ansari, et al. "Chito oligosaccharide-mediated neuroprotection is associated with modulation of Hsps expression and reduction of MAPK phosphorylation." Int J Biol Macromol **48**(5): 726-35.

Results: 2. Neural cell behaviour *in vitro* and *in vivo* on flat and micro patterned chitosan films

- Kim, H., C. H. Tator, et al. (2011). "Chitosan implants in the rat spinal cord: Biocompatibility and biodegradation." Journal of Biomedical Materials Research Part A **97A**(4): 395-404.
- Lakard, S., G. Herlem, et al. (2004). "Adhesion and proliferation of cells on new polymers modified biomaterials." Bioelectrochemistry **62**(1): 19-27.
- Lee, J. E., S. E. Kim, et al. (2004). "Effects of a chitosan scaffold containing TGF-beta1 encapsulated chitosan microspheres on *in vitro* chondrocyte culture." Artif Organs **28**(9): 829-39.
- Martínez-Ramos, C., S. Lainez, et al. (2008). "Differentiation of Postnatal Neural Stem Cells into Glia and Functional Neurons on Laminin-Coated Polymeric Substrates" Tissue Engineering Part A **14**(8): 1365-1375.
- Martín-López, E., M. Nieto-Díaz, et al. (2012). "Differential Adhesiveness and Neurite-promoting Activity for Neural Cells of Chitosan, Gelatin, and Poly-L-Lysine Films." Journal of Biomaterials Applications **26**(7): 791-809.
- Matthews, J. A., J. L. Belof, et al. (2007). "Glucosamine-induced increase in Akt phosphorylation corresponds to increased endoplasmic reticulum stress in astroglial cells." Mol Cell Biochem **298**(1-2): 109-23.
- Mattotti, M., Z. Alvarez, et al. (2012). "Inducing functional radial glia-like progenitors from cortical astrocyte cultures using micropatterned PMMA." Biomaterials **33**(6): 1759-1770.
- Menei, P., V. Daniel, et al. (1993). "Biodegradation and brain tissue reaction to poly(D,L-lactide-co-glycolide) microspheres." Biomaterials **14**(6): 470-478.
- Nisbet, D. R., J. S. Forsythe, et al. (2009). "Review Paper: A Review of the Cellular Response on Electrospun Nanofibers for Tissue Engineering" Journal of Biomaterials Applications **24** (1): 7-29
- Ortega, J. A. and S. Alcantara (2010) "BDNF/MAPK/ERK-induced BMP7 expression in the developing cerebral cortex induces premature radial glia differentiation and impairs neuronal migration." Cerebral Cortex **20**: 2132-44.
- Pangestuti, R. and S. K. Kim "Neuroprotective properties of chitosan and its derivatives." Mar Drugs **8**(7): 2117-28.
- Ren, Y. J., H. Zhang, et al. (2009). "In vitro behavior of neural stem cells in response to different chemical functional groups." Biomaterials **30**(6): 1036-1044.
- Rolls A., R. Shechter (2009) "The bright side of the glial scar in CNS repair." Nat Rev Neurosci:**10**:235-241.
- Salloum, D. S. and J. B. Schlenoff (2004). "Protein adsorption modalities on polyelectrolyte multilayers." Biomacromolecules **5**(3): 1089-96.
- Soria J. M., M. S. Sánchez, et al. (2006). "Survival and differentiation of embryonic neural explants on different biomaterials." Journal of Biomedical Materials Research Part A **79A**(3): 495-502.
- Soria J. M., Bahamonde, D. M. et al. (2007). "Influence of the substrate's hydrophilicity on the *in vitro* Schwann cells viability." Journal of Biomedical Materials Research Part A **83A**(2): 463-470.
- Supler M. L., S. L. Semple-Rowland (1994). "Oligodendrocytes produce low molecular weight glycoproteins containing N-acetyl-D-glucosamine in their Golgi apparatus." Glia **10**(3): 193-201.
- Tangpasuthadol, V., N. Pongchaisirikul, et al. (2003). "Surface modification of chitosan films.: Effects of hydrophobicity on protein adsorption." Carbohydrate Res **338**(9): 937-942.
- Tian, W., S. P. Hou, et al. (2005). "Hyaluronic Acid-Poly-D-Lysine-Based Three-Dimensional Hydrogel for Traumatic Brain Injury." Tissue Engineering Part A **11**(3-4): 513-525.
- Ueno, H., T. Mori, et al. (2001). "Topical formulations and wound healing applications of chitosan." Ad Drug Delivery Rev Drug Delivery App of Chit **52**(2): 105-115.
- Von Recum, A. F., T.G., Van Kooten, (1996) "The influence of micro-topography on cellular response and the implications for silicone implants." Journal of Biomaterials Science, Polymer Edition, **7**(2): 181-198.
- Vogt, A. K., F. D. Stefani, et al. (2004). "Impact of micropatterned surfaces on neuronal polarity." J Neurosci Methods **134**(2): 191-8.

Results: 2. Neural cell behaviour *in vitro* and *in vivo* on flat and micro patterned chitosan films

Wakana, S., H. Jiang, et al. (2004). "Fiber Tract-based Atlas of Human White Matter Anatomy." Radiology **230**(1): 77-87.

White R. E., L. B. Jakeman "Don't fence me in: harnessing the beneficial roles of astrocytes for spinal cord repair." Restor Neurol Neurosci 2008;**26**:197-214.

3. EFFECT OF MODEL SURFACES ON GLIAL ADHESION AND DIFFERENTIATION

Abstract

In the CNS, the use of neural electrodes to provide a treatment to degenerative diseases is finding increasing application. However, as a consequence of electrode implant, the inflammatory response lead to the formation of reactive glial cells, that encapsulates the electrode. Looking for better materials to promote implantable electrodes, recent studies have shown that material properties can be manipulated to reduce reactivity in glial cells. It is well known that surface chemistry and wettability are extremely important to determine cell attachment and behavior. In this study we asses the effect of wettability and surface chemistry on glial cells adhesion and differentiation, in order to better understanding the relationship between adhesion and phenotype. Glass was functionalized by SAMs technique using appropriate organosilanes that expose CH₃, OH, COOH and NH₂ groups at the surface. Glial cells from newborn mice cerebral cortex were cultured on top either for 5h or 5 days. Immunocytochemistry was used to determine adhesion and spreading after 5h and differentiation after 5 days. Glial cells showed a different behavior on model surfaces. Surfaces with intermediate wettability (with contact angle values from 40° to 60°) promoted a better cell adhesion both at 5h and 5 days, induce less cell loss and wide and round morphologies. Differences in cell morphology on all the other surfaces were almost absent after 5 days, with an exception for hydrophobic surfaces. Indeed, surfaces with low wettability (CH₃ functionalized, contact angle: 103°) promoted elongated morphologies that were maintained during the 5 days periods, despite the initial low cell adhesion. Moreover, these elongated cells were positive for nestin, a radial glia progenitor marker, and they were similar to the reference condition of progenitor cells. Those results suggest that hydrophobicity and low adhesion strength might be key element in directing astrocytes toward immature or progenitor phenotypes, while intermediate wettability promote better cell adhesion and spreading, probably liked with glia maturation. Even though further studies are needed to better characterize the glial response, these findings could be helpful for improving the design and the outcome of brain electrodes and implants.

3.1 Introduction

In the last 50 years, technological advances lead to the development of brain implants. Brain implants consist in electrodes in direct contact with parts of the cerebral cortex and are currently used as cochlear implants, to treat Parkinson disease, epilepsy and tinnitus. (Cogan 2008; Marin and Fernandez 2010; Ereifej et al. 2011). Despite their therapeutic utility, the procedure of electrode implant is always traumatic and lead to the development of a situation of inflammation and foreign body reaction. Glial cells are the first type of cells that contact the implant surface and a common drawback is the electrode encapsulation (McConnell et al. 2009; Ereifej et al. 2011). Astrocytes, along with fibroblasts, endothelial cells, and macrophages, are the major component of the CNS wound-healing process. In response to an injury or to the implant of an electrode, astrocytes become reactive and form a barrier which separate and protect the healthy tissue from the damaged one. (Polikov et al. 2006; White and Jakeman 2008).

However, astrocytes reaction can be moderate and controlled by multiple strategies. For instance, it has been shown that glial cells could de-differentiate *in vitro*, acquiring progenitor phenotypes, permissive for neural growth (Yu et al. 2006; Vaccarino et al. 2007; Moon et al. 2008). In our previous work, we observed that mature glial cells can turn into more immature radial glia like cells driven by line micropatterns presented by a polymer, PMMA. An interesting observation was that PMMA itself, a slightly hydrophobic polymer (contact angle: $76^{\circ}\pm 4$), already had an effect on astrocyte de-differentiation (Mattotti et al. 2012).

In the case of electrodes, inflammatory response and biocompatibility can be modulated by modifying the electrode surface. This include the preparation of smooth or rough surfaces, chemical modification with anti-inflammatory compounds, adhesion proteins, bioactive molecules or coating materials (He et al. 2006; Marin and Fernandez 2010).

Physical and chemical characteristics of the materials, such as wettability and surface chemistry are key in determine glial cell behavior. Some characteristics can promote cell attachment and proliferation, and others can induce a less reactive state in glial cells (Cameron J. Wilson 2005). In the last years, cell response to surface chemistry *in vitro* was matter of study of various research groups. For instance, Ren et al studied the behaviour of neural stem cells (NSCs) cultured on glass surfaces modified by different chemical groups. NSC demonstrated to be extremely sensitive to surface chemistry, changing their adhesion, migration and lineage specification according to the different chemical groups (Ren et al. 2009). Another example is the study by Soria et al, which cultured peripheral nervous system glial cells (Schwann cells) on polymers with different wettability. These polymers included polymethylacrylate, chitosan, polyethylacrylate, polyhydroxyethylacrylate, and a series of random copolymers containing ethylacrylate and hydroxyethylacrylate monomeric units. They observed that Schwann cells are influenced by the substrate's surface chemistry in terms of cell attachment and proliferation. In particular, they conclude that hydrophobic biomaterials based on polymethylacrylate, polyethylacrylate, and the copolymers polyethylacrylate, polyhydroxyethylacrylate in a narrow composition window were better substrates to promote cell attachment and proliferation (Soria JM 2007).

Based on these evidences, this work was designed to study the role of wettability on glial cells response. We assessed glial cells adhesion and differentiation to four model surfaces presenting different chemical groups (CH_3 , OH , COOH and NH_2). The substrates consisted in glass functionalized by the self-assembling monolayer (SAM) technique. This method provides the capability to control surface properties varying only surface chemistry, without interfering with stiffness or bulk chemistry. We characterized glial cells response after 5h in terms of cell adhesion and overall morphology; subsequently, we studied cell differentiation state after 5 days using immunocytochemical techniques.

3.2. Materials and methods


3.2.1 Preparation of model surfaces

Glass coverslips (22x22 mm, Fisher Bioblock, Thermo Fisher Scientific, Waltham, MA, USA) were functionalized according to a previously described protocol (Gustavsson et al. 2008; Coelho et al. 2010; Coelho et al. 2011). To obtain hydrophilic OH surfaces, Glass coverslips were cleaned in an ultrasonic bath for 10 min in a 1:1 mixture of 2-propanol and tetrahydrofuran. The samples were then exposed to piranha solution (30% (v/v) H₂O₂ and 70% (v/v) H₂SO₄) for 30 min followed by a copious rinsing with milliQ water (18.2 MΩ) and dried. To obtain CH₃, NH₂ and COOH functionalized surfaces, the samples were pre-cleaned as above and allow reacting with the correspondent silane. For CH₃ functionalization, samples were placed in a solution containing 12.5 ml of carbon tetrachloride, 37.5 ml of heptane and 220 μl ODS (organosilane trichloro-(octadecyl)-silane (ODS), Sigma (St. Louis, MO, USA). The samples were left in this solution for 18 min at room temperature and the excess of silane was washed away with pure heptane. Samples were then heated for one hour at 80°C (Coelho NM 2010). For NH₂functionalization the samples were immersed for 18 min at room temperature in a solution containing 30 ml methanol, 10 ml of 4% acetic acid glacial and 3-(2-aminoethylamino) propyltrimethoxysilane (C₈H₂₂N₂O₃Si, Sigma-Aldrich, Madrid, Spain) to yield a final 1% concentration. Excess of silane was washed away by immersion in excess solvent solution. Samples were air dried and then heated at 80°C for 1h. COOH functionalization was performed in two steps; first the samples were immersed in a 1:3 mixture of CCl₄ and *n*-C₇H₁₆ containing 0.01M 10-(carbomethoxy) decyl dimethylchlorosilane (C₁₄H₂₉ClO₂Si, ABCR GmbH &Co) for 4h at 4°C, which create COOHCH₃ functions. Samples were then washed in silane-free solvent, heated as above and immersed overnight in a 12M HCl solution remove methyl moieties. Un-functionalized glass (Glass) was used as control, while poly-D-lysine coated glass (LysGlass) was used as a reference substrate for good cell adhesion. To obtain LysGlass, a standard cell adhesive surface, glass coverslips were incubated at 37°C during 30 min with an aqueous solution containing 10μg/ml poly-D-lysine. Excess of the aminoacid was washed away with water.

3.2.2 Surface characterization

The wettability of surfaces was estimated in previous works with water contact angle measurements using sessile drop technique performed on Dataphysics Contact Angle Systems OCA15. Average values of water contact angles are reported in **Table 1**. Surfaces functionalized with OH groups were the most hydrophilic (contact angle: $25^\circ \pm 7$) (Coelho et al. 2010), followed by the COOH surfaces (contact angle: $34^\circ \pm 4$) (Coelho et al. 2011) and the positive control poly-D-lysine coated glass (contact angle: $42^\circ \pm 3$). HN_2 and Glass had increased contact angles (53 ± 7 and 73 ± 3 respectively) (Coelho et al. 2011), and CH_3 was the most hydrophobic (contact angle: 103 ± 3) (Coelho et al. 2010).

Table 1. Values of water contact angle of model surfaces. Values of OH and CH_3 are from (Coelho et al. 2010), while values of COOH and NH_2 are from (Coelho et al. 2011)



| Surface | Contact angle ($^\circ$) |
|-----------------|----------------------------|
| -OH | 25 ± 7 |
| -COOH | 34 ± 4 |
| LysGlass | 42 ± 3 |
| - NH_2 | 53 ± 7 |
| Glass | 73 ± 3 |
| - CH_3 | 103 ± 3 |

3.2.3 Primary mouse glial cell culture

Glial cells were derived from the cerebral cortex of newborn mice like described elsewhere (Ortega and Alcantara 2010; Mattotti et al. 2012). All animal housing and procedures were approved by the Institutional Animal Care and Use Committee in accordance with Spanish and EU regulations. Briefly, brain cortices were dissected out free of meninges in dissection buffer (PBS 0.6% glucose (Sigma), 0.3% BSA (Sigma)) and digested with trypsin (Biological Industries) and DNase I (Sigma) for 10 min at 37°C . The tissue was dissociated in Dulbecco's Modified Eagle Medium (DMEM, Biological Industries) 10% Normal Horse Serum (NHS, GIBCO), 1% Penicillin-Streptomycin (Pen-

Results: 3. Effect of model surfaces on glial adhesion and differentiation

Strep, Biological Industries), 2mM L-Glutamine (Biological Industries). After centrifugation and resuspension, cells were plated and grown to confluence at 37°C, 5% CO₂ (approximately 25-30 days *in vitro*, DIV). All the experiments were performed using glial cells from the first passage (Ps1) To assess the influence of different surface chemistry, glial cells were cultured at a density of 2×10^5 cells/cm² for either 5 h or 5 DIV on Glass, LysGlass, OH, CH₃, NH₂ and COOH surfaces in the experimental medium (EM) which consisted in Neurobasal (NB, Sigma), 3% Normal Horse Serum (NHS, GIBCO), 1% Penicillin-Streptomycin (Pen-Strep, Biological Industries), 2mM L-Glutamine (Biological Industries).

To compare biochemical changes of glial cells on model surfaces we used two reference conditions (Mattotti et al. 2012). Briefly, reactive/mature glia was obtained by culturing Ps1 glial cells for 8 DIV in EM and with EM supplemented with dibutyril cyclic AMP (dcAMP, 500 μM, SIGMA) during 7 more days. Progenitor glia was obtained by culturing Ps1 glial cells for 24h in EM and then in NB supplemented with G5 (GIBCO) for 7 DIV.

3.2.4 Cell count and overall cell morphology

To study the overall cell morphology of glial cells adhering to different samples, 5×10^4 cells/well were seeded in 24-well TCP containing modified glass surfaces for 5h in EM. At the end of the incubation, the cells were fixed with 4% paraformaldehyde (15min) and permeabilized with 0.5% Triton X-100 for 5min. For the overall morphology studies and cell adhesion measurements the actin cytoskeleton was stained with 20μg/mL AlexaFluor 488 phalloidin (Molecular Probes) in PBS and then the samples were washed and mounted in Mowiol. The samples were analyzed with a fluorescent microscope (Nikon Eclipse E800) or with a spectral confocal microscope (Leica TCS-SL, Leica Microsystems, Mannheim, Germany), and at least three representative images of each condition were acquired. Morphological parameters such as the number of adhered cells, the mean cell surface area and the cell circularity were evaluated using the ImageJ plug-ins (National Institutes of Health, USA; <http://rsb.info.nih.gov/ij/>). Circularity index describe cell shape, where 1 is round, while 0 is linear.

3.2.5 Immunocytochemistry

For immunofluorescence, fixed samples (4% PFA for 15min at RT) were incubated with primary antibodies and appropriate Alexa488 or Alexa555 secondary antibodies (1:500, Molecular Probes, Eugene, Oregon). TO-PRO-3 iodide (1:500, Molecular Probes, Eugene, Oregon) was used to stain nuclei and AlexaFluor 555 phalloidin (1:2000, Sigma) to stain cytoskeleton. The following primary antibodies were used: rabbit anti-GFAP (Mature and Reactive Glia marker, 1:500, Dako) and mouse anti-Nestin (Radial Glia marker, 1:200, Abnova Corporation).

3.2.6 Statistical analysis

Statistical analysis was performed using the Statgraphic-plus software. One-way ANOVA and Fisher's least significant difference (LSD) procedure were used to discriminate between the means.

3.3 Results

3.3.1. Glial cells adhesion and survival

In order to characterize the effect of wettability on glial cells primary adhesion and proliferation, glial cells were seeded on our model surfaces during 5 h or 5 DIV. Then cell nuclei were stained and counted by the aid of ImageJ software.

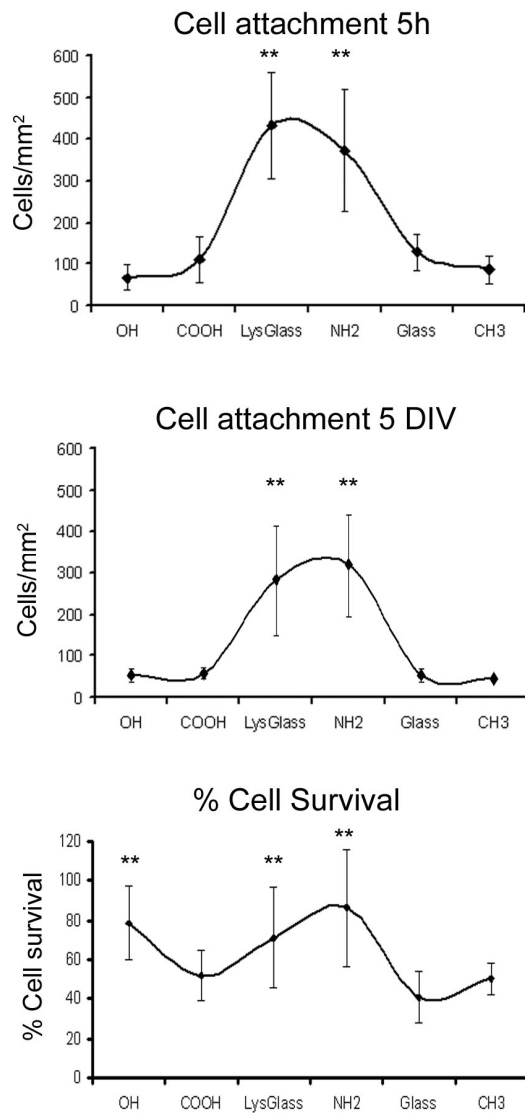


Figure 1. Glial cell attachment on model surfaces with increasing hydrophobicity after 5h and 5 DIV and the respective percentage of cell survival. Significant difference ** $p < 0.01$ respect to Glass.

Glial cells showed different adherent behavior on the different model surfaces. After 5h, the number of adhered cells was significantly higher on the surfaces with intermediate hydrophobicity values (NH₂ and LysGlass functionalized surfaces, with 372 ± 145 cells/mm² and 432 ± 126 cells/mm² respectively). On the other hand, on OH, CH₃ and COOH functionalized surfaces numbers were not significantly different from the un-functionalized glass (67 ± 31 , 87 ± 32 , 111 ± 53 and 129 ± 44 cells/mm² respectively). After 5 DIV, the same trend was maintained. On NH₂ functionalized surfaces and on LysGlass cell number was significantly higher (292 ± 139 cells/mm² and 330 ± 129 cells/mm² respectively), while on OH,

CH₃ and COOH functionalized surfaces numbers were not significantly different from the un-functionalized glass (52 ± 16 , 44 ± 6 , 58 ± 14 and 52 ± 16 cells/mm² cells/mm² for OH, CH₃, COOH and glass respectively). However, the cell number was significantly reduced in all surfaces,

indicative of some cell loss. Surfaces with intermediate hydrophobicity values had the higher cell survival rate ($71 \pm 26\%$ and $86 \pm 30\%$ for NH_2 and LysGlass), together with the hydrophilic OH surfaces ($79 \pm 19\%$), while control glass had the smaller cell survival rate ($41 \pm 13\%$), followed by CH_3 and COOH functionalized surfaces ($50 \pm 8\%$ and $52 \pm 13\%$ respectively) (**Fig.1**).

3.3.2 Glial cells morphometric characterization after 5h

In order to characterize the effect of wettability on glial cells morphology, glial cells were seeded on the different model surfaces during 5h. Then cells were stained for actin cytoskeleton and the morphometric parameters analyzed with the aid of the ImageJ software. The overall morphology and morphometric parameters of glial cells adhering for 5h are shown in **Fig.2**.

Cells grown on surfaces with intermediate hydrophobicity had bigger cell area values than cells on control glass (4576 ± 2097 , 4443 ± 1099 and 3082 ± 741 pixels for NH_2 , LysGlass and Glass respectively), and a circularity index close to 1, similar than control Glass ($0,78 \pm 0,03$, $0,78 \pm 0,04$ and $0,64 \pm 0,09$ for NH_2 , LysGlass and Glass respectively). The combinations of these parameters describe cells on NH_2 and LysGlass surfaces as round and spread, while cells on glass can be considered round and small. Cells grown on the more hydrophilic COOH functionalized surface had also big cell areas, but they were characterized by a lower circularity index (area: 4392 ± 1180 pixels and circularity index: $0,47 \pm 0,06$). These parameters together are indicative of big and elongated and/or ramified morphologies. These morphologies are visible from phalloidin staining pictures (**Fig.2**). Cells grown on the most hydrophilic (OH) and the most hydrophobic (CH_3) surfaces were both small, with no significant differences from cells on control glass surfaces (cell area values 1914 ± 599 and 3989 ± 1728 for OH and CH_3 respectively). However, cells on hydrophilic surfaces had a significantly higher circularity index ($0,58 \pm 0,19$) compared to hydrophobic surfaces ($p \leq 0.01$), indicative of round shapes, while cells on hydrophobic surfaces had a lower cell circularity index, indicative of elongated morphology ($0,40 \pm 0,07$).

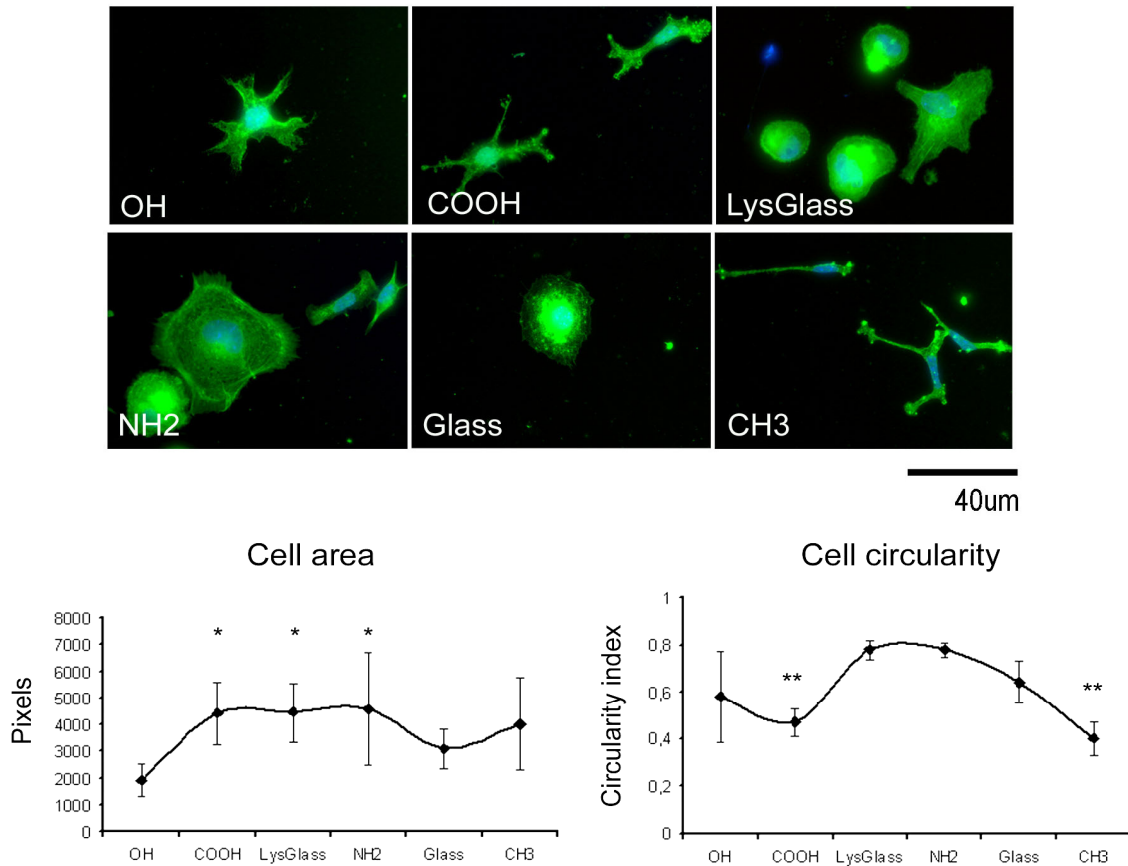


Figure 2. Glial cell morphology and morphometric parameters after 5 h on model surfaces with increasing hydrophobicity. **A.** Confocal pictures for actin staining. Scale bar = 40 μ m. **B.** Glial cells area (pixels) and cell circularity. Circularity index values range from 0 to 1, where 0 = linear shape and 1= circular shape. * $p \leq 0.05$ and ** $p \leq 0.01$ respect to Glass.

3.3.3 Glial cells differentiation after 5 DIV

In order to determine if the initial cell attachment and morphology had an influence on cell differentiation, cells on model surfaces were cultured for 5 DIV. Reactive and progenitor glial cells were used as two reference conditions. Cells were stained for GFAP, a marker for astroglia, and Nestin, a progenitor cell marker.

Concerning cell morphology, we observed that despite the differences presented after 5h, after 5 DIV glial cells assumed quite similar morphologies on all the conditions, except the CH₃ functionalized surface (**Fig.3**). Cells on Glass, LysGlass, COOH, NH₂ and OH were spread, express GFAP and in lower amount nestin. This phenotype does not differ from control Glass condition and in any case they resemble the stellate and ramified morphologies of reactive glial cells. On the other hand, cells on CH₃ surfaces

had an elongated morphology and express more markedly nestin. This kind of morphology and immunoreactivity strongly resemble radial glia-like progenitor cells.

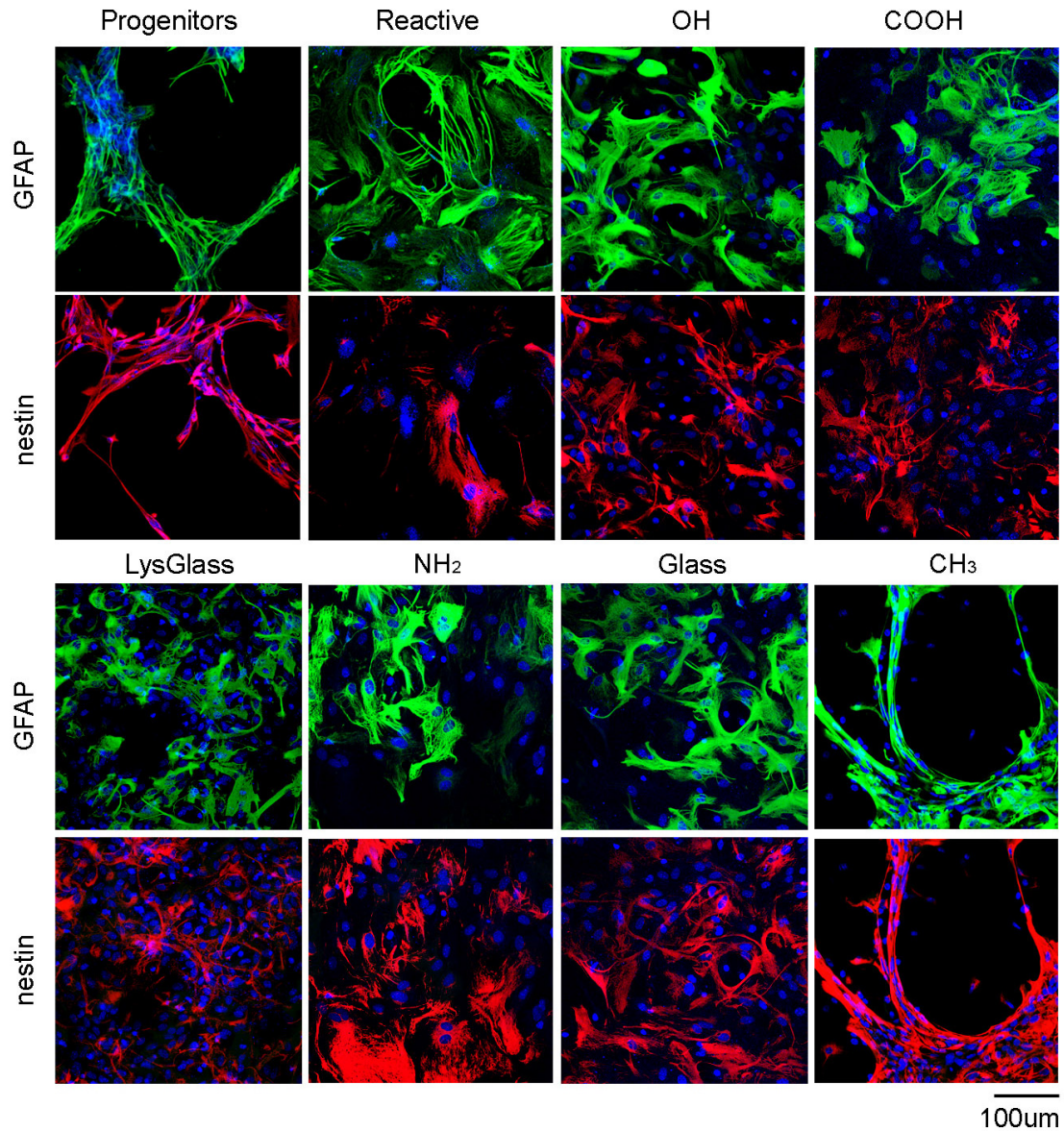


Figure 3. Cellular composition of glial cultures. Confocal images of glial cells immunostained for GFAP (astroglia) and Nestin (progenitors). Nuclei are stained with TO-PRO-3 (blue). Scale bar = 100µm.

3.4. Discussion

When electrodes are implanted in CNS, a common drawback is inflammation and consequently the encapsulation caused by glial reaction. Astrocytes respond to the insult becoming hypertrophic, proliferating, increasing the expression of the intermediate filament protein GFAP, and produce elevated extra cellular matrix proteins (White and Jakeman 2008). Thus, understanding and controlling glial response to materials could help to select appropriate coatings for implant that minimize glial reaction. The aim of this work was to characterize the response of astrocytes to substrates with different wettability and surface chemistry. We analyzed in a first place, initial adhesion and morphology and, in a second place, the morphology and phenotype after 5 DIV.

The result showed a marked preference of astrocytes for NH_2 and LysGlass functionalized surfaces, which had intermediate wettability values (contact angles: $42^\circ \pm 3$ to $53^\circ \pm 7$ respectively). These surfaces promoted a better cell adhesion, increased cell survival and induce wide and round morphology. Apart from wettability, these surfaces are also characterized by the presence of amino groups, which at physiological pH are positively charged (Takehara et al. 2008). It is known since 1976 that cells are negatively charged and adhere with more affinity to positively charged surfaces (Maslow 1976). More recently, this has been shown by several authors. For instance, Dadsetan et al cultured DRG explant and Schwann cells on positively charged hydrogels. They conclude that charged hydrogels are better substrates than not-charged hydrogels in supporting neurons and Schwann cells. Moreover, Schwann cells on positively charged surfaces differentiated to a myelinating phenotype, and they formed myelin sheaths on newly formed DRG axons (Dadsetan et al. 2009). These evidences suggest that positive charges play fundamental roles in promoting neurons and glial cells adhesion and perhaps differentiation toward a more mature phenotype.

On the other surfaces (OH, COOH, Glass and CH_3), cell attachment was lower and cell morphologies were different. However, the differences in cell morphology present after 5h were almost absent after 5 DIV, with an exception for CH_3 surfaces. Those

results suggest that primary cell adhesion does not predict the direction of cell differentiation in culture. Similar results were obtained also by Biran et al, which cultivate glial cells on several different materials of biomedical interest having contact angles values ranging from 35° to 75°. They observed that despite the initial differences among the materials, after 12 DIV astrocytes were similar in all conditions (Biran et al. 1999).

Surprisingly, cells on hydrophobic surfaces (CH₃) assume stretched and aligned morphologies, which resemble progenitor radial glia cells (**Fig.3**). The fact that no significant proliferation was observed means that the changes seen in the morphology and immunoreactivity of glial cells are induced directly by the surfaces on the seeded cells, and mostly exclude the possibility of the expansion or the suppression of a determined cell population.

It has been documented that surface hydrophobicity does have an effect on protein conformation, possibly making the protein's cell binding domain unavailable for cells to attach (Ni M 2009). Moreover, Burton et al found that hydrophobicity is inversely correlated to adhesive strength; an increase in hydrophobic characteristics therefore reduces adhesive force (Burton and Bhushan 2005). Ereifej et al, observed that C6 rat astrocytoma cell line adhere with poor strength on PMMA and SU-8, two slightly hydrophobic materials, in comparison to other hydrophilic substrates. (Ereifej et al. 2011). Moreover, they confirmed the biocompatibility of the polymers and a slight decrease of astrocyte reactivity compared to silicon and platinum, two standard electrode reference surfaces (Ereifej et al. 2011).

In our previous study, we observed that glial cells on PMMA express some progenitor cells markers (Mattotti et al. 2012). Considering these observation, we hypothesized that low adhesion strength induced by hydrophobic surfaces might be a key element in directing astrocytes toward an immature phenotype. However, further studies are needed to better characterize astrocytes behavior and phenotype on hydrophobic surfaces, like Western Blot and proliferation analysis.

3.5 Conclusions

Surface chemistry and wettability have an important influence on glial attachment and differentiation. Cells adhere and spread better on NH₂ and Lysine functionalized surfaces, which had intermediate wettability (42°±3 and 53°±7 respectively). However, despite the low initial adhesion, cells on hydrophobic CH₃ functionalized surfaces were positive for nestin and had elongated morphologies, resembling radial glia progenitor cells. Those results suggest that hydrophobicity and low adhesion strength might be key element in directing astrocytes toward immature or progenitor phenotypes, while intermediate wettability promote better cell adhesion and spreading. Even though further studies are needed to better characterize glial response, these findings could be helpful for improve the design of brain electrodes to minimize adverse glial scar reaction and to prolong electrode life.

3.6 References

- Biran, R., M. D. Noble, et al. (1999). "Characterization of cortical astrocytes on materials of differing surface chemistry." Journal of Biomedical Materials Research **46**(2): 150-159.
- Burton, Z. and B. Bhushan (2005). "Hydrophobicity, Adhesion, and Friction Properties of Nanopatterned Polymers and Scale Dependence for Micro- and Nanoelectromechanical Systems." Nano Lett. **5**(8): 1607-1613.
- Cameron J., R. E. C. Wilson, et al. (2005). "Mediation of Biomaterial–Cell Interactions by Adsorbed Proteins: A Review." Tissue Engineering. **11**((1-2)): 1-18.
- Coelho, N. M., C. Gonzalez-Garcia, et al. (2010). "Different assembly of type IV collagen on hydrophilic and hydrophobic substrata alters endothelial cells interaction." Eur Cell Mater **19**: 262-72.
- Coelho, N. M., C. Gonzalez-Garcia, et al. (2011). "Arrangement of type IV collagen on NH and COOH functionalized surfaces." Biotechnol Bioeng **108**(12): 3009-18.
- Cogan, S. F. (2008). "Neural stimulation and recording electrodes." Annu Rev Biomed Eng **10**: 275-309.
- Dadsetan, M., A. M. Knight, et al. (2009). "Stimulation of neurite outgrowth using positively charged hydrogels." Biomaterials **30**(23-24): 3874-3881.
- Ereifej, E. S., S. Khan, et al. (2011). "Characterization of astrocyte reactivity and gene expression on biomaterials for neural electrodes." Journal of Biomedical Materials Research Part A **99A**(1): 141-150.
- Gustavsson, J., G. Altankov, et al. (2008). "Surface modifications of silicon nitride for cellular biosensor applications." J Mater Sci Mater Med **19**(4): 1839-50.
- He, W., G. C. McConnell, et al. (2006). "Nanoscale laminin coating modulates cortical scarring response around implanted silicon microelectrode arrays." J Neural Eng **3**(4): 316-26.
- Marin, C. and E. Fernandez (2010). "Biocompatibility of intracortical microelectrodes: current status and future prospects." Front Neuroeng **3**: 8.
- Maslow, D. E. and L. Weiss (1976). "Some effects of positively charged surface groups on cell aggregation." J. Cell Sci. **21**: 219-225.
- Mattotti, M., Z. Alvarez, et al. (2012). "Inducing functional radial glia-like progenitors from cortical astrocyte cultures using micropatterned PMMA." Biomaterials **33**(6): 1759-70.
- McConnell G. C., H. D. Rees (2009). "Implanted neural electrodes cause chronic, local inflammation that is correlated with local neurodegeneration." Journal of Neural Engineering **6**(5): 056003
- Moon, J. H., B. S. Yoon, et al. (2008). "Induction of neural stem cell-like cells (NSCLCs) from mouse astrocytes by Bmi1." Biochem Biophys Res Commun **371**(2): 267-72.
- Ni M, T., W.H., Choudhury, D, Abdul Rahim, N.A., Iliescu, C. and Yu H. (2009). "Cell Culture on MEMS Platforms: A Review." Int J Mol Sci. **10**(12): 5411–5441.
- Ortega, J. A. and S. Alcantara (2010). "BDNF/MAPK/ERK-induced BMP7 expression in the developing cerebral cortex induces premature radial glia differentiation and impairs neuronal migration." Cereb Cortex **20**(9): 2132-44.
- Polikov, V. S., M. L. Block, et al. (2006). "In vitro model of glial scarring around neuroelectrodes chronically implanted in the CNS." Biomaterials **27**(31): 5368-5376.
- Ren, Y.-J., H. Zhang, et al. (2009). "In vitro behavior of neural stem cells in response to different chemical functional groups." Biomaterials **30**(6): 1036-1044.

Results: 3. Effect of model surfaces on glial adhesion and differentiation

Soria J. M., C. Martínez Ramos et al. (2007). "Influence of the substrate's hydrophilicity on the *in vitro* Schwann cells viability." Journal of Biomedical Materials Research Part A **83A**(2): 463-470.

Takehara, M., M. Saimura, et al. (2008). "Poly(β -l-diaminobutanoic acid), a novel poly(amino acid), coproduced with poly(ϵ -l-lysine) by two strains of *Streptomyces celluloflavus*." FEMS Microbiology Letters **286**(1): 110-117.

Vaccarino, F. M., D. M. Fagel, et al. (2007). "Astroglial cells in development, regeneration, and repair." Neuroscientist **13**(2): 173-85.

White, R. E. and L. B. Jakeman (2008). "Don't fence me in: harnessing the beneficial roles of astrocytes for spinal cord repair." Restor Neurol Neurosci **26**(2-3): 197-214.

Yu, T., G. Cao, et al. (2006). "Low temperature induced de-differentiation of astrocytes." J Cell Biochem **99**(4): 1096-107.

GENERAL DISCUSSION & CONCLUSIONS

In this chapter the main findings of the thesis are discussed with a particular focus on the effect of material wettability, chemistry, charge, and topography on glial and neuronal behaviour.

The results of the first, the second and the third chapter are correlated between themselves to have a wider view.

“No great thing is created suddenly.”

Epictetus AD 55-c.135

1. GENERAL DISCUSSION

The main goal of this thesis work was to assess the effects of different materials and micropatterns on glial and neuronal behaviour and to identify key parameters for inducing regeneration after injury. In order to do that, we studied functionalized glass surfaces, line micropatterned chitosan and PMMA. Even none of the materials studied herein will find direct application in nerve regeneration, there is some useful information that improves the knowledge in this field.

Summarizing the results concerning glial cells, PMMA showed to be a suitable substrate for glial cell growth. Surprisingly, it not only allowed the growth of glial cells, but also induced a mild de-differentiation. On the other hand, chitosan exerted on glial cells a maturation effect. On model surfaces with different wettability, a trend toward de-differentiation of glial cells was observed on hydrophobic surfaces, while on surfaces with intermediate wettability cells attach in greater numbers and spread.

1.1 Wettability

Among all the factors, wettability play an important, even not exclusive, role in determining glial cell response, as experienced before by other authors (Faucheux et al. 2004; Soria JM 2006; Arima and Iwata 2007; Soria 2007). In this thesis, materials with different wettabilities were considered: from the most hydrophilic to the most hydrophobic, we used OH surfaces (CA=25°), chitosan and COOH surfaces (CA=34° for both), LysGlass (CA=42°), NH₂ surfaces (CA=53°), Glass (CA= 73°), PMMA (CA=76°) and CH₃ surfaces (CA=103°). On hydrophobic surfaces, like PMMA and CH₃ functionalized glass, glial cells had a trend to de-differentiate; on surfaces with intermediate wettability, like Lys-glass and NH₂, glial cells were spread, while on the hydrophilic chitosan glial cells matured.

Overall, it seems like hydrophobicity is a necessary surface property to induce glial cells to assume immature and progenitor phenotypes. Hydrophobicity is known to affect the adsorption and the conformation of ECM proteins, modifying the protein's cell

binding domain and thus regulating cell adhesion and proliferation (Soria 2007; Soria JM 2007). Cell adhesion strength to biomaterial depends on how adhesive proteins adhere to the substrates. Kesselowsky et al. reported that surface chemistry modulates the structure and molecular composition of cell-matrix adhesions. According to his study, the neutral hydrophilic OH functionality supported the highest levels of recruitment of proteins to adhesive structures. The positively charged NH₂ and negatively charged COOH surfaces exhibited intermediate levels of recruitment of focal adhesion components, while the hydrophobic CH₃ substrate displayed the lowest levels (Kesselowsky et al. 2004). However, the strength of protein adhesion is the one that determine cell response. A recent study by Sethuraman et al. on seven different proteins demonstrated that proteins adhere weakly on –OH surfaces, while they adhere strongly on –CH₃ surfaces (Sethuraman et al. 2004). This process induces conformational changes in proteins exposing or hiding the integrin adhesion binding sites (Soria JM 2007; Coelho et al. 2011)

To support the hypothesis that hydrophobic surfaces are low adhesive for cell attachment, there are the studies of Burton, Ereifej and Biran. Burton et al observed that hydrophobicity is inversely correlated to cell adhesive strength; an increase in hydrophobic characteristics therefore reduces adhesive force (Burton and Bhushan 2005). This trend was confirmed by Ereifej et al, which reported that C6 rat astrocytoma cell line adhere with poor strength on PMMA and SU-8, two slightly hydrophobic materials, in comparison to other hydrophilic substrates. (Ereifej et al. 2011). The study of Biran et al., demonstrated that astrocytes exhibit lower adhesion and increased proliferation with increasing material hydrophobicity (Biran 1999; Soria 2007). In addition, to demonstrate the opposite effect, it is proved that strong cell adhesion favors the formation of focal contacts, probably limiting cell division (Engler 2006; Discher 2009).

An example of low cell adhesive culture is the case of neural stem cells (NSC). Protocols to expand NSC, known also as neurospheres, require that the cells are maintained floating, and differentiate when they attach to substrates functionalized with adhesive

molecules (Alaerts 2001; Martinez et al. 2008; Discher 2009). Thus, high hydrophobicity helps cells not to attach strongly, maintaining some characteristics of proliferative progenitor cells.

Considering all of those references, it can be assumed that slight hydrophobicity (CA from 76°) might be a key parameter to induce glial cell de-differentiation, promoting a favorable environment for nerve regeneration. This specific effect of hydrophobic surfaces may be considered also for the design of neural electrodes, where the need is to it minimize cell attachment and glial scarring, improving and making more time-lasting the electrode function (Lakard et al. 2005; Polikov et al. 2006; Bellamkonda 2009; Ereifej et al. 2011).

However, wettability itself is not enough to explain the behaviors of glial cells. Wettability is only one descriptor of material properties, and it is clear that we can not dissociate material properties like if they were parts of mathematical equations. An example we encountered here is the case of glass and PMMA: both the materials have similar contact angles (73° and 76° respectively), but they generate a completely different glial response. On glass we did not observe dedifferentiation. There are other characteristics of the materials, like surface charge, chemical composition and stiffness, which all together determine the final performance of the surface. The combination of all these properties at the surface will determine the final biomaterial – cell interaction.

1.2. Surface chemistry and charge

Studying the response of glial cells to model surfaces with variable wettability, we observed that materials with intermediate wettability (contact angles ranging from 40° to 60°) promoted good glial cell adhesion and spreading, probably linked with an increased maturation, while from the 2nd chapter, we learned that chitosan (contact angle 33°) led to glial cell maturation. More than wettability, the common element that links together those three materials with similar performances probably is the presence of amino groups. Amino groups are positively charged at physiological pH

(Takehara et al. 2008), and, according to Sallum, surface charge play a stronger influence than wettability in determining protein adsorption and thus cell response (Salloum and Schlenoff 2004). It has been shown by several authors that positive charges promote cell attachment (Maslow 1976). For instance, Dadsetan et al. demonstrated that charged hydrogels are better substrates than not-charged hydrogels in supporting Schwann cells attachment and growth. Schwann cells on positively charged surfaces differentiated to a myelinating phenotype, and they formed myelin sheaths on newly formed DRG axons (Dadsetan et al. 2009). Moreover, it is known that strong cell adhesion to substrates favors the formation of focal contacts and actin-myosin stress fibers, leading cells to attach and spread and probably mature (García et al. 1999; Engler 2006; Discher 2009). Thus, it can be concluded that positive charges have to be taken into account since they are a key parameter in promoting glial cells adhesion and perhaps differentiation towards a more mature phenotype.

The conclusions concerning positive charges and amino groups are suitable also for neurons. Neurons attach and grow on substrates containing NH₂ moieties like chitosan and LysGlass, while they are not capable to grow on uncoated glass or PMMA (data not shown). The good affinity of neurons is probably due to the interaction of the cationic amine groups and the negative cell surface charge (Chung and Wang 2004; Cho et al. 2010). This correlates well with previous studies showing that neurons preferentially adhere to and form neural networks on positively charged surfaces such as poly-lysine coated glass slides (Lakard et al. 2004). In addition, amino groups are known to be good for neuronal adhesion and in some cases in promoting neural differentiation (Soria JM 2006; Soria JM 2007; Ren et al. 2009). This work support and confirm the above mentioned trend, even if this does not mean that neurons could not grow on hydrophobic or negatively charged surfaces. To claim that, further specific studies would be needed and it has to be taken into account that wettability or surface charge are not the only properties that play a relevant role on biomaterials for medical applications.

1.3. Stiffness

Another parameter that should be taken into account is surface stiffness. It is known from various studies that stiffness directs cell phenotype (Engler et al. 2004; Discher 2005; Even-Ram et al. 2006; Georges et al. 2006). In this thesis we use chitosan, that compared to glass and PMMA, was a quite soft material. Soft materials have been demonstrated to favour neuronal attachment (Georges et al. 2006), while discourage glial cell adhesion (Moshayedi et al. 2012). This can be a parameter, together with surface chemistry, charge and wettability, which promoted good neuronal adhesion and good glial cell adhesion, in presence of low serum concentrations. Again we find ourselves in front of a situation that is not black or white, in which one material feature alone is not sufficient to explain the whole biological performance.

1.4. Topography

Another great finding of this thesis work is related to line topography and its effects on neural cell behavior. On line patterned PMMA glial cells align following the patterns and their phenotype was reverted into a progenitor like state, permissive for neuronal growth and migration. On the other hand, on micropatterned chitosan, glial cells could align but no radial glia-like morphologies were observed. It seems like the line patterns synergistically enhance the effects that the materials already exert on glial cells, and they cannot be considered separately from the substrate in which they are incorporated. This proves the idea that material properties are stronger than surface pattern in driving cell response.

Line dimension is also important since it determines cell organization. In the case of neuronal culture, axons organize following the patterns, forming bundles in the bigger ones (10 μ m) and growing as separate axons in smaller ones (2 μ m). In the case of glial cells cultured on PMMA, ln2, a size similar than the size of radial glia processes, promoted better alignment and dedifferentiation than ln10 patterns. Thus, line size in the range of natural structures can be modulated to select the desired morphological organization of cells.

Interestingly, in neuronal cultures grown on patterned chitosan substrates, axons and dendrites behave differently since axons align in the direction of the pattern, while dendrites orient randomly. Probably this behavior has to do with the phases of polarization of neural cells. During development, at the first stages of polarization, neurons extend randomly undifferentiated neurites and the first to exceed a critical length becomes the axon (Fukata et al. 2002). Gomez et al. demonstrated that in axons topographical cues are stronger than biochemical cues in promoting neuronal polarization (Gomez et al. 2007). This concept is supported by Vogt et al, which showed that the presence of one more adhesive pathway is sufficient as a trigger to orient neuronal polarity, especially when biochemical signals are absent (Vogt et al. 2004). Physical guidance in this case probably promote the elongation of neurites grown anisotropically, marking their fate as axons.

1.5 Final statements

Material properties can be chosen to induce specific biological responses. If the desirable effect is to reactivate progenitors or to contrast the glial scarring reaction, like after a traumatic injury in CNS, then the use of a line patterned hydrophobic materials like PMMA is appropriate. However, for *in vivo* applications, lines should be presented into other forms, like gels or fibers, which allow for cell infiltration and avoid glial encapsulation; moreover, the material used should summarize all the good properties that cooperate to good neuronal and glial phenotype and axonal growth guidance. Biodegradability is also a desirable characteristic. Materials which summarize those properties (hydrophobicity, biodegradability) could be synthetic biodegradable polyesters, like poly-lactic acid (PLA), poly-glycolic acid (PGA), poly-lactic-co-glycolic acid (PLGA) and poly-3-caprolactone (PCL). PLA fibers are currently studied in our laboratory with excellent performances in terms of neuronal and glia cell attachment and infiltration, alignment and differentiation toward a permissive phenotype.

However, there are situations in which the reactivation of progenitor is not desired, like after the removal of tumors. Indeed, the reactivation of the proliferation could result in the reestablishment of a new tumor. In these cases the selected materials should permit cellular growth, but induce maturation. For this purposes a material like chitosan, which induce glial maturations and permit neuronal growth, could be preferential. Chitosan could be a good material used also in situations in which the desired aim is to reconnect neural fiber, without the stimulation of progenitor glial cells.

A part from extrapolating knowledge in the field of nervous system tissue engineering, this thesis work also helped to develop good *in vitro* models to study radial glia. On one side, the progenitor control condition established using the commercial available supplement G5 in chapter 1, resulted to be a very good reference for radial glia *in vitro*. Moreover, 2 μ m line patterned PMMA can be used as a model not only to study radial glia, but also to study radial glia – neuron interaction such as gliophilic neuronal migration. In the literature there are only few models for this kind of experimental settings, an example is the one reported by Yu et al. (Yu et al. 2006). A system like this could also allow studying factors involved in neuronal migration without using *in vivo* models.

Overall this thesis work helped to increase the knowledge in the field of CNS tissue engineering, giving useful insights on the *in vitro* and *in vivo* response of glial cell and neurons.

2. CONCLUSIONS

According to the established goals, the conclusions of this thesis work are:

1. Slightly hydrophobic materials, like PMMA, promote glial cell de-differentiation towards a radial glia-like phenotype.
2. Chitosan, like other hydrophilic and positively charged surfaces containing the NH₂ moiety (LysGlass and NH₂ functionalized surface), induced an overall maturation of glial cells and permitted the adhesion of both glial cells and neurons.
3. Line micropatterns generally induce cell alignment and changes in cell morphology and phenotype in a size dependent manner. In addition, topography enhance the effect already exerted by the material: line patterned PMMA induced glial cell to assume an aligned radial glia like phenotype, permissive for neuronal growth and migration, while line patterns on chitosan promote glial maturation.
4. Neuronal axons and dendrites respond differently to line micropatterns presented on chitosan, since axons align following the pattern and dendrites do not.
5. Overall, none of the material properties alone is sufficient to explain the biological response to cells to the biomaterial. The final performance of a material is given by the synergistic combination of all the properties (wettability, chemistry, charge, stiffness, topography etc).
6. The right material has to be chosen carefully depending on the biological desired responses.

3. Epilogue

A small personal and social point of view

Due to the complexity and marvellous structure of CNS, the main thought I had doing this thesis is that everyone should be aware and take care of his CNS. This means taking care of one owns body, mind and soul. Looking at the huge technological progresses made in other fields of tissue engineering (like bone, skin or vascular tissue engineering), hopefully in a near future, researchers together with doctors and surgeons, will be able to design multidisciplinary strategies to support CNS regeneration. However, this perspective seems to be at medium- long term and, considered the difficulty of the regenerative process, together with the costs that it implies, the take home message I would like to give to the lectors and that I learned during these years is “take care of your self”!

Currently the “enriched environment”, is considered as the most efficient plasticity- and regeneration-promoting paradigm for rehabilitation (Nilsson and Pekny). To support that, recent studies have shown the importance of the “enriched environment” and the voluntary physical exercise on neural stem/progenitor activation, especially after injuries such as stroke and other CNS disorders. (Horner P.J. 2000; Komitova et al. 2005 ; Matsumori et al. 2006; Nithianantharajah and Hannan 2006).

Our brains need to be fed with good nutrients, including positive emotions, willpower, thoughts, relationships and creativity, and need to be supported by a healthy body. All of these elements play important roles in health, in prevention and in recovery from injuries. Step by step, science is starting to unravel the underlying molecular mechanisms of CNS injury and regeneration. This knowledge, together with biomaterial science and rehabilitation therapies, will help the field of neural regeneration to make big steps in the future. Meanwhile, we should take care of ourselves and our beloved. Life is so marvellous and complex that once we are alive, we cannot loose the chance we’ve been given to live.

“I like nonsense, it wakes up the brain cells. Fantasy is a necessary ingredient in living, it's a way of looking at life through the wrong end of a telescope. Which is what I do, and that enables you to laugh at life's realities.”

Theodor Seuss Geisel 1904-1991

“Every man can, if he so desires, become the sculptor of his own brain”
Santiago Ramon Y Cajal

4. References

- Alaerts, J. A., De Cupere, V.M., Moser, S., van den Bosh de Aguilar, P., Rouxhet, P.G. (2001). "Surface characterization of poly(methyl methacrylate) microgrooved for contact guidance of mammalian cells." Biomaterials **22**: 1635-1642.
- Arima, Y. and H. Iwata (2007). "Effect of wettability and surface functional groups on protein adsorption and cell adhesion using well-defined mixed self-assembled monolayers." Biomaterials **28**(20): 3074-3082.
- Bellamkonda, G. C. M. et al. (2009). "Implanted neural electrodes cause chronic, local inflammation that is correlated with local neurodegeneration." Journal of Neural Engineering **6**(5): 056003
- Biran, R., Noble, M.D., Tresco, P.A. . (1999). "Characterization of cortical astrocytes on materials of different surface chemistry." J Biomed Mater Res, **46**(2): 150-159.
- Burton, Z. and B. Bhushan (2005). "Hydrophobicity, Adhesion, and Friction Properties of Nanopatterned Polymers and Scale Dependence for Micro- and Nanoelectromechanical Systems." Nano Letters **5**(8): 1607-1613.
- Cho, Y., R. Shi, et al. (2010). "Chitosan produces potent neuroprotection and physiological recovery following traumatic spinal cord injury " Journal of Experimental Biology **213** (9): 1513-1520.
- Chung, Y., Su, Y,Chen, Chiing-chang, Jia, Guang, and H. Wang, Wu,J C, Lin J (2004). "Relationship between antibacterial activity of chitosan and surface characteristics of cell wall." Acta Pharmacol Sin **25**(7): 932-936.
- Coelho, N. M., C. Gonzalez-Garcia, et al. (2011). "Arrangement of type IV collagen and laminin on substrates with controlled density of -OH groups." Tissue Eng Part A **17**(17-18): 2245-57.
- Dadsetan, M., A. M. Knight, et al. (2009). "Stimulation of neurite outgrowth using positively charged hydrogels." Biomaterials **30**(23-24): 3874-3881.
- Discher, D. E., Janmey, P., Wang, Y.L. (2005). "Tissue cells feel and respond to the stiffness of their substrate. ." Science **310**(5751): 1139-1143.
- Discher, D. E., Mooney, D.J., Zandstra, P.W. . (2009). "Growth factors, matrices, and forces combine and control stem cells." Science **324**(5935): 1673-167.
- Engler, A., L. Bacakova, et al. (2004). "Substrate compliance versus ligand density in cell on gel responses." Biophys J **86**(1 Pt 1): 617-28.
- Engler, A. J., Sen, S., Sweeney, H.L., Discher, D.E. (2006). "Matrix elasticity directs stem cell lineage specification." Cell **126**(4): 677-689.
- Ereifej, E. S., S. Khan, et al. (2011). "Characterization of astrocyte reactivity and gene expression on biomaterials for neural electrodes." Journal of Biomedical Materials Research Part A **99A**(1): 141-150.
- Even-Ram, S., V. Artym, et al. (2006). "Matrix control of stem cell fate." Cell **126**(4): 645-7.
- Faucheux, N., R. Schweiss, et al. (2004). "Self-assembled monolayers with different terminating groups as model substrates for cell adhesion studies." Biomaterials **25**(14): 2721-2730.
- Fukata, Y., T. Kimura, et al. (2002). "Axon specification in hippocampal neurons." Neuroscience Research **43**(4): 305-315.
- García, A. J., M. D. Vega, et al. (1999). "Modulation of Cell Proliferation and Differentiation through Substrate-dependent Changes in Fibronectin Conformation." Molecular Biology of the Cell **10**(3): 785-798.
- Georges, P. C., W. J. Miller, et al. (2006). "Matrices with compliance comparable to that of brain tissue select neuronal over glial growth in mixed cortical cultures." Biophys J **90**(8): 3012-8.
- Gomez, N., S. Chen, et al. (2007). "Polarization of hippocampal neurons with competitive surface stimuli: contact guidance cues are preferred over chemical ligands" Journal of The Royal Society Interface **4** (13): 223-233.

General Discussion & Conclusions

- Horner P.J., F. H. G. (2000). "Regenerating the damaged central nervous system." Nature **407**: 963-970.
- Keselowsky, B. G., D. M. Collard, et al. (2004). "Surface chemistry modulates focal adhesion composition and signaling through changes in integrin binding." Biomaterials **25**(28): 5947-5954.
- Komitova, M., B. Mattsson, et al. (2005). "Enriched Environment Increases Neural Stem/Progenitor Cell Proliferation and Neurogenesis in the Subventricular Zone of Stroke-Lesioned Adult Rats" Stroke **36** (6): 1278-1282.
- Lakard, S., G. Herlem, et al. (2004). "Adhesion and proliferation of cells on new polymers modified biomaterials." Bioelectrochemistry **62**(1): 19-27.
- Lakard, S., G. Herlem, et al. (2005). "Culture of neural cells on polymers coated surfaces for biosensor applications." Biosensors and Bioelectronics Part II **20**(10): 1946-1954.
- Martinez, E., E. Engel, et al. (2008). "Focused ion beam/scanning electron microscopy characterization of cell behavior on polymer micro-/nanopatterned substrates: a study of cell-substrate interactions." Micron **39**(2): 111-6.
- Maslow, D. E. a. W., L. (1976). "Some effects of positively charged surface groups on cell aggregation." J. Cell Sci. **21**: 219-225.
- Matsumori, Y., S. M. Hong, et al. (2006). "Enriched environment and spatial learning enhance hippocampal neurogenesis and salvages ischemic penumbra after focal cerebral ischemia." Neurobiology of Disease **22**(1): 187-198.
- Moshayedi, P., F. Costa Lda, et al. (2012). "Mechanosensitivity of astrocytes on optimized polyacrylamide gels analyzed by quantitative morphometry." J Phys Condens Matter **22**(19): 194114.
- Nilsson, M. and M. Pekny "Enriched environment and astrocytes in central nervous system regeneration." Journal of Rehabilitation Medicine **39**(5): 345-352.
- Nithianantharajah, J. and A. J. Hannan (2006). "Enriched environments, experience-dependent plasticity and disorders of the nervous system." **7**(9): 697-709.
- Polikov, V. S., M. L. Block, et al. (2006). "In vitro model of glial scarring around neuroelectrodes chronically implanted in the CNS." Biomaterials **27**(31): 5368-5376.
- Ren, Y.-J., H. Zhang, et al. (2009). "In vitro behavior of neural stem cells in response to different chemical functional groups." Biomaterials **30**(6): 1036-1044.
- Salloum, D. S. and J. B. Schlenoff (2004). "Protein adsorption modalities on polyelectrolyte multilayers." Biomacromolecules **5**(3): 1089-96.
- Sethuraman, A., M. Han, et al. (2004). "Effect of Surface Wettability on the Adhesion of Proteins." Langmuir **20**(18): 7779-7788.
- Soria, J. M., Martínez Ramos, C., Bahamonde, O., García Cruz, D.M., Salmerón Sánchez, M., García Esparza, M.A. et al. (2007). "Influence of the substrate's hydrophilicity on the in vitro Schwann cells viability." J Biomed Mater Res A. **83**(2): 463-70.
- Soria JM, et al. (2006). "Survival and differentiation of embryonic neural explants on different biomaterials." Journal of Biomedical Materials Research Part A **79A**(3): 495-502.
- Takehara, M., M. Saimura, et al. (2008). "Poly(β -l-diaminobutanoic acid), a novel poly(amino acid), coproduced with poly(ϵ -l-lysine) by two strains of *Streptomyces celluloflavus*." FEMS Microbiology Letters **286**(1): 110-117.
- Vogt, A. K., F. D. Stefani, et al. (2004). "Impact of micropatterned surfaces on neuronal polarity." J Neurosci Methods **134**(2): 191-8.
- Yu, T., G. Cao, et al. (2006). "Low temperature induced de-differentiation of astrocytes." J Cell Biochem **99**(4): 1096-107.

APPENDIX

1. SCIENTIFIC COMUNICATIONS DERIVED FROM THE THESIS

Oral presentations

M. Mattotti, L. Delgado, J. Planell, C. Aparicio, S. Alcántara and E. Engel, "Differential Behaviour of Cortical Neural Cells Related to Material Properties". TERMIS, 7-13th June, 2011, Granada, Spain.

M. Mattotti, L. Delgado, J. Planell, C. Aparicio, S. Alcántara and E. Engel, "Differential Behaviour of Cortical Neural Cells Related to Material Properties". 22nd European Conference on Biomaterials, 08-12th September, 2009, Lausanne, Switzerland.

Mattotti M, Planell JA, Alcantara S, Engel E "Micropatterned PMMA substrates influence glial cells phenotype" XXIV Trobades Científiques de la Mediterrània, La Física a les Ciències de la Vida. Octubre 2008, Maó, Spain.

Flash presentations (3-5min)

Mattotti M, Z. Alvarez, J.A. Planell, E. Engel and S. Alcántara. "Inducing functional radial glia-like progenitors from cortical astrocyte cultures using micropatterned PMMA" Second ECMNET Conference, Satellite event of FENS, 12th and 13th July 2012, Barcelona, Spain.

M. Mattotti, Z. Alvarez, J.A. Planell, E. Engel and S. Alcántara, "Micro-patterns switch astrocytes phenotype into a permissive state for neuronal growth" 3rd IBEC symposium, 1st and 2nd June 2010, Barcelona, Spain.

M. Mattotti, L. Delgado, J. Planell, C. Aparicio, S. Alcántara and E. Engel, "Differential Behaviour of Cortical Neural Cells Related to Material Properties". 2nd IBEC Symposium –14th and 15th April 2009, Barcelona, Spain.

Posters

Mattotti M, Z. Alvarez, J.A. Planell, E. Engel and S. Alcántara. "Inducing functional radial glia-like progenitors from cortical astrocyte cultures using micropatterned PMMA" 8th FENS July 14-18, 2012, Barcelona, Spain

M. Mattotti, N. Coelho, J.A. Planell, G. Altankov, E. Engel and S. Alcántara, "Effect of model surfaces on glial cell adhesion and differentiation". 24th European Conference on 04-08 September 2011, Dublin, Ireland.

M. Mattotti, Z. Alvarez, J.A. Planell, E. Engel and S. Alcántara, "Inducing in vitro astrocytes de-differentiation using a micropatterned polymer". 7th Forum of European Neuroscience- 02-07 July 2010, Amsterdam, The Netherlands

M. Mattotti, Z.Alvarez, J.A. Planell, E. Engel and S. Alcántara, “Micro-patterns switch astrocytes phenotype into a permissive state for neuronal growth”. TERMIS, 13-17 June 2010, Galway, Ireland.

M. Mattotti, Z.Alvarez, J.A. Planell, E. Engel and S. Alcántara, “Micro-patterns switch astrocytes phenotype into a permissive state for neuronal growth”3rd IBEC symposium, 1st and 2nd June 2010, Barcelona, Spain.

M. Mattotti, L. Delgado, J.Planell, C. Aparicio, S. Alcántara and E. Engel, “Differential Behaviour of Cortical Neural Cells Related to Material Properties”. ESF-EMBO Symposium on 'Biological Surfaces and Interfaces', 27 June - 2 July 2009, Sant Feliu de Guixols, Spain.

M. Mattotti, L. Delgado, J.Planell, C. Aparicio, S. Alcántara and E. Engel, “Differential Behaviour of Cortical Neural Cells Related to Material Properties”. 2nd IBEC Symposium –14th and 15th April 2009, Barcelona, Spain.

M.Mattotti, Ortega A, Planell JA, Alcantara, S, Engel E. “Patterned polymeric matrices direct orientation of cortical glial cells.” 8th World Biomaterial Congress, 28 May- 1 June 2008, Amsterdam, The Netherlands.

Publications

M. Mattotti , Z.Alvarez, J.A. Planell, E. Engel and S. Alcántara. “Inducing functional radial glia-like progenitors from cortical astrocyte cultures using micropatterned PMMA”. *Biomaterials* **33**(6): 1759-1770.

M. Mattotti, Z. Alvarez, L. Delgado, J.Planell, C. Aparicio, S. Alcántara and E. Engel “Differential neuronal and glial behavior from cerebral cortex on flat and micro patterned chitosan films”. Submitted to *Acta Biomaterialia*.



Inducing functional radial glia-like progenitors from cortical astrocyte cultures using micropatterned PMMA

Marta Mattotti^{a,b,d}, Zaida Alvarez^{b,d}, Juan A. Ortega^d, Josep A. Planell^{a,b,c}, Elisabeth Engel^{a,b,c}, Soledad Alcántara^{d,*}

^aDpt. Material Science and Metallurgical Engineering, Technical University of Catalonia-UPC, Barcelona, Spain

^bInstitute for Bioengineering of Catalonia-IBEC, Barcelona, Spain

^cCentro de Investigación Médica en Red. Biomecánica, Biomateriales y Nanotecnología-CiberBBN, Barcelona, Spain

^dDpt. of Pathology and Experimental Therapeutics, Medical School (Bellvitge Campus), University of Barcelona-UB, Barcelona, Spain

ARTICLE INFO

Article history:

Received 9 September 2011

Accepted 10 October 2011

Available online 1 December 2011

Keywords:

Polymethylmethacrylate

Micropatterning

Surface topography

Astrocyte

Nerve guide

Co-culture

ABSTRACT

Radial glia cells (RGC) are multipotent progenitors that generate neurons and glia during CNS development, and which also served as substrate for neuronal migration. After a lesion, reactive glia are the main contributor to CNS regenerative blockage, although some reactive astrocytes are also able to de-differentiate *in situ* into radial glia-like cells (RGLC), providing beneficial effects in terms of CNS recovery. Thus, the identification of substrate properties that potentiate the ability of astrocytes to transform into RGLC in response to a lesion might help in the development of implantable devices that improve endogenous CNS regeneration. Here we demonstrate that functional RGLC can be induced from *in vitro* matured astrocytes by using a precisely-sized micropatterned PMMA grooved scaffold, without added soluble or substrate adsorbed biochemical factors. RGLC were extremely organized and aligned on 2 μm line patterned PMMA and, like their embryonic counterparts, express nestin, the neuron-glial progenitor marker Pax6, and also proliferate, generate different intermediate progenitors and support and direct axonal growth and neuronal migration. Our results suggest that the introduction of line patterns in the size range of the RGC processes in implantable scaffolds might mimic the topography of the embryonic neural stem cell niche, driving endogenous astrocytes into an RGLC phenotype, and thus favoring the regenerative response *in situ*.

© 2011 Elsevier Ltd. All rights reserved.

1. Introduction

Despite the presence of multipotent neural stem cells (NSC) in the adult central nervous system (CNS), their ability to regenerate after an injury is very limited and there is currently no effective treatment to improve CNS healing. The formation of a glial scar is one of the most important causes of the lack of spontaneous CNS regeneration. Reactive astrocytes, fibroblasts and other glial cells within the scar produce inhibitory molecules for axon growth [1,2]. However, current evidence indicate that astrocytes also play beneficial effects for CNS recovery, as they restart the hemato-

encephalic barrier, secrete neurotrophic factors and provide support and guidance for axonal growth [3–5]. Moreover, a pool of early reactive astrocytes changes their phenotype adopting many of the molecular traits of embryonic radial glia and NSC [6,7]. Therefore, a promising strategy can be enhancing the beneficial astrocytic response to obtain a permissive glial environment for neural growth and the re-establishment of functional connections after an injury.

Cell-based approaches to CNS regeneration have had little success, partly because of the limited survival and integration of the implanted cells, which is probably due to the absence of biochemical and topographical cues normally present at the NSC niche. To overcome this problem, the tissue engineering approach aims to provide instructive information to regenerative capable cells through the implantation of intelligent materials that mimic the natural NSC microenvironment. There is increasing evidence that surface topography can modulate the cell response by changing cell morphology and differentiation state. The most

* Corresponding author. Cell Biology Unit, Department of Experimental Pathology and Therapeutics, School of Medicine (Bellvitge Campus), University of Barcelona, 08907 L'Hospitalet de Llobregat, Spain. Tel./fax: +34 954024288.

E-mail address: salcantara@ub.edu (S. Alcántara).

recent findings and theories have been elegantly reviewed by Bettinger et al. [8] and Hoffman-Kim [9], the latter focusing specifically on nerve regeneration. Among the results they mention, micropatterned or aligned fibers of poly-caprolactone enhanced the differentiation of retinal progenitor cells into neurons and glia [10] or Schwann cells maturation [11], respectively, while the diameter of electrospun fibers influenced NSC differentiation [12]. Furthermore, mature astrocytes have been shown to de-differentiate *in vitro* under certain specific conditions. For instance, induction of the polycomb transcription factor Bmi1 and exposure to FGF-2 or sulfated hyaluronan can induce stem cell-like features in quiescent astrocytes [13,14]. Astrocytes may also de-differentiate by physical methods, such as freeze-thawing [15] or by mechanical and scratch insults [7]. These findings suggest that differentiated glial cells retain a certain plasticity that might be manipulated to evoke a reparative response to damage by presenting the appropriate signals.

Several recent studies have used micropatterned polymer substrates to direct the growth and differentiation of NSC [16]. However, glial cells and, in particular, astrocytes are the most likely cell types to contact the material after *in vivo* implant. To identify instructive cues that could induce astrocytes to adopt a radial glia-like phenotype permissive for neural growth, we analyzed *in vitro* the differentiation of glial cells in response to linear patterns imprinted on a substrate of poly(methyl methacrylate) (PMMA).

PMMA is a transparent synthetic material that, thank to its thermoplastic nature, can be structured by hot embossing with high resolution [17–19]. It has been used for nerve tissue engineering *in vitro* [20,21] and has recently been successfully employed for rat sciatic nerve regeneration *in vivo* [22]. Here therefore, we used uncoated PMMA films carrying line topographies of different dimensions in order to determine whether the introduction of topographical cues might bias glial differentiation toward a supportive phenotype for neuronal growth.

2. Materials and methods

2.1. PMMA characterization and microstructuring

Characterization of PMMA wettability was achieved via contact angle measurements using an OCA 20 system (Dataphysics, GmbH, Germany). Advancing contact angle measurements were taken using 3 μ L Milli-Q water. Four substrates and at least four different measurements were performed on each. Z-potential measurements were carried out using a SurPASS apparatus and VisioLab software (Anton Paar Ltd. - UK). All the measurements were performed four times at the pH of the electrolyte (KCL 1 mM, pH 5.5) after 2h of equilibration using the Adjustable Gap Cell for small samples (20 mm \times 10 mm).

Micropatterns were introduced on 125 μ m thick PMMA sheets (Goodfellow Ltd., UK) by nano-imprinting lithography (NIL) (Obducat AB, Sweden) and following the protocol described by Mills et al. [17]. Micropatterns consisted of 2 μ m and 10 μ m wide lines (ln2 and ln10), all 1 μ m deep/tall and 1.5'' length. The silicon molds were provided by AMO GmbH (Aachen, DE) and consisted of 1.5'' \times 1.5'' silicon squares. For cell culture, PMMA films were sterilized with 70% ethanol for 15 min and cut to fit in 60 mm ϕ tissue culture dishes. The characterization of patterned PMMA films was achieved by white light interferometry (WYKO NT1100 apparatus and the software Vision 32 V2.303 (Veeco Instruments, Inc, USA)).

2.2. Cell culture

All animal housing and procedures were approved by the Institutional Animal Care and Use Committee in accordance with Spanish and EU regulations. Glial cells were derived from brain cortex of postnatal mice as described elsewhere [23]. Briefly, P0 brain cortices were dissected out free of meninges in dissection buffer (PBS 0.6% glucose (Sigma), 0.3% BSA (Sigma)) and digested with trypsin (Biological Industries) and DNase I (Sigma) for 10 min at 37 °C. The tissue was dissociated in Dulbecco's Modified Eagle Medium (DMEM, Biological Industries) 10% normal horse serum (NHS, Gibco), 1% penicillin-streptomycin (Pen-Strep, Biological Industries), and 2 mM L-glutamine (Biological Industries), referred to in this text as growing medium (GM). After centrifugation and resuspension, cells were plated and grown to confluence at 37 °C, 5% CO₂ (approximately 25–30 days *in vitro*, DIV). All the experiments were performed using glial cells from the first passage (Ps1).

To assess the influence of different line topographies on glial cell morphology and differentiation state, Ps1 cells were cultured at a density of 2×10^5 cells/cm² for 5 DIV in Neurobasal™ (NB), 3% NHS, 1% Pen-Strep, and 2 mM L-glutamine (experimental medium = EM) on PMMA ln2, ln10 or flat (non patterned = NP). To avoid any confusion caused by the heterogeneity of glia culture types described in the literature, we defined three reference conditions within the *in vitro* system used here to compare biochemical changes of glial cells on PMMA. Control glia were Ps1 glial cells cultured on non-coated culture plastic (for Western blotting) or glass (for ICC) under the same conditions as for PMMA. Reactive/mature glia were obtained by culturing Ps1 glial cells for 8 DIV in EM and with EM supplemented with dibutyl cyclic AMP (dcAMP, 500 mM, SIGMA) during 7 more days [24,25]. Progenitor glia were obtained by culturing Ps1 glial cells for 24h in EM and then in NB supplemented with G5 (GIBCO) for 7 DIV. G5 supplement contains mitogens, such as FGF-2 and EGF, and it is used to maintain neural stem cells in culture; it significantly promotes the proliferation of neuronal precursor cells, radial glial cells and astrocytes *in vitro* [15,26]. The choice of culture conditions for progenitor and reactive glia, and of the EM, was made after numerous preliminary studies using different culture mediums, supplements, serum types and concentrations.

Neurons were obtained from embryonic brains. Brain cortices from E16 mice were isolated in dissection buffer, digested with trypsin-DNase I, dissociated and preplated for 30 min in preplating medium (CO₂-equilibrated Neurobasal™ supplemented with 5% NHS, 1% Pen-Strep, 0.5 mM L-glutamine, 5.8 μ M/ml NaHCO₃ (Sigma–Aldrich, Saint Louis, MO)). The supernatant was then collected, centrifuged and resuspended in serum-free neuronal culture medium (NB, 1% Pen-Strep, 0.5 mM L-glutamine, 1x B27, 5.8 μ M/ml NaHCO₃). Neurons were plated at a density of 2.5×10^5 cells/cm², directly on top of 5DIV glial cell cultures, and then cultured for 5 more days in neuronal culture medium.

Explants were obtained from the cerebral cortex of E16 actin-GFAP transgenic mice. Brains were isolated and then cut into 350 μ m thick slices with a McIlwain Tissue Chopper (Camden Instruments, UK). Explants of approximately 300 μ m diameter were obtained by microdissection, incubated in preplating medium for 1h and seeded on top of glial layers in neuronal culture medium for 2 DIV.

2.3. Western blot

Total extract proteins were separated by SDS-polyacrylamide gel and electrotransferred to a nitrocellulose membrane. Membranes were first blocked in 5% non-fat milk and then incubated with primary antibodies overnight at 4 °C, followed by their corresponding secondary HRP-conjugated antibodies (1:3000, Santa Cruz Biotechnology, San Diego). Protein signal was detected using the ECL chemiluminescent system (Amersham, Buckinghamshire, UK). Densitometric analysis, standardized to actin as a control for protein loading, was performed using ImageJ software (National Institutes of Health, USA).

For quantification, triplicate samples were analyzed.

2.4. Immunocytochemistry and primary antibodies

For immunofluorescence, fixed samples (4% PFA for 1h at RT) were incubated with primary antibodies and appropriate Alexa488 or Alexa555 secondary antibodies (1:500, Molecular Probes, Eugene, Oregon). Phalloidin was used to stain F-actin (1:2000, Sigma–Aldrich, Saint Louis, MO) and To-Pro-3 iodide (1:500, Molecular Probes, Eugene, Oregon) to stain nuclei. Finally, the preparations were coverslipped with Mowiol (Calbiochem, San Diego) for imaging.

The following primary antibodies were used: rabbit anti-GFAP (mature and reactive glia marker, 1:500–1:8000, Dako), mouse anti-Vimentin (reactive glia marker 1:1000, Santa Cruz Biotechnology, INC), rabbit anti-EAAT-2 (mature glia marker 1:500, Cell Signaling) rabbit anti-BLBP (radial glia marker, 1:1000–1:8000, Chemicon), mouse anti-Nestin (progenitor and radial glia marker, 1:250, Abnova Corporation), goat anti-Actin (cytoskeleton Marker, 1:2000, Santa Cruz Biotechnology, INC), mouse anti-Tuj-1 (neuronal marker 1:10000, Covance) and rabbit anti-PH3 (proliferation marker, 1:250, Millipore), goat anti-Pax6 (neurogenic radial glia marker, 1:250, Santa Cruz Biotechnology, INC) and rabbit anti-TBR2 (neurogenic intermediate progenitor cells marker, 1:500, Abcam), rabbit anti-NG2 (oligodendrocytes precursor cells marker, 1:200, Millipore), rabbit anti-Ki67 (proliferation marker, 1:500, Abcam), mouse anti A2B5 (glial precursor cell marker, 1:100, Miltenyi Biotec) and goat anti-Tuj-1 (neuronal marker 1:1000, Covance).

2.5. Flow cytometry analysis

The absolute number of living and dead cells was determined at 1–4 DIV by flow cytometry using a FACScalibur apparatus (Becton Dickinson). For absolute live/dead cell number counts we used propidium iodide (PI, Sigma, 5 μ g/mL) to label dead cells and CountBright™ absolute counting beads (Molecular Probes, Invitrogen), according to the protocol suggested by the provider. Ps1 cells were cultured at a density of 2×10^5 cells/cm², then trypsinized at 1–4 DIV, and resuspended in 1 ml of PBS. Ten thousand CountBright™ counting beads (Molecular Probes, Invitrogen) were recorded and cell populations were determined based on cell size (FSC) and granularity of the cytoplasm (SSC). The cell suspensions were analyzed after PI incubation. Percentage of positive cells and sample relative fluorescence were

calculated for each window, as determined by the monoparametric analysis. All the samples were measured in triplicates.

2.6. Scanning electron microscopy (SEM)

For SEM imaging, samples were fixed in 2.5% glutaraldehyde in 0.1M PB for 2 h at 4 °C, washed three times, frozen in liquid nitrogen and dehydrated by freeze-drying over 24 h. Then they were gold sputter-coated and observed using a Jeol JSM-6400 scanning electron microscope.

2.7. Video time lapse analysis

For video time lapse analysis, neurons were obtained from the cerebral cortex of E16 actin-GFP transgenic mice and cultured on top of pre-seeded glial cells as described above. After 8 h, the co-cultured cells were placed in the incubation chamber of an Observer.Z1m inverted fluorescent microscope (Carl Zeiss, USA) at 37 °C with 5% CO₂. Cells were imaged in phase contrast and under 488-nm wavelength light. Pictures were taken every 3 min during 3 h. Cell displacement, speed and trajectory were calculated by the aid of the “Manual Tracking” plug-in of the ImageJ software (National Institutes of Health, USA).

2.8. Imaging and analysis of cell orientation and co-localization

Cells were observed using an Axiovert 40 CFL light inverted microscopy (Carl Zeiss, USA). Digital images were taken throughout experimentation using a digital camera controlled by software. Fluorescent preparations were visualized and micrographs were captured with either a Leica TCS-SL Spectral confocal microscope (Leica Microsystems, Mannheim, Germany) or a Nikon Eclipse 800 light microscope (Nikon, Tokyo, Japan). Images were assembled in Adobe Photoshop (v. 7.0), with adjustments for contrast, brightness and color balance to obtain optimum visual reproduction of data. Morphometric and quantitative image analysis was performed using ImageJ software (National Institutes of Health, USA).

Cell alignment was quantified using the FTT-Oval Profile method described previously by Alexander et al. [27]. This method generates plots that represent alignment by a peak at 90° and randomness by a flat line. To this end, astrocytes stained for actin, BLBP and GFAP were considered. Neuron-glia co-localization was quantified using the Intensity Correlation Analysis plug-in on pictures of glial cells stained with BLBP and neurons stained with Tuj-1. Co-localization was represented by Pearson's correlation coefficient (Rr), whose values range between 1 and -1, where 1 represent maximal co-localization and -1 maximal exclusion [28]. Axon alignment from brain explants was analyzed fitting a line along the emitted axons, measuring their angles and plotting their relative frequencies.

The percentage of immunoreactive cells for the distinct differentiation markers was calculated with respect to the total number of cell nuclei stained with TO-PRO-3. Cells were counted manually on a minimum of 10 pictures for each condition.

2.9. Statistical analysis

Statistical analysis was performed using the Statgraphic-plus software. One-way ANOVA and Fisher's least significant difference (LSD) procedure were used to discriminate between the means.

3. Results

3.1. Glial cell orientation and morphology

Besides their distinct composition, glass PMMA and culture plastic (polypropylene) are harder than brain and considered stiff substrates (<http://matbase.com>; <http://goodfellow.com>). PMMA and glass were slightly hydrophobic and negatively charged (contact angle: 76°±4 and 73°; Z-potential: -45 ± 5 mV and -80 ± 14 mV respectively), while tissue culture treated polystyrene was slightly hydrophilic and negatively charged [29].

The choice of the pattern type and dimension was taken after an initial screening of different geometries (lines and posts) and width (2, 5, 10 and 20 μm) based on previous studies involving the alignment of osteoblast-like cells [17], and mesenchymal stem cells [19]. Glial cells spread in posts (not shown) and aligned in lines of all sizes. Glial cells on 2 μm lines exhibited better alignment and higher nestin expression than on 10 μm and 20 μm lines, where they behave similarly. Thus, lines of 2 μm and 10 μm were selected for the present study. The replication of micropatterns on PMMA was confirmed by white light interferometry imaging (Fig. 1). Height and width of both 2 μm and 10 μm line patterns were replicated faithfully (ln2: height 0.76 ± 0.3 μm, width 1.92 ± 0.2 μm; ln10: height 0.97 ± 0.02 μm, width 9.9 ± 0.31 μm; n = 5).

Using E16 primary neuronal cultures we determined that neurons do not attach to uncoated PMMA films, glass or culture plastic (not shown). By contrast, primary glial cultures from P0 cortices attached and grew on uncoated PMMA, glass and culture plastic. Cells were then stained with phalloidin or actin antibodies for morphometric analysis. Glial cells grown in the control condition (glass and culture plastic) adopted a flattened and well-spread morphology, with the occasional presence of elongated, bipolar or small ramified cells (Fig. 2A). In the presence of dcAMP, the reactive/mature condition, glial cells acquired a stellar morphology with

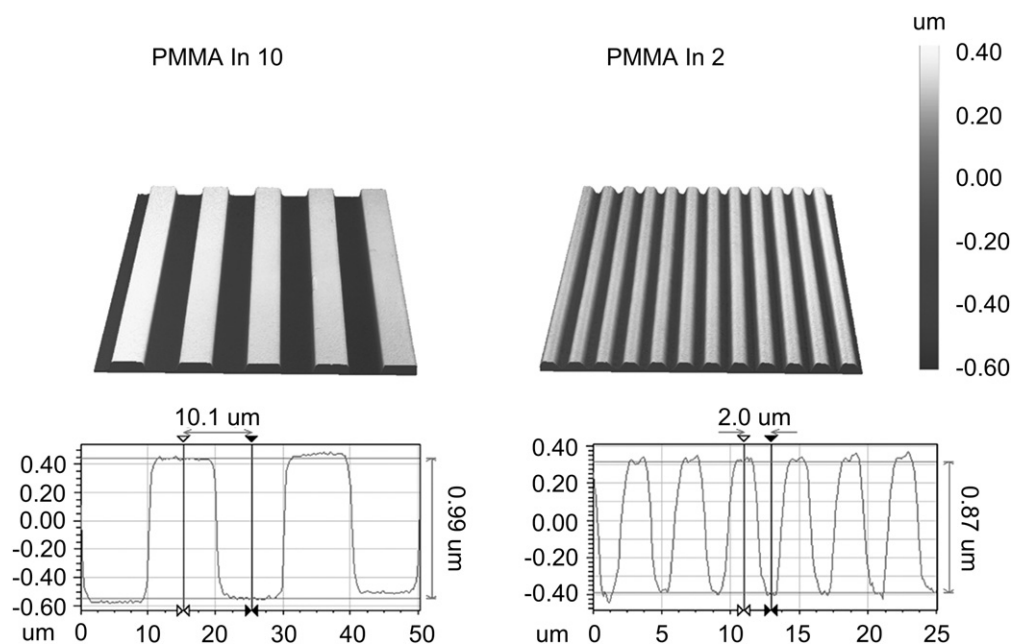


Fig. 1. White light interferometer 3D images and profiles of 10 μm and 2 μm patterned PMMA.

a highly ramified cytoskeleton characteristic of reactive glia (Fig. 2B), while cells grown in the progenitor condition were elongated and bipolar with reduced cytoplasm, a morphology that resembles radial glia and progenitor cells (Fig. 2C). On flat PMMA, as in controls, well-spread astrocytes, small ramified cells and bipolar radial glia-like cells (RGLC) were present (Fig. 2D). However, the branched cytoskeleton arrangements typical of reactive glia were not observed. In the presence of grooved topographies, glial cells adopted elongated shapes resembling RGLC and aligned following the pattern (Fig. 2E–F). FTT-Oval Profile analysis demonstrated that the alignment was better on In2 than on In10 (Fig. 2G), which is represented by a higher peak at 90°. SEM images revealed that elongated glial cells extended their processes, with a preference toward the mesa of the topography. They grew on top of the pattern and covered the grooves only in the case of higher cell density (Fig. 2H).

3.2. Biochemical characterization of glial cells

In order to determine whether micropatterns can induce RGLC we characterized glial cultures by immunocytochemistry and Western blot. Glial cultures were immunostained with antibodies

against GFAP and BLBP to identify astrocytes, and against nestin to identify progenitors and radial glia-like cells (Fig. 3). Astrocytes expressing GFAP predominated in the reactive, control, NP and In10 PMMA conditions ($78 \pm 10\%$, $75 \pm 13\%$, $89 \pm 9\%$, $81 \pm 11\%$ respectively), while they were reduced in progenitor and In2 PMMA conditions ($25 \pm 3\%$ and $45 \pm 7\%$ respectively). BLBP + astrocytes predominated in the progenitor condition ($93 \pm 11\%$), being less abundant in the reactive, control, NP, In10 and In2 PMMA ($61 \pm 17\%$, $69 \pm 13\%$, $63 \pm 21\%$, $65 \pm 6\%$ and $68 \pm 4\%$ respectively). Many astrocytes expressed both GFAP and BLBP and when we analyzed their morphology, the number of bipolar cells was significantly increased in the In2 and In10 PMMA conditions ($43 \pm 17\%$ and $27 \pm 7\%$ respectively) with respect to NP PMMA and control conditions ($17 \pm 3\%$ and $16 \pm 11\%$ respectively). Nestin + progenitors were scarce in the control and reactive conditions ($26 \pm 8\%$ and $23 \pm 1\%$ respectively), they were abundant in the progenitor condition ($81 \pm 6\%$) and intermediate levels were found in NP, In10 and In2 PMMA ($35 \pm 11\%$, $33 \pm 16\%$ and $55 \pm 18\%$ respectively).

Western blotting was then used to quantify the relative proportion of the different cell types and their maturation state (Fig. 4A). Densitometry analysis revealed that when glial cells were

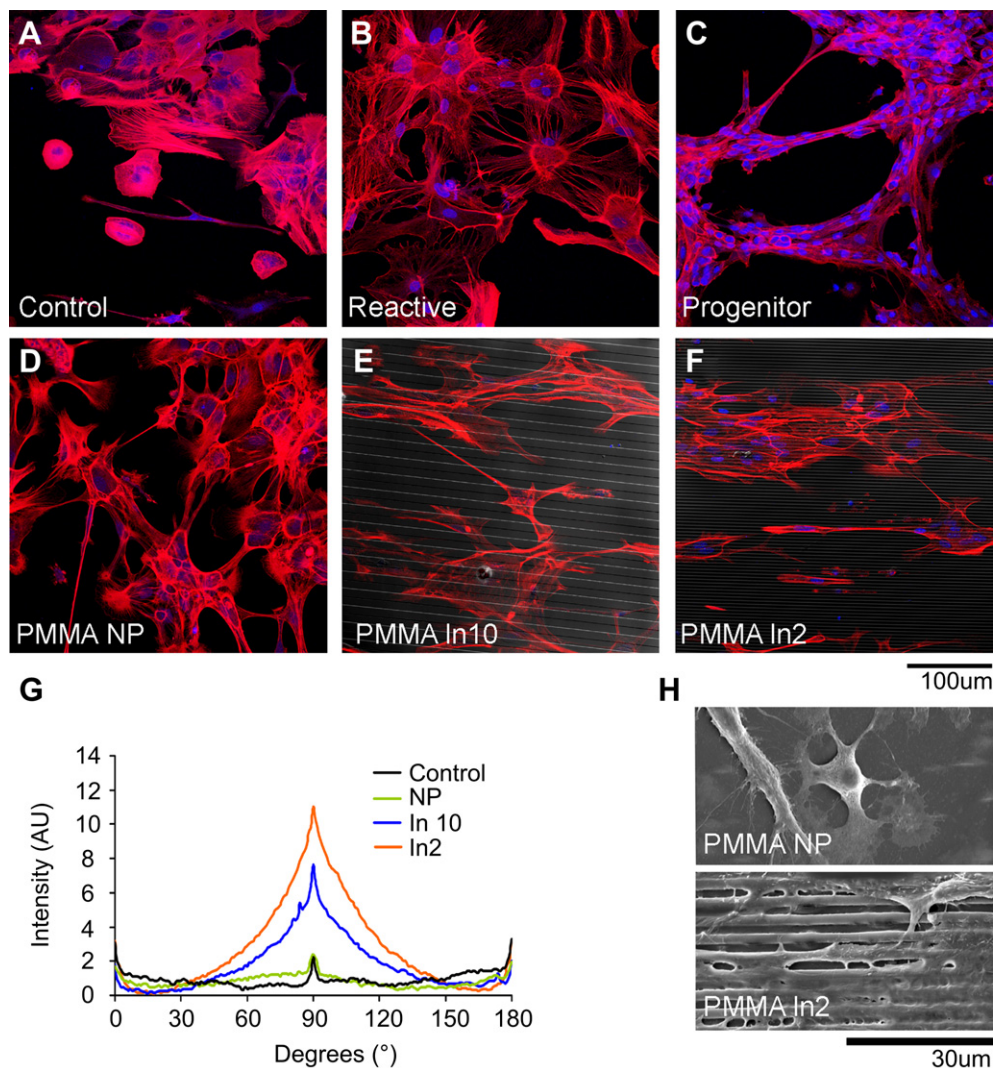


Fig. 2. Effect of PMMA and micropattern on glial cells morphology and orientation. A–F, Confocal images of actin staining (phalloidin, red) and nuclei (TO-PRO-3, blue). G, Graphic representing cell alignment by FTT-Oval profile measurement. Flat line indicates random distribution; peak at 90° indicates alignment parallel to the topography. H, SEM pictures of glial cells on NP and 2 μm lines PMMA. Scale bar A–F = 100 μm; Scale bar H = 30 μm. **Indicates statistical significance respect to control $p \geq 0.001$. (For interpretation of the references to colour in this figure legend, the reader is referred to the web version of this article.)

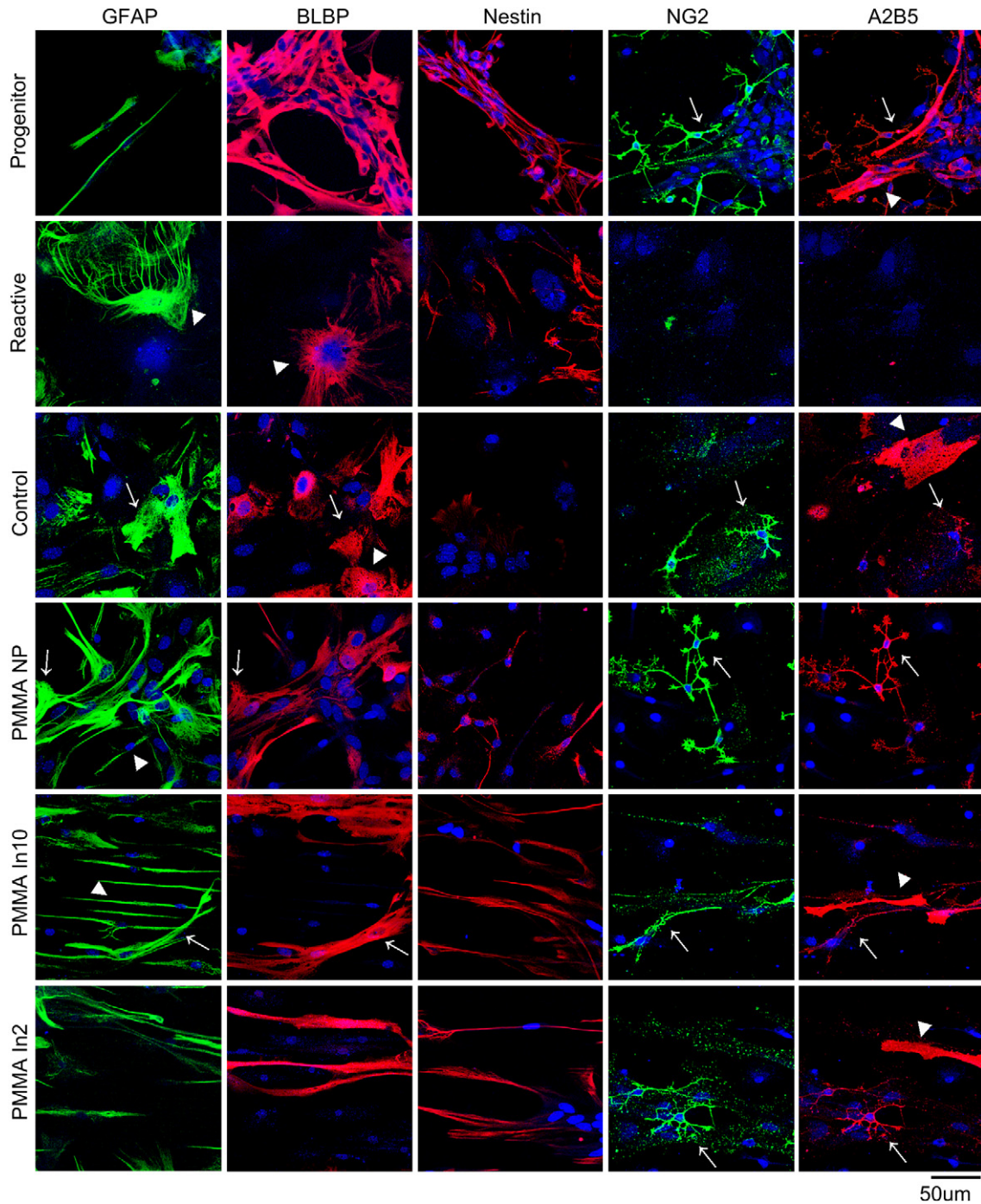


Fig. 3. Cellular composition of glial cultures. Confocal images of glial cells immunostained for different glial and progenitor markers: GFAP and BLBP for astroglia, Nestin for progenitors, and NG2 and A2B5 for different glia-restricted progenitors. Nuclei are stained with TO-PRO-3 (blue). Scale bar = 50 μ m. (For interpretation of the references to colour in this figure legend, the reader is referred to the web version of this article.)

grown in the progenitor condition the expression of immaturity markers, such as nestin, and the mitotic marker PH3 dramatically increased with respect to the control, while maturity and reactive markers such as GFAP, vimentin, and the glutamate transporter EAAT-2 were markedly reduced. By contrast, the opposite was observed in the reactive condition where EAAT-2 increased while immature and progenitor markers dramatically decreased with respect to control (Fig. 4B and C). Glial cells grown on PMMA increased the expression of immaturity markers (nestin) while maturation markers decreased (GFAP, EAAT-2). The induction of

a progenitor-like phenotype was more dramatic on In2 PMMA, where proliferation (identified by PH3 expression) was also increased (Fig. 4B and C).

To investigate whether gliogenic or neurogenic progenitors were favored by the micropattern, we analyzed by Western blot the expression of several lineage-specific markers. Pax6 homeodomain transcription factor was used to identify radial glia-like cells that can produce neurons and glia, along with Tbr2, a T-domain transcription factor expressed by intermediate progenitors that produce only neurons, and Tuj-1, a neuronal tubulin expressed by

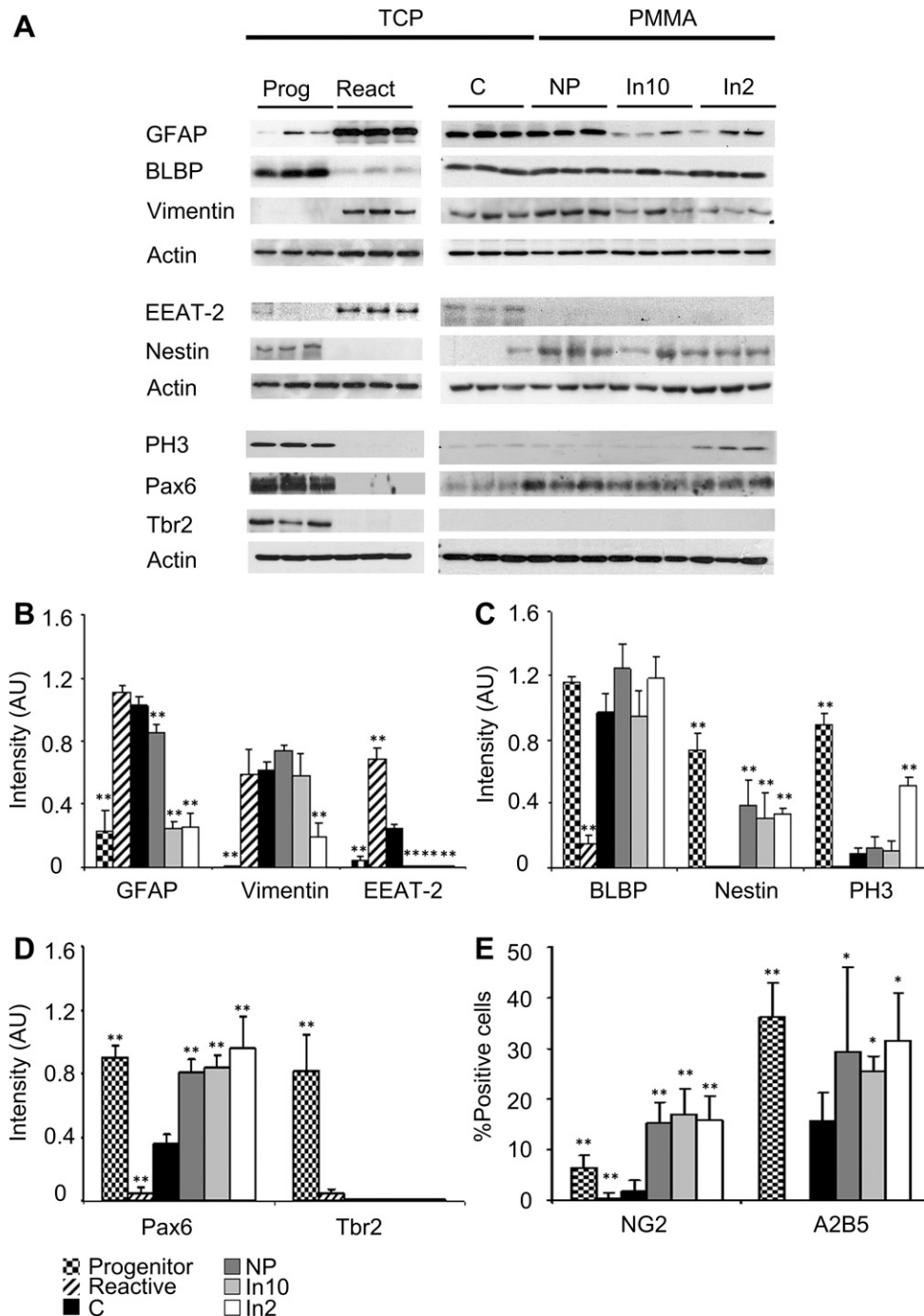


Fig. 4. Biochemical characterization of glial differentiation. A, Western Blots showing the expression of different progenitors and glial differentiation markers. B–D, Quantitative representation of the western blot densitometry (intensity values normalized to actin) grouped by categories: B, mature and reactive glial markers (GFAP, Vimentin and EEAT-2); C, progenitor glial markers (BLBP, Nestin and PH3); and D, neurogenic progenitor markers (Pax6 and Tbr2). E, Graph representing the percentage of immunoreactive cells for glial restricted progenitors markers (NG2 and A2B5) respect the total number of cells by unit area. Prog = progenitor; React = reactive glia; C = control (tissue culture plate); NP = no patterned PMMA; In10 = 10 μ m line patterned PMMA; In2 = 2 μ m line patterned PMMA. **Indicates statistical significance respect to control $p < 0.01$.

postmitotic neurons [30]. Tuj-1 expression was never found in our glial cultures, indicating the absence of differentiated neurons (not shown). Pax6 expression was induced by culture in the progenitor condition and by PMMA whereas Tbr2 expression was only induced by culture in the progenitor condition (Fig. 4A, D).

We then analyzed whether the use of PMMA substrates favored the development of specific sub-populations of glial progenitors. A2B5 ganglioside is a marker of glial restricted progenitors, Olig2 is a helix-loop-helix transcription factor that is early expressed by

oligodendrocyte progenitors, while NG2 proteoglycan is expressed by the recently described NG2 glia, a progenitor cell type that can generate oligodendrocytes and protoplasmic astrocytes [31]. Olig2 was not detected by Western blot or ICC in our culture conditions (not shown), while A2B5 and NG2 could only be detected by ICC. A2B5+ glia-restricted progenitors were mostly small bipolar or multipolar cells, although large and elongated flat cells were also occasionally seen. They were abundant in glial cultures grown in the progenitor condition and on In2 PMMA (36 ± 6.8 and 30.5 ± 5

respectively), less frequently seen in control or on flat and In10 PMMA (21.4 ± 8.7 ; 21.3 ± 5.6 and 25.1 ± 6.9 respectively) and absent in the reactive condition (0 ± 0). NG2+ progenitors were small bipolar or mostly multipolar cells, and double labeling studies revealed that most of them were also A2B5 positive. NG2 cells were rare in the control and reactive conditions (1.7 ± 2.2 and 0.5 ± 0.9 respectively), whereas their number increased significantly in the progenitor condition (6.4 ± 2.4) and even greatly on PMMA (flat 15.3 ± 4.1 ; In10 17.2 ± 5.1 ; In2 15.9 ± 4.6) (Figs. 3 and 4E). Taken together these data suggest that PMMA and more dramatically In2 PMMA induce RGLC and progenitor phenotypes on glial cultures.

3.3. Glial cell differentiation on patterned PMMA

In2 PMMA substrate might induce RGLC through different mechanisms. RGLC might be: 1) the progeny of RGC that contaminated the initial culture; 2) the result of cell selection through induced death of particular cell sub-populations; or 3) the product of the de-differentiation of mature astrocytes. Therefore, we analyzed the level of cell death and total number of cells in glial cultures grown in control and In2 PMMA conditions from 1 to 4 div. The total number of cells during the 4 days period analyzed remains almost constant in controls while was slightly reduced at day 4 in In2 PMMA (Fig. 5A). Only minor differences were found between control and In2 PMMA substrates at 1 and 4 div. Cell number doubling was not achieved in this 4 days period in neither condition, a result that is concordant with the cell cycle asynchronicity and extremely low proliferation rates observed in our primary culture conditions. The number of dead cells labeled with PI was low and decreased with time, between 9% (control) and 12% (In2 PMMA, $p < 0.05$) at day 1, and between 2% (control) and 3% (In2 PMMA) at day 4 (Fig. 5B). These small changes in cell death and proliferation suggest that the most probable source of RGLC in In2 PMMA is the de-differentiation of mature astrocytes.

3.4. Neuronal adhesion and migration on topography-modified glial cells

In the developing CNS newborn neurons attach to radial glia which is the main substrate for neuronal migration. Thus, we then analyzed the neuronal supportive behavior of RGLC induced by PMMA substrates. To determine whether oriented RGLC can direct neuronal migration and neurite growth, explants from E16 cerebral cortex were grown on top of aligned (In 2 PMMA) or random (NP PMMA) glial cells. After 36–48 h axons and some neurons were able to migrate outside the explants. Neuronal outgrowth was radial when grown in random oriented glia with only the 14% of axons aligned (Fig. 6A, C), while on In2 PMMA they follow the pattern of the aligned glia underneath, with the 80% of axons having an angle less than 20° (Fig. 6B, D). In addition to fibers, neurons also abandoned the explants in some cases, migrating on the aligned glia (Fig. 6E, F).

To corroborate whether topography induced RGLC support and directed neuronal migration we used video time lapse microscopy. Glial cultures from wild type mice were first grown on control (uncoated glass) and In2 PMMA for 5 DIV, and dissociated E16 neurons from actin-GFP transgenic mice were then seeded on top of them in serum-free neuronal medium. After 8 h, neurons were attached to the subjacent glia and the co-cultures were then placed in the microscope incubation chamber and recorded every 3 min for 3 h. In the control conditions GFP+ neurons remained static or exhibited a minimal random movement with an average speed of $14 \pm 12 \mu\text{m/h}$ ($n = 24$), and final displacement of $7 \pm 6 \mu\text{m}$ (Fig. 7A, C, G, supplementary video 1). On In2 PMMA neurons migrate for relative long distances on RGLC ($37 \pm 23 \mu\text{m}$) with an average speed

of $39 \pm 11 \mu\text{m/h}$ ($n = 24$) (Fig. 7B, D, E, supplementary video 2). Neurons moved along the RGLC, and in some cases, they reverted their direction of movement when they reach the end of the RGLC.

Supplementary material associated with this article can be found, in the online version, at doi:10.1016/j.biomaterials.2011.10.086.

To discard the possibility that the neuronal cultures provided RGC that act as substrates for migration, WT glial co-cultures with GFP neurons were left for a further 5 div, fixed and stained for BLBP to identify the origin of glial cells (Fig. 7F, G). In both control and In2 PMMA conditions, neurons were GFP+ and almost all BLBP+ glial cells were negative for GFP. This data indicate that embryonic neuronal dissociates does not provide a significant number of glial cells. After 5div, in the control condition BLBP+ glial cells were flattened and well-spread and GFP+ neurons were well developed and exhibited ramified dendritic branches (Fig. 7F). However, in In2 PMMA glial cells were elongated and GFP+ neurons were mostly bipolar, oriented along the BLBP+ RGLC processes and with few or none dendritic branches (Fig. 7G). In both conditions, Z reconstruction showed that neurons grew on the top of glial cells. To quantify the differences in neuron-glia attachment we stained WT co-cultures with Tuj-1 and BLBP. Then we measured the degree of Tuj-1/BLBP co-localization, using the intensity correlation analysis 5 days after the neuronal seeding. The degree of co-localization can be calculated according to the value of Pearson's coefficient (Rr), where Rr equal to 1 indicates maximal co-localization and Rr of -1 indicates maximal exclusion. Glia-neuron co-localization was significantly higher in In2 PMMA culture (Rr: 0.59 ± 0.11) than in control (Rr: 0.15 ± 0.08) (Fig. 7H–J). Taking together, those results indicate that In2 PMMA-induced RGLC recapitulates the functions of embryonic RG, providing a good substrate for neural attachment and promoting directional neuronal migration.

4. Discussion

Although glial cells have long been regarded as responsible for the lack of CNS regeneration, due to the formation of the non-

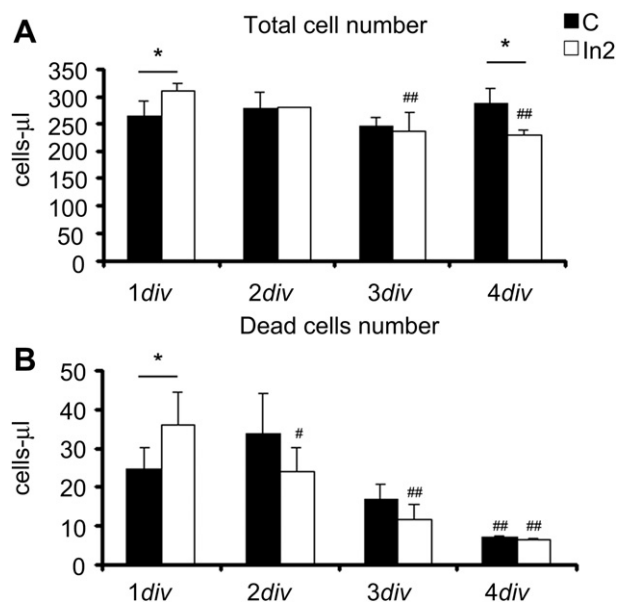


Fig. 5. Graft from flow cytometry analysis showing the evolution of the total cell number and dead cell number on control and PMMA In2 during 4 days. *Indicates statistical significance between control and PMMA In2, $p < 0.05$; # indicates statistical significance with respect to 1div in each substrate, # $p < 0.05$, ## $p < 0.01$.

permissive glial scar, it is now clear that they are also beneficial and may play an active role in the induction of neurogenesis from adult neural stem cells [6,32,33]. During embryonic development, radial glia generate directly or indirectly most CNS neurons [34], while at

the end of neurogenesis most radial glia transform into parenchymal astrocytes [35], and also originate the adult neural stem cells [36,37]. The direction of differentiation can be partially reverted after a lesion *in vivo*, and some astrocytes can de-

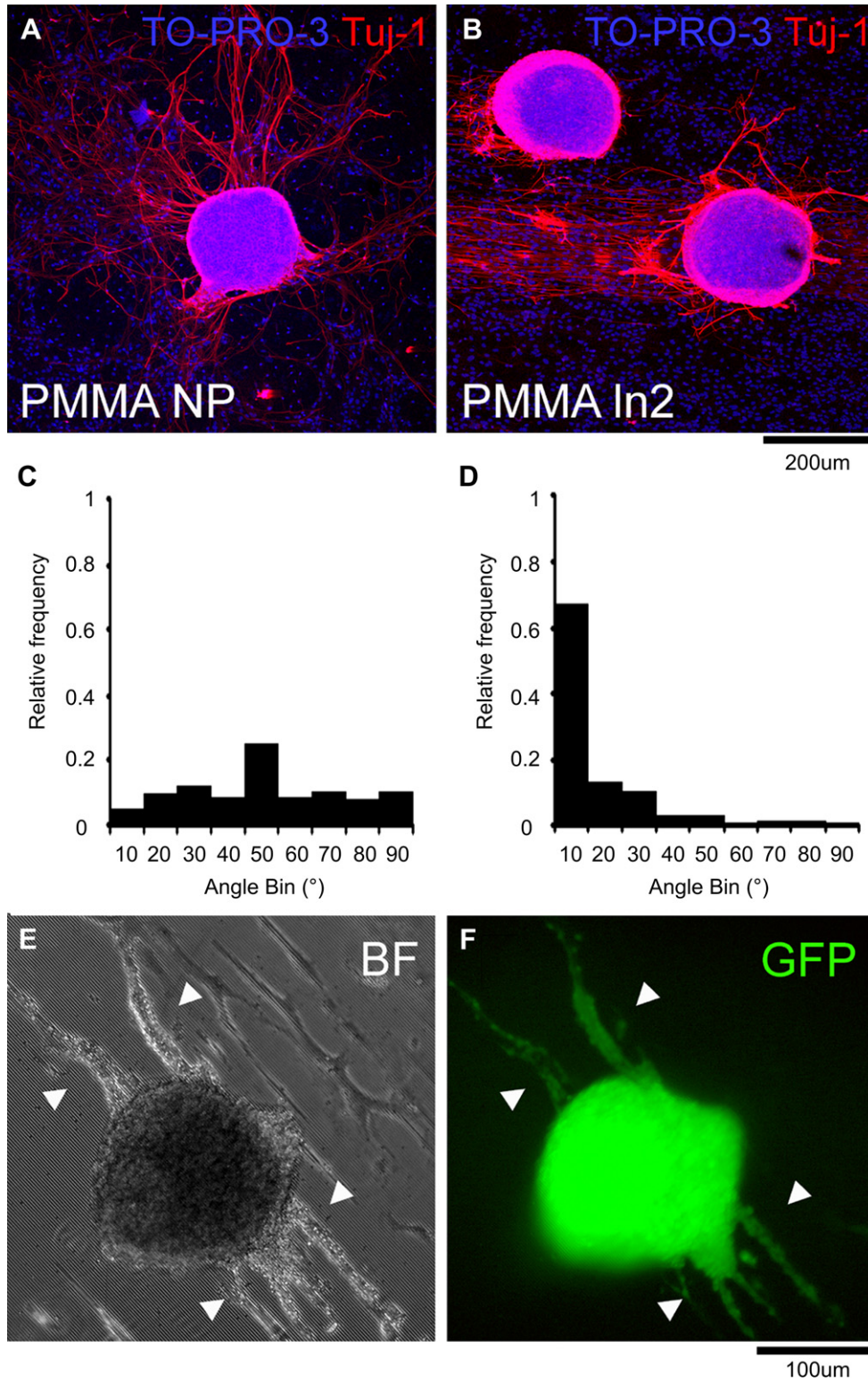


Fig. 6. Effect role of pattern-induced RGLC in neural growth and axonal guidance. A, B, Images showing explants from E16 cerebral cortex cultured on glial cells grown on NP PMMA (A) or Ln2 PMMA (B). Cell nuclei are marked with TO-PRO-3 (blue) and neurons with Tuj-1 antibody (red). Frequency plots representing axonal outgrowth orientation on PMMA NP (C) and PMMA Ln2 (D) substrates. E–F, explants from E16 GFP mice cerebral cortex seeded on top of on glia grown on PMMA Ln2. E = bright field and F = GFP fluorescence. Neurons exiting from the explants are identified by GFP expression. Scale bars = 200 μm (A, B); 100 μm (E, F). (For interpretation of the references to colour in this figure legend, the reader is referred to the web version of this article.)

differentiate into a radial glia-like phenotype that supports the migration of embryonic transplanted neurons [3]. On this basis, a recent experimental strategy for CNS regeneration is to develop mechanisms that restore the embryonic radial glia neurogenic competence into parenchymal astrocytes [38,39]. Extracellular stimuli, including soluble and adhesive factors *in vivo* and in culture media are important modulators of glial cell phenotype and function [4,40]. However these factors are usually derived from animal sources, they are expensive, and it is difficult to control their optimum concentration and side effects. Recent evidence claims that topographical cues cause changes in cell phenotype [21,41–43]. For instance, Evelyn K.F. Yim et al., promoted hMSC transdifferentiation into neuronal lineages using a collagen coated PDMS carrying line patterns of 350 nm [44], while MR Lee et al. obtained the same from hESC [45]. Thus it can be assumed that by providing appropriate physical stimuli it is possible to bias the response of glial cells to injury, i.e. from the reactive to the radial glia phenotype, the later being more supportive for successful endogenous repair.

The major finding of this study is that *in vitro* matured astrocytes can be reverted to an RGLC phenotype by a precisely-sized micropatterned PMMA scaffold without added biochemical factors. As do their embryonic counterparts, induced RGLC express the neuronal glial progenitor marker Pax6, and also proliferate, generate intermediate A2B5 and NG2 progenitors, and support and direct neuronal migration and axonal outgrowth.

The composition and physiological status of a primary glial culture is highly heterogeneous and depends on several factors, including the tissue origin and mode of preparation, the selected growth substrate and substrate coating, and the culture medium composition. To overcome this heterogeneity we defined three reference conditions: progenitor, reactive/mature and control (see material and methods for detailed definitions), thus enabling us to compare the physiological changes of cortical glial cells on the different substrates. In these reference conditions, progenitor glia were small bipolar cells characterized by a high proliferation rate and the expression of the progenitor markers (nestin, Pax6, A2B5), whereas reactive/mature glia were large cells with flat or ramified shapes, mostly quiescent, and expressing high levels of maturity markers (GFAP, EAAT-2). Control glia were mostly flat and well-spread, proliferated slowly, and expressed high levels of mature markers, characteristics that define them as cells closer to the reactive/mature condition. When PMMA was used as the substrate, the glial morphology and biochemical marker expression indicate a bias toward a more immature RGLC progenitor phenotype that was dramatically potentiated when PMMA was micropatterned, with grooves no bigger than 2 μm wide/1 μm deep. These results suggest that intrinsic material properties might act synergistically with the micro-topography in the modulation of the astrocytic phenotype. Biophysical and material cues regulate stem cell behavior (reviewed in Keung et al., 2010 [46]). For example, substrate stiffness differentially directs neural stem cells differentiation to neural and glial phenotypes [47–49] and substrate hydrophobicity regulates glial cells adhesion and proliferation [50,51]. PMMA is the most hydrophobic substrate we used here and the study of Biran et al., demonstrated that astrocytes exhibit lower adhesion and increased proliferation with increasing material hydrophobicity [50]. Material chemistry and surface energy affect the adsorption of ECM proteins and thus might regulate cell adhesion and proliferation by modulating integrin signaling [51]. ECM protein adsorption on PMMA is 5–10 times smaller than the amount adsorbed in tissue culture treated polystyrene [52]. Thus, one possibility is that the hydrophobicity and low protein adsorption of PMMA might act synergistically with the micro-topography in the induction of the RGLC phenotype.

After initial seeding, primary glial cultures were grown *in vitro* for 1 month until reach confluence, reflecting the extremely slow proliferation rate in our experimental conditions. One possibility is that the threefold increase in RGLC in Ln2 PMMA was the progeny of RGC that contaminated the initial culture, selected through induced death of particular cell sub-populations. However, our data strongly argue against this possibility because cell number doubling was not achieved in any substrate in the first 4 days of the study, and the number of dead cells was similar in Ln2 PMMA and control substrates. Therefore, although complementary experiments will be required to fully resolve this question, our results support that the most probably source of RGLC is the dedifferentiation of mature astrocytes.

Recent studies have focused on the effect of nano- and micro-topography on cell function (reviewed by Bettinger et al. [8]), and grooved substrates have been tested for neural tissue engineering purposes showing a size-dependent response [9]. For instance, line topographies larger than the cell body (30–200 μm) promote perpendicular alignment, called “cell bridging”, in several cell types such as dorsal root ganglion and Schwann cells [53]. Moreover, mesenchymal stem cell differentiation and cell fate might be directed by changing the groove dimension [44,54]. Cell shape elongation on grooved surfaces is mostly due to oriented mechanical tension created by integrin and focal adhesion rearrangements. The elongation of cytoskeleton and nucleus has been correlated with changes in cell function and differentiation, in part through intracellular calcium regulation [55,56]. Nevertheless the strong proliferative induction of 2 μm grooves that we observed here was rather surprising, as it is reported in the literature that, in general, cells grown on grooved topographies exhibit lower proliferation rates [8,48]. However, in most studies the material surface was modified by adding reactive groups or through coatings with extracellular matrix proteins to improve cell adhesion. It is known that strong cell adhesion to stiff substrates favors the formation of focal contacts and actin-myosin stress fibers [57,58], thus probably limiting cell division. We have observed that RGLC on PMMA or in the progenitor condition gradually lose their adhesion to the substrate, and some of their radial processes detach from them. NSC proliferate when grown as neurospheres, and differentiate when they are forced to adhere to stiff substrates through the addition of adhesive molecules [21,58]. Thus, a loose adherent phenotype might be a requisite to maintain NSC competence and proliferative capacity, and optimizing cell adhesion to the substrate might therefore introduce a bias toward cell differentiation.

Recent evidence strongly supports the idea that in order to maintain or promote proliferation it is also necessary to recreate certain physical characteristics of the specialized progenitor niche [59]. In the embryonic CNS, progenitors and neuroblasts are densely packed in the ventricular areas, with the long processes of radial glia spanning from the ventricular surface to the surrounding pia mater. As the size of radial glia processes is around 2 μm [60], one possibility is that 2 μm grooves mimic the physical structure of the NSC niche during brain development.

Lineage tracing experiments suggest that CNS neural progenitors are heterogeneous and mostly arise from sequential differentiation of an early multipotent neuroepithelial progenitor that progressively transforms into radial glia. Radial glia cells, which express Pax6 in the cerebral cortex, can originate neurons and glia, and as development proceeds they also generate different intermediate neuronal restricted (TBR2 positive) or glial restricted (A2B5 positive) amplifying progenitors [30,61]. In our experimental conditions, RGLC and glia-restricted progenitors could be induced by material chemistry and topographical cues, but this was not the case of neuronal restricted progenitors or mature neurons,

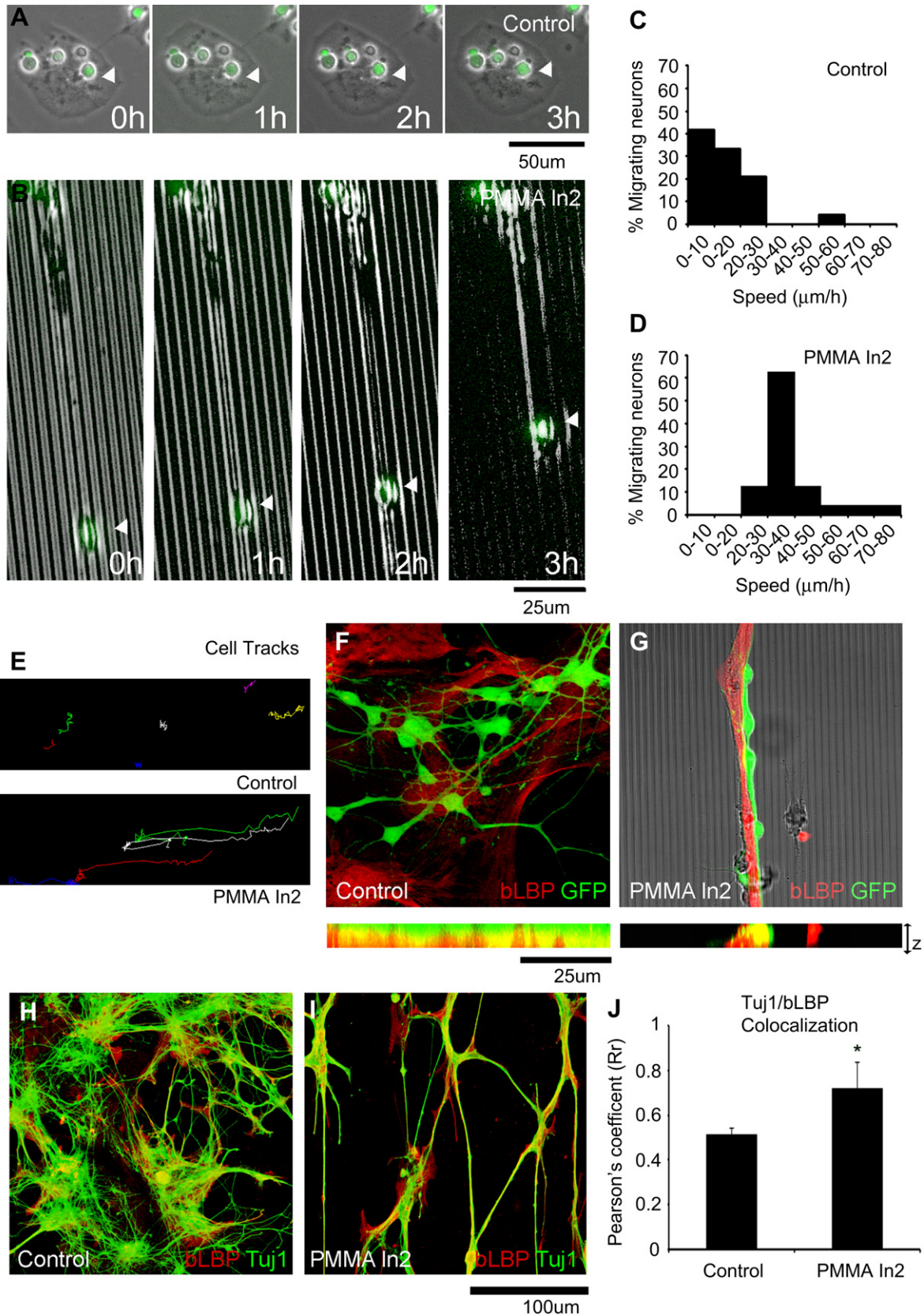


Fig. 7. Role of pattern-induced RGLC in neural migration. Representative time lapse images of E16 GFP neurons (green) seeded on glial cells grown on control (A) and In2 PMMA (B) of glial cells (bright field). White arrows indicate the position of a representative neuronal body showing its stativity on control condition (A) and its migration on In2 induced RGLC process (B). C–D, Frequency plot showing the distribution of the speed (μ m/h) of migrating neurons ($n = 24$) in control and In2 PMMA conditions. E, Particle tracks showing neuronal trajectories in control and In2 PMMA during a 3h record. F–G, GFP neurons (green) grown on WT glial cells stained with BLBP (red) after 5div in control (F) and In2 PMMA (G) and their Z projections. H–I, neurons labeled with Tuj-1 (green) grown on glial cells labeled with BLBP (red) in control (H) and In2 PMMA (I) substrates. (J), Graph representing the Pearson's coefficient for neuron/glia co-localization in those cultures. $0 \leq Rr \leq 1$, where $1 = \text{max co-localization}$ and $0 = \text{maximal exclusion}$. **Indicates statistical significance, $p < 0.01$. Scale bar = 100 μ m. Scale bars (A) = 50 μ m; (B, F, G) = 25 μ m; (E) = 20 μ m; (H, I) 100 μ m. (For interpretation of the references to colour in this figure legend, the reader is referred to the web version of this article.)

suggesting that the cues which guide progenitor specification to neuronal and glial lineages might be different.

During embryonic development, RGC not only act as NSC but also serve as scaffold for directed neuronal migration [33]. The ability of glial cells to support and orient neural growth has already been studied by other authors. For instance, dorsal root ganglions grew longer neurites on aligned astrocytes and meningeal-coated substrates [62], while neurons grew and oriented on electric field-induced aligned astrocytes [27]. One interesting study reported that neurons could align on top of an astrocyte monolayer even after 3 weeks, and they were able to read the pattern “buried” beneath astrocytes [63]. In our experimental conditions, embryonic cortical neurons adhered to glial cells but not to the substrates themselves; thus, changes in neuronal adhesion directly reflect different glial physiology. RGLC induced by 2 μm grooved PMMA provided better neuronal substrates than did glial cells grown on naive PMMA, glass or culture plastic, and neuronal bodies and neurites align perfectly with the oriented glia. Moreover, neurons migrate relatively long distances using the RGLC as rails, at a speed that is comparable with the embryonic neuronal radial migration [64]. Significant participation of contaminant RGC from neural cultures was also ruled out, as GFP+/BLBP glial cells were rarely observed in our co-cultures. Thus, induced RGLC are functional and reproduce the normal roles of RGC during development, providing a guiding substrate for migrating neurons.

Embryonic neurons are known in turn to direct astrocyte transformation into radial glia through neuregulin secretion and BLBP induction in astrocytes [54]. Here we found that 2 μm patterned PMMA synergizes with embryonic neurons, potentiating astrocyte de-differentiation into RGLC. This effect was manifested by a reduction of the surface covered by glial cells, since they adopted bipolar shapes, and an increase in neuron-glia co-localization compared to control (from 15% to 60%).

The present work report morphological and physiological RGLC progenitor induction from *in vitro* matured astrocytes in response to material composition and topography without the concurrence of biochemical cues. Although PMMA is not the material of choice for *in vivo* implantation after a lesion, our results suggest that substrate-mediated induction of RGLC phenotype in mature astrocytes might improve their ability to sense and respond to other potential regenerative cues, whether provided externally or already present locally.

Although much more work remains to be done, the findings raise the possibility of designing implantable devices that restore *in situ* the embryonic radial glia competence into parenchymal astrocytes. Successful regeneration might then require that implantable materials not only promote neuronal cell growth, but also drive glial physiological responses into a neuron permissive or even a neurogenic phenotype. In this regard, the introduction of line patterns within the size range of RGC processes in implantable scaffolds might mimic the topography of the embryonic neural stem cell niche, and could be a useful tool for driving endogenous astrocytes into a neurogenic RGLC phenotype and a regenerative response *in situ*.

5. Conclusions

This study has demonstrated that in the absence of other biochemical cues, the intrinsic composition and line topography of PMMA is sufficient to drive glial cell de-differentiation into RGLC progenitors. Glial cells, and in particular astrocytes, align and orient in a wide range of line topographies, although, only those in the size range of normal RGC processes ($\sim 2 \mu\text{m}$) strongly induced astrocyte transformation into RGLC progenitors. These cells reproduce *in vitro* some of the normal functions of radial glia itself, including the

generation of different types of intermediate progenitors and the support and orientation of neuronal growth. Our results also suggest that the design of an implantable device to promote CNS regeneration must take in account the glial cell response.

Acknowledgments

This study was supported in part by grants from Spain's Ministerio de Ciencia e Innovación [MAT2008-06887-C03-02/MAT] and [MAT2008-06887-C01/MAT], co-financed by the European Regional Development Fund, to S.A. and J.A.P. respectively; from 2009 SGR 719 to S.A. as well as through the fellowship FPU AP2008-01868 to M.M.

We are grateful to M. Maudsley for editorial assistance and to B. Torrejon and E. Castaño from the Scientific-Technical Services UB (Campus Bellvitge) for technical support in confocal microscopy and cytometry.

References

- [1] Yiu G, He Z. Glial inhibition of CNS axon regeneration. *Nat Rev Neurosci* 2006; 7:617–27.
- [2] Fitch MT, Silver J. CNS injury, glial scars, and inflammation: inhibitory extracellular matrices and regeneration failure. *Exp Neurol* 2008;209:294–301.
- [3] Leavitt BR, Hernit-Grant CS, Macklis JD. Mature astrocytes transform into transitional radial glia within adult mouse neocortex that supports directed migration of transplanted immature neurons. *Exp Neurol* 1999;157:43–57.
- [4] White RE, Jakeman LB. Don't fence me in: harnessing the beneficial roles of astrocytes for spinal cord repair. *Restor Neurol Neurosci* 2008;26:197–214.
- [5] Rolls A, Shechter R, Schwartz M. The bright side of the glial scar in CNS repair. *Nat Rev Neurosci* 2009;10:235–41.
- [6] Buffo A, Rolando C, Ceruti S. Astrocytes in the damaged brain: molecular and cellular insights into their reactive response and healing potential. *Biochem Pharmacol* 2010;79:77–89.
- [7] Lang B, Liu HL, Liu R, Feng GD, Jiao XY, Ju G. Astrocytes in injured adult rat spinal cord may acquire the potential of neural stem cells. *Neurosci* 2004;128: 775–83.
- [8] Bettinger CJ, Langer R, Borenstein JT. Engineering substrate topography at the micro- and nanoscale to control cell function. *Angew Chem Int Ed Engl* 2009; 48:5406–15.
- [9] Hoffman-Kim D, Mitchel JA, Bellamkonda RV. Topography, cell response, and nerve regeneration. *Annu Rev Biomed Eng* 2010;12:203–31.
- [10] Steedman M, Tao S, Klassen H, Desai T. Enhanced differentiation of retinal progenitor cells using microfabricated topographical cues. *Biomed Microdevices* 2010;12:363–9.
- [11] Chew SY, Mi R, Hoke A, Leong KW. The effect of the alignment of electrospun fibrous scaffolds on Schwann cell maturation. *Biomaterials* 2008;29:653–61.
- [12] Christopherson GT, Song H, Mao H-Q. The influence of fiber diameter of electrospun substrates on neural stem cell differentiation and proliferation. *Biomaterials* 2009;30:556.
- [13] Moon JH, Yoon BS, Kim B, Park G, Jung HY, Maeng I, et al. Induction of neural stem cell-like cells (NSCLCs) from mouse astrocytes by Bmi1. *Biochem Biophys Res Commun* 2008;371:267–72.
- [14] Yamada T, Sawada R, Tsuchiya T. The effect of sulfated hyaluronan on the morphological transformation and activity of cultured human astrocytes. *Biomaterials* 2008;29:3503–13.
- [15] Tao Y, Guan C, Linyin F. Low temperature induced de-differentiation of astrocytes. *J Cell Biochem* 2006;99:1096–107.
- [16] Recknor JB, Sakaguchi DS, Mallapragada SK. Directed growth and selective differentiation of neural progenitor cells on micropatterned polymer substrates. *Biomaterials* 2006;27:4098–108.
- [17] Mills CA, Fernandez JG, Martinez E, Funes M, Engel E, Errachid A, et al. Directional alignment of MG63 cells on polymer surfaces containing point microstructures. *Small* 2007;3:871–9.
- [18] Engel E, Martinez E, Mills CA, Funes M, Planell JA, Samitier J. Mesenchymal stem cell differentiation on microstructured poly (methyl methacrylate) substrates. *Ann Anat* 2009;191:136–44.
- [19] Martinez E, Engel E, Lopez-Iglesias C, Mills CA, Planell JA, Samitier J. Focused ion beam/scanning electron microscopy characterization of cell behavior on polymer micro-/nanopatterned substrates: a study of cell-substrate interactions. *Micron* 2008;39:111–6.
- [20] Johansson P, Carlberg P, Danielsen N, Montelius L, Kanje M. Axonal outgrowth on nano-imprinted patterns. *Biomaterials* 2006;27:1251–8.
- [21] Martínez-Ramos C, Lainez S, Sancho F, García Esparza MA, Planells-Cases R, García Verdugo JM, et al. Differentiation of postnatal neural stem cells into glia and functional neurons on laminin-coated polymeric substrates. *Tissue Eng Part A* 2008;14:1365–75.

- [22] Merolli A, Rocchi L, Catalano F, Planell J, Engel E, Martinez E, et al. In vivo regeneration of rat sciatic nerve in a double-halved stitch-less guide: a pilot-study. *Microsurgery* 2009;29:310–8.
- [23] Ortega JA, Alcantara S. BDNF/MAPK/ERK-induced BMP7 expression in the developing cerebral cortex induces premature radial glia differentiation and impairs neuronal migration. *Cereb Cortex* 2010;20:2132–44.
- [24] Fedoroff S, McAuley WA, Houle JD, Devon RM. Astrocyte cell lineage. V. Similarity of astrocytes that form in the presence of dBcAMP in cultures to reactive astrocytes in vivo. *J Neurosci Res* 1984;12:14–27.
- [25] Wu VW, Schwartz JP. Cell culture models for reactive gliosis: new perspectives. *J Neurosci Res* 1998;51:675–81.
- [26] Gregg C, Weiss S. Generation of functional radial glial cells by embryonic and adult forebrain neural stem cells. *J Neurosci* 2003;23:11587–601.
- [27] Alexander JK, Fuss B, Colello RJ. Electric field-induced astrocyte alignment directs neurite outgrowth. *Neuron Glia Biol* 2006;2:93–103.
- [28] Comeau JWD, Costantino S, Wiseman PW. A guide to accurate fluorescence microscopy colocalization measurements. *Biophys J* 2006;91:4611–22.
- [29] van Kooten TG, Spijker HT, Busscher HJ. Plasma-treated polystyrene surfaces: model surfaces for studying cell-biomaterial interactions. *Biomaterials* 2004;25:1735–47.
- [30] Englund C, Fink A, Lau C, Pham D, Daza RA, Bulfone A, et al. Pax6, Tbr2, and Tbr1 are expressed sequentially by radial glia, intermediate progenitor cells, and postmitotic neurons in developing neocortex. *J Neurosci* 2005;25:247–51.
- [31] Zhu X, Bergles DE, Nishiyama A. NG2 cells generate both oligodendrocytes and gray matter astrocytes. *Development* 2008;135:145–57.
- [32] Song H, Stevens CF, Gage FH. Astroglia induce neurogenesis from adult neural stem cells. *Nature* 2002;417:39–44.
- [33] Vaccarino FM, Fagel DM, Ganat Y, Maragnoli ME, Ment LR, Ohkubo Y, et al. Astroglial cells in development, regeneration, and repair. *Neuroscientist* 2007;13:173–85.
- [34] Kriegstein A, Alvarez-Buylla A. The glial nature of embryonic and adult neural stem cells. *Annu Rev Neurosci* 2009;32:149–84.
- [35] Voigt T. Development of glial cells in the cerebral wall of ferrets: direct tracing of their transformation from radial glia into astrocytes. *J Comp Neurol* 1989;289:74–88.
- [36] Alvarez-Buylla A, Garcia-Verdugo JM, Tramontin AD. A unified hypothesis on the lineage of neural stem cells. *Nat Rev Neurosci* 2001;2:287–93.
- [37] Chojnacki AK, Mak GK, Weiss S. Identity crisis for adult periventricular neural stem cells: subventricular zone astrocytes, ependymal cells or both? *Nat Rev Neurosci* 2009;10:153–63.
- [38] Berninger B. Making neurons from mature glia: a far-fetched dream? *Neuropharmacology* 2010;58:894–902.
- [39] Costa MR, Gotz M, Berninger B. What determines neurogenic competence in glia? *Brain Res Rev* 2010;63:47–59.
- [40] Discher DE, Janmey P, Wang YL. Tissue cells feel and respond to the stiffness of their substrate. *Science* 2005;310:1139–43.
- [41] Recknor JB, Recknor JC, Sakaguchi DS, Mallapragada SK. Oriented astroglial cell growth on micropatterned polystyrene substrates. *Biomaterials* 2004;25:2753–67.
- [42] Thompson DM, Buettner HM. Schwann cell response to micropatterned laminin surfaces. *Tissue Eng* 2001;7:247–65.
- [43] Yang IH, Co CC, Ho CC. Spatially controlled co-culture of neurons and glial cells. *J Biomed Mater Res A* 2005;75:976–84.
- [44] Yim EK, Pang SW, Leong KW. Synthetic nanostructures inducing differentiation of human mesenchymal stem cells into neuronal lineage. *Exp Cell Res* 2007;313:1820–9.
- [45] Lee MR, Kwon KW, Jung H, Kim HN, Suh KY, Kim K, et al. Direct differentiation of human embryonic stem cells into selective neurons on nanoscale ridge/groove pattern arrays. *Biomaterials* 2010;31:4360–6.
- [46] Keung JA, Kumar S, Schaffer DV. Presentation counts: microenvironmental regulation of stem cells by biophysical and material cues. *Annu Rev Cell Dev Biol* 2010;26:533–56.
- [47] Hynes SR, Millicent FR, Bertram JP, Lavik EB. A library of tuneable poly(ethylene glycol)/poly(L-lysine) hydrogels to investigate the material cues that influence neural stem cell differentiation. *J Biomed Mater Res A* 2009;89:499–509.
- [48] Saha K, Keung AJ, Irwin EF, Li Y, Little L, Schaffer DV. Substrate modulus directs neural stem cell behaviour. *Biophys J* 2008;95:4426–38.
- [49] Leipzig ND, Shoichet MS. The effect of substrate stiffness on adult neural stem cell behaviour. *Biomaterial* 2009;30:6867–78.
- [50] Biran R, Noble MD, Tresco PA. Characterization of cortical astrocytes on materials of different surface chemistry. *J Biomed Mater Res* 1999;46:150–9.
- [51] Soria JM, Martínez Ramos C, Bahamonde O, García Cruz DM, Salmerón Sánchez M, García Esparza MA, et al. Influence of the substrate's hydrophilicity on the *in vitro* Schwann cells viability. *J Biomed Mater Res A* 2007;83:463–70.
- [52] Alaerts JA, De Cupere VM, Moser S, van den Bosh de Aguilar P, Rouxhet PG. Surface characterization of poly(methyl methacrylate) microgrooved for contact guidance of mammalian cells. *Biomaterials* 2001;22:1635–42.
- [53] Goldner JS, Bruder JM, Li G, Gazzola D, Hoffman-Kim D. Neurite bridging across micropatterned grooves. *Biomaterials* 2006;27:460–72.
- [54] Tay CY, Yu H, Pal M, Leong WS, Tan NS, Ng KW, et al. Micropatterned matrix directs differentiation of human mesenchymal stem cells towards myocardial lineage. *Exp Cell Res* 2010;316:1159–68.
- [55] Dalby MJ, Riehle MO, Yarwood SJ, Wilkinson CD, Curtis AS. Nucleus alignment and cell signaling in fibroblasts: response to a micro-grooved topography. *Exp Cell Res* 2003;284:274–82.
- [56] Itano N, Okamoto S, Zhang D, Lipton SA, Ruoslahti E. Cell spreading controls endoplasmic and nuclear calcium: a physical gene regulation pathway from the cell surface to the nucleus. *Proc Natl Acad Sci U S A* 2003;100:5181–6.
- [57] Engler AJ, Sen S, Sweeney HL, Discher DE. Matrix elasticity directs stem cell lineage specification. *Cell* 2006;126:677–89.
- [58] Discher DE, Mooney DJ, Zandstra PW. Growth factors, matrices, and forces combine and control stem cells. *Science* 2009;324:1673–7.
- [59] Keung AJ, Healy KE, Kumar S, Schaffer DV. Biophysics and dynamics of natural and engineered stem cell microenvironments. *Rev Syst Biol Med* 2010;2:49–64.
- [60] Anton ES, Marchionni MA, Lee KF, Rakic P. Role of GGF/neuregulin signaling in interactions between migrating neurons and radial glia in the developing cerebral cortex. *Development* 1997;124:3501–10.
- [61] Baracskey KL, Kidd GJ, Miller RH, Trapp BD. NG2-positive cells generate A2B5-positive oligodendrocyte precursor cells. *Glia* 2007;55:1001–10.
- [62] Biran R, Noble MD, Tresco PA. Directed nerve outgrowth is enhanced by engineered glial substrates. *Exp Neurol* 2003;184:141–52.
- [63] Sørensen A, Alekseeva T, Katechia K, Robertson M, Riehle MO, Barnett SC. Long-term neurite orientation on astrocyte monolayers aligned by microtopography. *Biomaterials* 2007;28:5498.
- [64] Youn YH, Pramparo T, Hirotsune S, Wynshaw-Boris A. Distinct dose-dependent cortical neuronal migration and neurite extension defects in Lis1 and Ndel1 mutant mice. *J Neurosci* 2009;29:15520–30.